

Determinants of Progressive Myocardial Deterioration in Human Heart Failure

Acknowledgements:

Financial support for printing this thesis by J. E. Jurriaanse Stichting, Menarini Framma Nederland BV and Pfizer BV is gratefully acknowledged. Additional financial support was kindly provided by Bio-Rad laboratories and tebu-bio

Determinants of Progressive Myocardial Deterioration in Human Heart Failure

Copyright © 2009 Nazha Hamdani, Amsterdam, The Netherlands

Thesis Vrije Universiteit van Amsterdam, Amsterdam, The Netherlands

VRIJE UNIVERSITEIT

Determinants of Progressive Myocardial Deterioration in Human Heart Failure

ACADEMISCH PROEFSCHRIFT

ter verkrijging van de graad Doctor aan
de Vrije Universiteit Amsterdam,
op gezag van de rector magnificus
prof.dr. L.M. Bouter,
in het openbaar te verdedigen
ten overstaan van de promotiecommissie
van de faculteit der Geneeskunde
op donderdag 4 juni 2009 om 13.45 uur
in de aula van de universiteit,
De Boelelaan 1105

Door

Nazha Hamdani

geboren te Amsterdam

Promotoren: prof.dr. W.J. Paulus
prof.dr. G.J.M. Stienen
Copromotor: dr. J. van der Velden

Contents

List of abbreviations.....	8
Chapter 1 General Introduction	11
Altered Sarcomeric Function in Cardiac Disease.....	30
Chapter 2 Sarcomeric Dysfunction in Heart Failure	31
Differences in Heart Failure with Different Phenotypes and Underlying Cause.....	56
Chapter 3 Diverse Alteration in Sarcomeric Protein Composition And Function in Ischemic and Idiopathic Dilated Cardiomyopathy.....	57
Chapter 4 Myofilament Degradation and Dysfunction in Human Cardiomyocytes with Fabry Disease	83
Chapter 5 Distinct Myocardial Effects of Beta-Blocker Therapy in Heart Failure with Normal and Reduced Left Ventricular Ejection Fraction	109
Chapter 6 Diastolic stiffness of the failing diabetic heart: Importance of fibrosis, advanced glycation end products, and myocyte resting tension.....	135
Chapter 7 Lack of Specificity of Antibodies Directed Against Human Beta-Adrenergic Receptors.....	157
Chapter 8 Myofilament Dysfunction in Cardiac Disease From Mice to Men.	171
Chapter 9 Summary, Conclusion & Future perspectives	199
Chapter 10 Nederlandse samenvatting	207
List of Publications.....	213
Dankwoord	219
Curriculum vitae.....	225

List of abbreviations

ACE-I	Angiotensin converting enzyme inhibitors
ARB	Angiotensin II receptor blockers
β_1 AR	Beta1-adrenergic receptor
β_2 AR	Beta2-adrenergic receptor
β -blockers	Beta-blockers
BMI	Body Mass Index
bpm	Beats per minute
CCB	Calcium channel blockers
CVF	Collagen volume fraction
DTT	Dithiothreitol
EGTA	Ethylene glycol-bis (amino-ethylether) N,N,N',N'-tetraacetic acid
F_{active}	Active Tension
FibD	Myofibrillar density
F_{passive}	Passive Tension
Gi	G-inhibitory proteins
Gs	G-stimulatory proteins
GRK2	G-coupled receptor kinase 2
GRK5	G-coupled receptor kinase 5
HF	Heart Failure
HFNEF	Heart Failure with Normal Ejection Fraction
HFREF	Heart Failure with Reduced Ejection Fraction
kDa	Kilodalton
Ktr	Rate of force redevelopment
LV	Left ventricular
LVEDP	LV end-diastolic pressure
LVEDVI	LV end-diastolic volume index
LVEF	Left ventricular Ejection Fraction
LVMi	LV mass index
LVPSP	LV peak systolic pressure
LVWT	LV wall thickness
M/F	Male/female
MHC	Myosin heavy chain
MyD	Myocyte diameter
n	Number of patients and myocytes

NADH	Nicotineamide adenine dinucleotide
NHill	Measure of calcium sensitivity
NMR	Nuclear magnetic resonance
NYHA	New York heart association
pCa ₅₀	Calcium sensitivity or Ca ²⁺ -sensitivity
pDesmin	Phosphorylated Desmin
PKA	Protein kinase A
PLB	Phospholamban
MLC-2	Myosin light chain-2
MyBP-C	Myosin-binding protein C
TnI	Troponin I
TnT	Troponin T
(p)MLC-2	(Phosphorylated) myosin light chain-2
(p)MyBP-C	(Phosphorylated) myosin-binding protein C
(p)TnI	(Phosphorylated) Troponin I
(p)TnT	(Phosphorylated) Troponin T
SEM	Standard error of the mean
SERCA2a	Sarcoplasmic reticulum (SR) Ca ²⁺ -ATPase 2a
SDS-PAGE	Sodium dodecyl sulphate-polyacrylamide gel Electrophoresis
TM	Tropomyosin

1

General Introduction

Heart failure

Heart failure is a major health care problem and one of the most frequent reasons for patients to be admitted to hospital. Heart failure is characterized by abnormalities of left ventricular (LV) function,¹ structural changes,² neurohumoral up-regulation³ and is accompanied with exercise intolerance,² reduced prognosis,⁴ altered hemodynamics,⁵ cytokine over-expression,^{3,6,7} vascular and endothelial dysfunction.⁸⁻¹⁰ The underlying pathophysiology is not well understood and may depend on cause and/or phenotype of cardiac disease. Therefore, in this present thesis, we focussed on heart failure with different clinical phenotypes, aimed to characterise underlying mechanisms and to identify possible target proteins for more patient tailored heart failure therapy.

The incidence of heart failure is increasing rapidly, particularly due to the aging of the population around the world.¹¹ In the Netherlands, there are 200.000 patients with heart failure and around 25.000 hospitalisations annually with a discharge diagnosis of heart failure.¹² Most of these patients are managed in primary care. Even with the significant advances in heart failure treatment,¹³ the prognosis remains poor. Heart failure is the final common pathway to death in cardiovascular disease, including pressure overload (i.e. hypertension), volume overload (i.e. mitral regurgitation), myocardial infarction, and inherited or acquired cardiomyopathies.

Human heart failure has many underlying causes. The major causes are: coronary heart disease, arterial hypertension, valvular heart disease, myocardial diseases (of which idiopathic dilated cardiomyopathy predominates), and diabetes mellitus (Table 1).¹⁴

In order to determine the best course of therapy, physicians often assess the stage of heart failure according to the New York Heart Association (NYHA) functional classification system. This system relates symptoms to everyday activities and the quality of life of the patients. The severity of heart failure is classified as mild in NYHA I to severe in NYHA IV (Table 2).¹⁵

Table 1.

Major causes of heart failure

- Coronary artery disease: many manifestations
 - Hypertension: often associated with LV hypertrophy and preserved ejection fraction
 - Valvular disease
 - Infectious myocarditis (e.g. viral, protozoal, bacterial)
 - Toxins (e.g. anthracyclines, cyclophosphamide, alcohol, cocaine, cobalt, lead)
 - Tachycardia-related cardiomyopathy
 - Endocrine disorders (e.g. sarcoidosis, amyloidosis)
 - Hypertrophic cardiomyopathy
 - Collagen vascular dystrophies
 - Peripartum cardiomyopathy
 - Nutritional deficiencies
 - Idiopathic
-

Table 2.

New York Heart Association classification system

Class I	no symptoms with ordinary physical activity
Class II	mild limitation of physical activity, symptoms with ordinary physical activity
Class III	marked limitation activity, symptoms with less than ordinary physical activity
Class IV	symptoms at rest and with any physical activity

The cardiac cycle

The cardiac cycle is divided into two major phases, both named for events in the ventricles: the period of ventricular contraction and blood ejection called **systole**, and the alternating period of ventricular relaxation and blood filling, **diastole**. Figure 1 represents an overview of the cycle, naming the phases and the key events. During the first part of systole, the ventricles are contracting but all valves in the heart are closed, and no blood can be ejected. This period is termed **isovolumetric ventricular contraction** because the ventricular volume is constant. The ventricular walls are developing tension and squeezing on the blood they enclose, raising the ventricular pressure. Once the pressure in the ventricles exceeds that in the aorta and pulmonary trunk, the aortic and pulmonary valves open, and the **ventricular ejection** period of systole occurs. Blood is forced into the aorta and pulmonary trunk as the contracting ventricular muscle fibers shorten.

During diastole, the ventricles begin to relax, and the aortic and pulmonary valves close. AS ventricular volume is not changing, this period is called **isovolumetric ventricular relaxation**. Next, the atrioventricular valves open, and ventricular filling occurs as blood flows in from the atria. Atrial contraction occurs at the end of diastole, after most of the ventricular filling has taken place.

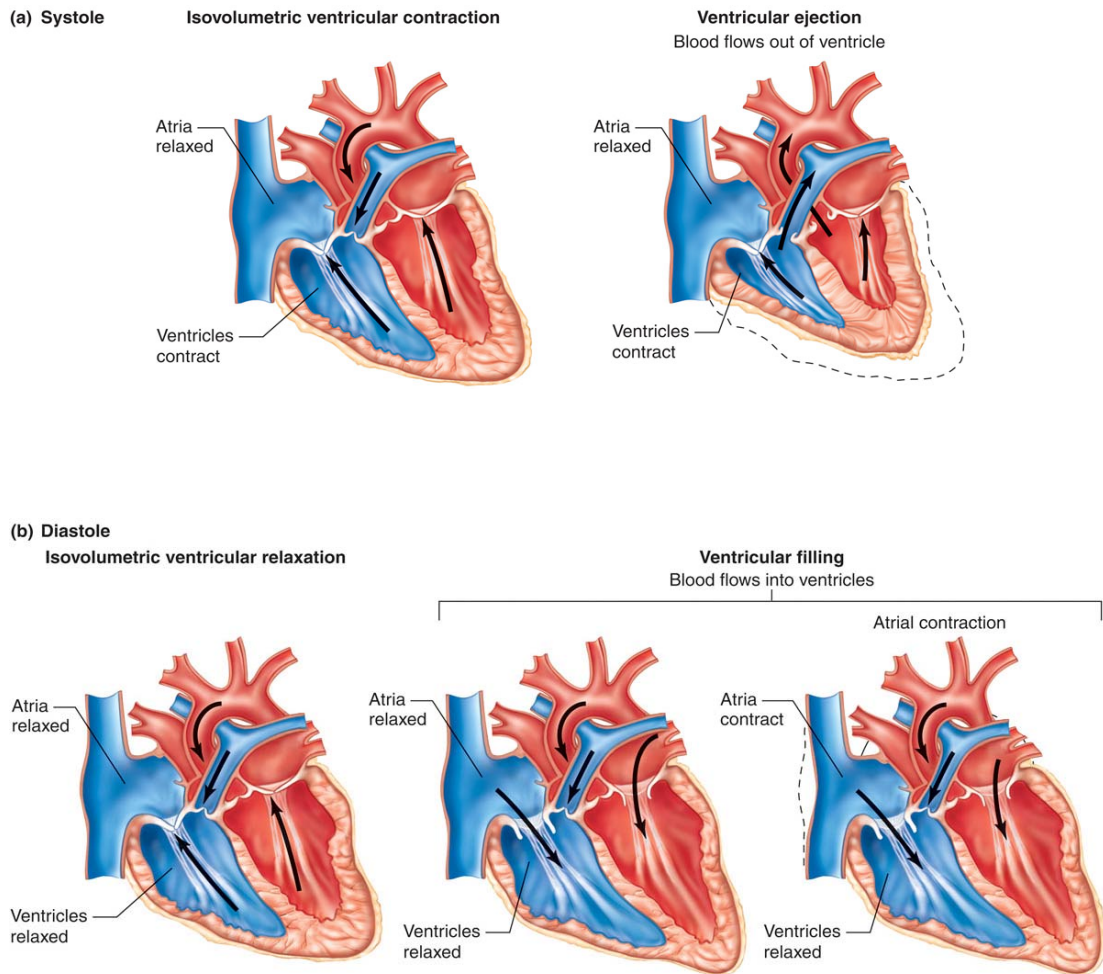
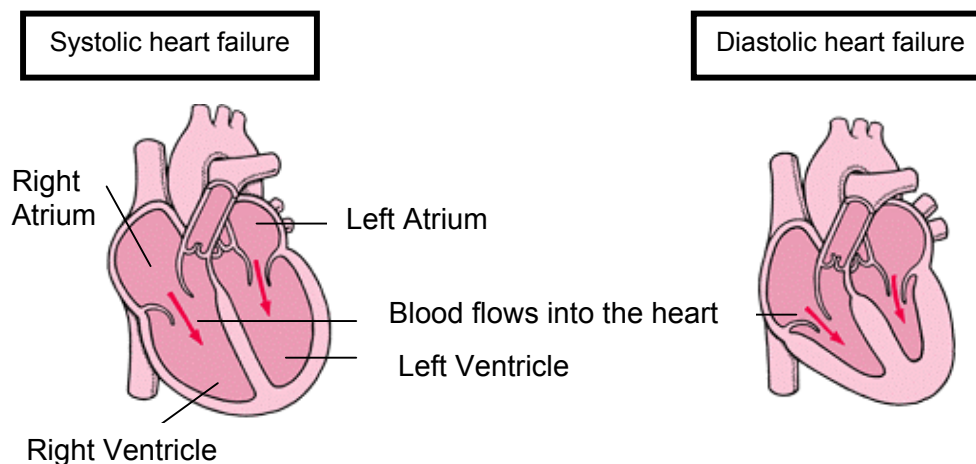


Figure 1. Cardiac cycle: (a) systolic and (b) diastolic phase. The phases of the cycle are identical in both halves of the heart. The direction in which the pressure difference favors flow in denoted by the arrow. Adapted from Widmaier, Raff and Strang. Vander's. Human Physiology; 2006; 11th Edition).

Systolic versus diastolic dysfunction

About half of all patients have systolic dysfunction. This group is referred to as systolic heart failure (SHF) or heart failure with reduced ejection fraction (HFREF) (Fig 2). The other half of the patients has normal systolic function (i.e. normal or preserved ejection fraction), but has diastolic dysfunction evident from increased LV end-diastolic pressure. This group is referred to as diastolic heart failure (DHF) or heart failure with normal ejection fraction (HFNEF).¹⁶



The enlarged ventricles fill with blood, but are less capable of ejecting blood during the systolic phase.

The stiff ventricles limit filling during the diastolic phase

Figure 2. The two major clinical heart failure phenotypes: Systolic heart failure (heart failure with reduced ejection fraction, HFREF) and diastolic heart failure (heart failure with normal ejection fraction, HFNEF).

Heart failure due to *systolic dysfunction* typically culminates in a progressively dilated heart with reduced LVEF lower than 40%, which is caused by impaired cardiac pump function. Patients with reduced ejection fraction have an increase of LV end-diastolic and end-systolic volumes (i.e. ventricular dilation), an increase in LV wall stress, cardiomyocyte hypertrophy and interstitial fibrosis.¹⁷ In systolic dysfunction contractility is depressed as evidenced by a downwardly displaced end-systolic pressure-volume relation. There is diminished capacity to eject blood during the systolic phase (Figure 3).

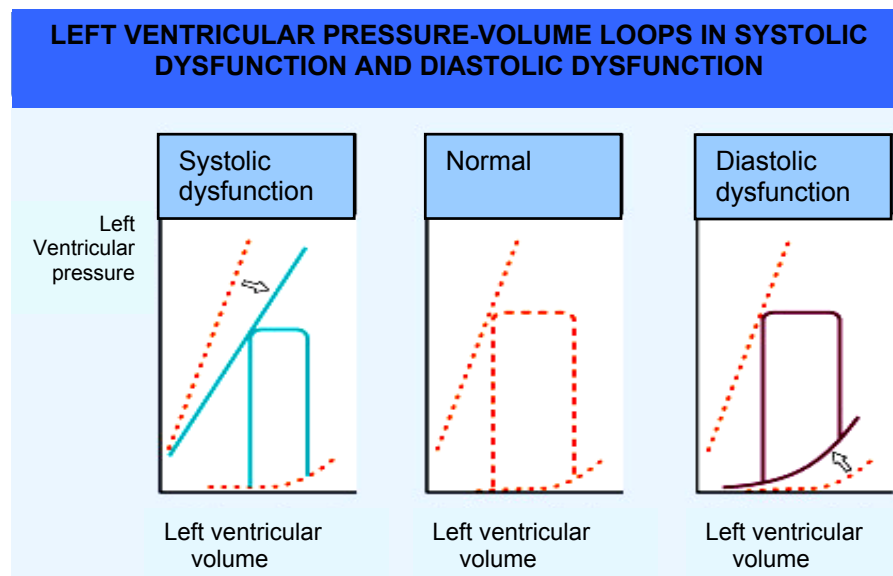


Figure 3. LV pressure-volume loops in systolic and diastolic dysfunction. Adapted from Crawford, Dimarco and Paulus: *Cardiology*; 2004; Second Edition.

LV *diastolic dysfunction* is present when there is evidence of increase passive stiffness and/or impaired relaxation of the ventricle. Patients with diastolic heart failure are clinically characterized by preserved or normal LVEF (> 50%), decreased LV end-systolic and end-diastolic volumes and increased LV end-diastolic pressure (> 16 mmHg). In diastolic HF the LV chamber size is usually normal. Diastolic dysfunction causes an upward shift in the diastolic pressure-volume relation, resulting in an increase in LV diastolic pressure without corresponding increase in diastolic volume (Fig 3). A number of cardiomyopathic processes can impair the ability of the left ventricle to fill at normal diastolic pressures. These include chronic high blood pressure, hypertrophic cardiomyopathy, aortic stenosis, diabetes mellitus, coronary artery disease, restrictive cardiomyopathy (a rare condition in which the heart muscle is infiltrated, and made stiff, by abnormal cells, protein, or scar tissue). The most common cause of restrictive cardiomyopathy is amyloidosis, a disease in which protein-like substance is deposited within the body's tissues. Other causes include sarcoidosis and hemochromatosis and aging.¹⁸

Cellular mechanisms involved in heart failure

Clinical and experimental studies have indicated that the two key components of heart failure progression are structural and functional adaptations of cardiac myocytes. Initially, these changes are compensatory in light of increased cardiac demand. However, with time they fail to correct the unfavorable changes in cardiomyocyte performance.^{16,19}

Contractile remodelling

The mechanisms underlying the progressive deterioration from LV pump dysfunction towards overt heart failure are still unclear, however, a primary event that may lead to heart failure is a decrease in the number of cardiomyocytes. This results from an imbalance between signaling pathways that promote cell survival and those that promote cell death (through apoptosis or necrosis).²⁰ Apart from loss of cardiomyocytes, the intrinsic cardiomyocyte function changes, due to alterations in proteins involved in calcium handling and myofilament contractility.

Alterations in Ca^{2+} handling have been reported in cardiac disease, and may contribute to the progression of LV pump dysfunction. Ca^{2+} is the central regulator of excitation-contraction coupling, which drives cyclical muscle contraction (Fig 4).

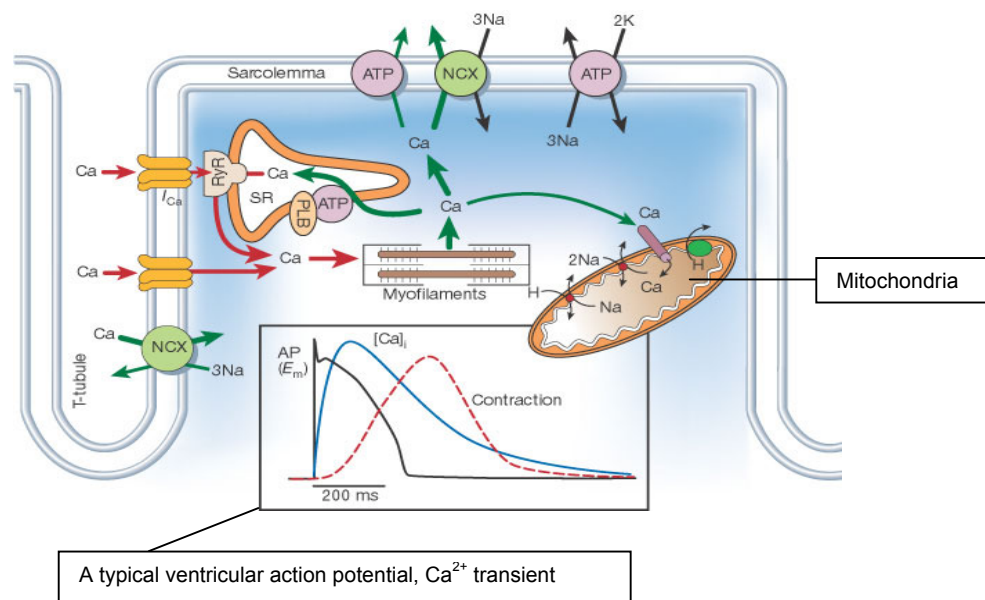


Figure 4. Ca^{2+} handling in myocytes in the heart adapted from Donald M. Bers. Cardiac excitation-contraction coupling. Nature 2002; 415:198-205. Abbreviations: Ca^{2+} : Calcium; NCX: $\text{Na}^+/\text{Ca}^{+2}$ exchange; AP: Action Potential; E_m : membrane potential; PLB: phospholamban; RYR: ryanodine receptor; ATP: Adenosine triphosphate; Na: sodium; K: potassium.

The contraction occurs from release of calcium ions from the sarcoplasmic reticulum (SR), the major intracellular calcium store in the cell. Calcium enters the cell via the opening of L-type calcium channels during the depolarization phase of the action potential. Subsequently, Ca^{2+} is released from the SR through the ryanodine channel (also known as the ryanodine receptor; RyR) and this is followed by re-uptake of Ca^{2+} into the sarcoplasmic reticulum by a Ca^{2+} uptake pump (SERCA2a) and removal of Ca^{2+} from the cell by the $\text{Na}^+/\text{Ca}^{2+}$ exchanger and the sarcolemmal Ca^{2+} pump (Fig 4). The activity of SERCA2a is regulated by phospholamban (PLB). In its unphosphorylated state, phospholamban inhibits SERCA2a activity, but upon phosphorylation (e.g. by protein kinase A (PKA)), this inhibition is released, thereby increasing Ca^{2+} uptake.

In the failing heart, Ca^{2+} uptake into the SR is impaired and Ca^{2+} concentrations in the SR are therefore decreased.²¹

The key components thought to be involved in altered calcium handling are 1) PKA-mediated hyperphosphorylation of the RyR, which may cause diastolic calcium leak and trigger arrhythmias;²² 2) impaired re-uptake of calcium by the SR due to reduced expression of the SR Ca^{2+} ATPase (SERCA2a) and up-regulation of phospholamban.²³ Moreover, decreased phosphorylation of PLB may limit SERCA2a function.²⁴

Contraction of cardiac muscle results from the molecular interaction of two myofilament proteins myosin in the thick myofilament and actin in the thin myofilament.

Structural remodelling

Increasing the size of cardiomyocytes referred to as physiological hypertrophy, which occurs to meet increased metabolic demands differs from pathological hypertrophy that occurs in response to myocardial stress signals and injury.²⁵ Initially hypertrophy is an adaptive response to an increased load resulting in improved cardiac pump function and decreased wall stress. However, during the progression of cardiac disease, cellular hypertrophy is detrimental.

Alterations in the structure of the extracellular matrix occur during development and progression of heart failure. This process is governed by the production of collagen by cardiac fibroblasts and the degradation of the extracellular matrix by matrix metalloproteinases (MMPs). Activation of MMPs is a key feature of the remodelling ventricle, particularly in the setting of post-myocardial infarction and LV dilatation.

β-Adrenergic receptor signalling

Apart from changes in cellular function at rest, alterations have been reported in the signaling pathway involved in cardiomyocyte function during exercise and increased cardiac stress. Activation of the sympathetic nervous system increases cardiac pump function via β-adrenergic receptor stimulation (Fig 5). The cardiac β-adrenergic receptor signal transduction pathway mediates the powerful effects of neuronally released and circulating catecholamines on the heart. The overall action of β-adrenergic receptor stimulation on the heart includes an increase in force of cardiac contraction (inotropism), an increase in rate of cardiac relaxation (lusitropism), an increase in heart rate (chronotropism), and an increase in impulse conduction (dromotropism).²⁶ The classic theory of biochemical and molecular events leading to these biological responses involves binding of catecholamines to the β-adrenergic receptors as well as triggering the interaction of guanine nucleotide-binding proteins (G-proteins) with adenylyl cyclases (ACs) to synthesize the second messenger cyclic AMP (cAMP) from ATP. It should be noted that β₁-adrenergic receptors (β₁ARs) activate only G-stimulatory (Gs) proteins, while β₂ARs stimulate both Gs and Gi (inhibitory) proteins. β₁ARs have been implicated as being pathological in heart failure, whereas β₂ARs have generally been perceived to be cardioprotective.^{27,28}

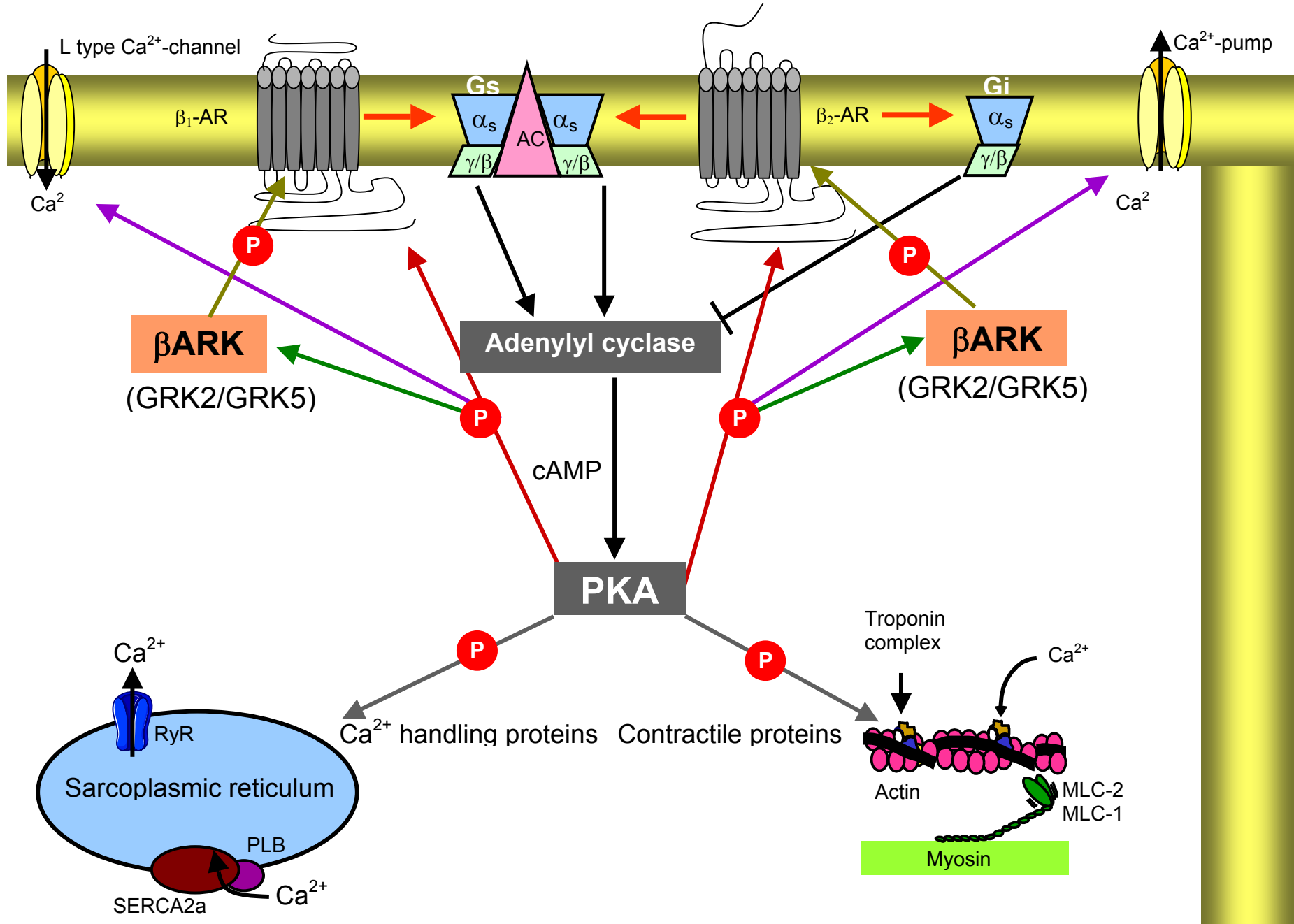


Figure 5. Activation of β -adrenergic signalling pathway in the heart. Abbreviations: β_1 ARs: β_1 -adrenergic receptors; β_2 ARs: β_2 -adrenergic receptors; Gs: G-stimulatory; Gi:G-inhibitory; GRK:G-coupled receptor kinase; Ca^{2+} :calcium; cAMP:cyclic AMP; MLC: myosin light chain; RyR: ryanodine receptor; PLB:Phospholamban; SERCA2a: SR Ca^{2+} ATPase.

The increase in intracellular cAMP level activates cAMP-dependent PKA, which then phosphorylates target proteins such as cardiac L-type Ca^{2+} -channels, phospholamban, troponin I and myosin binding protein C, leading to various physiological responses.²⁹ Physiologic and molecular analyses indicate that the β -adrenergic signaling cascade is an important regulator of myocardial function, and several lines of investigation support alterations in β -adrenergic receptor signal transduction mechanisms as primary determinants of heart failure.¹⁹ The regulation of β -adrenergic signalling requires a synchronised and subtle balance among different processes involving receptor activation, desensitisation, and resensitisation.

Desensitization refers to the reduction of receptor signalling because of persistent attendance of agonist stimulation. Many of these events involve regulation of activity of G protein-coupled receptors such as β AR, while others occur down stream of the receptors. By using β_2 AR as a model, three events namely, uncoupling, internalisation, and down regulation were found to be involved in the process of desensitisation at the receptor level.³⁰

Uncoupling of receptors from G-proteins results from receptor phosphorylation, which rapidly desensitises the receptor. Phosphorylation can occur by the actions of three classes of kinases, namely, PKA and protein kinase C (PKC) and G-coupled receptor kinases (GRKs). PKA and PKC phosphorylate and directly uncouple β_2 -AR from Gs-protein. GRK phosphorylation of receptors does not directly inhibit receptor G-protein interaction, but the GRK-mediated phosphorylation of receptors rather serves as a binding site for certain cytosolic proteins, members of the arrestin family.^{31,32} Binding of arrestin protein sterically blocks β_2 AR mediated G-protein activation.

Internalisation occurs once the receptor has been phosphorylated and uncoupled from the signalling pathway. The receptor will be removed and translocates from the plasma membrane to an intracellular endosomal compartment.³³⁻³⁶

Down regulation occurs after desensitisation and internalisation and represents a decrease in the total number of receptors after prolonged agonist stimulation that may result from degradation of the receptors by lysosomes. The internalised receptor may be dephosphorylated by protein phosphatase, PP2a, which

thereby prevents degradation by lysosomes and leads to recycling back to the plasma membranes as fully functional receptors.

Treatment of heart failure

Therapy of heart failure has undergone several large shifts, moving from a focus on hemodynamics only, to a focus on the targeting of a specific disease mechanism. Early diagnosis and treatment can help people with heart failure to live longer. The aim of treatment is to relieve symptoms, to prevent progression to more severe cardiac dysfunction or to prolong survival. Diuretics and digoxin are often indicated for these patients because they reduce symptoms in the chronic phase, and reduce hospitalisations, but do not reduce deaths.³⁷ Treatment of LV diastolic dysfunction has two major objectives. First to eliminate or reduce the factors that cause diastolic dysfunction (e.g. fibrosis), and second to reverse the consequences of diastolic dysfunction (e.g. improve ventricular relaxation).³⁸ Beta-adrenergic stimulators (such as isoproterenol, forskolin or norepinephrine) and calcium channel blockers are used to improve ventricular relaxation, while diuretics, ACE inhibitors, and angiotensin II receptor blocking agents are used for the treatment of hypertension and heart failure.^{39,40} The mechanism underlying mortality benefit is likely complex, however, it has been shown that these agents can attenuate or even reverse structural remodelling of the heart. In addition, β -blockers and Ca^{2+} channel blockers are used to treat and prevent myocardial ischemia, control hypertension and promote regression of hypertrophy.^{41,42} Multiple trials have demonstrated evidence of attenuated or reversed remodelling with β -blocker treatment in heart failure.⁴³⁻⁴⁶

Beta-blockers are one of the few classes of drugs that have been shown to improve cardiac function and reduce morbidity and mortality rates in patients with congestive heart failure.⁴⁸⁻⁵⁴ Because β -blockers are known to depress cardiac function in healthy hearts, it seems rather counter-intuitive to use this class of drugs for the treatment of heart failure. Recent data, however, showed the molecular mechanism by which β -blockers might improve cardiac contractility in patients with congestive heart failure (CHF).⁵⁵ β -blockers reduce the chronic hyperactivity of the sympathetic nervous system. Lowered plasma levels of circulating catecholamines are associated with reduced intracellular cAMP levels, and thus reversal of PKA hyperphosphorylation of RyR, which might in part explain the improved cardiac function observed in heart failure patients treated with β -blockers.^{55,56} Moreover, β -blockers might improve the energy balance in failing hearts. Finally, β -blockers reverse failure-specific alterations in cardiac gene expression, which might be

involved in progression of the disease.⁵⁷ However, knowledge about the effects of β -blockers on myofilament function is lacking. Moreover, most studies have been performed in patients with systolic dysfunction.

Aim of this thesis

The main objective of this thesis is to investigate diverse alterations in heart failure with different underlying cause and phenotype, and effects of β -blocker therapy. The different patient groups studied are summarized in the schematic diagram given in Fig 6.

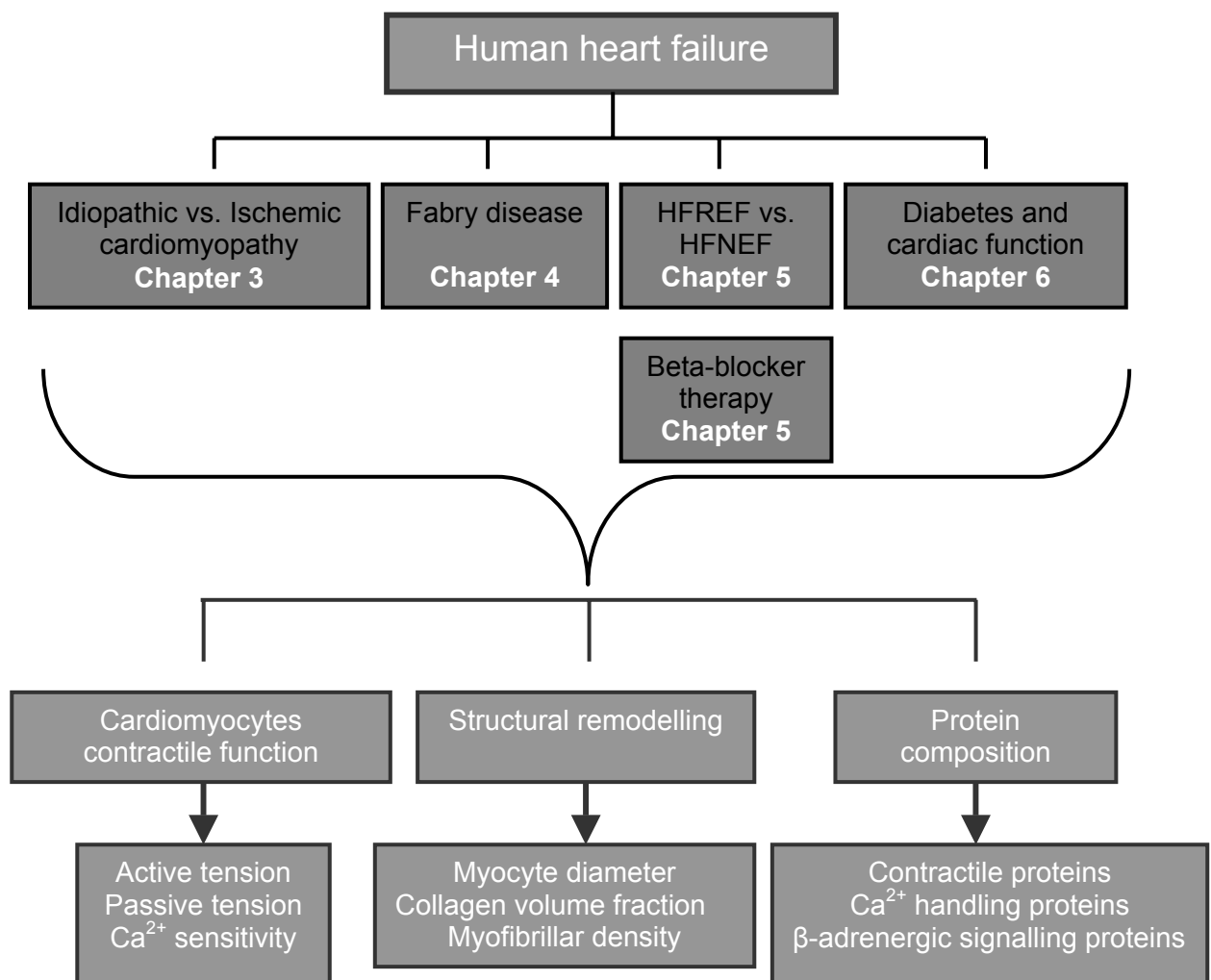


Figure 6. Schematic outline of this thesis.

The questions addressed in this thesis are important to obtain insight into the cellular pathomechanisms underlying progressive deterioration of LV pump function in human heart failure, and the differences between all phenotypes. This information is important to develop novel targeted therapeutic interventions for the treatment of

heart failure.

The outline of this thesis is as follows:

In **Chapter 2** a review is given of the alterations that have been found in sarcomeric proteins in failing myocardium. Previous studies in human failing myocardium indicate that sarcomeric dysfunction mainly results from altered protein phosphorylation, caused by neurohumoral-induced alterations in the kinase-phosphatase balance inside the cardiomyocytes. Modulation of phosphorylation of the sarcomeric proteins, by kinases and phosphatases, could represent a target for novel therapy in heart failure.

In **Chapter 3** alterations in the adrenergic receptor cascade, which coincide with diverse changes in cellular function and structure in failing human myocardium with different underlying cause, are described. A comparison was made between LV tissue samples from patients with ischemic and idiopathic cardiomyopathy. Donor hearts samples served as non-failing controls.

In **Chapter 4** functional and structural myofilament changes, which occur in Fabry disease cardiomyopathy, are discussed. Fabry disease is an X-linked lysosomal storage disorder caused by the deficiency of the enzyme α -galactosidase A, resulting in progressive intracellular glycosphingolipid deposition in multiple organ systems, including the heart. In this study, we investigated cardiomyocyte function in LV endomyocardial biopsies from Fabry patients, and from patients with mitral stenosis and normal LV function. Cardiomyocyte cross-sectional area, glycosphingolipid vacuole area, myofibrilolysis, and extent of fibrosis were also determined. These data were correlated with results of tissue Doppler imaging i.e. myocardial long axis shortening and lengthening velocities.

In **Chapter 5** it is shown that LV myocardial structure and function differ in heart failure with normal and reduced LV ejection fraction. This difference could underlie the unequal outcome of trials with β -blockers in both phenotypes. To investigate if β -blockers have distinct myocardial effects in different phenotypes, myocardial structure, cardiomyocyte function and myocardial protein composition were compared in the two patient groups treated without or with β -blockers.

In **Chapter 6** the role of fibrosis, advanced glycation endproducts (AGEs), and cardiomyocyte resting tension in diastolic stiffness in diabetic heart failure patients

with normal or reduced LVEF was studied, since diastolic LV stiffness is an important contributor to heart failure in patients with diabetes mellitus.

In **Chapter 7** the specificity of antibodies directed against human β -adrenergic receptors was studied.

In **Chapter 8** a review is given of altered PKA-mediated myofilament protein phosphorylation in different animal and human studies, and the roles of troponin I, myosin binding protein C and titin in regulating myofilament dysfunction in cardiac function are discussed.

In **Chapter 9** a summary and conclusion of the major findings of the studies presented in this thesis is given followed by future perspectives.

References

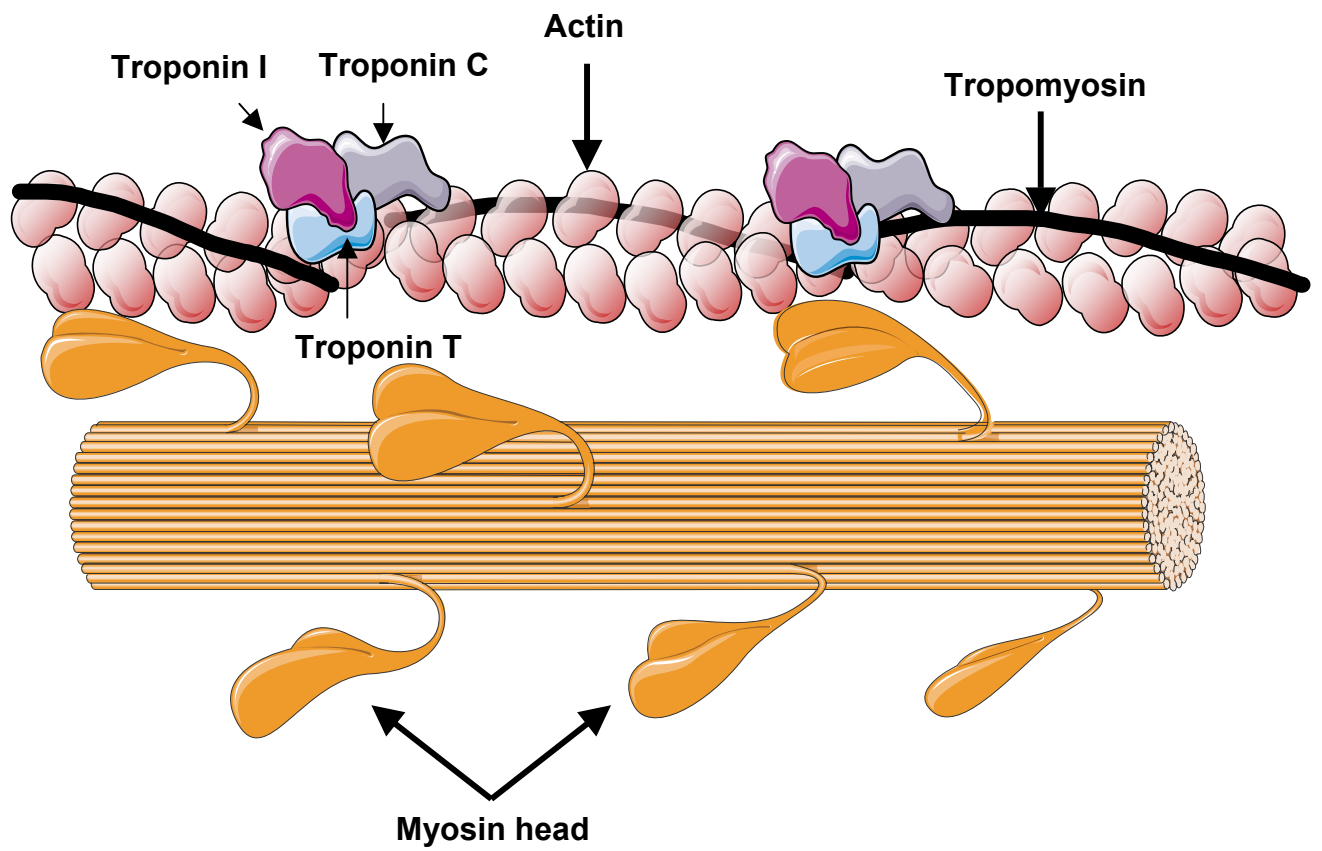
1. Conraads VM, Bosmans JM, Vrints CJ. Chronic heart failure: an example of a systemic chronic inflammatory disease resulting in cachexia. *Int J Cardiol* 2002; 85:33-49.
2. Francis GS. Pathophysiology of chronic heart failure. *Am J Med* 2001; 110:37-46.
3. Braunwald E, Bristow MR. Congestive Heart Failure: Fifty Years of Progress. *Circulation* 2000; 102:IV-14.
4. Meyer FJ, Borst MM, Zugck C. Respiratory muscle dysfunction in congestive heart failure: clinical correlation and prognostic significance. *Circulation* 2001; 103:2153-2158.
5. Guérin AP, Marchais SJ, Metivier F, London GM. Arterial structural and functional alterations in uraemia. *Eur J Clin Invest* 2005; 3:85-88.
6. Paulus WJ. How are cytokines activated in heart failure? *The European Journal of Heart Failure* 1999; 1:309-312.
7. Blum A, Miller H. Role of cytokines in heart failure. *Am Heart J* 1998; 135:181-186.
8. Bank AJ, Lee PC, Kubo SH. Endothelial dysfunction in patients with heart failure: relationship to disease severity. *J Card Fail* 2000; 6:29-36.
9. Nakamura M. Peripheral vascular remodeling in chronic heart failure: clinical relevance and new conceptualization of its mechanisms. *J Card Fail* 1999; 5:127-138.
10. Brutsaert DL. Cardiac Endothelial-Myocardial Signaling: Its Role in Cardiac Growth, Contractile Performance, and Rhythmicity. *Physiology* 2003; 83:59-115.
11. Terman A, Brunk UT. The aging myocardium: roles of mitochondrial damage and lysosomal degradation. *Heart Lung Circ* 2005; 14:107-114.
12. Jaarsma T, Haaijer-Ruskamp FM, Sturm H, Van Veldhuisen DJ. Management of heart failure in The Netherlands. *Eur J Heart Fail* 2005; 16:371-375.
13. Doba N, Tomiyama H, Nakayama T. Drugs, heart failure and quality of life: what are we achieving? What should we be trying to achieve? *Drugs Aging* 1999; 14:153-163.
14. Paulus WJ, Tschöpe C, Sanderson JE, Rusconi C, Flachskampf FA, Rademakers FE, Marino P, Smiseth OA, De Keulenaer G, Leite-Moreira AF, Borbély A, Edes I, Handoko ML, Heymans S, Pezzali N, Pieske B, Dickstein K, Fraser AG, Brutsaert DL. How to diagnose diastolic heart failure: a consensus statement on the diagnosis of heart failure with normal left ventricular ejection fraction by the Heart Failure and Echocardiography Associations of the European Society of Cardiology. *Eur Heart J* 2007; 28:2539-2550.
15. Bayrak F, Kahveci G, Degertekin M, Mutlu B. Echocardiographic predictors of severe heart failure symptoms in hypertrophic cardiomyopathy patients with sinus rhythm. *Trials* 2008; 9:1-11.
16. Tilley DG, Rockman HA. Role of β -adrenergic receptor signaling and desensitization in heart failure: new concepts and prospects for treatment. *Expert Rev Cardiovasc Ther* 2006; 4:417-432.
17. van Heerebeek L, Borbély A, Niessen HW, Bronzwaer JG, van der Velden J, Stienen GJ, Linke WA, Laarman GJ, Paulus WJ. Myocardial structure and function differ in systolic and diastolic heart failure. *Circulation* 2006; 113:1966-1973.

18. Stephen J. McPhee, Maxine A. Papadakis, Lawrence M. Tierney. *Current Medical Diagnosis and Treatment*. 2008, 47th edition
19. Feldman DS, Carnes CA, Abraham WT, Bristow MR. Mechanisms of disease: β -adrenergic receptors—alterations in signal transduction and pharmacogenomics in heart failure. *Nat Clin Pract Cardiovasc Med* 2005; 2: 475-483.
20. Feldman DS, Elton TS, Sun B, Martin MM, Ziolo MT. Mechanisms of Disease: detrimental adrenergic signaling in acute decompensated heart failure. *Nat Clin Pract Cardiovasc Med* 2008; 5: 208-218.
21. Bers DM. Altered Cardiac Myocyte Ca Regulation In Heart Failure. *Physiology* 2006; 21: 380-387.
22. Vest JA, Wehrens XH, Reiken SR, Lehnart SE, Dobrev D, Chandra P, Danilo P, Ravens U, Rosen MR, Marks AR. Defective cardiac ryanodine receptor regulation during atrial fibrillation. *Circulation* 2005; 111:2025-2032.
23. Wehrens XH, Lehnart SE, Marks A. Intracellular calcium release and cardiac disease. *Annu Rev Physiol* 2005; 67:69-98.
24. Braz JC, Gregory K, Pathak A, Zhao W, Sahin B, Klevitsky R, Kimball TF, Lorenz JN, Nairn AC, Liggett SB, Bodi I, Wang S, Schwartz A, Lakatta EG, DePaoli-Roach AA, Robbins J, Hewett TE, Bibb JA, Westfall MV, Kranias EG, Molkenstein JD. PKC-alpha regulates cardiac contractility and propensity toward heart failure. *Nat Med* 2004; 10:248-254.
25. Olson EN. A decade of discoveries in cardiac biology. *Nat Med* 2004; 10:467-474. Review
26. Opie LH. *The Heart Physiology from Cell to Circulation: Receptors and signal transductions*. Lippincott-Raven Publishers, Philadelphia, 173-207.
27. Lohse MJ, Engelhardt S, Eschenhagen T. What is the role of β -adrenergic signaling in heart failure? *Circ Res* 2003; 93:896-906.
28. Vatner SF, Vatner DE, Homcy CJ. β -Adrenergic receptor signaling: an acute compensatory adjustment-inappropriate for the chronic stress of heart failure? Insights from G α overexpression and other genetically engineered animal models. *Circ Res* 2000; 86:502-506.
29. Omens JH, Covell JW. Transmural distribution of myocardial tissue growth induced by volume-overload hypertrophy in the dog. *Circulation* 1998; 84: 1235-1245.
30. Lefkowitz RJ, Pitcher J, Krueger K, Daaka Y. Mechanisms of beta adrenergic receptor desensitization and resensitization. *Adv Pharmacol* 1998; 42:416-420.
31. Inglese J, Freedman NJ, Koch WJ, Lefkowitz RJ. Structure and mechanism of the G protein-coupled receptor kinases. *J Biol Chem* 1993; 268: 23735-23738.
32. Premont RT, Inglese J, Lefkowitz RJ. Protein kinases that phosphorylate activated G protein-coupled receptors. *FASEB J* 1995; 9:175-182.
33. Ferguson SS, Menard L, Barak LS, Koch WJ, Colapietro AM, Caron MG. Role of phosphorylation in agonist-promoted β 2-adrenergic receptor sequestration. Rescue of a sequestration-defective mutant receptor by b ARK1. *J Biol Chem* 1995; 270:24782-24789.

34. Ferguson SS, Downey WE, Colapietro AM, Barak LS, Menard L, Caron MG. Role of β -arrestin in mediating agonist-promoted G protein-coupled receptor internalization. *Science* 1996; 271:363-366.
35. Goodman OB Jr, Krupnick JG, Santini F, Gurevich VV, Penn RB, Gagnon AW, Keen JH, Benovic JL. β -arrestin acts as a clathrin adaptor in endocytosis of the β 2-adrenergic receptor. *Nature* 1996; 383:447-450.
36. Zhang J, Ferguson SG, Barak LS, Menard L, Caron MG. Dynamin and β -arrestin reveal distinct mechanisms for G protein-coupled receptor internalization. *J Biol Chem* 1996; 271:18302-18305.
37. South-Paul JE, Matheny SC, Lewis EL. *Current Diagnosis & Treatment in Family Medicine*. Published by McGraw-Hill Professional 2007.
38. Rusconi C. Diastolic heart failure- are treatment options available? *European cardiovascular disease* 2006.
39. Devereux RB, Dahlöf B, Gerdts E, Boman K, Nieminen MS, Papademetriou V, Rokkedal J, Harris KE, Edelman JM, Wachtell K. Regression of hypertensive left ventricular hypertrophy by losartan compared with atenolol: the Losartan Intervention for Endpoint Reduction in Hypertension (LIFE) trial. *Circulation* 2004;110:1456-1462.
40. Wong M, Staszewsky L, Latini R, Barlera S, Volpi A, Chiang YT, Benza RL, Gottlieb SO, Kleemann TD, Rosconi F, Vandervoort PM, Cohn JN. Heart Failure Trial Investigators. Valsartan benefits left ventricular structure and function in heart failure: Val-HeFT echocardiographic study. *J Am Coll Cardiol* 2002; 40:970-975.
41. Zile MR, Brutsaert DL. New Concepts in Diastolic Dysfunction and Diastolic Heart Failure: Part II: Causal Mechanisms and Treatment. *Circulation* 2002; 105:1503-1508.
42. Bassett AL, Chakko S, Epstein M. Are calcium antagonists proarrhythmic? *J Hypertens* 1997; 15:915-923.
43. Dubach P, Myers J, Bonetti P, Schertler T, Froelicher V, Wagner D, Scheidegger M, Stuber M, Luchinger R, Schwitzer J, Hess O. Effects of bisoprolol fumarate on left ventricular size, function, and exercise capacity in patients with heart failure: analysis with magnetic resonance myocardial tagging. *Am Heart J* 2002; 143:676-683.
44. Hall SA, Cigarroa CG, Marcoux L,RC, Grayburn PA, Eichhorn EJ. Time course of improvement in left ventricular function, mass and geometry in patients with congestive heart failure treated with beta-adrenergic blockade. *J Am Coll Cardiol* 1995; 25:1154-1161.
45. Lowes BD, Gill EA, Abraham WT, Larrain JR, Robertson AD, Bristow MR, Gilbert EM. Effects of carvedilol on left ventricular mass, chamber geometry, and mitral regurgitation in chronic heart failure. *Am J Cardiol* 1999; 83:1201-1205.
46. Waagstein F, Stromblad, Andersson B, Böhm M, Darius M, Delius W, Goss F, Osterziel KJ, Sigmund M, Trenkwalder SP, Wahlqvist I. Increased exercise ejection fraction and reversed remodeling after long-term treatment with metoprolol in congestive heart failure: a randomized, stratified, double-blind, placebo-controlled trial in mild to moderate heart failure due to ischemic or idiopathic dilated cardiomyopathy. *Eur J Heart Fail* 2003; 5:679-691.
47. Dobre D, Haaijer-Ruskamp FM, Voors AA, van Veldhuisen DJ. Beta. Adrenoceptor antagonists in elderly patients with heart failure: a critical review of their efficacy and tolerability. *Drugs Aging* 2007 24:1031-1044.

48. CIBIS Investigators and Committees. A randomized trial of beta-blockade in heart failure: the Cardiac Insufficiency Bisoprolol Study (CIBIS). *Circulation* 1994; 90:1765-1773.
49. CIBIS-II Investigators and Committees. The Cardiac Insufficiency Bisoprolol Study II (CIBIS-II). *Lancet* 1999; 353:9-13.
50. The International Steering Committee, MERIT-HF. Rationale, design, and organization of the Metoprolol CR/XL Randomized Intervention Trial in Heart Failure (MERIT-HF). *Am J Cardiol* 1997; 80: 54J-58J.
51. Cohn JN, Fowler MB, Bristow MR, Colucci WS, Gilbert EM, Kinhal V, Krueger SK, Lejemtel T, Narahara KA, Packer M, Young ST, Holcslaw TL, Lukas MA. Safety and efficacy of carvedilol in severe heart failure: the US Carvedilol Heart Failure Study Group. *J Card Fail* 1997; 3:173-179.
52. Packer M, Bristow MR, Cohn JN, Colucci WS, Fowler MB, Gilbert EM, Shusterman NH. The effect of carvedilol on morbidity and mortality in patients with chronic heart failure: US Carvedilol Heart Failure Study Group. *N Engl J Med* 1996; 334:1349-1355.
53. Goldstein S, Hjalmarson A. The mortality effect of metoprolol CR/XL in patients with heart failure: results of the MERIT-HF Trial. *Clin Cardiol* 1999; 22 (suppl 5):V30-V35.
54. MERIT-HF, Effect of metoprolol CR/XL in chronic heart failure: Metoprolol CR/XL Randomised Intervention Trial in Congestive Heart Failure (MERIT-HF). *Lancet* 1999; 353:2001–2007.
55. Reiken S, Wehrens XH, Vest JA, Barbone A, Klotz S, Mancini D, Burkhoff D, Marks AR. Beta-blockers restore calcium release channel function and improve cardiac muscle performance in human heart failure. *Circulation* 2003; 107:2459-2466.
56. Yano M, Kobayashi S, Kohno M, Doi M, Tokuhisa T, Okuda S, Suetsugu M, Hisaoka T, Obayashi M, Ohkusa T, Kohno M, Matsuzaki M. FKBP12.6-mediated stabilization of calcium-release channel (ryanodine receptor) as a novel therapeutic strategy against heart failure. *Circulation* 2003; 7:477-484.
57. Lowes BD, Gilbert EM, Abraham WT, Minobe WA, Larrabee P, Ferguson D, Wolfel EE, Lindenfeld J, Tsvetkova T, Robertson AD, Quaife RA, Bristow MR. Myocardial gene expression in dilated cardiomyopathy treated with beta-blocking agents. *N Engl J Med* 2002; 346:1357-1365.

Altered Sarcomeric Function in Cardiac Disease



2

Sarcomeric Dysfunction in Heart Failure

Nazha Hamdani, Viola Kooij, Sabine van Dijk, Daphne Merkus,
Walter J Paulus, Cris dos Remedios, Dirk J Duncker, Ger JM Stienen,
Jolanda van der Velden

Abstract

Sarcomeric dysfunction plays a central role in reduced cardiac pump function in heart failure. This review focuses on the alterations in sarcomeric proteins in diseased myocardium that range from altered isoform expression to post-translational protein changes such as proteolysis and phosphorylation. Recent studies in animal models of heart failure and human failing myocardium converge and indicate that sarcomeric dysfunction, including altered maximum force development, Ca^{2+} -sensitivity and increased passive stiffness, largely originates from altered protein phosphorylation, caused by neurohumoral-induced alterations in the kinase-phosphatase balance inside the cardiomyocytes. Novel therapies, which specifically target phosphorylation sites within sarcomeric proteins or the kinases and phosphatases involved, might improve cardiac function in heart failure.

Sarcomeric dysfunction

The failing heart is characterized by reduced contractility (systolic dysfunction) and/or impaired filling (diastolic dysfunction). A number of factors, including changes in cardiac structure (dilation and hypertrophy), apoptotic and necrotic cell death, maladaptive remodeling of the extracellular matrix, abnormal energy metabolism, impaired calcium handling and neurohumoral disturbances have been implicated in the initiation and progression of heart failure.¹⁻⁴ Recent studies revealed that alterations in sarcomeric function play a prominent role in reduced cardiac pump function.

Sarcomeric function is determined by the expression levels of multiple isoforms and by post-translational modifications of sarcomeric proteins. During muscle contraction a molecular interaction takes place between the thin (actin) and thick (myosin) filament of the sarcomeres, which is triggered by a rise in the intracellular calcium and is driven by the energy from ATP hydrolysis.⁵ The tropomyosin-troponin complex inhibits the actin-myosin interaction at low intracellular free calcium (Fig 1A). This inhibition is released when intracellular free calcium increases and binds to troponin C (Fig 1B). Alterations in sarcomeric protein composition under pathological conditions will influence contractile performance of the heart. Within the first part of this review we discuss the functional role of individual sarcomeric protein isoforms and of post-translational protein modifications such as proteolysis and phosphorylation. In the second part we highlight the major changes in sarcomeric function reported in failing myocardium and discuss the most likely underlying protein modifications.

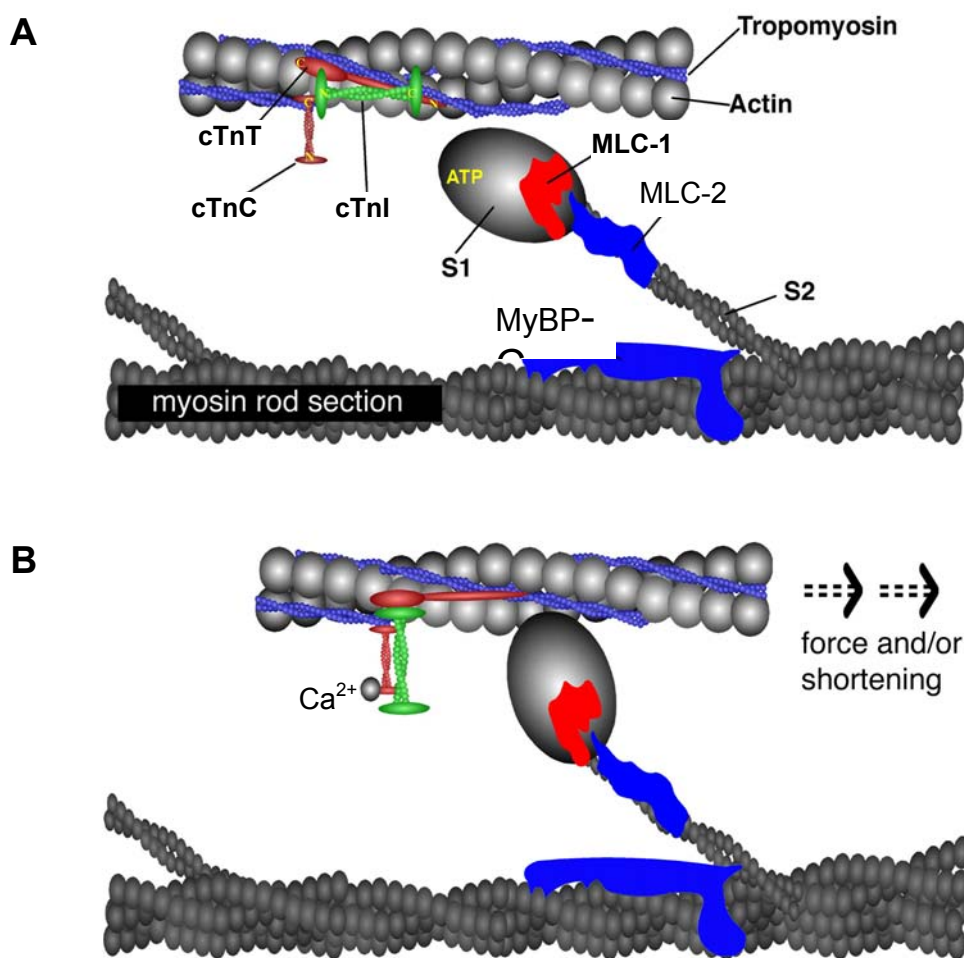


Figure 1. Schematic representation of the cardiac sarcomere during diastole (**A**) and systole (**B**). **A.** The thin filament is composed of actin, tropomyosin, and the troponin complex (composed of troponin T, cTnT; troponin C, cTnC; and troponin I, cTnI). The thick filament is composed of myosin, an asymmetric dimer composed of a globular head portion (S1), a hinged stalk region (S2) and a rod section. The S1 portion of myosin contains both the ATP hydrolysis domain and the actin-binding domain. Each myosin head is associated with a pair of myosin light chains, which consists of an essential light chain (MLC-1) and a regulatory light chain (MLC-2). MyBP-C, myosin binding protein C. **B.** Calcium binding to cTnC induces a conformational rearrangement in the troponin-tropomyosin complex. Movement of tropomyosin exposes a myosin-binding site on actin allowing cross-bridge formation to take place. This results in force development and/or shortening of the sarcomere (Modified from de Tombe, *J Biomech* 2003;36:721-730, with permission).

Isoform composition and sarcomeric dysfunction

Myosin heavy chains

The thick filament is composed of myosin, which consists of two myosin heavy chains (MHC), and two pairs of myosin light chains (MLC) (Fig 1). One of the major isoform changes which has been observed in hypertrophied and failing ventricular myocardium is the shift from the fast α -MHC to the slow β -MHC.⁶⁻⁸ The magnitude of the MHC shift largely depends on the amount of endogenous α -MHC present in ventricular tissue, which is species-dependent, being largest in small rodents and smallest in human.⁶⁻¹¹ Hence, the functional significance of the shift in MHC composition in diseased human ventricles is still a matter of debate.^{8,10,12}

The MHCs carry the site for ATP hydrolysis and are important determinants of the rate of energy consumption and the speed of contraction of the sarcomeres, which are closely related.¹³ In vitro studies have shown that the α -MHC isoform has a higher ATPase activity¹⁴ and a higher actin filament sliding velocity compared to the β -MHC isoform.¹⁵ From experiments in permeabilized cardiac preparations from small mammals and humans it followed that the β -MHC is 3-5 times more economical,^{11,16,17} but is associated with reduced power output¹⁸ and shortening velocity^{17,18} compared to the α -MHC isoform. Consequently, in rats a shift from α - to β -MHC coincided with significant reductions in ATPase activity,^{7,19} tension cost¹⁹ and power output.¹⁸ Evidence that a shift in MHC may be of pathophysiological relevance for human sarcomeric dysfunction was already provided in 1962 by Alpert and Gordon who reported reduced myofibrillar ATPase activity in human congestive heart failure.²⁰ However, subsequent human studies failed to unequivocally link this observation with a MHC isoform shift in failing ventricular myocardium. Firstly, no differences were found in functional properties of myosin isolated from non-failing and failing hearts,^{10,21,22} indicating that protein alterations other than a change in myosin composition are responsible for the reduction in myofilament ATPase activity.^{20,23} Moreover, various expression levels of α -MHC (ranging from 0 to 30%) have been reported in the ventricles of different individuals.^{8,10,12,24} This may be due to age-dependent changes in MHC composition and heterogeneous expression of MHC isoforms within the ventricular wall.^{25,26} Both in human²⁵ and rat²⁶ ventricular tissue, a regional difference in MHC expression has been observed, characterized by a higher expression of the fast α -MHC in the subepicardial than in the subendocardial layer, consistent with the shorter action potential and contraction duration in the subepi- as compared to the subendocardium. Thus, in human ventricular myocardium the

change in MHC isoform composition during heart failure will be variable and this may have obscured significant effects on sarcomeric function. However, recent studies have shown that even a small shift will have a significant impact on cardiomyocyte contractility.^{11,27} In contrast to ventricular human tissue, human atria contain ~80% of α -MHC.^{12,24} In atrial fibrillation the β -MHC expression increased almost two-fold, which coincided with a reduction in kinetics of force redevelopment.²⁸

Overall, the shift towards the slow and more economical β -MHC isoform occurs in human diseased atria and to a lesser extent in diseased human ventricular myocardium. The MHC shift may be beneficial under pathological conditions, since less energy is required to maintain cardiac pump function at rest, though at the expense of reduced speed of contraction and power output.

Myosin light chains

Apart from the shift in MHC, changes may occur in the expression pattern of myosin light chains within the heart. In particular, isoform changes have been reported for myosin light chain 1 (MLC-1, or essential MLC), both in atrial and ventricular tissue. MLC-1 not only interacts with MHC, but also binds to actin with its N-terminus. It exists in two forms, a ventricular (VLC-1) and an atrial (ALC-1) form.²⁹ The latter is expressed in the entire heart muscle during fetal and early life and is subsequently replaced by the ventricular form. In the ventricles of patients with hypertrophic obstructive cardiomyopathy relatively high amounts of ALC-1 were found, which correlated with the maximal rate of force development.³⁰ Apart from its positive effect on dynamics of contraction, replacement of VLC-1 by ALC-1 increased isometric force development of ventricular preparations at maximal and submaximal activation.²⁹ Morano et al. hypothesized that MLC-1 tethers MHC to actin and thereby restrains cross-bridge cycling and reduces force generation.³¹ As actin-binding affinity of ALC-1 is less than of VLC-1, improved cardiac function in ventricular tissue expressing ALC-1 may be explained by weakening of the interaction between actin and MLC-1. However, although up-regulation of ALC-1 may represent a compensatory mechanism to improve cardiac function, it is not a consistent protein alteration in ischemic and idiopathic cardiomyopathy, as large individual differences exist.^{29,30,32}

Alternatively, addition of the N-terminal region of MLC-1 may be used to promote sarcomeric function. Cardiac function may be enhanced by disruption of the actin-MLC-1 interaction by additional expression of N-terminal MLC-1 fragments, which competitively bind to actin.^{29,31} Another explanation for MLC-1 induced

increase in function was given by Rarick et al.³³ who reported increased myofibrillar MgATPase activity at submaximal $[Ca^{2+}]$ upon addition of an N-terminal VLC-1 fragment. These authors suggested that the MLC-1 N-terminal peptide directly affects protein interactions and exerts an inotropic effect via cooperative mechanisms, which activate the entire thin filament. Hence, the N-terminus of MLC-1 seems to exert a beneficial effect on sarcomeric function as increased systolic force generation and rates of contraction and relaxation were observed in hearts from transgenic rats harboring minigenes encoding the N-terminal domain of MLC-1.³⁴ Thus, although endogenous heterogeneous expression of MLCs may be of minor relevance in failing human myocardium, up-regulation of the MLC-1 N-terminal fragment might provide a therapeutic tool to enhance cardiac performance.

Troponin T

Anderson et al.³⁵ have proposed that re-expression of fetal troponin T (cTnT) may also contribute to the reduced ATPase activity in human heart failure. A significant inverse negative relationship was found between (re-)expression of fetal cTnT and myofibrillar ATPase activity in human ventricular tissue from normal and end-stage failing hearts. However, this observation has not been confirmed by others, and similar to the expression of α -MHC, the expression levels of fetal cTnT is variable among individuals.³⁶⁻³⁸ While Anderson et al.³⁵ observed re-expression of fetal cTnT in all end-stage failing human hearts, Solaro et al.³⁶ only observed this fetal cTnT isoform in one out of ten failing heart samples. Similarly, we have observed fetal cTnT in only one out of 24 patients with end-stage heart failure.³⁸ Mesnard-Rouiller et al.³⁷ found expression of fetal cTnT in half of the failing ventricles and suggested that re-expression of fetal cTnT isoforms is not a common characteristic of heart failure and most likely depends on other factors such as intensity and duration of the elevation of wall stress.

The consequences of fetal cTnT on sarcomeric contraction were studied upon exchange of endogenous cTnT with fetal cTnT in rat cardiomyocytes.³⁹ No differences were found in myofilament force development at maximal and submaximal Ca^{2+} concentrations at a sarcomere length of 2.2 μm between cardiomyocytes exchanged with troponin complex containing adult or fetal cTnT.³⁹ Akella et al.⁴⁰ observed a decrease in Ca^{2+} -responsiveness at low (1.9 μm), but not at high (2.4 μm) sarcomere length in skinned cardiac trabeculae from diabetic rats which coincided with alterations in cTnT composition. More recently, it was shown by Gomes et al.⁴¹ that fetal cTnT modulates Ca^{2+} -sensitivity in the presence of fetal

(skeletal) TnI. Hence, the effect of fetal cTnT on sarcomeric function seems to be dependent on sarcomere length and protein background in the heart.

In conclusion, most isoform changes might be an intrinsic part of the so-called “fetal” (hypertrophic) program yet their expression appears to be highly variable within human ventricular tissue. Minor shifts in MHC and MLC composition do not explain sarcomeric dysfunction in heart failure, but are of compensatory nature.

Proteolysis and sarcomeric dysfunction

Troponin I

There is ample evidence that proteolytic activity is enhanced after an acute ischemic insult. Degradation products of several sarcomeric proteins⁴²⁻⁴⁷ have been observed, which may subsequently induce sarcomeric dysfunction. One of the main proteins thought to be responsible for impaired cardiac function upon ischemia/reperfusion is cardiac troponin I (cTnI) (Fig 1).⁴²⁻⁴⁵ In rodents, McDonough et al.⁴⁴ showed that with moderate ischemia/reperfusion, cTnI is cleaved at its C-terminus, which results in a truncated cTnI product (cTnI₁₋₁₉₃, in human cTnI₁₋₁₉₂). More recently, it was postulated that degradation of cTnI might also impair cardiomyocyte function and contribute to reduced pump function in heart failure.⁴⁸ Myocardial infarction in pigs induced a reduction in the maximal force generating capacity of single permeabilized cardiomyocytes isolated from remodeled non-infarcted left ventricular tissue, in which minor degradation of cTnI (4%) was observed.⁴⁹ In addition, independent of ischemia, cTnI degradation has been demonstrated in human myocardium from coronary artery disease patients with different degrees of heart failure.^{45,50,51} To investigate if truncated cTnI may contribute to depressed cardiac pump function in human ischemic cardiomyopathy and heart failure, we recently investigated the direct functional effects of cTnI₁₋₁₉₂ in human cardiomyocytes. Force measurements were performed in non-failing human cardiomyocytes permeabilized with Triton-X 100 and exchanged with troponin complex containing either full length (cTnI_{FL}) or truncated cTnI.⁵² Surprisingly, truncated cTnI did not significantly alter maximal force development (Fig 2A). Likewise, passive force was not different between cells containing cTnI_{FL} and cTnI₁₋₁₉₂. However, myofilament Ca²⁺-sensitivity was significantly higher in cTnI₁₋₁₉₂ exchanged preparations compared to cTnI_{FL} cells (Fig 2B). This implicates that in humans truncation of cTnI may limit relaxation of the heart muscle, while systolic function would benefit from the increase in Ca²⁺-responsiveness of the myofilaments.

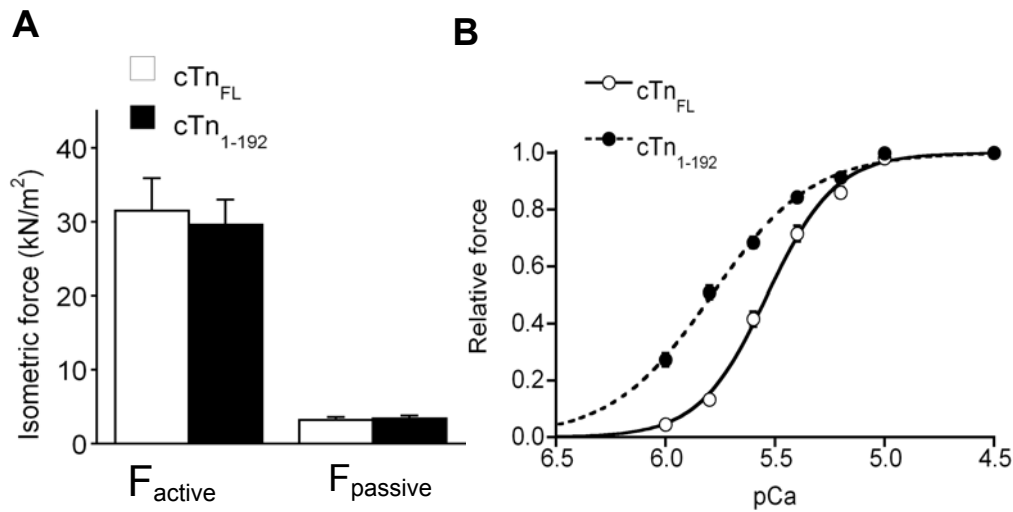


Figure 2. Isometric force was measured in single permeabilized human cardiomyocytes upon activation in solutions containing maximal (pCa 4.5) and submaximal Ca^{2+} concentrations (pCa 5 to 6) and in relaxing solution (pCa 9) to determine maximal (F_{max}) and passive (F_{pas}) force development (**A**) and Ca^{2+} -sensitivity of force development (**B**). Force at submaximal activation was normalized to the force obtained during maximal activation. **A.** The maximal force generating capacity (F_{max}) and F_{pas} did not differ between cardiomyocytes containing truncated cTnI (cTn₁₋₁₉₂) or full-length cTnI (cTn_{FL}). **B.** Ca^{2+} -sensitivity increased in cTn₁₋₁₉₂ cardiomyocytes compared to cTn_{FL} exchanged cells (From Narolska et al. *Circ Res* 2006;**99**:1012-1020: Figures printed with permission).

Role of protein phosphorylation in sarcomeric dysfunction

Protein kinase A-mediated phosphorylation

Not only truncation of cTnI, but also its phosphorylation status is a prominent determinant of sarcomeric function, both in health and disease. Upon β -adrenergic stimulation, protein kinase A (PKA)-mediated cTnI phosphorylation at serines 23/24 is associated with a decrease in myofilament Ca^{2+} -sensitivity^{32,53,54} and contributes to an acceleration of cardiac relaxation.^{55,56} Since β -adrenergic signaling is reduced in heart failure due to down-regulation and desensitization of β -adrenoceptors,⁵⁷⁻⁵⁹ PKA-mediated cTnI phosphorylation might be less pronounced in failing myocardium. In agreement with reduced β -adrenergic signaling, reduced phosphorylation levels of cTnI have been reported in failing human myocardium compared to non-failing donor hearts.⁶⁰⁻⁶² More specifically, phosphorylation at PKA sites 23/24 was significantly reduced in end-stage failing compared to donor human myocardium.^{61,62} At the functional level, reduced PKA-mediated cTnI phosphorylation would result in an increase in Ca^{2+} -sensitivity of the myofilaments, as was observed in single

permeabilized human cardiomyocytes isolated from end-stage failing hearts.^{32,54,61,63}

In comparison to cells from non-failing donor myocardium, Ca^{2+} -sensitivity was significantly higher in cardiomyocytes from patients with idiopathic or ischemic cardiomyopathy (Fig 3A). This sarcomeric defect was normalized upon treatment of cardiomyocytes with the catalytic subunit of PKA (Fig 3B), as the reduction in pCa_{50} was larger in cardiomyocytes from failing compared to donor hearts.³² Recently, Messer et al.⁶² have shown that altered cTnI phosphorylation most likely underlies the increased Ca^{2+} -responsiveness as isolated thin filaments from failing human hearts displayed higher Ca^{2+} -responsiveness compared to filaments from donor myocardium in an in vitro motility assay. One should be careful when using non-failing donor myocardium as “normal”, because of the high blood catecholamine levels at the time of tissue procurement. The high level of cTnI phosphorylation and relatively small effect of PKA on myofilament Ca^{2+} -responsiveness might reflect overstimulation of the β -adrenergic pathway in donors and thereby augment the difference between healthy and failing samples. However, a similar increase in myofilament Ca^{2+} -responsiveness has been observed in several animal models of heart failure.^{49,64-66}

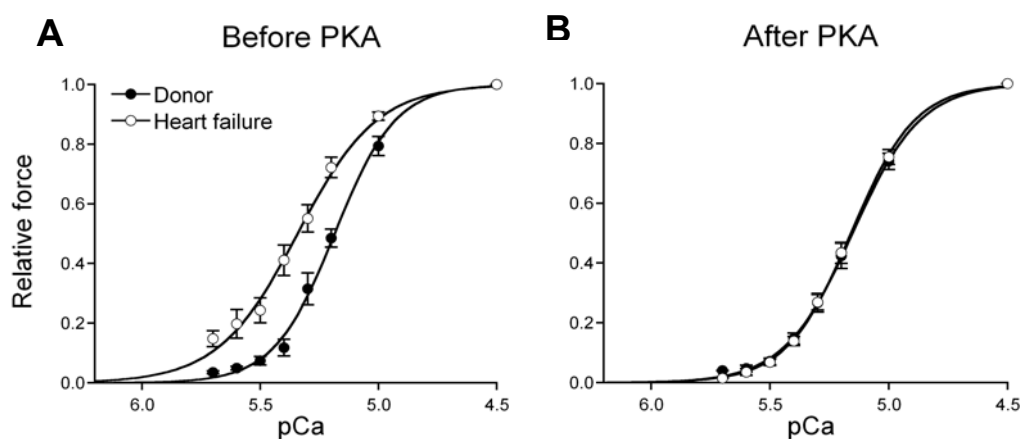


Figure 3. **A.** Ca^{2+} -sensitivity was significantly higher in cardiomyocytes isolated from end-stage failing ($n=10$) compared to donor ($n=6$) hearts. **B.** Incubation of cells with the catalytic subunit of PKA reduced pCa_{50} (ΔpCa_{50} : 0.20 ± 0.01 and 0.03 ± 0.01 in failing and donor cells, respectively) and abolished the difference between both groups (Modified from van der Velden et al. *Cardiovasc Res* 2003;**57**:37-47, with permission).

To minimize variable receptor stimulation at the time of biopsy procurement, we recently conducted a series of experiments on single cardiomyocytes from pigs with a myocardial infarction or sham-operated animals isolated from transmural

needle biopsies, which were instantly frozen in liquid nitrogen. Biopsies were taken from remote left ventricular tissue 3 weeks after myocardial infarction induced by ligation of the left circumflex coronary artery or from sham-operated animals. Consistent with previous observations (Fig 4),⁴⁹ Ca^{2+} -responsiveness was significantly higher in cells from infarct compared to sham animals, while the shift upon PKA was smaller in sham than in post-infarct remodeled myocardium (unpublished data). These data clearly show that alterations in β -adrenergic signaling and the concomitant reduction in PKA-mediated cTnI phosphorylation impair sarcomeric function. The increased Ca^{2+} -sensitivity of the myofilaments might contribute to diastolic dysfunction via impaired relaxation of failing myocardium.

Protein kinase C and D

Apart from the β -adrenergic pathway, other signaling routes might be involved in the alterations in phosphorylation and function of sarcomeric proteins in heart failure. Noteworthy, overall phosphorylation status of cTnI, determined on ProQ Diamond stained gels,⁶⁷ did not significantly differ between sham-operated and MI pigs (unpublished data), while the shift in Ca^{2+} -sensitivity upon PKA treatment was larger in infarct compared to sham animals (Fig 4B). This implies that, whereas PKA-mediated cTnI phosphorylation is down-regulated in infarct animals, cTnI phosphorylation by other kinases should be increased. One of the most likely candidates is protein kinase C (PKC). Its activity and expression levels are increased in heart failure^{66,68-71} and both cTnI and cTnT contain specific PKC phosphorylatable sites (i.e. serine 43/45 and threonine 144 in cTnI and serine 201 and threonine 197/206/287 in cTnT).⁷²⁻⁷⁴ In addition to PKC, an increase in protein kinase D (PKD) has been reported in heart failure.⁷⁵ PKD can be activated upon phosphorylation by PKC, and thus may act down-stream of PKC, or it also may be directly activated upon receptor stimulation by e.g. endothelin 1.⁷⁶ It has been shown that PKD is able to reduce myofilament Ca^{2+} -sensitivity via phosphorylation of PKA-sites (serine 23/24) in cTnI.⁷⁷ Consequently, the regulatory window of PKC and PKD in sarcomeric function might be widened in diseased myocardium.

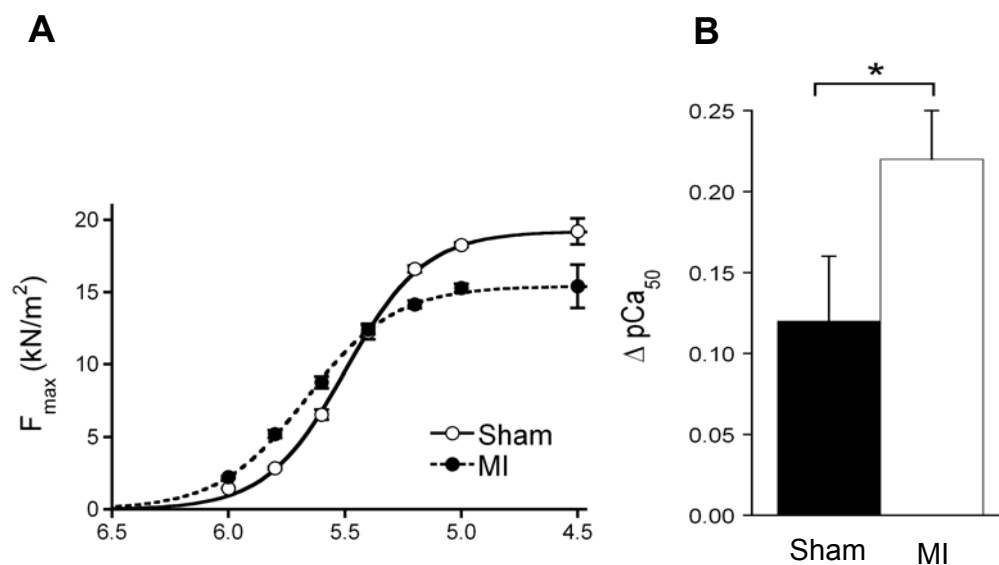


Figure 4. Isometric force measurements were performed in single Triton-permeabilized cardiomyocytes isolated from remote left ventricular tissue from pigs three weeks after myocardial infarction (MI). Maximal force development (F_{\max}) was significantly lower in MI compared to sham-operated animals (**A**). Similar to the observations in human heart failure, Ca^{2+} -sensitivity was significantly higher (**A**) and the PKA-mediated reduction in Ca^{2+} -sensitivity was larger (**B**) in cells from MI compared to sham animals (Modified from van der Velden et al. *Circ Res* 2004;**95**:e85-e95, with permission).

The functional consequences of PKC-mediated protein phosphorylation have been investigated in rodent models and indicated a central role for cTnI and cTnT in reducing maximal myofilament force development.^{73,74,78} Apart from its effect on maximal force, PKC has been shown to reduce myofilament Ca^{2+} -sensitivity in rodent and human myocardium.^{61,71,73,74,78} The possible involvement of PKC-mediated protein phosphorylation in sarcomeric function in failing myocardium was shown recently in rat models of end-stage heart failure resulting from chronic pressure overload (aortic banding) and myocardial infarction.⁷¹ In both models increased expression and activation of PKC α were observed in the late, but not in the early phase of heart failure. Maximal force generating capacity and Ca^{2+} -sensitivity of permeabilized cardiomyocytes were significantly reduced in end-stage failing animals compared to age-matched controls,^{71,79} and both parameters increased upon treatment with protein phosphatase 1 (PP-1). In contrast, PKC α did not significantly alter cardiomyocyte function of failing cardiomyocytes, while it reduced both maximal force and its Ca^{2+} -sensitivity in cells from the control group. In a previous study, the same group performed experiments where in failing cardiomyocytes the endogenous Tn-complex was exchanged by unphosphorylated troponin complex, while control

cells were exchanged with troponin complex extracted from failing hearts.⁷⁹ Upon exchange, Ca²⁺-sensitivity of failing cardiomyocytes was restored towards the value observed in controls, while failing troponin complex induced a significant reduction in Ca²⁺-sensitivity in control cells. However, troponin exchange did not affect maximal tension, indicating that PKC-mediated phosphorylation of troponin is not involved in the reduced force generating capacity. Overall, the data confirm that altered myofilament Ca²⁺-sensitivity can be attributed to altered troponin phosphorylation, while changes in maximal force generating capacity most likely rely on the permissive action of other sarcomeric proteins.

Whether PKC- and PKD-mediated phosphorylation and a concurrent reduction in Ca²⁺-responsiveness is detrimental for cardiac function or represents an alternative mechanism to preserve positive lusitropy during exercise and compensates for reduced PKA-mediated cardiac relaxation requires further investigation.

Sarcomeric dysfunction in heart failure

Increased versus decreased Ca²⁺-sensitivity

Opposite to the increased myofilament Ca²⁺-sensitivity observed in human end-stage failing myocardium (Fig 2)^{32,54,61,63} and in several animal models of cardiac disease (Fig 3)^{49,64-66}, a decrease in myofilament Ca²⁺-sensitivity was reported in rodent models of heart failure resulting from chronic pressure overload (aortic banding) and myocardial infarction.^{71,79} One possible explanation for these contrasting observations might be the level of neurohumoral stimulation present at the time of tissue procurement. An intricate balance exists between kinase and phosphatase activities within the cardiomyocyte as was shown recently by Braz et al.⁶⁸ They reported that both PKA and PKC may alter phosphorylation status of proteins *indirectly* via phosphorylation of protein phosphatase inhibitor-1 (I-1). Opposite to PKA, which suppresses PP-1 activity,⁸⁰ PKC enhances PP-1 activity via phosphorylation of I-1. This illustrates the delicate balance between kinases and phosphatases within a cell. An increase in PKC and a decrease in PKA-mediated phosphorylation of I-1 would enhance PP-1 activity⁸¹ and thereby induce hypophosphorylation of sarcomeric proteins.

Apart from differences in neurohumoral status when tissue is retrieved from the heart, diverse alterations in the signaling pathways known to alter sarcomeric protein phosphorylation upon neurohumoral stimulation most likely underlie diverse functional properties of the sarcomeres. Already in 1991 Bristow et al.⁸² have shown

different alterations in the β -adrenergic pathway in hearts with ischemic heart disease (ISHD) and idiopathic cardiomyopathy (IDCM). Analysis of sarcomeric protein phosphorylation on ProQ Diamond stained gradient gels (Fig 5A)⁶⁷ revealed significant differences between left ventricular myocardial tissue from end-stage failing patients with IDCM and ISHD (Fig 5B). Phosphorylation of cTnI was significantly higher in non-failing donor compared to end-stage failing myocardium. In addition, myosin binding protein C, which is phosphorylated upon β -adrenergic stimulation is lower in failing compared to donor hearts.^{67,83} Noteworthy, MLC-2 phosphorylation was significantly higher in ISHD compared to donor and IDCM myocardium, and statistical analysis revealed significant different phosphorylation of cTnI between ISHD and IDCM samples. In line with a higher level of cTnI phosphorylation in ISHD samples, myofilament Ca^{2+} -sensitivity was significantly lower in ISHD compared to IDCM myocardium.^{32,54} These data provide evidence that diverse alterations in sarcomeric protein composition and function in failing hearts are related to underlying cause or phenotype.

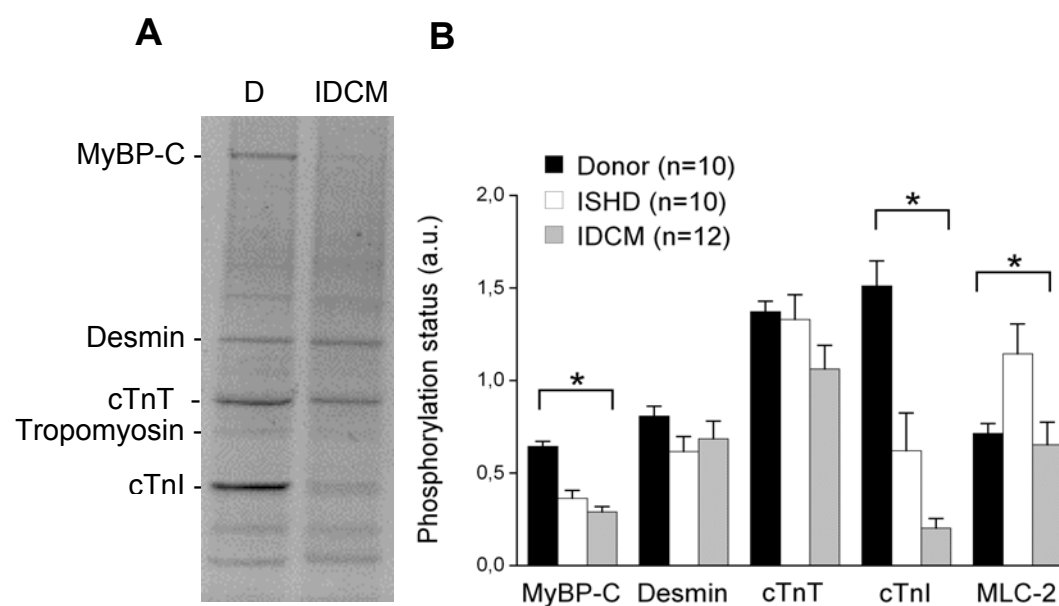


Figure 5. A. Human heart samples (D, donor and IDCM, idiopathic dilated cardiomyopathy; 20 $\mu\text{g}/\text{lane}$) separated on 4-15% gradient gels. Phosphorylation of myosin binding protein C (MyBP-C), desmin, troponin T (cTnT), troponin I (cTnI) and myosin light chain 2 (MLC-2) was determined with Pro-Q Diamond stain. **B.** Bar graph to illustrate differences in sarcomeric protein phosphorylation between human donor hearts and failing myocardium (ISHD, ischemic heart failure). * $P < 0.05$ in one-way ANOVA. n = number of hearts.

Reduction in maximal force generating capacity

Reduced maximal force has been observed in diverse models of cardiomyopathy (Fig

4A).^{49,65,79,84} In rat with pressure-overload and infarction-induced cardiomyopathy, the reduction in F_{\max} amounted to 35% and 42%, respectively.⁷⁹ As reduced F_{\max} was only partly reversed by PP-1 (15%),⁷¹ and as described above, may not directly involve the troponin complex,⁷⁹ alternative signaling routes and other sarcomeric proteins may be of relevance. Moreover, depressed cardiomyocyte force development was also observed in enzymatically isolated preparations from failing rat hearts,⁸⁴ in which the isolation procedure most likely reduced phosphorylation status of most sarcomeric proteins. Therefore, part of the reduction in maximal force might at least in part be related to altered isoform composition and/or proteolysis of sarcomeric proteins. A recent study in transgenic mice by Vahebi et al.⁸⁵ in which p38 MAPK (mitogen activated protein kinase) was constitutively active in the heart revealed a possible role for tropomyosin dephosphorylation in the depression of maximal force of the sarcomeres. Activation of p38 MAPK, as occurs in pressure overload-induced hypertrophy, has been shown to exert a negative effect on cardiomyocyte contractility without altering Ca^{2+} -handling.⁸⁶ The study in transgenic mice⁸⁵ indicated that apart from its role in remodeling and apoptosis, activated p38 MAPK leads to sarcomeric dysfunction, possibly via activation of phosphatases and a subsequent dephosphorylation of tropomyosin. The level of tropomyosin phosphorylation appears to be species-dependent, being relatively high in mice⁸⁵ and lower in human myocardium (Fig 5A). However, similar to isoform changes in MHC, small changes in phosphorylation may exert a significant effect on sarcomeric function. Therefore, the (patho)physiological role of tropomyosin phosphorylation for sarcomeric function requires further investigation.

In conclusion, depressed force development cannot be explained by a single protein alteration, though seems to be the result of complex interactions between various sarcomeric proteins.

Increased cardiomyocyte stiffening

Subtle, though functionally important changes in protein phosphorylation, induced by kinases and phosphatases other than PKA, may have been obscured in failing human myocardium in comparison to donor hearts. Separation of patients with heart failure into subgroups, based on severity, cause or phenotype, represents a powerful approach to reveal the causes and functional implications of alterations in sarcomeric function in human heart failure. Comparison of patients with diastolic (DHF) and systolic heart failure (SHF) revealed an increased passive force development in cardiomyocytes from DHF compared to SHF patients (Fig 6).⁸⁷ A significant positive

correlation was present between in vivo left ventricular end-diastolic pressure (LVEDP) and F_{passive} ,⁸⁸ indicating that cardiomyocyte stiffening contributes to high filling pressures in DHF. Increased cardiomyocyte passive force was corrected to values observed in hearts with preserved ejection fraction and normal LVEDP⁸⁸ upon incubation with PKA (Fig 6), indicative for hypophosphorylation of sarcomeric proteins. The hypophosphorylated sarcomeric protein, possibly titin,^{89,90} could be a specific myocardial target for drug therapy to lower LVEDP in DHF.

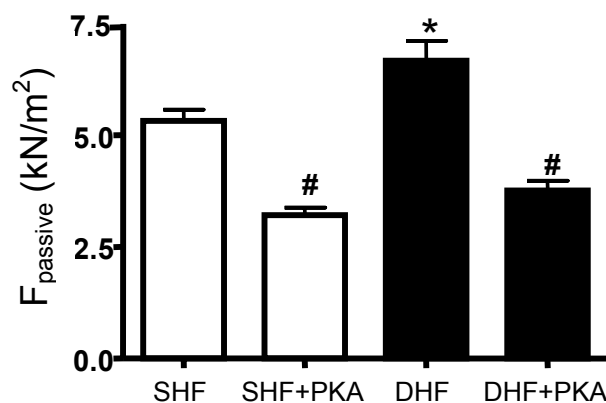


Figure 6. Cardiomyocyte stiffening in human heart failure. Cardiomyocyte passive force (F_{passive}) was significantly higher in DHF than in SHF (* $P < 0.05$). PKA treatment reduced F_{pas} in SHF and DHF (# $P < 0.05$ in paired t-test) (From van Heerebeek et al. *Circulation* 2006;113:1966-1973, with permission).

Future perspectives

The question if depressed cardiomyocyte contractility is involved in heart failure has been positively answered. Overall, there seems to be general consensus that sarcomeric dysfunction in heart failure results from altered protein phosphorylation, which is the result of complex changes in kinase and phosphatase expression and activity. The balance between kinases and phosphatases in the cardiomyocyte are humoral and heart rate-dependent and as a consequence the activities of kinases and phosphatases vary in time. Apart from temporal changes, spatial changes occur, as complex interactions have been shown between kinases and phosphatases regulating calcium homeostasis within cardiomyocytes.^{91,92} Such complex signaling may also apply to the myofilaments. Moreover, within the complex pattern of sarcomeric protein phosphorylation each protein and its phosphorylation status influences the behaviour of other sarcomeric proteins.^{93,94} As sarcomeric function most likely reflects differences in phosphorylation status and depend on the neurohumoral status and heart rate at the time of tissue procurement, investigation of

the functional properties of the sarcomeres should be performed in cardiac tissue, which is obtained under standardized conditions. The use of catheter biopsies has proven to be a major leap forward in unraveling sarcomeric dysfunction in human myocardium.^{87,88} Linkage of in vivo hemodynamic data with cardiomyocyte force measurements revealed that stiffening of the sarcomeres contributes to impaired filling of the heart in DHF patients.⁸⁸ To obtain insight in dynamic signaling cardiac samples could be retrieved upon receptor stimulation.⁶⁷ This approach allows determination of the direct relation between functional, structural and protein characteristics at the cellular level with in vivo hemodynamics measured at the time of tissue harvesting.

The sarcomeric proteome will be even more complex than described in the present review, since other signaling routes, apart from the β -adrenergic pathway, may be triggered under pathological conditions and affect sarcomeric function.^{68,75,76,86,95,96} Only recently, Yuan et al.⁹⁷ discovered novel phosphorylation sites within the N-terminus of MyBP-C, which were differentially phosphorylated upon stunning in canine and rat myocardium. Apart from phosphorylation, post-translational modifications resulting from oxidative stress might impair sarcomeric function. Moreover, mutant sarcomeric proteins as found in inherited cardiomyopathies^{98,99} further complicate analysis of causality between protein alterations and function of the sarcomere. Over the past years knowledge on mutated sarcomeric proteins present in cardiomyopathies increased swiftly. However the exact consequences of these mutations on cardiomyocyte function in human cardiac tissue are still unclear and knowledge concerning additional (mal)adaptive changes in sarcomeric proteins is scarce. Hence, it remains to be elucidated if and to what extent altered sarcomeric protein expression and/or posttranslational changes impair sarcomeric function in inherited cardiomyopathies.

The combination of sarcomeric force measurements with proteomic analysis (i.e. functional proteomics) will reveal (novel) post-translational modifications involved in cardiomyocyte dysfunction in heart failure. The use of transgenic animal models and protein exchange experiments in cardiac preparations are required to define the specific role of post-translational protein modifications and mutant sarcomeric proteins in cardiac function.

Clinical implications

The recently obtained data in human myocardium (Fig 5 and 6) indicate that divergent disturbance of receptor-signaling cascades depend on underlying cause

and phenotype. Diverse alterations in signaling pathways might alter the responsiveness of patients to drug therapy and therefore the current strategy of treating heart failure should be re-evaluated. Large randomized, double-blind, placebo-controlled multicenter trials have shown that treatment of heart failure patients (classified according to the New York Heart Association into class II-IV) with neurohumoral receptor blockers, such as ACE-inhibitors and beta-blockers, reduces both morbidity and mortality. However, it remains to be investigated if and to what extent reversal of sarcomeric dysfunction contributes to the beneficial effects of beta-blocker and ACE-inhibitor therapy in different patient groups.

Interestingly, exercise in mice with a myocardial infarction reversed depressed sarcomeric function to values observed in controls.⁶⁵ The beneficial effects appeared to be the result of improved β -adrenergic signaling. Future studies should investigate if the combination of currently used neurohumoral blockers with exercise yield added benefit.

Novel therapy may include drugs targeted to mediators down-stream of the adrenergic and angiotensin receptors. Cardiac performance may be improved by targeting a specific myofilament protein^{34,100} to directly modulate sarcomeric function. Further exploration of the complex signaling routes underlying defects in sarcomeric function is required in order to develop more precise, individualized therapy in heart failure patients.

References

1. De Tombe PP. Altered contractile function in heart failure. *Cardiovasc Res* 1998;37:367-380.
2. Houser SR, Margulies KB. Is depressed myocyte contractility centrally involved in heart failure? *Circ Res* 2003;92:350-358.
3. Nakayama H, Chen X, Baines CP, Klevitsky R, Zhang X, Zhang H et al. Ca^{2+} - and mitochondrial-dependent cardiomyocyte necrosis as a primary mediator of heart failure. *J Clin Invest* 2007;117:2431-2444.
4. Jane-Lise S, Corda S, Chassagne C, Rappaport L. The extracellular matrix and the cytoskeleton in heart hypertrophy and failure. *Heart Fail Rev* 2000;5:239-250.
5. De Tombe PP. Cardiac myofilaments: mechanics and regulation. *J Biomech* 2003;36:721-730.
6. Lompre AM, Schwartz K, d'Albis A, Lacombe G, Van Thiem N, Swynghedauw B. Myosin isoenzyme redistribution in chronic heart overload. *Nature* 1979;282:105-107.
7. Mercadier JJ, Lompre AM, Wisnewsky C, Samuel JL, Bercovici J, Swynghedauw B, Schwartz K. Myosin isoenzyme changes in several models of rat cardiac hypertrophy. *Circ Res* 1981;49:525-532.
8. Miyata S, Minobe W, Bristow MR, Leinwand LA. Myosin heavy chain isoform expression in the failing and nonfailing human heart. *Circ Res* 2000;86:386-390.
9. Lompre AM, Mercadier JJ, Wisnewsky C, Bouveret P, Pantaloni C, d'Albis A, Schwartz K. Species- and age-dependent changes in the relative amounts of cardiac myosin isoenzymes in mammals. *Develop Biol* 1981;84:286-290.
10. Mercadier JJ, Bouveret P, Gorza L, Schiaffino S, Clark WA, Zak R, Swynghedauw B, Schwartz K. Myosin isoenzymes in normal and hypertrophied human ventricular myocardium. *Circ Res* 1983;53:52-62.
11. Narolska NA, van Loon RB, Boontje NM, Zaremba R, Penas SE, Russell J, Spiegelberg SR, Huybregts MA, Visser FC, de Jong JW, van der Velden J and Stienen GJM. Myocardial contraction is 5-fold more economical in ventricular than in atrial human tissue. *Cardiovasc Res* 2005;65:221-229.
12. Narolska NA, Eiras S, van Loon RB, Boontje NM, Zaremba R, Spiegelberg SR, Spiegelberg SR, Huybregts MA, Visser FC, de Jong JW, van der Velden J and Stienen GJM. Myosin heavy chain composition and the economy of contraction in healthy and diseased human myocardium. *J Muscle Res Cell Motil* 2005;26:39-48.
13. Barany M. ATPase activity of myosin correlated with speed of muscle shortening. *J Gen Physiol* 1967;50:Suppl:197-218.
14. Pope B, Hoh JF, Weeds A. The ATPase activities of rat cardiac myosin isoenzymes. *FEBS Lett* 1980;118:205-208.
15. Harris DE, Work SS, Wright RK, Alpert NR, Warshaw DM. Smooth, cardiac and skeletal muscle myosin force and motion generation assessed by cross-bridge mechanical interactions in vitro. *J Muscle Res Cell Motil* 1994;15:11-19.
16. Van der Velden J, Moorman AF, Stienen GJM. Age-dependent changes in myosin composition correlate with enhanced economy of contraction in guinea-pig hearts. *J Physiol* 1998;507:497-510.

17. Rundell VL, Manaves V, Martin AF, de Tombe PP. Impact of beta-myosin heavy chain isoform expression on cross-bridge cycling kinetics. *Am J Physiol Heart Circ Physiol* 2005;288:H896-H903.
18. Korte FS, Herron TJ, Rovetto MJ, McDonald KS. Power output is linearly related to MyHC content in rat skinned myocytes and isolated working hearts. *Am J Physiol Heart Circ Physiol* 2005;289:H801-H812.
19. Rundell VL, Geenen DL, Buttrick PM, de Tombe PP. Depressed cardiac tension cost in experimental diabetes is due to altered myosin heavy chain isoform expression. *Am J Physiol Heart Circ Physiol* 2004;287:H408-H413.
20. Alpert NR, Gordon MS. Myofibrillar adenosine triphosphatase activity in congestive heart failure. *Am J Physiol* 1962;202:940-946.
21. Nguyen TT, Hayes E, Mulieri LA, Leavitt BJ, ter Keurs HE, Alpert NR, Warshaw DM. Maximal actomyosin ATPase activity and in vitro myosin motility are unaltered in human mitral regurgitation heart failure. *Circ Res* 1996;79:222-226.
22. Noguchi T, Camp P Jr, Alix SL, Gorga JA, Begin KJ, Leavitt BJ, Vanburen P. Myosin from failing and non-failing human ventricles exhibit similar contractile properties. *J Mol Cell Cardiol* 2003;35:91-97.
23. Pagani ED, Alousi AA, Grant AM, Older TM, Dziuban SW Jr, Allen PD. Changes in myofibrillar content and Mg-ATPase activity in ventricular tissues from patients with heart failure caused by coronary artery disease, cardiomyopathy, or mitral valve insufficiency. *Circ Res* 1988;63:380-385.
24. Reiser PJ, Portman MA, Ning XH, Schomisch Moravec C. Human cardiac myosin heavy chain isoforms in fetal and failing adult atria and ventricles. *Am J Physiol Heart Circ Physiol* 2001;280:H1814-H1820.
25. Kuro-o M, Tsuchimochi H, Ueda S, Takaku F, Yazaki Y. Distribution of cardiac myosin isozymes in human conduction system. Immunohistochemical study using monoclonal antibodies. *J Clin Invest* 1986;77:340-347.
26. Carnes CA, Geisbuhler TP, Reiser PJ. Age-dependent changes in contraction and regional myocardial myosin heavy chain isoform expression in rats. *J Appl Physiol* 2004;97:446-453.
27. Herron TJ, McDonald KS. Small amounts of alpha-myosin heavy chain isoform expression significantly increase power output of rat cardiac myocyte fragments. *Circ Res* 2002;90:1150-1152.
28. Eiras S, Narolska NA, van Loon RB, Boontje NM, Zaremba R, Jimenez CR, Visser FCW, Stoker W, van der Velden J, Stienen GJM. Alterations in contractile protein composition and function in human atrial dilatation and atrial fibrillation. *J Mol Cell Cardiol* 2006;41:467-477.
29. Morano I. Tuning the human heart molecular motors by myosin light chains. *J Mol Med* 1999;77:544-555.
30. Ritter O, Luther HP, Haase H, Baltas LG, Baumann G, Schulte HD, Morano I. Expression of atrial myosin light chains but not alpha-myosin heavy chains is correlated in vivo with increased ventricular function in patients with hypertrophic obstructive cardiomyopathy. *J Mol Med* 1999;77:677-685.
31. Morano I, Ritter O, Bonz A, Timek T, Vahl CF, Michel G. Myosin light chain-actin interaction regulates cardiac contractility. *Circ Res* 1995;76:720-725.

32. Van der Velden J, Papp Z, Zaremba R, Boontje NM, de Jong JW, Owen VJ, Burton PB, Goldmann P, Jaquet K, Stienen GJ. Increased Ca^{2+} -sensitivity of the contractile apparatus in end-stage human heart failure results from altered phosphorylation of contractile proteins. *Cardiovasc Res* 2003;57:37-47.
33. Rarick HM, Opgenorth TJ, von Geldern TW, Wu-Wong JR, Solaro RJ. An essential myosin light chain peptide induces supramaximal stimulation of cardiac myofibrillar ATPase activity. *J Biol Chem* 1996;271:27039-27043.
34. Haase H, Dobbernack G, Tunnemann G, Karczewski P, Cardoso C, Petzhold D, Schlegel WP, Lutter S, Pierschalek P, Behlke J, Morano I. Minigenes encoding N-terminal domains of human cardiac myosin light chain-1 improve heart function of transgenic rats. *FASEB J* 2006;20:865-873.
35. Anderson PA, Malouf NN, Oakeley AE, Pagani ED, Allen PD. Troponin T isoform expression in the normal and failing human left ventricle: a correlation with myofibrillar ATPase activity. *Basic Res Cardiol* 1992;87:Suppl 1:117-127.
36. Solaro RJ, Powers FM, Gao L, Gwathmey JK. Control of myofilament activation in heart failure. *Circulation* 1993;87:Suppl VII:VII38-VII43.
37. Mesnard-Rouiller L, Mercadier JJ, Butler-Browne G, Heimbürger M, Logeart D, Allen PD, Samson F. Troponin T mRNA and protein isoforms in the human left ventricle: Pattern of expression in failing and control hearts. *J Mol Cell Cardiol* 1997;29:3043-3055.
38. Van der Velden J, Klein LJ, van der Bijl M, Huybregts MA, Stooker W, Witkop J, Eijnsman L, Visser CA, Visser FC, Stienen GJ. Isometric tension development and its calcium sensitivity in skinned myocyte-sized preparations from different regions of the human heart. *Cardiovasc Res* 1999;42:706-719.
39. Van der Velden J, Chandra M, Stienen GJM, Solaro RJ, de Tombe PP. Exchange of troponin T in single cardiomyocytes from rat. *J Muscle Res Cell Motil* 2000;21:803 (Abstract).
40. Akella AB, Ding XL, Cheng R, Gulati J. Diminished Ca^{2+} sensitivity of skinned cardiac muscle contractility coincident with troponin T-band shifts in the diabetic rat. *Circ Res* 1995;76:600-606.
41. Gomes AV, Venkatraman G, Davis JP, Tikunova SB, Engel P, Solaro RJ, Potter JD. Cardiac troponin T isoforms affect the Ca^{2+} sensitivity of force development in the presence of slow skeletal troponin I: insights into the role of troponin T isoforms in the fetal heart. *J Biol Chem* 2004;279:49579-49587.
42. Gao WD, Atar D, Liu Y, Perez NG, Murphy AM, Marban E. Role of troponin I proteolysis in the pathogenesis of stunned myocardium. *Circ Res* 1997;80:393-399.
43. Van Eyk JE, Powers F, Law W, Larue C, Hodges RS, Solaro RJ. Breakdown and release of myofilament proteins during ischemia and ischemia/reperfusion in rat hearts: identification of degradation products and effects on the pCa-force relation. *Circ Res* 1998;82:261-271.
44. McDonough JL, Arrell DK, Van Eyk JE. Troponin I degradation and covalent complex formation accompanies myocardial ischemia/reperfusion injury. *Circ Res* 1999;84:9-20.
45. Murphy AM, Kogler H, Georgakopoulos D, McDonough JL, Kass DA, Van Eyk JE, Marbán E. Transgenic mouse model of stunned myocardium. *Science* 2000;287:488-491.

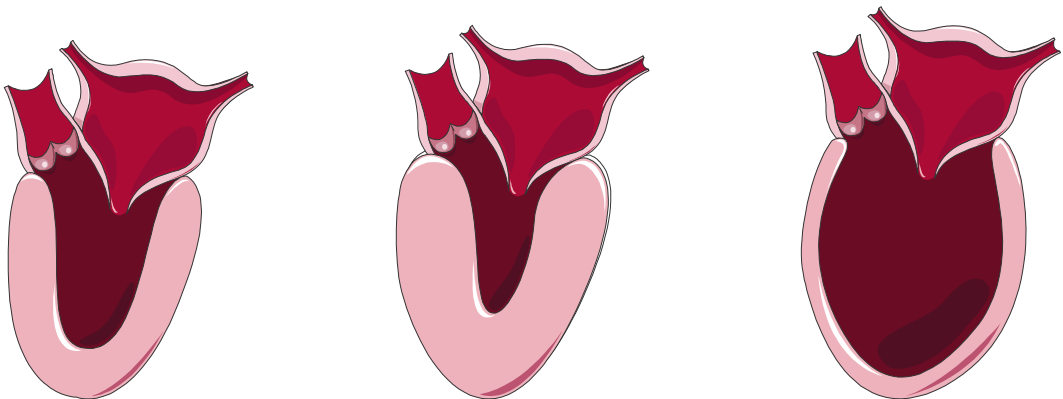
46. Papp Z, van der Velden J, Stienen GJM. Calpain-I induced alterations in the cytoskeletal structure and impaired mechanical properties of single myocytes of rat heart. *Cardiovasc Res* 2000;45:981-993.
47. Decker RS, Decker ML, Kulikovskaya I, Nakamura S, Lee DC, Harris K, Klocke FJ, Winegrad S. Myosin-binding protein C phosphorylation, myofibril structure, and contractile function during low-flow ischemia. *Circulation* 2005;111:906-912.
48. Van der Laarse A. Hypothesis: troponin degradation is one of the factors responsible for deterioration of left ventricular function in heart failure. *Cardiovasc Res* 2002;56:8-14.
49. Van der Velden J, Merkus D, Klarenbeek BR, James AT, Boontje NM, Dekkers DH, Stienen GJM, Lamers JMJ, Duncker DJ. Alterations in myofilament function contribute to left ventricular dysfunction in pigs early after myocardial infarction. *Circ Res* 2004;95:e85-e95.
50. McDonough JL, Labugger R, Pickett W, Tse MY, MacKenzie S, Pang SC, Atar D, G. Ropchan, Van Eyk JE. Cardiac troponin I is modified in the myocardium of bypass patients. *Circulation* 2001;103:58-64.
51. Neagoe C, Kulke M, del Monte F, Gwathmey JK, de Tombe PP, Hajjar RJ, Linke WA. Titin isoform switch in ischemic human heart disease. *Circulation* 2002;106:1333-1341.
52. Narolska NA, Piroddi N, Belus A, Boontje NM, Scellini B, Deppermann S, et al. Impaired diastolic function after exchange of endogenous troponin I with C-terminal truncated troponin I in human cardiac muscle. *Circ Res* 2006;99:1012-1020.
53. Solaro RJ, Moir AJ, Perry SV. Phosphorylation of troponin I and the inotropic effect of adrenaline in the perfused rabbit heart. *Nature* 1976;262:615-617.
54. Wolff MR, Buck SH, Stoker SW, Greaser ML, Mentzer RM. Myofibrillar calcium sensitivity of isometric tension is increased in human dilated cardiomyopathies. *J Clin Invest* 1996;98:167-176.
55. Zhang R, Zhao J, Mandveno A, Potter JD. Cardiac troponin I phosphorylation increases the rate of cardiac muscle relaxation. *Circ Res* 1995;76:1028-1035.
56. Metzger JM, Westfall MV. Covalent and noncovalent modification of thin filament action. The essential role of troponin in cardiac muscle regulation. *Circ Res* 2004;94:146-158.
57. Bristow MR, Ginsburg R, Fowler M, Minobe W, Rasmussen R, Zera P, Menlove R, Shah P, Jamieson S. β_1 - and β_2 -adrenergic receptor subpopulations in normal and failing human ventricular myocardium: coupling of both receptor subtypes to muscle contraction and selective β_1 -receptor downregulation in heart failure. *Circ Res* 1986;59:297-309.
58. Brodde OE, Schuler S, Kretsch R, Brinkmann M, Borst HG, Hetzer R. Regional distribution of β -adrenoceptors in the human heart: coexistence of functional β_1 - and β_2 -adrenoceptors in both atria and ventricles in severe congestive cardiomyopathy. *J Cardiovasc Pharmacol* 1986;8:1235-1242.
59. Harding SE, Jones SM, Vescovo G, Del Monte F, Poole-Wilson PA. Reduced contractile responses to forskolin and a cyclic AMP analogue in myocytes from failing human ventricle. *Eur J Pharmacol* 1992;223:39-48.
60. Bodor GS, Oakeley AE, Allen PD, Crimmins DL, Ladenson JH, Anderson PA. Troponin I phosphorylation in the normal and failing adult human heart. *Circulation*

- 1997;96:1495-1500.
61. Van der Velden J, Narolska NA, Lamberts RR, Boontje NM, Borbely A, Zaremba R, et al. Functional effects of protein kinase C-mediated myofilament phosphorylation in human myocardium. *Cardiovasc Res* 2006;69:876-887.
 62. Messer AE, Jacques AM, Marston SB. Troponin phosphorylation and regulatory function in human heart muscle: dephosphorylation of Ser23/24 on troponin I could account for the contractile defect in end-stage heart failure. *J Mol Cell Cardiol* 2007;42:247-259.
 63. Van der Velden J, Klein LJ, Zaremba R, Boontje NM, Huybregts MA, Stooker W, Eijnsman L, de Jong JW, Visser CA, Visser FC, Stienen GJM. Effects of calcium, inorganic phosphate, and pH on isometric force in single skinned cardiomyocytes from donor and failing human hearts. *Circulation* 2001;104:1140-1146.
 64. Wolff MR, Whitesell LF, Moss RL. Calcium sensitivity of isometric tension is increased in canine experimental heart failure. *Circ Res* 1995;76:781-789.
 65. De Waard MC, van der Velden J, Bito V, Ozdemir S, Biesmans L, Boontje NM, Dekkers DH, Schoonderwoerd K, Schuurbiens HC, de Crom R, Stienen GJ, Sipido KR, Lamers JM, Duncker DJ. Early exercise training normalizes myofilament function and attenuates left ventricular pump dysfunction in mice with a large myocardial infarction. *Circ Res* 2007;100:1079-1088.
 66. Lamberts RR, Hamdani N, Soekhoe TW, Boontje NM, Zaremba R, Walker LA, de Tombe PP, van der Velden J, Stienen GJ. Frequency-dependent myofilament Ca^{2+} desensitisation in failing rat myocardium. *J Physiol* 2007;582:695-709.
 67. Zaremba R, Merkus D, Hamdani N, Lamers JM, Paulus WJ, dos Remedios C, Duncker DJ, Stienen GJ van der Velden J. Quantitative analysis of myofilament protein phosphorylation in small cardiac biopsies. *Proteomics Clin Appl* 2007, in press.
 68. Braz JC, Gregory K, Pathak A, Zhao W, Sahin B, Klevitsky R, Kimball TF, Lorenz JN, Nairn AC, Liggett SB, Bodi I, Wang S, Schwartz A, Lakatta EG, DePaoli-Roach AA, Robbins J, Hewett TE, Bibb JA, Westfall MV, Kranias EG, Molkentin JD. PKC- α regulates cardiac contractility and propensity toward heart failure. *Nature Med* 2004;10:248-254.
 69. Bowling N, Walsh RA, Song G, Estridge T, Sandusky GE, Fouts RL, Mintze K, Pickard T, Roden R, Bristow MR, Sabbah HN, Mizrahi JL, Gromo G, King GL, Vlahos CJ. Increased protein kinase C activity and expression of Ca^{2+} -sensitive isoforms in the failing human heart. *Circulation* 1999;99:384-391.
 70. Noguchi T, Hunlich M, Camp PC, Begin KJ, El-Zaru M, Patten R, Leavitt BJ, Ittleman FP, Alpert NR, LeWinter MM, VanBuren P. Thin filament-based modulation of contractile performance in human heart failure. *Circulation* 2004;110:982-987.
 71. Belin RJ, Sumandea MP, Allen EJ, Schoenfelt K, Wang H, John Solaro R, de Tombe PP. Augmented Protein Kinase C- α -induced myofilament protein phosphorylation contributes to myofilament dysfunction in experimental congestive heart failure. *Circ Res* 2007;101:195-204.
 72. Noland TA, Raynor RL, Kuo JF. Identification of sites phosphorylated in bovine cardiac troponin I and troponin T by protein kinase C and comparative substrate activity of synthetic peptides containing the phosphorylation sites. *J Biol Chem* 1989;264:20778-20785.
 73. Burkart EM, Sumandea MP, Kobayashi T, Nili M, Martin AF, Homsher E. Phosphorylation or glutamic acid substitution at protein kinase C sites on cardiac

- troponin I differentially depress myofilament tension and shortening velocity. *J Biol Chem* 2003;278:11265-11272.
74. Sumandea MP, Pyle WG, Kobayashi T, de Tombe PP, Solaro RJ. Identification of a functionally critical protein kinase C phosphorylation residue of cardiac troponin T. *J Biol Chem* 2003;278:35135-35144.
75. Bossuyt J, Wu X, Avkiran M, Martin JL, Pogwizd SM, Bers DM. CaMKII and PKD overexpression seen in heart failure maintains the HDAC5 redistribution from the nucleus to the cytosol. *Circulation* 2006;114:396 (Abstract).
76. Cuello F, Bardswell SC, Haworth RS, Yin X, Lutz S, Wieland T, Mayr M, Kentish JC, Avkiran M. Protein kinase D selectively targets cardiac troponin I and regulates myofilament Ca²⁺ sensitivity in ventricular myocytes. *Circ Res* 2007;100:864-873.
77. Haworth RS, Cuello F, Herron TJ, Franzen G, Kentish JC, Gautel M, Avkiran M. Protein kinase D is a novel mediator of cardiac troponin I phosphorylation and regulates myofilament function. *Circ Res* 2004;95:1091-1099.
78. Montgomery DE, Chandra M, Huang QQ, Jin JP, Solaro RJ. Transgenic incorporation of skeletal TnT into cardiac myofilaments blunts PKC-mediated depression of force. *Am J Physiol* 2001;260:H1011-H1018.
79. Belin RJ, Sumandea MP, Kobayashi T, Walker LA, Rundell VL, Urboniene D, Yuzhakova M, Ruch SH, Geenen DL, Solaro RJ, de Tombe PP. Left ventricular myofilament dysfunction in rat experimental hypertrophy and congestive heart failure. *Am J Physiol Heart Circ Physiol* 2006;291:H2344-H2353.
80. Neumann J, Gupta RC, Schmitz W, Scholz H, Nairn AC, Watanabe AM. Evidence for isoproterenol-induced phosphorylation of phosphatase inhibitor-1 in the intact heart. *Circ Res* 1991;69:1450-1457.
81. Neumann J, Eschenhagen T, Jones LR, Linck B, Schmitz W, Scholz H, Zimmermann N. Increased expression of cardiac phosphatases in patients with end-stage heart failure. *J Mol Cell Cardiol* 1997;29:265-272.
82. Bristow MR, Anderson FL, Port JD, Skerl L, Hershberger RE, Larrabee P, O'Connell JB, Renlund DG, Volkman K, Murray J. Differences in β -adrenergic neuroeffector mechanisms in ischemic versus idiopathic dilated cardiomyopathy. *Circulation* 1991;84:1024-1039.
83. El-Armouche A, Pohlmann L, Schlossarek S, Starbatty J, Yeh YH, Nattel S et al. Increased phosphorylation levels of cardiac myosin-binding protein-C in human and experimental heart failure. *J Mol Cell Cardiol* 2007;43:223-229.
84. Fan D, Wannenburg T, de Tombe PP. Decreased myocyte tension development and calcium responsiveness in rat right ventricular pressure overload. *Circulation* 1997;95:2312-2317.
85. Vahebi S, Ota A, Li M, Warren CM, de Tombe PP, Wang Y, Solaro RJ. p38-MAPK induced dephosphorylation of alpha-tropomyosin is associated with depression of myocardial sarcomeric tension and ATPase activity. *Circ Res* 2007;100:408-415.
86. Liao P, Wang SQ, Wang S, Zheng M, Zheng M, Zhang SJ, Cheng H, Wang Y, Xiao RP. p38 Mitogen-activated protein kinase mediates a negative inotropic effect in cardiac myocytes. *Circ Res* 2002;90:190-196.
87. Van Heerebeek L, Borbely A, Niessen HW, Bronzwaer JG, van der Velden J, Stienen GJM, Paulus WJ. Myocardial structure and function differ in systolic and diastolic heart failure. *Circulation* 2006;113:1966-1973.

88. Borbély A, van der Velden J, Papp Z, Bronzwaer JG, Edes I, Stienen GJM, et al. Cardiomyocyte stiffness in diastolic heart failure. *Circulation* 2005;111:774-781.
89. Yamasaki R, Wu Y, McNabb M, Greaser M, Labeit S, Granzier H. Protein kinase A phosphorylates titin's cardiac-specific N2B domain and reduces passive tension in rat cardiac myocytes. *Circ Res* 2002;90:1181-1188.
90. Kruger M, Linke WA. Protein kinase-A phosphorylates titin in human heart muscle and reduces myofibrillar passive tension. *J Muscle Res Cell Motil* 2006;27:435-444.
91. Wehrens XH, Lehnart SE, Reiken SR, Marks AR. Ca^{2+} /calmodulin-dependent protein kinase II phosphorylation regulates the cardiac ryanodine receptor. *Circ Res* 2004;94:e61-e70.
92. Huke S, Bers DM. Temporal dissociation of frequency-dependent acceleration of relaxation and protein phosphorylation by CaMKII. *J Mol Cell Cardiol* 2007;42:590-599.
93. Van der Velden J, Papp Z, Boontje NM, Zaremba R, de Jong JW, Janssen PM, Hasenfuss G, Stienen GJ. The effect of myosin light chain 2 dephosphorylation on Ca^{2+} -sensitivity of force is enhanced in failing human hearts. *Cardiovasc Res* 2003;57:505-514.
94. Verduyn SC, Zaremba R, van der Velden J, Stienen GJ. Effects of contractile protein phosphorylation on force development in permeabilized rat cardiac myocytes. *Basic Res Cardiol* 2007;102:476-487.
95. Buscemi N, Foster DB, Neverova I, Van Eyk JE. p21-activated kinase increases the calcium sensitivity of rat triton-skinned cardiac muscle fiber bundles via a mechanism potentially involving novel phosphorylation of troponin I. *Circ Res* 2002;91:509-516.
96. Chen Y, Rajashree R, Liu Q, Hofmann P. Acute p38 MAPK activation decreases force development in ventricular myocytes. *Am J Physiol Heart Circ Physiol* 2003;285:H2578-H2586.
97. Yuan C, Guo Y, Ravi R, Przyklenk K, Shilkofski N, Diez R, Cole RN, Murphy AM. Myosin binding protein C is differentially phosphorylated upon myocardial stunning in canine and rat hearts: evidence for novel phosphorylation sites. *Proteomics* 2006;6:4176-4186.
98. Chang AN, Potter JD. Sarcomeric protein mutations in dilated cardiomyopathy. *Heart Fail Rev* 2005;10:225-235.
99. Tardiff JC. Sarcomeric proteins and familial hypertrophic cardiomyopathy: linking mutations in structural proteins to complex cardiovascular phenotypes. *Heart Fail Rev* 2005;10:237-248.
100. Day SM, Westfall MV, Metzger JM. Tuning cardiac performance in ischemic heart disease and failure by modulating myofilament function. *J Mol Med* 2007;85:911-921.

Differences in Heart Failure with Different Phenotypes and Underlying Cause



3

Diverse Alteration in Sarcomeric Protein Composition And Function in Ischemic and Idiopathic Dilated Cardiomyopathy

Nazha Hamdani, Attila Borbely, Sophie PGR Veenstra, Viola Kooij, Wim
Vrydag, Ruud Zaremba, Cris dos Remedios, Hans WM Niessen,
Martin C. Michel, Walter J Paulus, Ger JM Stienen,
Jolanda van der Velden

Submitted

Abstract

Previous studies revealed differences in the β -adrenergic receptor (β AR) signalling pathway between ischemic cardiomyopathy (ISHD) and idiopathic dilated cardiomyopathy (IDCM) patients.

To reveal if one or more components of the β AR pathway are responsible for altered cardiomyocyte function and structure in failing hearts, key components of the β AR signalling pathway were studied in left ventricular tissue samples from patients with IDCM and ISHD and compared with non-failing donor hearts. This analysis was combined with force measurements in single permeabilized cardiomyocytes, protein analysis of regulatory proteins involved in cardiomyocyte contractility and histological analysis.

Total β AR density was significantly reduced in IDCM patients compared to non-failing hearts, while this reduction was less in ISHD myocardium. Expression of the G-protein coupled receptor kinase, GRK5, was significantly higher in ISHD than in IDCM, while the expression of GRK2 and the stimulatory G-protein (Gs) was similarly reduced in both failing groups compared to donor. Expression level of the inhibitory G-protein (Gi) was significantly higher in IDCM than in ISHD, though an increase was observed in both failing groups relative to donor. Expression of protein phosphatase 1 was significantly lower in ISHD than IDCM, consistent with significantly higher phosphorylation of myosin light chain 2. Phosphorylation of the β AR target proteins, Myosin binding protein C (MyBPC) and cTroponin I (cTnI) was lower in IDCM than in ISHD, which was associated with a significantly higher Ca^{2+} -sensitivity in IDCM compared to ISHD. Expression of phospholamban (PLB) was increased in both failing groups compared to donor, while SERCA2a expression was solely reduced in IDCM. Consequently, the PLB/SERCA2a ratio was significantly higher in ISHD compared to IDCM. Histological analysis revealed lower collagen volume fraction in ISHD compared to IDCM.

Our data indicate that alterations in β -adrenergic signaling pathway and cardiomyocyte function and structure depend on underlying cause of the cardiomyopathy.

Introduction

In patients with heart failure the sympathetic nervous system is chronically activated to maintain perfusion of vital organs via peripheral vasoconstriction, an increase in heart rate and an increase in myocardial contractility. Although aimed at maintaining cardiac pump function, chronic neurohumoral stimulation is detrimental for cardiac function and results in uncoupling and down-regulation of adrenergic receptors (AR).¹⁻³ The adverse effects of neurohumoral overstimulation is illustrated by the negative correlation between noradrenaline plasma levels and prognosis of the patients,⁴ and by the improvement of symptoms and prolonged survival of patients treated with β -adrenergic receptor (β AR) blockers.⁵

In human myocardium, the main β AR are the β_1 AR and β_2 AR subtypes, which are coupled to stimulatory (Gs, both receptors) or inhibitory (Gi, only β_2 AR) guanine nucleotide binding proteins. Agonist binding to β AR triggers interaction of Gs with adenylyl cyclase, which subsequently stimulates the production of the second messenger cyclic AMP from ATP, leading to activation of the down-stream kinase, protein kinase A (PKA).⁶ Active PKA phosphorylates several cellular target proteins involved in Ca^{2+} -handling and myofilament contraction.^{7,8} It increases Ca^{2+} influx (via the L-type Ca^{2+} -channel), accelerates Ca^{2+} reuptake into the sarcoplasmic reticulum (via phosphorylation of phospholamban (PLB)) and decreases myofilament Ca^{2+} sensitivity.^{9,10} These PKA-induced cellular changes exert a positive inotropic and lusitropic effect on cardiac pump function.^{7,11,12} The β_2 ARs also couple to Gi, which results in the opposite effects by lowering cAMP levels.⁶ The β AR itself is also regulated by phosphorylation. Beta-adrenergic receptors are uncoupled from G-proteins, and thereby lose their responsiveness to agonist stimulation, upon phosphorylation by PKA or by G-protein-coupled receptor kinases (GRK).^{6,13} Increased GRK activity has been related to uncoupling and down-regulation of adrenergic receptors in human cardiac disease.^{14,15}

Diverse alterations in myocardial β AR density have been reported in ischemic heart disease (ISHD) and idiopathic dilated cardiomyopathy (IDCM).^{16,17} In IDCM patients β_1 AR has been found to be 50-70% downregulated, while β_2 AR remained unchanged.^{16,17} In contrast, no change in β AR density¹⁶ or a reduction of both β_1 AR and β_2 AR was reported in ISHD patients.¹⁷ Apart from altered β AR composition, a change in G-protein expression is thought to underlie depressed responsiveness to catecholamines in heart failure.^{6,18} Neumann et al.¹⁸ reported increased expression of Gi in patients with IDCM. Analysis of Gi in IDCM and ISHD revealed significantly higher Gi expression in IDCM than in ISHD.^{19,20} It is however, unknown whether

these changes at the receptor level translate into diverse functional and structural alterations. To assess the impact of changes in the adrenergic receptor pathway on cellular structure, function and protein composition, a careful comparison was made between myocardium from patients with IDCM and ISHD. Radioligand binding studies were performed to determine β AR density. Protein analysis included downstream components of the adrenergic signaling cascade, the phospho-proteome of the myofilaments, and SERCA2a and PLB expression levels. Myofilament function was determined in permeabilized single cardiomyocytes. Histological analysis of cardiomyocyte diameter, collagen volume fraction and myofibrillar density were performed using light and electron microscopy.

Methods

Human ventricular tissue

Left ventricular (LV) tissue samples were obtained during heart transplantation surgery from end-stage heart failure patients (NYHA III-IV) with IDCM (n=13; 9 males, 4 females; mean age 49 ± 5 yrs) or ISHD (n=10; 7 males, 3 females; mean age 51 ± 2 yrs). Medication included angiotensin-converting-enzyme inhibitors, angiotensin II receptor antagonists, diuretics, β -blockers, digoxin and anti-arrhythmic agents. Tissue from 10 donor hearts (n=10; 8 males, 2 females; mean age 38 ± 6 yrs) served as reference for non-failing myocardium. The tissue was collected in cardioplegic solution and stored in liquid nitrogen. Samples were obtained after informed consent and with approval of the local Ethical Committee (St Vincents' Hospital Human Research Ethics Committee: File number: H03/118; Title: Molecular Analysis of Human Heart Failure). The investigation conforms with the principles outlined in the Declaration of Helsinki (Cardiovascular Research 1997;35:2-4).

Protein analysis

Radioligand binding

Tissues (~200 mg wet weight) were thawed in ice-cold 1 mM KHCO_3 solution, minced with scissors and then homogenized with an Ultra-Turrax (Janke & Kunkel, Staufen, Germany) for 10 sec at maximum speed followed by twice 20 sec at 2/3 of maximum speed. The homogenates were centrifuged for 15 min at 250 g and 4°C. The supernatant was filtered through medical gauze and centrifuged for 20 min at 50,000 g at 4°C. The sediment was resuspended in binding buffer (10 mM Tris, 154 mM NaCl, pH 7.4). Protein content was measured by the method of Bradford using bovine IgG as standard. Radioligand binding was performed using a 90 min

incubation at 37°C with [¹²⁵I]iodocyanopindolol (ICYP; specific activity 2200 Ci/mmol, Perkin Elmer, Zaventem, Belgium) in a total volume of 250 µl. Non-specific binding was defined as binding in the presence of 100 µM isoproterenol (Sigma-Aldrich). All experiments were performed in duplicates in 96 well plates, and incubations were terminated by rapid vacuum filtration over Whatman GF/C using a Filtermate harvester (Perkin Elmer). Each filter was washed with approximately 10 ml of buffer. Radioactivity adherent to the filters was quantified in a Topcount NXT (Perkin Elmer) using Microsint O scintillator (Perkin Elmer). To determine the relative amount of β₁AR and β₂AR, membranes were incubated with ICYP (100 pM) in the presence or absence of eight concentrations (range 10⁻¹⁰ to 10⁻³ M) of the highly selective β₁-AR antagonist CGP 20712 A [21]. Specific binding was determined as described earlier [21]. CGP 20712A is an abbreviation of 1-[2-((3-carbamoyl-4 hydroxy)phenoxy)ethylamino]-3-[4-(1-methyl-4-trifluoromethyl-2imidazolyl)phenoxy]-2-propanol methanesulfonate.

Components of the β-adrenergic pathway

Protein expression levels of GRK2 and GRK5, G-proteins (Gs and Gi) and protein phosphatase 1 (PP-1) were analyzed by one-dimensional 15% SDS-polyacrylamide gel electrophoresis (1D-PAGE) and subsequent Western blotting. Samples were applied in concentrations which were within the linear range of detection: 20 µg for GRK2, GRK5, Gs and PP-1, and 10 µg for Gi. After 1D separation proteins were transferred to Hybond-ECL nitrocellulose membranes. Blots were pre-incubated with 0.5% milk powder in TTBS (Tween-tris-buffered-saline: 10 mM Tris-HCl pH 7.6, 75 mM NaCl, 0.1% Tween) for one hour at room temperature. The blots were incubated overnight at 4°C with primary rabbit polyclonal antibodies (Santa Cruz) against GRK2 (dilution 1:1000; sc-562), GRK5 (dilution 1:1000; sc-565), Gs (G_{s/olf}; dilution 1:1000; sc-383), Gi (dilution 1:1000; G_{i-1} sc-262, G_{i-2} sc-7276, G_{i-3} sc-262) or primary mouse polyclonal antibody against PP-1 (dilution 1:50; sc-7482, Santa Cruz). After washing with TTBS, primary antibody binding was visualized using a secondary horseradish peroxidase-labeled goat-anti-rabbit/mouse antibody (dilution 1:2000; Dako-Cytomation) and enhanced chemiluminescence (ECL plus Western blotting detection, Amersham Biosciences). All signals were normalized to actin (dilution 1:1000; clone KJ43A; Sigma) stained on the same blots.

Myofilament protein phosphorylation

Myofilament protein phosphorylation was determined using Pro-Q Diamond Phosphoprotein Stain as described previously.²² To preserve the endogenous phosphorylation status, frozen biopsies were homogenized in liquid nitrogen and re-suspended in 1 ml cold 10% trichloroacetic acid solution (TCA; dissolved in acetone containing 0.1% (w/v) dithiothreitol (DTT)). TCA-treated tissue pellets were homogenized in sample buffer containing 15% glycerol, 62.5 mM Tris (pH 6.8), 1% (w/v) SDS and 2% (w/v) DTT. Tissue samples were separated on gradient gels (Criterion tris-HCl 4-15% gel, BioRad) and proteins were stained for one hour with Pro-Q Diamond Phosphoprotein Stain. Fixation, washing and de-staining were performed according to the manufacturer's guidelines (Molecular Probes). To assess protein content subsequently gels were stained overnight with SYPRO Ruby stain (Molecular Probes). Phosphorylation status of myofilament proteins was expressed relative to protein expression of cardiac myosin-binding protein C (cMyBP-C) to correct for differences in sample loading. Staining was visualized using the LAS-3000 Image Reader and signals were analyzed with AIDA.

Bisphosphorylation of cardiac troponin I (cTnI) at PKA sites Ser-23/24 was detected with a primary rabbit polyclonal antibody (dilution 1:500; Cell signaling) in Western blotting. In addition, the recently developed Phos-tagTM acrylamide (FMS Laboratory; Hiroshima University, Japan)²³ was used to visualize phosphorylated cTnI species using alkoxide-bridged dinuclear metal (Mn^{2+}) complex as phosphate-binding tag (Phos-tag) molecule. Mn^{2+} -Phos-tag molecules preferentially capture phosphomonoester dianions bound to Ser, Thr and Tyr residues. Non-phosphorylated and phosphorylated cTnI species were separated in 1D-PAGE with polyacrylamide-bound Mn^{2+} -Phos-tag and transferred to Western blots. Phosphorylated cTnI species in the gel are visualized as slower migration bands compared to the corresponding dephosphorylated cTnI form.

SERCA2a and PLB

SERCA2a protein levels were determined immunochemically by dot-blot analysis, as described before, with minor modifications.²⁴ Briefly, homogenized tissue samples (typically 0.5 μ g total protein) were spotted in triplo onto a nitrocellulose membrane. The blot was then incubated with a 1:2500 dilution of a polyclonal antiserum to SERCA2a²⁵ and subsequently with ¹²⁵I-labeled anti-rabbit immunoglobulin G (0.05 mg/ml, specific activity 7 mCi/mg). To detect PLB expression, blots were first incubated with a 1:2500 dilution of a monoclonal anti mouse antibody (Affinity

Bioreagents) and subsequently with ¹²⁵I-labeled anti-mouse immunoglobulin G. Blots were exposed to Phosphor Imager screens, which were then scanned and spots were quantified using ImageQuant software (Molecular Dynamics).

All protein values for ISHD and IDCM samples were normalized to the average value observed in donor hearts, which was set to 1.

Force measurements in isolated cardiomyocytes

Force measurements were performed in single, mechanically isolated cardiomyocytes as described previously.^{26,27} Tissue samples were defrosted in relaxing solution (in mmol/L: free Mg, 1; KCl, 145; EGTA, 2; MgATP, 4; imidazole, 10; pH7.0), mechanically disrupted and incubated for 5 minutes in relaxing solution supplemented with 0.5% Triton X-100 to remove all membrane structures. Subsequently, cells were washed twice in relaxing solution, after which single cardiomyocytes were attached with silicone adhesive between a force transducer and a motor. Sarcomere length of isolated cardiomyocytes was adjusted to 2.2 μ m. The pCa ($-\log_{10}[\text{Ca}^{2+}]$) ranged from 9.0 (relaxation solution) to 4.5 (maximal activation). All force values were normalized for cardiomyocyte cross-sectional area. Exposure to a series of solutions with intermediate pCa values (pCa 6.0-5.0) yielded the baseline force-pCa relation. On transfer of the cardiomyocyte from relaxing to activating solution, isometric force started to develop. Once a steady state force level was reached, the cell was shortened within 1 ms to 80% of its original length to determine the baseline of the force transducer. The distance between the baseline and the steady force level is the total force (F_{total}). After 20 ms, the cell was restretched and returned to the relaxing solution, in which a second slack test, of 10 s duration was performed to determine passive force (F_{passive}). Active force was obtained by subtracting passive force from the total force, i.e. $F_{\text{active}} = F_{\text{total}} - F_{\text{passive}}$.

Quantitative histomorphometry

Histomorphologic analysis of tissues was performed on elastica-von-Giesson and hematoxylin-eosin stained, 4 μ m thick sections of tissue fixed in 5% formalin.²⁷ Images of these sections were acquired using a projection microscope (x50). Subsequent image analysis, using SlidebookTM 4.0 software (3i, Denver, Co), was performed to determine cardiomyocyte diameter (MyD, μ m) and the extent of interstitial fibrosis, which was expressed as collagen volume fraction (CVF, %). Areas of reparative and perivascular fibrosis were excluded. As previously validated,²⁷ MyD was determined perpendicularly to the outer contour of the cell membrane at nucleus

level in 15 representative myocytes of the section, and CVF was calculated as the sum of all connective tissue areas divided by the sum of all connective tissue and muscle areas averaged over 4-6 representative fields of the section.

Tissues samples were fixed in 2% (v/v) gluteraldehyde for 30 min and 1.5% (w/v) osmium tetroxide for 10 min dehydrated with acetone and embedded in Epon812. Ultrathin sections were collected on 300-mesh Formavar-coated Nickel-grids. The sections were contrasted with uranyl acetate and lead citrate and were examined in a Jeol-1200EX electron microscope. Quantitative analysis was performed with the above mentioned automated image analyzer. Cardiomyocyte myofibrillar density (FibD, %) was calculated from the sum of the myofibrillar areas related to total cellular area in 4-6 representative myocytes.

Data analysis

Competition binding data were analyzed by fitting mono- and biphasic sigmoidal functions to the experimental data; a biphasic fit was accepted only if it resulted in a significant improvement as judged by an F-test. Resulting IC_{50} values for the high and low affinity component of inhibition were converted to K_i values based upon the Cheng-Prusoff equation²⁸ and assuming a K_d value of ICYP of 72 pM (n=4). Due to limited tissue availability, receptor density (B_{max}) was estimated based upon the specific binding (SB) of the single radioligand concentration (L) in the competition experiments relative to its K_d using the equation $B_{max} = SB / (1 - 1 / (L / K_d + 1))$. The statistical significance of inter-group differences was assessed by one-way ANOVA followed by Dunnett's post-hoc tests.

Force-pCa relations were fit to the Hill equation as described previously.²⁶ Values are given as mean \pm SEM of n observations. The mean data values of protein and histological analysis and force measurements in ISHD, IDCM and donor samples were compared using one-way ANOVA and Bonferroni-post tests. $P < 0.05$ was considered significant. All statistical analysis were performed with the Prism program (version 4.01, Graphpad Software, San Diego, CA, USA).

Results

Diverse changes in components of the β AR pathway in IDCM and ISHD

With one exception competition by the highly β_1 -selective CGP 20712A resulted in biphasic curves in all cases (Fig 1). The high and low affinity sites had $-\log K_i$ values of 8.84 ± 0.10 and 6.04 ± 0.11 , identifying β_1 AR and β_2 AR respectively in the non-failing donor group (n=7). The $-\log K_i$ values were not significantly different in either IDCM

(n=8) or ISHD (n=8). The calculated percentages of β_1 ARs were $52\pm 6\%$, $50\pm 4\%$ and $47\pm 9\%$ in donor, IDCM and ISHD, respectively ($P>0.05$). Single point estimates of total β AR density were 13.5 ± 2.2 , 6.6 ± 1.5 and 9.9 ± 1.8 fmol/mg protein in donor, IDCM and ISHD, respectively ($P<0.05$ for IDCM vs. non-failing donor).

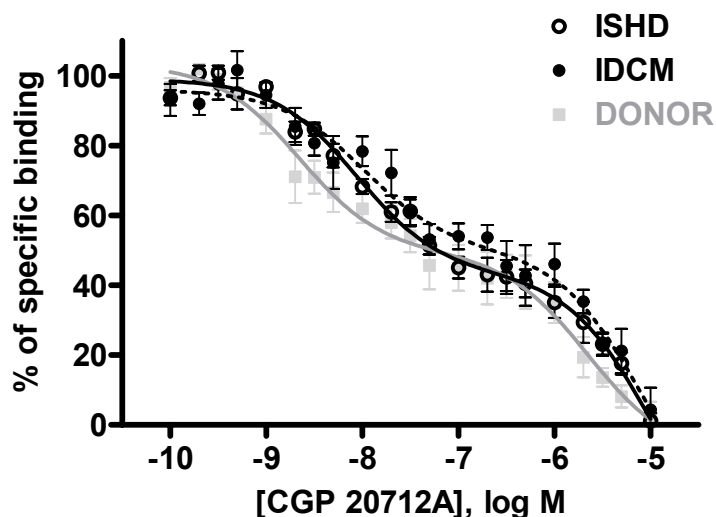


Figure 1. Competition curve of radioligand binding as a function of CGP 20712A. These measurements revealed significantly lower β AR density in IDCM compared to non-failing donor myocardium, but the receptor distribution remained the same.

An overview of the Western blot analysis of components of the β AR pathway in failing and donor myocardium is given in Figure 2. All signals in failing samples were normalized to the value observed in donor myocardium, which was set to 1. One-way ANOVA revealed significant differences in expression of GRK2 and GRK5 among groups. The expression level of GRK2 (Fig 2A) was significantly lower in both failing groups compared to non-failing tissue, while GRK5 (Fig 2B) was significantly higher in ISHD compared to IDCM and non-failing myocardium. Gs expression was significantly lower in both failing groups compared to donor hearts (Fig 2C). In the present study, we have analyzed three forms of inhibitory G-protein: $G_{i\alpha-1}$, $G_{i\alpha-2}$ and $G_{i\alpha-3}$. The heterotrimeric G-proteins are composed of α , β and γ subunits, of which the α subunit confers specificity to the G-protein.⁶ The α subunit contains the GTP binding site and the intrinsic GTPase activity. $G_{i\alpha-1}$ expression (Fig 2D) was significantly higher in IDCM than in ISHD and donor, while $G_{i\alpha-2}$ (Fig 2E) was significantly higher in both failing groups compared to donor. No significant differences were found in $G_{i\alpha-3}$ expression level (Fig 2F).

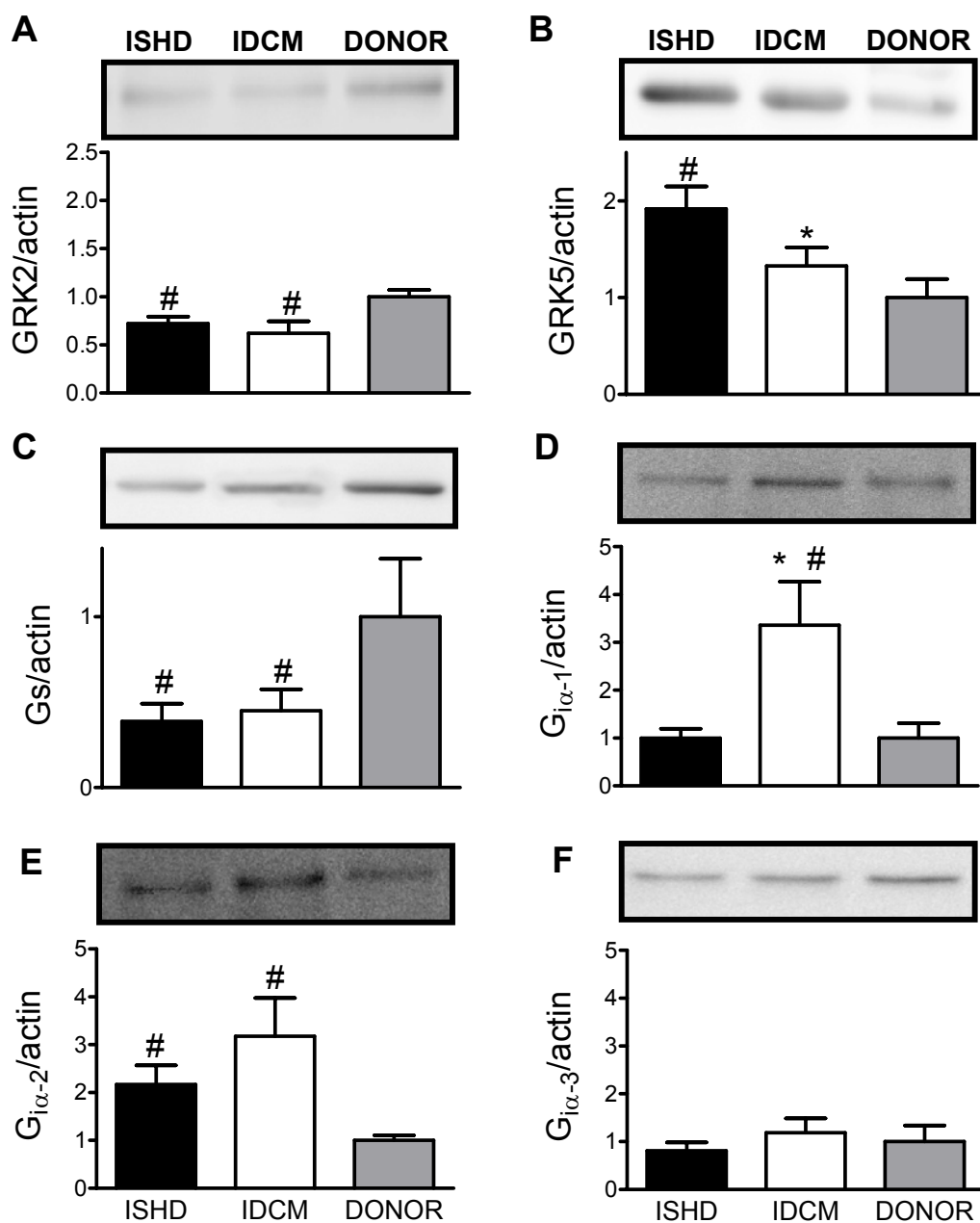


Figure 2. Western blot examples of the β AR pathway proteins in IDCM, ISHD and donor myocardium. The expression of GRK2 was significantly lower in both ISHD and IDCM compared to donor (A), while GRK5 expression was significantly higher in ISHD compared to IDCM and donor (B). Expression of Gs was significantly lower in failing compared to donor (C). The expression level of the three isoforms of Gi (D, $G_{i\alpha-1}$; E, $G_{i\alpha-2}$ and F, $G_{i\alpha-3}$) were different among groups ($P < 0.05$, in one-way ANOVA). Post-test Bonferroni analysis revealed a significantly higher level of $G_{i\alpha-1}$ in IDCM compared to ISHD and donor, while $G_{i\alpha-2}$ was significantly higher in both failing groups compared to donor. * $P < 0.05$ in Bonferroni-post tests, CM vs. ISHD; # $P < 0.05$, in Bonferroni-post tests, failing vs. donor.

Myofilament protein phosphorylation

ProQ Diamond phosphostaining was used to detect phosphorylation of myofilament proteins. Figure 3A shows ProQ Diamond-stained cardiac samples from ISHD, donor (D) and IDCM myocardium separated on a gradient gel. The same gel was subsequently stained with SYPRO Ruby for analysis of total protein content (Fig 3B). The ProQ signals of phosphorylated proteins were corrected by the SYPRO-stained cMyBP-C band to correct for small differences in protein loading. The ProQ Diamond stained gel shows lower endogenous phosphorylation of the PKA-target proteins cMyBP-C and cTnI in failing compared to non-failing donor myocardium. Noteworthy, cTnI phosphorylation was significantly higher in ISHD compared to IDCM (Fig 3C). In addition, phosphorylation of cMyBP-C was higher in ISHD, though not significantly ($P=0.07$).

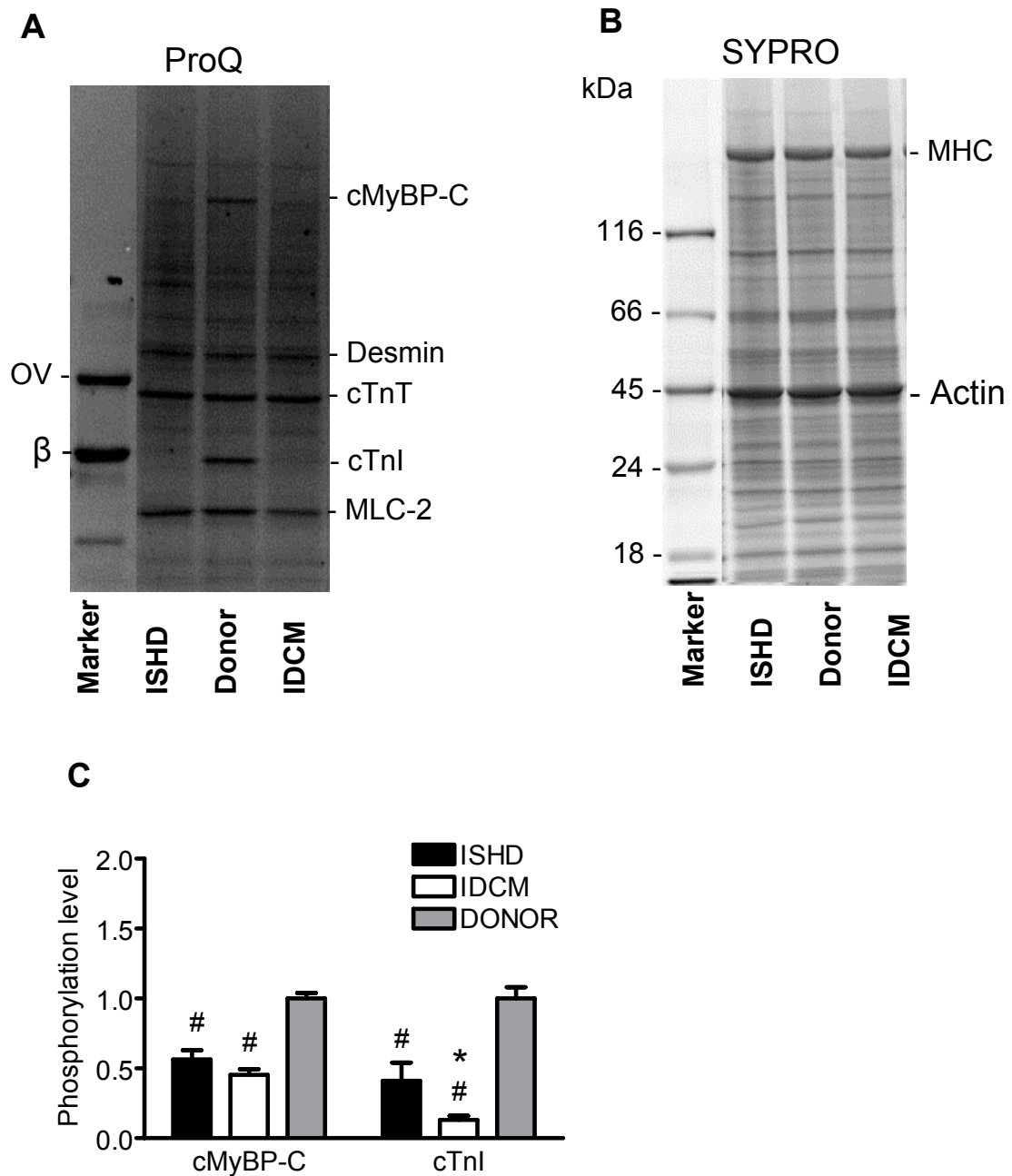


Figure 3. Pro-Q Diamond-stained (**A**) and SYPRO-stained (**B**) gel of ISHD, donor (D) and IDCM samples. The ProQ Diamond stained gel clearly shows higher phosphorylation of cardiac myosin binding protein C (cMyBP-C) and troponin I (cTnI) in donor compared to the ISHD and IDCM sample. The mean values are shown in the bar graph (**C**). Phosphorylation of cTnI was significantly higher in ISHD compared to IDCM. *Abbreviations:* n, number of heart samples; MHC, myosin heavy chain; cTnT, troponin T; M, molecular weight marker (PeppermintStick Phosphoprotein marker in which ovalbumin (OV) and β -casein (β) are phosphorylated). *P<0.05 in Bonferroni-post tests, IDCM vs. ISHD; #P<0.05, in Bonferroni-post tests, failing vs. donor.

Higher PKA-mediated phosphorylation of cTnI (at Ser 23/24, i.e. PKA sites) in ISHD compared to IDCM was confirmed in Western blotting ($P < 0.05$, ISHD vs. IDCM; Fig 4A). Consistent with ProQ Diamond analysis of cTnI phosphorylation, the Western blots revealed higher cTnI phosphorylation at PKA-sites in non-failing donor myocardium compared to failing hearts.

Analysis of cTnI species separated by Phos-tag polyacrylamide gels revealed three bands upon staining of Western blots with a specific anti-cTnI antibody (8I-7, Spectral Diagnostics Inc.) in non-failing donor myocardium, while only two bands were observed in the failing sample shown in Figure 4B. The lower band was recognized by an antibody directed against cTnI non-phosphorylated at PKA sites (22B11, Research Diagnostics). The upper band was recognized by the PKA-specific cTnI antibody indicating that this band is the PKA-bisphosphorylated cTnI form. Based the latter analysis we assume that the second band is the mono-phosphorylated form of cTnI. The distribution of the cTnI forms was significantly different among the three groups. The non-phosphorylated form was highest in IDCM, while the bisphosphorylated form was highest in non-failing donor hearts.

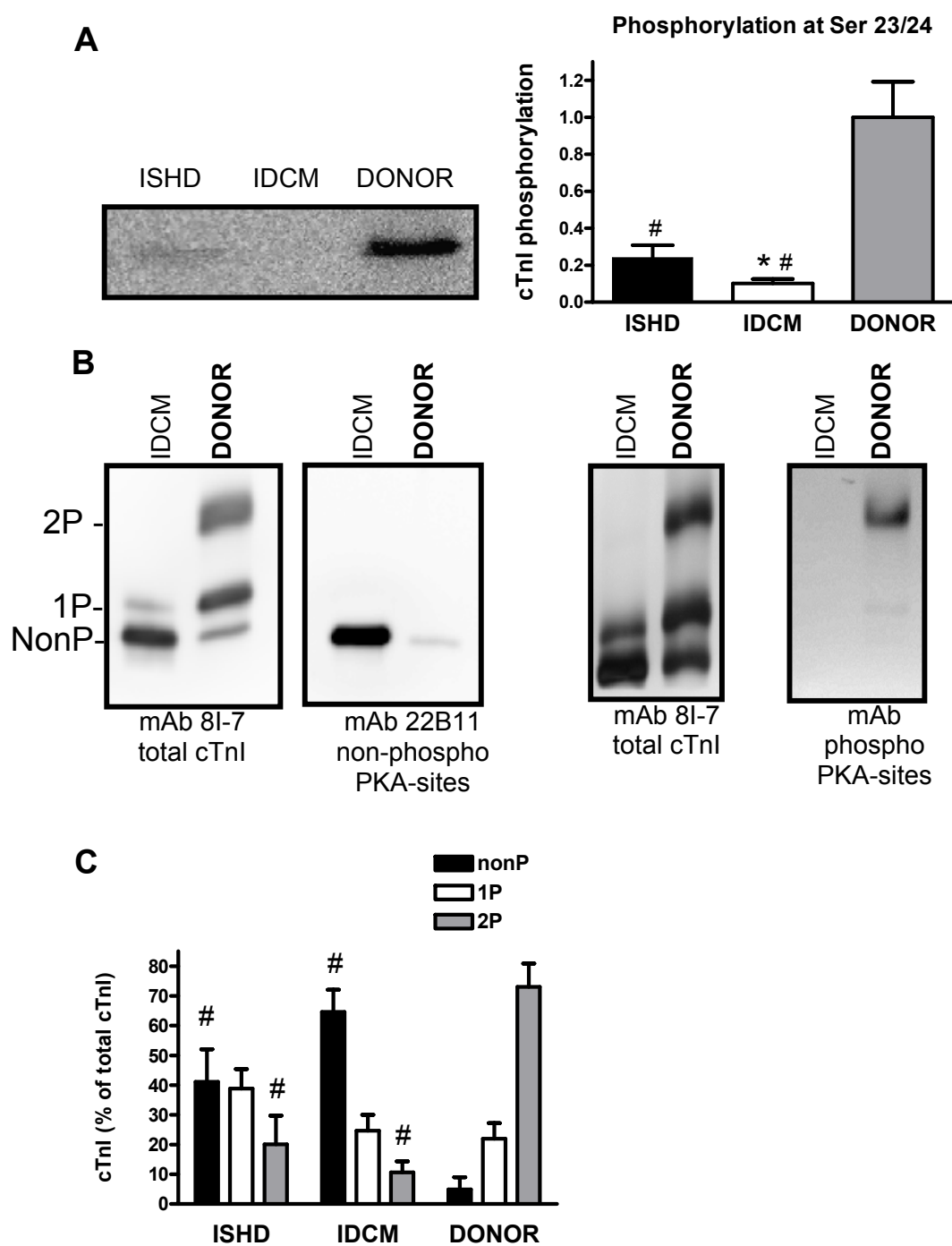


Figure 4. A. Western blot analysis of cTnI phosphorylation at the PKA-sites Ser 23/24 revealed significantly higher cTnI phosphorylation in ISHD compared to IDCM, while cTnI phosphorylation was lower in both failing groups compared to donor. **B.** Phos-tag analysis of cTnI species revealed three cTnI bands in non-failing donor myocardium, of which the lowest band stained with an antibody directed against non-phosphorylated cTnI (22B11), and the highest band stained with the anti-PKA-bis phosphorylated sites in cTnI. **C.** The distribution of cTnI species was significantly different among groups. * $P < 0.05$ in Bonferroni-post tests, IDCM vs. ISHD; # $P < 0.05$, in Bonferroni-post tests, failing vs. donor.

ProQ Diamond analysis also revealed higher phosphorylation of myosin light chain 2 (MLC-2) in ISHD compared to both IDCM and donor (Fig 5C), while there were no significant differences in phosphorylation of the other myofilament proteins, desmin and troponin T (data not shown). MLC-2 protein expression was similar in all groups ISHD, IDCM and donor (Fig 5A). The difference in MLC-2 phosphorylation may be in part explained by differences in PP-1 expression. Western blot analysis of PP-1 revealed significantly higher PP-1 expression in IDCM compared to ISHD and donor myocardium (Fig 5B).

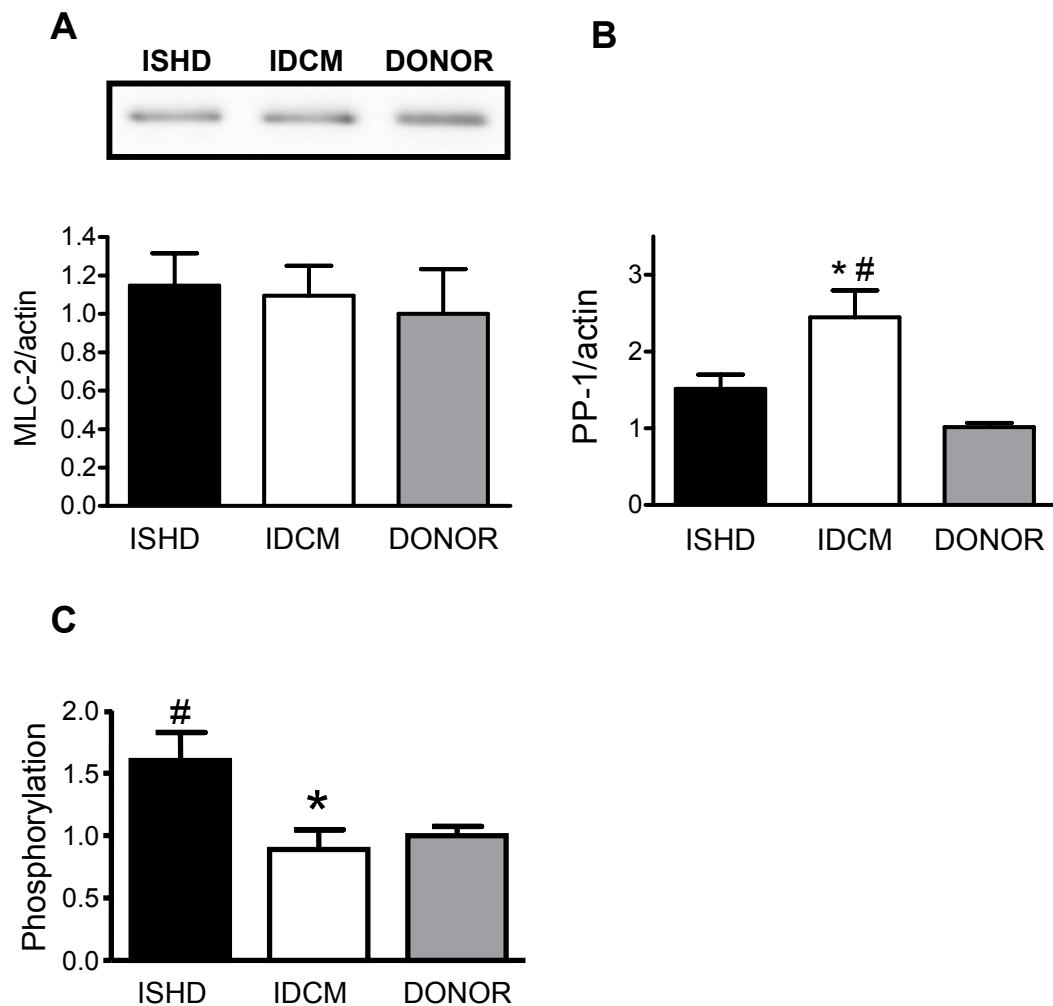


Figure 5. A. Expression of MLC-2 was similar in all groups. B. Expression of protein phosphatase 1 (PP-1) was significantly higher in IDCM compared to ISHD and donor. C. Phosphorylation of myosin light chain 2 (MLC-2) was significantly higher in ISHD compared to IDCM. * $P < 0.05$ in Bonferroni-post tests, IDCM vs. ISHD; # $P < 0.05$, in Bonferroni-post tests, failing vs. donor.

Diverse changes in PLB and SERCA2a expression in IDCM and ISHD

Western immunoblot analysis revealed increased PLB expression (Fig 6A) in IDCM and ISHD compared to non-failing donor hearts and a significantly lower SERCA2a expression level (Fig 6B) in IDCM compared to both ISHD and donor. The ratio of PLB over SERCA2a (Fig 6C) significantly differed among groups, being highest in IDCM and lowest in donor.

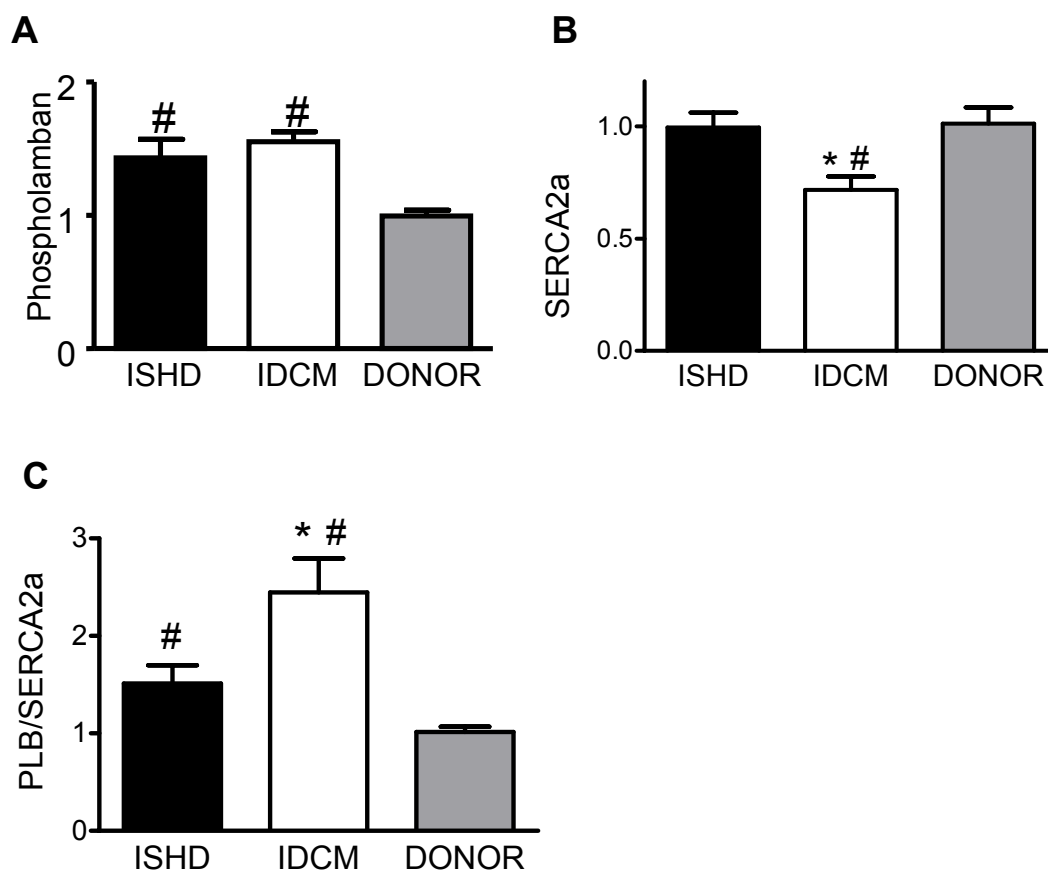


Figure 6. Western blot analysis revealed significant differences in protein levels of the Ca^{2+} -handling proteins phospholamban (PLB) and SERCA2a among groups. PLB was significantly higher in both failing groups compared to donor (A), while SERCA2a was significantly lower in IDCM compared to ISHD and donor (B). The ratio of PLB over SERCA2a was significantly higher in both failing groups compared to donor. The PLB/SERCA2a ratio of IDCM group was significantly higher compared to the value observed in the ISHD group (C). * $P < 0.05$ in Bonferroni-post tests, IDCM vs. ISHD; # $P < 0.05$, in Bonferroni-post tests, failing vs. donor.

Higher Ca^{2+} -sensitivity in IDCM than in ISHD

Force measurements were performed in single cardiomyocytes isolated from 9 IDCM (42 cardiomyocytes), 8 ISHD (27 cardiomyocytes) and 11 donor (41 cardiomyocytes) samples. Cross-sectional area of the cardiomyocytes determined at a sarcomere length of 2.2 μm was significantly higher in IDCM ($556 \pm 44 \mu\text{m}^2$) and ISHD ($690 \pm 75 \mu\text{m}^2$) compared to non-failing donor hearts ($339 \pm 26 \mu\text{m}^2$) ($P < 0.05$ in one-way ANOVA).

F_{active} did not differ (Fig 7A), while F_{passive} was significantly lower in failing compared to donor (Fig 7B). A significantly higher pCa_{50} was found in failing heart compared to non-failing donor hearts (Fig 7C,D). Noteworthy pCa_{50} was significantly lower in ISHD compared to IDCM (Fig 7C,D). Moreover, the steepness of the force- pCa relationship (n_{Hill}) was significantly higher in ISHD (4.05 ± 0.12) compared to IDCM (3.58 ± 0.10) and non-failing donor (3.70 ± 0.14).

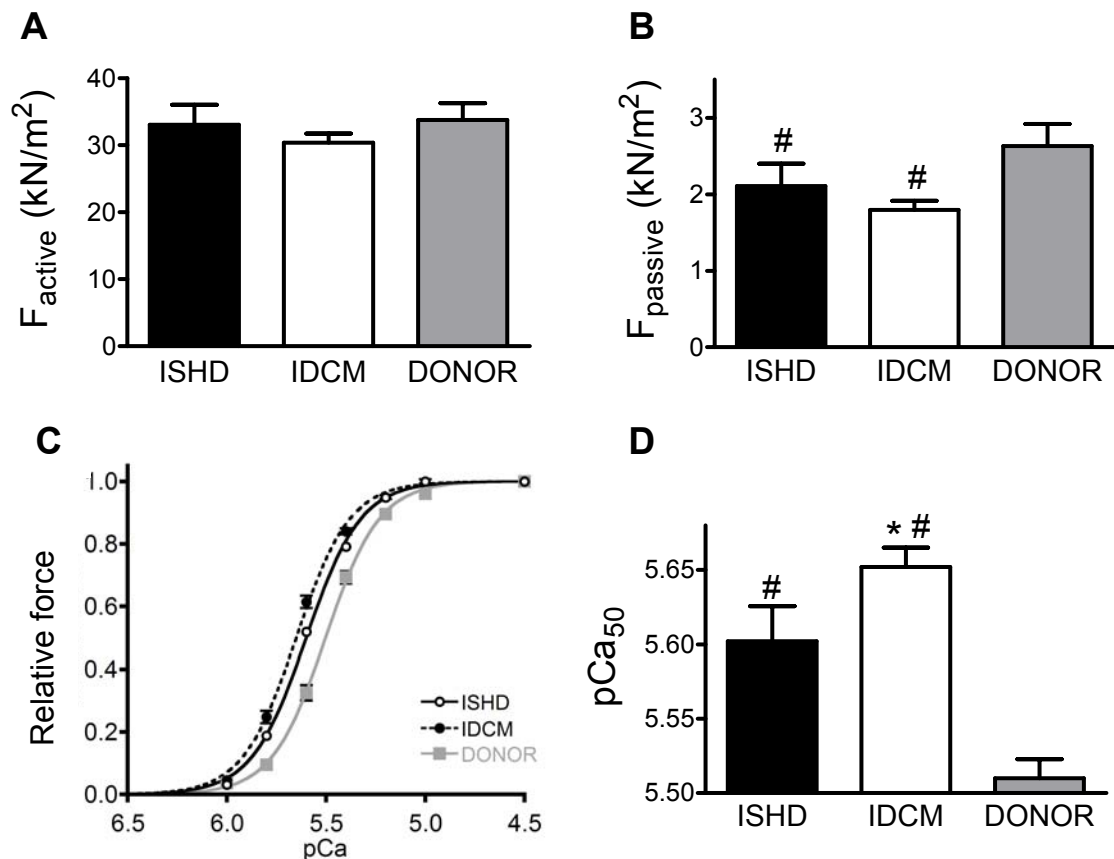
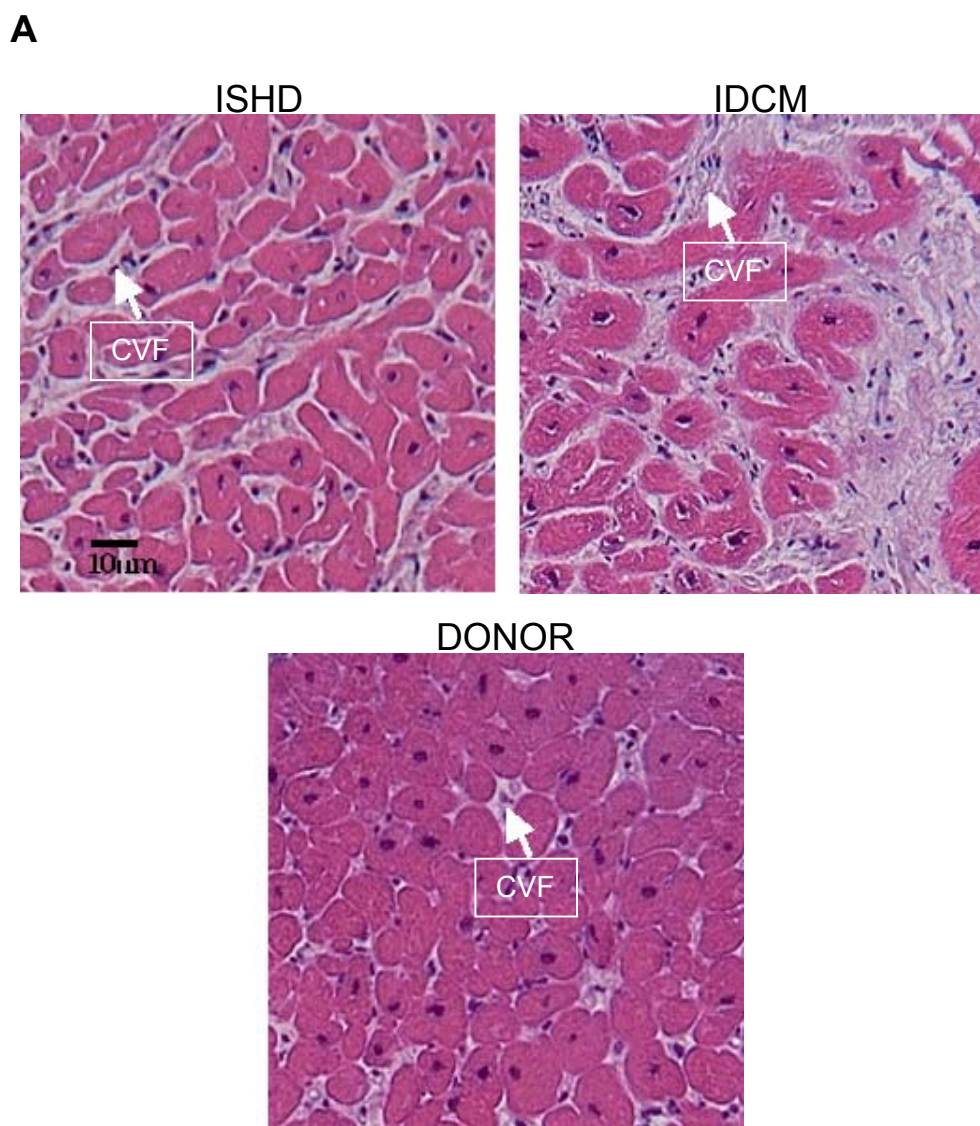


Figure 7. Maximal active tension (F_{active}) did not differ among groups (A). Passive (F_{passive}) force was significantly lower in failing hearts compared to donor (B). Ca^{2+} -sensitivity (pCa_{50}) was significantly higher in failing hearts compared to the donor group (C,D). The pCa_{50} was significantly lower in ISHD compared to IDCM (C,D). * $P < 0.05$ in Bonferroni-post tests, IDCM vs. ISHD; # $P < 0.05$, in Bonferroni-post tests, failing vs. donor.

Alterations in cellular structures

Representative examples of light microscopy images of LV sections from the three groups are shown in Figure 8A. MyD did not differ between ISHD and IDCM, although MyD values in both failing groups were higher than observed in donor myocardium (Fig 8B). CVF was significantly higher in both failing compared to the donor group. Moreover, CVF was significantly higher in IDCM compared to ISHD (Fig 8C). No differences were found in FibD between ISHD and IDCM, while FibD was significantly lower in both IDCM and ISHD compared to non-failing donor ($P < 0.05$ in post-test Bonferroni analysis; Fig 8D).



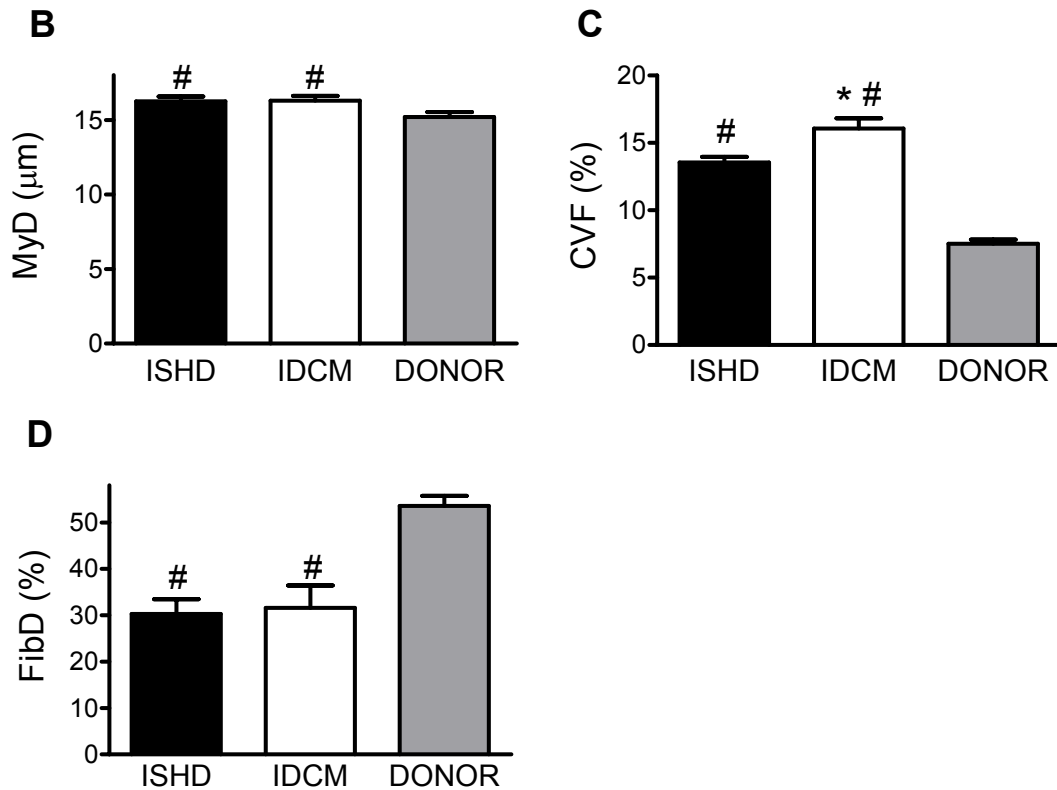


Figure 8. A. Light microscopy images of LV sections from the three groups. B. Bar graphs showing cardiomyocyte diameter (MyD), C. collagen volume fraction (CVF) and D. myofibrillar density (FibD). A significant increase was observed in MyD and CVF in both failing groups compared to donor. In addition, a significantly lower FibD was present in failing hearts compared to donor. CVF in IDCM was significantly higher compared to ISHD. * $P < 0.05$ in Bonferroni-post tests, IDCM vs. ISHD; # $P < 0.05$, in Bonferroni-post tests, failing vs. donor. Representative example of collagen (arrows) of the IDCM, ISHD and non-failing donor.

Discussion

Diverse changes in components of the β -adrenergic pathway

Bristow et al. showed down-regulation of β ARs in dilated cardiomyopathy patients,² which were mainly attributed to a reduction of the β_1 AR subtype. In our study, total β AR density was significantly reduced in IDCM patients compared non-failing hearts, while this reduction was less in ISHD myocardium. No change was found in percentage of β_1 AR among groups. The number of β AR may change as a result of reduced mRNA levels.²⁹ In addition, β AR may be degraded upon internalization of receptors, which is preceded by the process of receptor uncoupling.⁶ The regulating step in the latter process is receptor phosphorylation, either by second-messenger activated kinases, or by GRKs, which only phosphorylate agonist occupied receptors.

Studies in transgenic mice overexpressing GRK2 (also known as β ARK1, β -adrenergic receptor kinase 1)¹³ or GRK5³⁰ revealed that both are determinants of β AR responsiveness of the heart, as they disrupt the interaction between receptors and the heterotrimeric G proteins. This process of receptor uncoupling is thought to be an important contributor to β AR desensitization and down-regulation due to increased sympathetic tone in cardiac disease. In failing human tissue, Ungerer et al.^{14,15} were the first to show increased GRK2 mRNA and activity in both ISHD and IDCM. In contrast, in the present study we observed lower GRK2 protein expression in both failing groups compared to non-failing myocardium, while GRK5 protein expression was significantly higher in ISHD compared to IDCM and non-failing myocardium. Our data indicate that apart from GRKs other mechanisms are involved in the reduction of β AR density.

Previous studies revealed no change in mRNA level and activity of Gs.^{31,32} In contrast, in our study a decreased Gs protein expression was detected in both patient groups compared to non-failing donor hearts, while no difference was present between IDCM and ISHD. Neumann et al. and Feldman et al.^{18,31} were the first to report an increase in Gi in preparations from IDCM patients. Noteworthy, in our study, Gai expression levels were highest in IDCM, with a significantly higher expression of Gai-1 in IDCM compared to ISHD.

Diverse changes in protein phosphorylation in ISHD and IDCM

Analysis of sarcomeric protein phosphorylation revealed significant differences in the β AR target proteins cMyBP-C and cTnI. Consistent with previous studies^{26,33} phosphorylation of cMyBP-C and cTnI was significantly lower in both failing groups compared to donor, which has been explained by reduced PKA-mediated phosphorylation due to β AR desensitization and down-regulation in cardiac disease.²⁶ Noteworthy, cTnI phosphorylation was significantly lower in IDCM compared to ISHD, which may be the resultant of the larger reduction in β AR density and larger increase in Gai-1 expression observed in IDCM compared to ISHD hearts.

MLC-2 phosphorylation was significantly higher in ISHD than in IDCM. MLC-2 dephosphorylation depends on expression level and activity of PP-1. The PP-1 level was significantly lower in ISHD compared to IDCM. However, it was similar in ISHD and non-failing donor. The activity of PP-1 is tightly regulated by its inhibitor, protein inhibitor 1 (I1).⁴⁶ Upon activation of β AR, PP-1 activity is depressed by PKA via phosphorylation of I1. Hence, the difference in MLC-2 phosphorylation between ISHD and donor myocardium may be caused by a difference in PP-1 activity.

Myofilament function

As PKA-mediated phosphorylation of cMyBP-C and cTnI result in a decrease in myofilament Ca^{2+} -sensitivity, the lower myofilament Ca^{2+} -sensitivity in ISHD compared to IDCM may be well explained by the significantly higher (PKA-mediated) phosphorylation of cTnI observed in ISHD. Interestingly, analysis of cTnI species using Phos-tag polyacrylamide gels (Fig 4B,C) showed that the difference in cTnI phosphorylation can be largely explained by a difference in the bis-phosphorylated form of cTnI. Thus it is tempting to speculate that a difference in bis-phosphorylated cTnI underlies the difference in Ca^{2+} -sensitivity between IDCM and ISHD.

Passive cardiomyocyte stiffness was reduced by 20% in ISHD and 32% in IDCM compared to donor hearts. The 30% reduction in FibD could have contributed to the low F_{passive} observed in both failing groups. However, F_{active} was comparable in all groups. Hence, it is unlikely that the reduction in cardiomyocyte stiffness can be explained by reduced FibD. Changes in passive stiffness have been ascribed to alterations in titin isoform composition.³⁵ The reduction in cardiomyocyte stiffness is most likely the resultant of a shift from the stiff N2B to the compliant N2BA titin isoform.

Diverse changes in protein expression in IDCM and ISHD

Increased activity and mRNA level of PP-1 has been reported previously in human IDCM.³⁶ Increased activity of PP-1 in a transgenic mouse model resulted in decreased contractility and dilated cardiomyopathy underscoring a detrimental role for PP-1 in heart failure.³⁴ Increased PP-1 will impair Ca^{2+} -handling by dephosphorylation of PLB. The resulting reduction in SR Ca^{2+} loading will be enhanced further by the reduction in SERCA2a expression in IDCM. Although several studies did not find differences in SERCA2a and PLB at mRNA levels between ISHD and IDCM,^{37,38} our study showed reduced SERCA2a protein expression only in IDCM, while expression of PLB was increased compared to donor myocardium in both failing groups. Based on these previous studies^{34,36} an increase in PP-1 and the reduction in SERCA2a expression will impair Ca^{2+} -handling and suggests that IDCM patients may benefit from SERCA2 transfection, which has been shown to restore cardiomyocyte function and cardiac pump function.⁴⁷

Structural changes in IDCM and ISHD

Previous studies identified three main structural alterations in patients with IDCM and ISHD: cardiomyocyte hypertrophy,⁴⁰ myofibrillar loss³⁹ and myocardial fibrosis.^{40,41} In our study, no difference was found in MyD and FibD between IDCM and ISHD, while CVF was significantly higher in IDCM compared to ISHD. Fibrosis is thought to result in abnormal myocardial stiffness, which can lead to left ventricular diastolic dysfunction⁴² and ultimately systolic dysfunction in IDCM and ISHD.⁴³ Our finding is in line with a previous study by Parodi et al,⁴⁴ which showed more fibrosis in IDCM than ISHD. The higher fibrosis in IDCM may be related to the inflammation⁴⁵ and warrants further research.

Clinical implications

As all patients received medication, which have been shown to reverse detrimental changes in cellular structure and expression of components of the β AR pathway, drug treatment may have obscured disease-related changes. Nevertheless, our results suggest that differences in β AR signalling result in alterations in cellular structure, function and protein composition and that responsiveness of patients to antagonist therapy may depend on the underlying cause of heart failure.

References

1. Bristow MR, Ginsburg R, Minobe W, Cubicciotti RS, Sageman WS, Lurie K, Billingham ME, Harrison DC, Stinson EB. Decreased catecholamine sensitivity and beta-adrenergic-receptor density in failing human hearts. *N Engl J Med* 1982;307:205-211.
2. Bristow MR, Ginsburg R, Umans V, Fowler M, Minobe W, Rasmussen R, Zera P, Menlove R, Shah P, Jamieson S. Beta1- and beta2-adrenergic-receptor subpopulations in nonfailing and failing human ventricular myocardium: coupling of both receptor subtypes to muscle contraction and selective beta 1-receptor down-regulation in heart failure. *Circ Res* 1986;59:297-309.
3. Packer M. Evolution of the neurohormonal hypothesis to explain the progression of chronic heart failure. *Eur Heart J* 1995;16:F4-6.
4. Cohn JN, Levine TB, Olivari MT, Garberg V, Lura D, Francis GS, Simon AB, Rector T. Plasma norepinephrine as a guide to prognosis in patients with chronic congestive heart failure. *N Engl J Med* 1984;311:819-823.
5. Bohm M, Maack C. Treatment of heart failure with beta-blockers. *Bas Res Cardiol* 2000;95:115-24.
6. Wang X, Dhalla NS. Modifications of β -adrenoceptor signal transduction pathway by genetic manipulation and heart failure. *Mol Cell Biochem* 2000;214:131-155.
7. Bers DM. Cardiac excitation-contraction coupling. *Nature* 2002;415:198-205.
8. Kranias EG, Garvey JL, Srivastava RD, Solaro RJ. Phosphorylation and functional modifications of sarcoplasmic reticulum and myofibrils in isolated rabbit hearts stimulated with isoprenaline. *Biochem J* 1985;226:113-121.
9. Wolff MR, Buck SH, Stoker SW, Greaser ML, Mentzer RM. Myofibrillar calcium sensitivity of isometric tension is increased in human dilated cardiomyopathies. *J Clin Invest* 1996;98:167-176.
10. Cazorla O, Szilagyi S, Salazar G, Krämer E, Vassort G, Carrier L, Lacampagne A. Length and protein kinase A modulations of myocytes in cardiac myosin binding protein C-deficient mice. *Cardiovasc Res* 2006;69:370-380.
11. Zhang R, Zhao J, Mandveno A, Potter JD. Cardiac troponin I phosphorylation increases the rate of cardiac muscle relaxation. *Circ Res* 1995;76:1028-1035.
12. Kentish JC, McCloskey DT, Layland J, Palmer S, Leiden JM, Martin AF, Solaro RJ. Phosphorylation of troponin I by protein kinase A accelerates relaxation and crossbridge cycle kinetics in mouse ventricular muscle. *Circ Res* 2001;88:1059-1065.
13. Koch WJ, Rockman HA, Samama P, Hamilton R, Bond RA, Milano CA, Lefkowitz RJ. Cardiac function in mice overexpressing the β -adrenergic receptor kinase or β ARK inhibitor. *Science* 1995;268:1350-1353.
14. Ungerer M, Böhm M, Elce JS, Erdmann E, Lohse MJ. Altered expression of beta-adrenergic receptor kinase and beta 1-adrenergic receptors in the failing human heart. *Circulation* 1993;87:652-654.
15. Ungerer M, Parruti G, Böhm M, Puzicha M, DeBlasi A, Erdmann E, Lohse MJ. Expression of beta-arrestins and beta-adrenergic receptor kinases in the failing human heart. *Circ Res* 1994;74:206-213.
16. Bristow MR, Anderson FL, Port JD, Skerl L, Hershberger RE, Larrabee P, O'Connell JB, Renlund DG, Volkman K, Murray J. Differences in beta-adrenergic neuroeffector

- mechanisms in ischemic versus idiopathic dilated cardiomyopathy. *Circulation* 1991;84:1024-1039.
17. Steinfath M, Geertz B, Schmitz W, Scholz H, Haverich A, Breil I, Hanrath P, Reupcke C, Sigmund M, Lo HB. Distinct down-regulation of cardiac beta1- and beta2-adrenoceptors in different human heart diseases. *Naunyn Schmiedebergs Arch Pharmacol* 1991;343:217-220.
 18. Neumann J, Schmitz W, Scholz H, von Meyerinck L, Döring V, Kalmar P. Increase in myocardial Gi-proteins in heart failure. *Lancet* 1988;2:936-937.
 19. Böhm M, Gierschik P, Jakobs KH, Pieske B, Schnabel P, Ungerer M, Erdmann E. Increase of Gi alpha in human hearts with dilated but not ischemic cardiomyopathy. *Circulation* 1990;82:1249-1265.
 20. Böhm M, Gierschik P, Erdmann E. Quantification of Gi alpha-proteins in the failing and nonfailing human myocardium. *Bas Res Cardiol* 1992;87 (Suppl 1):37-50.
 21. Niclauss N, Michel-Reher MB, Alewijnse AE, Michel MC. Comparison of three radioligands for the labelling of human β -adrenoceptor subtypes. *Naunyn-Schmiedeberg's Arch Pharmacol* 2006;374:99-105
 22. Zaremba R, Merkus D, Hamdani N, Lamers MJM, Paulus WJ, dos Remedios C, Duncker DJ, Stienen GJM and van der Velden J. Quantitative analysis of myofilament protein phosphorylation in small cardiac biopsies. *Proteomics Clin Appl* 2007;1:1285-1290.
 23. Kinoshita E, Kinoshita-Kikuta E, Takiyama K, Koike T. Phosphate-binding tag, a new tool to visualize phosphorylated proteins. *Mol Cell Proteomics* 2006;5:749-757.
 24. Muller A, van der Linden GC, Zuidwijk MJ, Simonides WS, van der Laarse WJ, van Hardeveld C. Differential effects of thyroid hormone on the expression of sarcoplasmic reticulum Ca^{2+} -ATPase isoforms in rat skeletal muscle fibers. *Biochem Biophys Res Commun* 1991;203:35-40.
 25. Eggermont JA, Wuytack F, Verbist J, Casteels R. Expression of endoplasmic-reticulum Ca^{2+} -pump isoforms and of phospholamban in pig smooth-muscle tissue. *Biochem J* 1990;271:649-653.
 26. Van der Velden J, Papp Z, Zaremba R, Boontje NM, de Jong JW, Owen VJ, Burton PB, Goldmann P, Jaquet K, Stienen GJM. Increased Ca^{2+} -sensitivity of the contractile apparatus in end-stage human heart failure results from altered phosphorylation of contractile proteins. *Cardiovasc Res* 2003;57:37-47.
 27. Borbély A, van der Velden J, Papp Z, Bronzwaer JG, Edes I, Stienen GJM, Paulus WJ. Cardiomyocyte stiffness in diastolic heart failure. *Circulation* 2005;111:774-781.
 28. Cheng Y, Prusoff WH. Relationship between the inhibition constant (K_i) and the concentration of an inhibitor, which causes 50 per cent inhibition (I_{50}) of an enzymatic reaction. *Biochemical Pharmacology* 1973;22:3099-3108.
 29. Hadcock JR, Malbon CC. Down-regulation of β -adrenergic receptors: agonist-induced reduction in receptor mRNA levels. *Proc Natl Acad Sci USA* 1998;85: 5021-5025.
 30. Rockman HA, Choi DJ, Rahman NU, Akhter SA, Lefkowitz RJ, Koch WJ. Receptor-specific in vivo desensitization by the G protein-coupled receptor kinase-5 in transgenic mice. *Proc Natl Acad Sci* 1996;93:9954-9959.
 31. Feldman AM, Cates AE, Veazey WB, Hershberger RE, Bristow MR, Baughman KL, Baumgartner WA, Van Dop C. Increase of the 40,000-mol wt pertussis toxin substrate

- (G protein) in the failing human heart. *J Clin Invest* 1988;82:189-197.
32. Feldman AM, Ray PE, Bristow MR. Expression of alpha-subunits of G proteins in failing human heart: a reappraisal utilizing quantitative polymerase chain reaction. *J Mol Cell Cardiol* 1991;23:1355-1358.
 33. El-Armouche A, Pohlmann L, Schlossarek S, Starbatty J, Yeh YH, Nattel S, Dobrev D, Eschenhagen T, Carrier L. Decreased phosphorylation levels of cardiac myosin-binding protein-C in human and experimental heart failure. *J Mol Cell Cardiol* 2007;43:223-229.
 34. Carr AN, Schmidt AG, Suzuki Y, del Monte F, Sato Y, Lanner C, Breeden K, Jing SL, Allen PB, Greengard P, Yatani A, Hoit BD, Grupp IL, Hajjar RJ, DePaoli-Roach AA, Kranias EG. Type 1 phosphatase a negative regulator of cardiac function. *Mol Cell Biol* 2002;22:4124-4135.
 35. Van Heerebeek L, Borbely A, Niessen HW, Bronzwaer JG, van der Velden J, Stienen GJ, Linke WA, Laarman GJ, Paulus WJ. Myocardial structure and function differ in systolic and diastolic heart failure. *Circulation* 2006;113:1966-1973.
 36. Neumann J, Eschenhagen T, Jones LR, Linck B, Schmitz W, Scholz H, Zimmermann N. Increased expression of cardiac phosphatases in patients with end-stage heart failure. *N.J Mol Cell Cardiol* 1997;29:265-272.
 37. Arai M, Alpert NR, Mac Lennan DH, Barton P, Petiasamy M. Alterations in sarcoplasmic reticulum gene expression in human heart failure A possible mechanism for alterations in systolic and diastolic properties of the failing myocardium. *Circ Res* 1993;72:463-469
 38. Flesch M, Schwinger RH, Schnabel P, Schiffer F, van Gelder I, Bavendiek U, Südkamp M, Kuhn-Regnier F, Böhm M. Sarcoplasmic reticulum Ca²⁺-ATPase and phospholamban mRNA and protein levels in end-stage heart failure due to ischemic or dilated cardiomyopathy. *J Mol Med* 1996;74:321-332.
 39. Gerdes AM, Capasso JM. Structural remodeling and mechanical dysfunction of cardiac myocytes in heart failure. *J Mol Cell Cardiol*. 1995; 27:849-56
 40. Anversa P, Ricci R, Olivetti G. Quantitative structural analysis of the myocardium during physiologic growth and induced cardiac hypertrophy: a review. *J Am Coll Cardiol*. 1986; 7:1140-1149
 41. Grossman W, Jones D, McLaurin LP. Wall stress and patterns of hypertrophy in the human left ventricle. *J Clin Invest*. 1975; 56:56-64
 42. Kass DA, Bronzwaer JG, Paulus WJ. What mechanisms underlie diastolic dysfunction in heart failure? *Circ Res* 2004;94:1533-1542
 43. Weber KT. Cardiac interstitium in health and disease: the fibrillar collagen network. *J Am Coll Cardiol* 1989;13:1637-1652.
 44. Parodi O, De Maria R, Oltrona L, Testa R, Sambuceti G, Roghi A, Merli M, Belingheri L, Accinni R, Spinelli F. Myocardial blood flow distribution in patients with ischemic heart disease or dilated cardiomyopathy undergoing heart transplantation. *Circulation* 1993;88:509-522
 45. Border WA, Noble AN. Transforming Growth Factor β in Tissue Fibrosis. *The N Engl J Med* 1994;331:1286-1292.
 46. Neumann J, Gupta RC, Schmitz W, Scholz H, Nairn AC, Watanabe AM. Evidence for isoproterenol-induced phosphorylation of phosphatase inhibitor-1 in the intact heart.

- Circ Res 1991;69:1450-1457.
47. Dally S, Bredoux R, Corvazier E, Andersen JP, Clausen JD, Dode L, Fanchaouy M, Gelebart P, Monceau V, Monte FD, Gwathmey JK, Hajjar R, Chaabane C, Bobe R, Raies A, Enouf J. Ca^{2+} -ATPases in non-failing and failing heart: evidence for a novel cardiac sarco/endoplasmic reticulum Ca^{2+} -ATPase 2 isoform (SERCA2c). *Biochem* 2006; 395: 249–258.

4

Myofilament Degradation and Dysfunction in Human Cardiomyocytes with Fabry Disease

Nazha Hamdani*, Cristina Chimenti*, Nicky M Boontje, Francesco DeCobelli,
Antonio Esposito, Jean GF Bronzwaer, Ger JM Stienen, Matteo A Russo,
Walter J Paulus, Andrea Frustaci, Jolanda van der Velden

The American Journal of Pathology 2008. 172:1482-1490. *Both authors contributed
equally

Abstract

Early detection of myocardial dysfunction in Fabry disease (FD) cardiomyopathy suggests possible compromise of myofilaments. Six males with untreated FD cardiomyopathy were submitted to cardiac studies, including Tissue Doppler imaging (TDI) and left ventricular endomyocardial biopsy. Active and resting tension before and after treatment with protein kinase A were determined in isolated Triton-permeabilized cardiomyocytes. Cardiomyocyte cross sectional area, area of glycosphingolipid vacuoles, myofibrilolysis and extent of fibrosis were also determined. Biopsies of donor hearts and mitral stenosis patients served as controls. Active tension was five times lower in FD cardiomyocytes and correlated with extent of myofibrilolysis. Resting tension was three times higher in FD than in controls. Protein kinase A treatment of FD cardiomyocytes decreased resting tension, but did not affect active force. Protein analysis revealed degradation products of troponin I and desmin. FD cardiomyocytes were significantly larger and filled with glycosphingolipids. Fibrosis was mildly increased compared with controls. TDI lengthening velocities were reduced in FD patients vs controls and correlated with resting tension. TDI shortening velocities were also reduced and correlated with active tension. In conclusion myofilament degradation and dysfunction appear as major determinants of FD cardiomyopathy. Partial reversal of cardiomyocytes high resting tension after protein kinase A suggests a potential benefit from enzyme replacement therapy and/or energy releasing agents.

Introduction

Fabry disease (FD) is an X linked lysosomal storage disorder caused by the deficiency of the enzyme α -galactosidase A, resulting in progressive intracellular glycosphingolipid deposition in multiple organ systems, including the heart.¹

In patients with FD, cardiac involvement is characterized by progressive left ventricular (LV) wall thickening, mimicking hypertrophic cardiomyopathy,²⁻³ with diastolic LV dysfunction and a preserved LV ejection fraction that may decline in the end stage of the disease.⁴ The diastolic LV dysfunction has usually been ascribed to myocardial fibrosis in addition to cardiomyocyte hypertrophy and engulfment by glycosphingolipids. Recently however, Tissue Doppler imaging (TDI) revealed reduced diastolic and systolic velocities even in the prehypertrophic phase of the disease,⁵ suggesting an early and direct involvement of cardiomyocyte function.

The present study therefore investigated in male patients with untreated FD active and resting tension of isolated cardiomyocytes, myofilament protein composition, myocardial collagen deposition and glycosphingolipids accumulation and correlated them with TDI myocardial long axis shortening and lengthening velocities.

Material and Methods

Patient population

From January 1996 to July 2005, 12 consecutive male patients with LV hypertrophy were diagnosed to have FD by means of biochemical, genetic and endomyocardial biopsy studies. Eight patients had not yet begun enzyme replacement therapy, 6 of them (47.1±8.3 yrs) had a complete clinical, morphometric and force measurement evaluation and constituted our patient population (Table 1). The patients belonged to unrelated families. Reduced peripheral blood alpha-galactosidase A activity was detected in all patients as previously described⁶ and causal mutations were identified by direct sequencing of alpha-galactosidase A gene in all families. The investigation conforms with the principles outlined in the Declaration of Helsinki.

Clinical studies

Extensive clinical examination, including the assessment of FD systemic manifestations, ECG, 2D echocardiography with Doppler analysis and cardiac magnetic resonance imaging (MRI) with late gadolinium enhancement, were performed in all patients. TDI analysis was performed in the pulsed Doppler mode to

record mitral annulus velocities at septal and lateral corners.^{5,7} Systolic (Sa), early diastolic (Ea) and late diastolic (Aa) velocities were measured and the E/Ea ratio was computed. Maximal wall thickness (MWT) was defined as the greatest thickness of any segment of the LV wall. Ten age-matched men with no evidence of LV hypertrophy or cardiac and systemic disease were used as controls. MRI was performed as previously described.⁷ Late enhancement assessment was performed 10-15 minutes after injection of gadolinium–DTPA (Shering AG) (0.2 mmol/kg of body weight), by using a 3D-Inversion Recovery T1-weighted sequence.

Cardiac catheterization and endomyocardial biopsy

All invasive studies were approved by the Ethical Committees of our Institutions and the patients provided written informed consent.

All FD patients underwent coronary and biventricular angiography with biventricular or LV endomyocardial biopsy. LV end-diastolic pressure >16 mm Hg was considered as indicative of LV diastolic dysfunction. Eight to 10 endomyocardial samples, approximately 3 mm³ each, were obtained from each patient. Five to 6 myocardial samples were processed for routine histological and histochemical analyses. Two samples were fixed in 2% glutaraldehyde in 0,1 M phosphate buffer (pH=7.3) and embedded in Epon resin; semi-thin sections were processed for Azur II staining and ultra-thin sections were stained with uranyl acetate and lead hydroxide for transmission electron microscopy (TEM).⁷ One-two endomyocardial biopsy samples were snap frozen in liquid nitrogen and used for cardiomyocyte force measurements and protein analysis.

Table 1. Characteristics of Fabry Disease Patients

A=arrhythmias; † CNS=central nervous system, AP=acroparesthesias, H=hypohidrosis; ‡ Values are the mean (± SD) results of three independent determinations on peripheral blood lymphocytes;§ EDP= left ventricular end diastolic pressure; ||LV=left ventricular, EDD=end diastolic diameter, MWT= maximal wall thickness, EF=ejection fraction; LVEDP= left ventricular end diastolic pressure; # MRI= Magnetic resonance imaging.

	Patient 1	Patient 2	Patient 3	Patient 4	Patient 5	Patient 6
Age (y)	50	46	53	58	41	35
Cardiac manifestations*	Dyspnea, Chest pain, A	Dyspnea, Chest pain, A	Dyspnea, Chest pain, A	Dyspnea, Chest pain, A	Dyspnea, Chest pain, A	Dyspnea, Chest pain, A
Extracardiac manifestations†	Skin, CNS, ears eyes, kidneys, H	Skin, CNS, ears eyes, kidneys, AP, H	Skin, eyes, kidneys, H	Eyes, ears, kidneys	Skin, eyes, ears, kidneys	Skin, CNS, eyes, ears, kidneys
Enzymatic activity‡ (nmol/hr/mg of protein)	70.3±9.6	20.9±1.5	79.2±8.5	50.2±5.6	23.1±2.6	15.2±0.8
LVEDP, mmHg§	26	24	21	19	20	22
Echocardiography						
LVEDD (mm)	49	46	44	43	45	40
MWT(mm)	20	21	23	19	18	18.5
LVEF (%)	50	51	67	65	63	65
Fractional shortening (%)	38	43	48	44	40	47
E/A ratio	0.82	0.93	0.91	0.89	0.94	0.95
Isovolumic relaxation time (ms)	115	110	108	111	107	108
E-wave deceleration time (ms)	285	270	275	240	205	210
<i>MRI data #</i>						
LV mass index, g/m ²	150.3	132.0	143.2	133.4	99.9	114.1
Late enhancement, %	6.7	6.3	4	7.4	1.6	7.9

Morphometric studies

Paraffin-embedded histologic sections stained with Masson's trichrome were examined at 400x magnification with a reticule containing 42 sampling points (105844, Wild Heerbrugg Instruments, Gals, Switzerland) to determine the percent area occupied by cardiomyocytes and by interstitial and replacement fibrosis.⁸

Cardiomyocyte cross sectional area was computed measuring the cardiomyocyte diameter across the nucleus in 50-100 cells cut transversely (78 ± 14 cells, range 58-97).⁹ At that level, the diameter of the perinuclear vacuoles was also measured and the percent cardiomyocyte area occupied by vacuoles was computed. In addition, endocardial thickness was determined. These measurements were performed in glutaraldehyde-fixed, Epon resin embedded, semi-thin sections stained with Azur II to visualize glycolipids droplets. Images of the histologic sections were analyzed using Lucia G software (version 4.82, Nikon, Japan).

Morphometric analysis of myofibrilolysis area was performed on ultra-thin sections, stained with uranyl acetate and lead hydroxide. Photographic negatives of TEM sections were analyzed using KS-300 software (Carl Zeiss Co, Germany, 1995).¹⁰ Ten surgical specimens of papillary muscles from age-matched male patients with mitral stenosis and normal LV function were used as normal controls for morphometric measurements.

Force Measurements in Isolated Cardiomyocytes

Biopsies were stored in liquid nitrogen for up to 41 months (20.2 ± 16.7 , range, 3 to 41 months). Previous studies have shown that these samples can be used for force measurements in single cardiomyocytes.¹¹ Force measurements were performed in mechanically isolated single cardiomyocytes of the six patients at 15°C as described previously.¹¹⁻¹³ The control group consisted of surgical biopsies from five age-matched male patients with mitral stenosis and normal LV end-diastolic pressure, chamber dimensions, and contractile function. Briefly, frozen biopsies were defrosted within 10 seconds in cold relaxing solution (in mmol/L: free Mg, 1; KCl, 100; EGTA, 2; MgATP, 4; imidazole, 10; pH7.0). Cells were mechanically isolated and incubated for 5 minutes in relaxing solution supplemented with 0.5% Triton X-100 to remove all membranes. Thereafter, cells were washed twice in relaxing solution and a single cardiomyocyte was attached between a force transducer and a piezoelectric motor using silicone adhesive (Fig 1, A and B). To enable attachment between the force transducer and motor single preparations were selected for measurements on the basis of cell length (~100 μm long). Resting sarcomere length of isolated

cardiomyocytes was $\sim 1.7 \mu\text{m}$ and was adjusted to $2.2 \mu\text{m}$ for measurements of isometric force. The composition of the relaxing [pCa ($-\log\{\text{Ca}^{2+}\}$), 9.0] and activating (pCa, 4.5) solution was previously described.¹⁴ All force values were normalized for cardiomyocyte cross-sectional area. A typical contraction-relaxation sequence in a cardiomyocyte from a Fabry sample is shown in Figure 1C. After curing of the glue for 50 minutes, the cardiomyocyte was transferred from the isolating solution on the mounting area to a small temperature-controlled well (volume, $80 \mu\text{l}$) containing relaxing solution. Isometric force was measured, after the preparation was transferred, by moving the stage of the inverted microscope to a temperature-controlled well containing activating solution.¹² On transfer of the cardiomyocyte from relaxing to activating solution, isometric force started to develop. Once a steady-state force level was reached, the cell was shortened within 1 ms to 80% of its original length to determine the base line of the force transducer. The distance between the base line and the steady force level is the total force (F_{total}). After 20 ms the cell was restretched and returned to the relaxing solution, in which a second slack-test of 10 seconds duration was performed to determine resting or passive force (F_{passive}). The difference between F_{total} and F_{passive} is the active force (F_{active}) developed by the cardiomyocyte. After measurements of F_{total} and F_{passive} , the cardiomyocytes were incubated for 40 minutes at 20°C in relaxing solution containing the catalytic subunit of protein kinase A (PKA) (100 U/ml, batch 12K7495; Sigma, Brooklyn, NY) and 6-mmol/L dithiothreitol (MP Biochemicals, Irvine, CA). Subsequently, force measurements were repeated. Control incubations in relaxing solution with 6 mmol/L dithiothreitol, but without PKA, did not alter F_{passive} and F_{active} of cardiomyocytes.

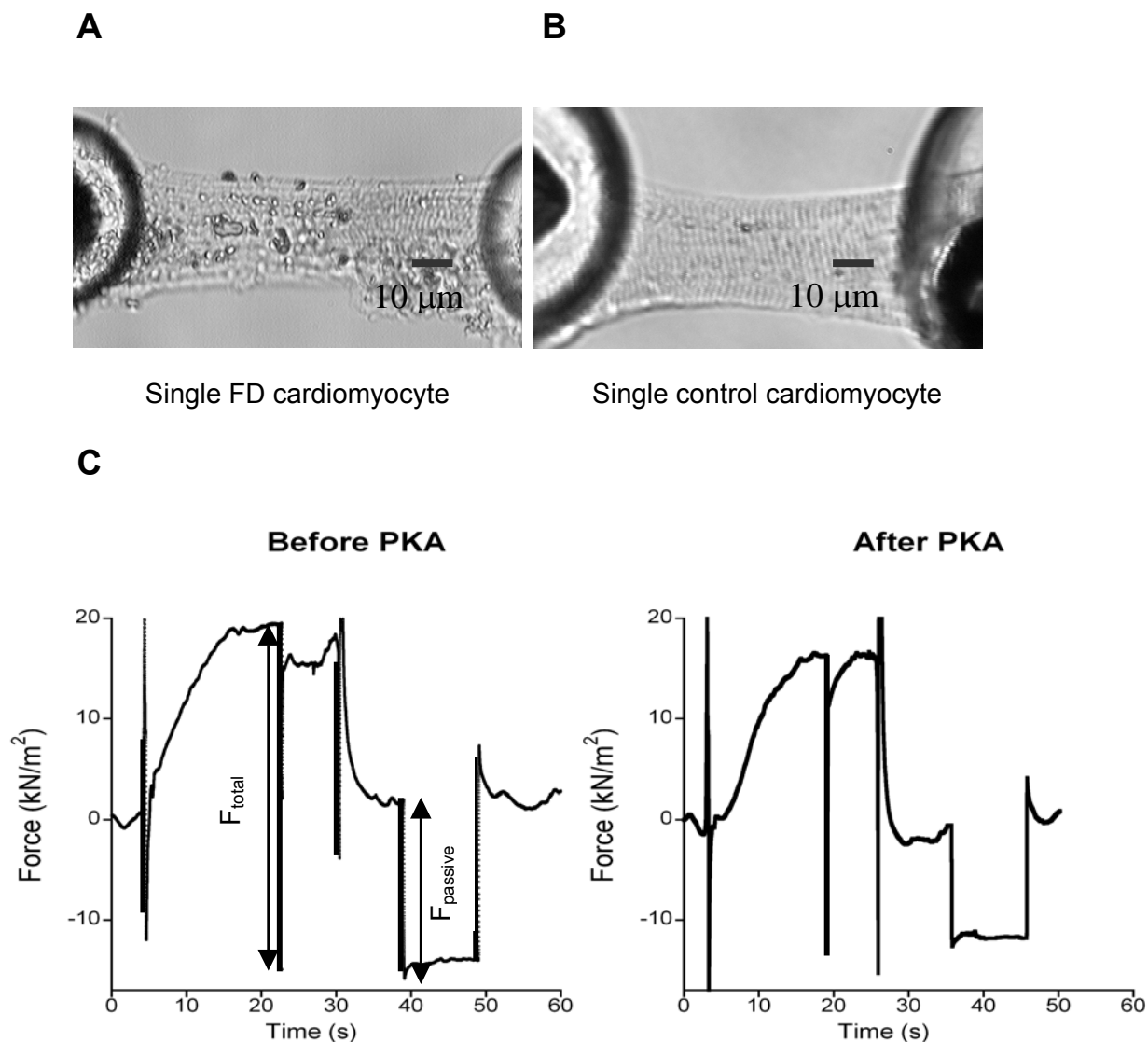


Figure 1. Single FD (A) and control (B) cardiomyocyte attached between a force transducer and a piezoelectric motor. C. Contraction-relaxation sequence in FD cardiomyocyte before (left) and after (right) treatment with PKA. The abrupt changes in force mark the transitions of the preparation through the interface between solution and air (i.e. transfers between wells containing relaxing and activating solutions).

Protein analysis

Protein analysis was performed on cardiomyocytes, which were not used for force measurements. After isolation and Triton treatment the remaining cell pellet was freeze dried and homogenized in sample buffer. To detect myofilament proteolysis, myofilament proteins were separated by one-dimensional gel electrophoresis containing 15% total acrylamide (acrylamide to bis-acrylamide ratio 37.5:1) followed by Western immunoblotting.¹⁵ Five μg (dry weight) of the tissue samples were applied

to the gels. Western immunoblot analysis was performed using specific monoclonal antibodies against troponin I (TnI) (clone 8I-7, Spectral Diagnostics Inc.; dilution 1:1000), desmin (clone DE-U-10, Sigma; dilution 1:1000), myosin light chain 1 (clone F109.16A12, Alexis biochemicals; dilution 1:200), myosin light chain 2 (clone F109.3E1, Alexis biochemicals; dilution 1:200) and α -actinin (clone EA-53, Sigma; dilution 1:1000) and signals were visualized using a secondary horseradish peroxidase-labeled goat-anti-mouse antibody and enhanced chemiluminescence (ECL plus Western blotting detection, Amersham Biosciences).

Statistical analysis

Normal distribution of variables was assessed with Kolmogorov Smirnov and Shapiro–Wilk tests. Variables showing normal distribution are presented as mean \pm SD. Variables not showing normal distribution are presented as median (interquartile range). Categorical variables are presented as proportions or percentages. Continuous variables, showing a normal distribution, were compared with Student t-test for independent samples (cases vs. controls). Continuous variables not showing a normal distribution were compared with Mann-Whitney test (cases vs. controls). Bivariate correlations were analyzed by Spearman rho coefficient computation. A two tailed $p < 0.05$ was considered statistically significant. Statistical analysis was performed with SPSS ver. 11.0.1 software (SPSS Inc., USA).

Results

Clinical studies

Patient's clinical characteristics, echocardiographic and MRI data are reported in Table 1. Alpha-galactosidase A activity was very low (mean value 43.4 \pm 7.4 nmol/h/mg of protein, normal range 3252-1623 nmol/h/mg of protein) and all patients had extra-cardiac clinical manifestations of the disease. All patients were normotensive, satisfied the ECG and echocardiographic criteria for LV hypertrophy, and showed an increase in LV mass index. Diastolic function was impaired in all patients but no restrictive filling pattern was detected. Conversely, systolic function, as measured by ejection fraction and fractional shortening, was within the normal range in all FD patients.

Gadolinium contrast-enhancement MRI study showed late enhancement in all patients typically localized in the basal or basal-medium segment of the lateral and infero-lateral wall (Fig 2A). Two patients (n°2 and n°6 of Table 1) showed additional

focal late enhancement in the apex. The mean percentage of myocardium involved was $5.7 \pm 2.4\%$ (range 1.6 to 7.9).

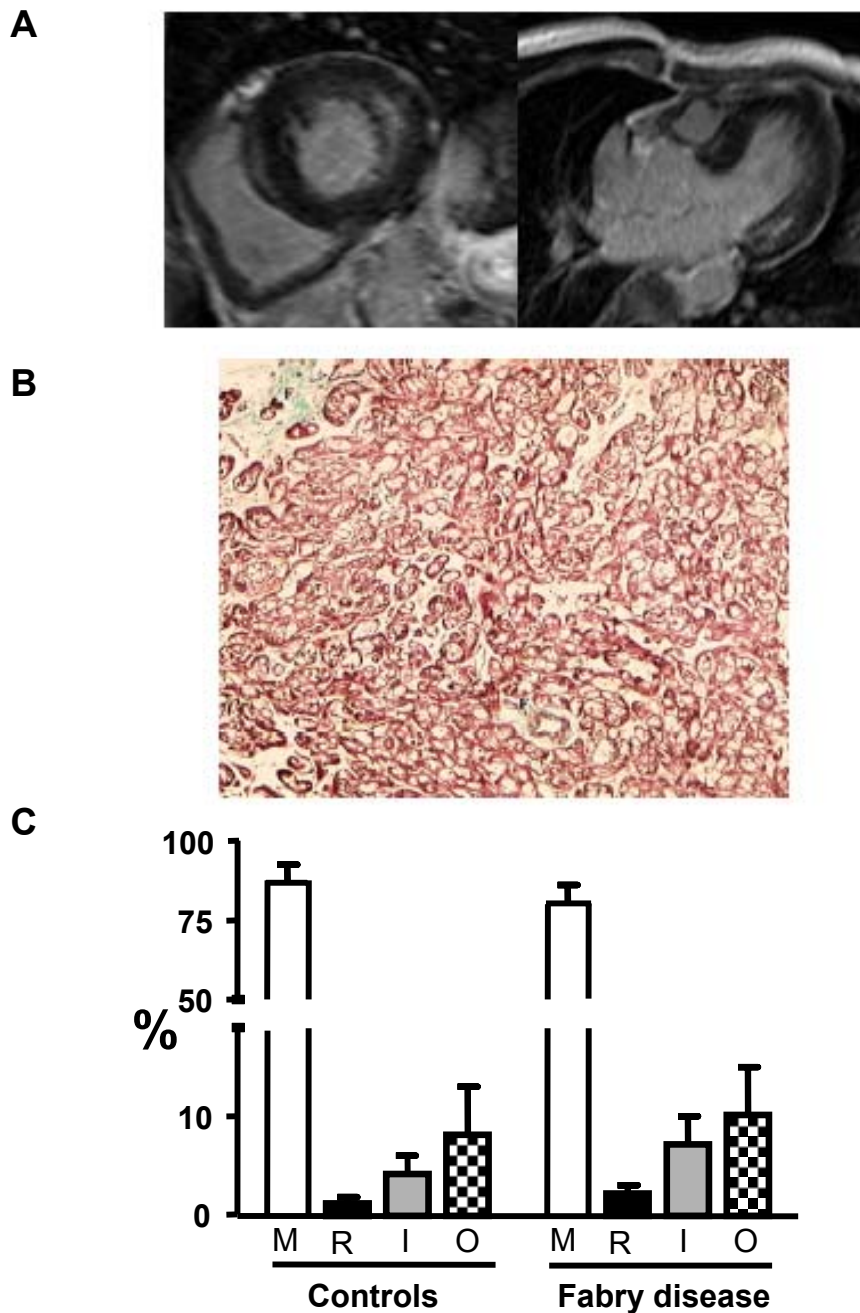


Figure 2. **A.** Cardiac MRI short (left) and long (right) axis view showing basal infero-lateral hyperenhancement in FD patient n°3 of Table 2. **B.** LV endomyocardial biopsy from the same patient showing mild interstitial and focal replacement fibrosis (F) and severe glycolipids engulfment of cardiomyocytes (Masson staining, magnification 40x). **C)** Volume composition of the myocardium in endomyocardial biopsies of FD compared with controls revealing no significant difference in percent of cardiomyocytes (M) and other interstitial components (O), while interstitial (IF) and replacement (RF) fibrosis showed a mild significant increase. Results are mean \pm SD. * $p < 0,05$ compared with controls.

On TDI examination all patients had significant reduction of long axis lengthening and shortening velocities measured at the septal and lateral corner of the mitral annulus (Table 2)

Table 2. TDI, morphometric and force measurements in patients with Fabry disease compared with controls

	Fabry disease	Controls *	p†
TDI velocities			
Septal Sa (cm/s)	5.9±0.4	14.6±1.2	<0.001
Septal Ea (cm/s)	5.7±0.5	15.5±1.3	<0.001
Septal Aa (cm/s)	6.0±0.5	10.3±0.9	<0.001
Septal E/Ea	11.2±0.5	6.0±1.3	<0.001
Lateral Sa (cm/s)	6.0±0.2	13.7±2	<0.001
Lateral Ea (cm/s)	5.9±0.4	14.0±0.4	<0.001
Lateral Aa (cm/s)	6.1±0.6	10.1±1.5	<0.001
Lateral E/Ea	10.5±0.3	5.8±1.2	<0.001
Morphometric data			
Fibrosis (%)	8.7±4.4	4.1±2.5	0.02
Interstitial	6.7±3.1	3.4±2.0	0.02
Replacement	1.9±1.5	0.7±0.6	0.03
Cardiomyocytes (%)	81.2±7.2	88.1±6.1	0.06
Cardiomyocyte area (µm ²)	861.0±208.4	215.4±90.1	<0.001
Cardiomyocyte area occupied by vacuoles (%)	57.3±4.1	0	<0.001
Myofibrilolysis area (%)	15.2±4.9	0	<0.001
Cardiomyocytes function			
F _{total} (kN/m ²)	13.7±3.9‡	17.6±5.3	NS
F _{active} (kN/m ²)	3.9±3.5	15.9±5.4	<0.001
F _{passive} (kN/m ²)	9.8±2.3‡	1.6±0.6	<0.001
F _{total} after PKA (kN/m ²)	11.1±2.6	18.2±5.4	0.02
F _{active} after PKA (kN/m ²)	4.3±3.3	16.8±5.4	<0.001
F _{passive} after PKA (kN/m ²)	6.6±2.6	1.4±0.6	<0.001

* Controls for TDI were n=10, for morphometric studies were n=10, for force measurements were n=8. † p values obtained comparing FD versus controls. ‡ p<0.001 versus after PKA treatment. Data are present as mean value ±SD; p<0.05 was considered statistically significant.

LV angiography revealed normal wall motion in all patients and coronary angiography showed absence of significant coronary stenoses.

On TDI examination all patients had significant reduction of long axis lengthening and shortening velocities measured at the septal and lateral corner of the mitral annulus (Table 2). LV angiography revealed normal wall motion in all patients and coronary angiography showed absence of significant coronary stenoses.

Histologic and morphometric studies

Histological examination of FD endomyocardial biopsies revealed regularly arranged and severely hypertrophied cardiomyocytes with large perinuclear vacuoles containing material that, on frozen sections, stained positively with periodic acid-Schiff and Sudan black stains. Fibrosis was predominantly interstitial (Fig 2B) with focal areas of replacement fibrosis. Computer-assisted histomorphometry showed only a mild, though significant, increase in fibrosis in FD patients compared to controls. The percent tissue area occupied by cardiomyocytes was similar (Fig 2C). Cardiomyocyte cross-sectional area was significantly increased in FD patients and more than 50% of it was occupied by glycosphingolipids vacuoles. The endocardium was thickened (mean FD value= 535 ± 201 μm , normal value= 18 ± 5 μm).

On ultrastructural electron microscopic examination intracellular vacuoles appeared to be represented by concentric lamellar structures in single-membrane bound vesicles, indicative of lysosomal glycosphingolipid accumulation. The cytoplasmic inclusions frequently displaced cardiac myofibrils to the periphery of the cell (Fig 3A). Focal areas of myofibrilolysis were also detected (Fig 3B) and myofibrilolysis area was calculated as $15\pm 5\%$. Lamellar inclusions were present also in the endothelial cells, smooth muscle cells and fibroblasts. Cardiomyocyte area and percent area occupied by glycolipid vacuoles closely correlated (correlation coefficient= 0.99 , $p < 0.0001$). This indicates that the increase of cardiomyocyte size is mainly due to intracytoplasmic glycosphingolipids vacuoles.

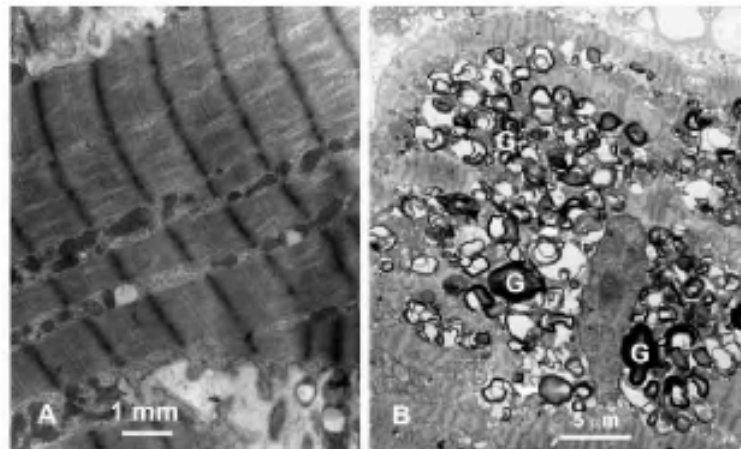
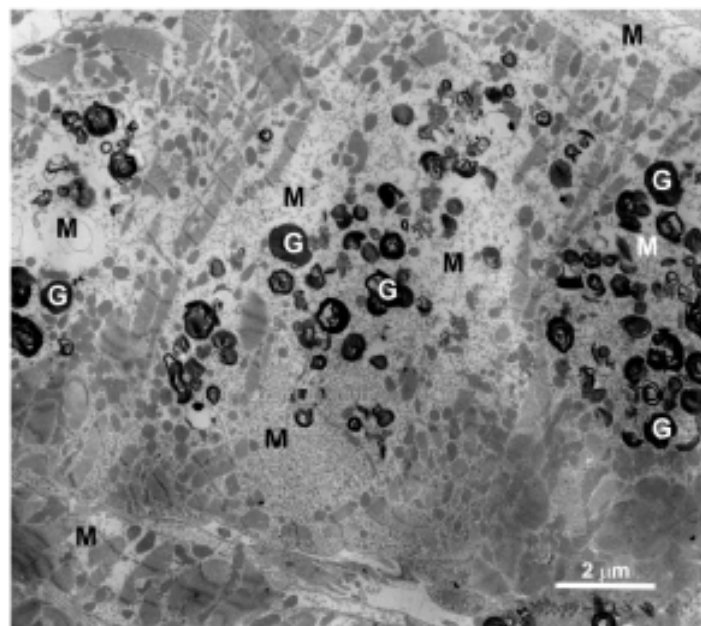
A**B**

Figure 3. A. Electron microscopy showing in comparison with the normal arrangement of myofilaments in a normal cardiomyocyte (A), myofilaments dislodgment and disarray due to glycosphingolipids accumulation in FD cardiomyopathy (B). **B.** Electron microscopy of FD cardiomyopathy showing myofibrilolysis areas (M) around glycolipid deposits (G).

Force measurements in isolated cardiomyocytes and protein analysis

Force measurement data of six FD patients (number of cardiomyocytes _ 17) and of five controls (number of cardiomyocytes _ 10) are presented in Table 2 as average value and in Table 3 as single patient value, in addition to the patients' gene mutation. When isolated cardiomyocytes were stretched to a sarcomere length of $2.2\mu\text{m}$ a significantly higher F_{passive} and a lower F_{active} was observed in FD patients compared to controls. Treatment with PKA significantly decreased F_{passive} , but it remained higher compared to controls. F_{active} was not altered (Fig 4A). PKA treatment did not alter F_{passive} and F_{active} in controls.

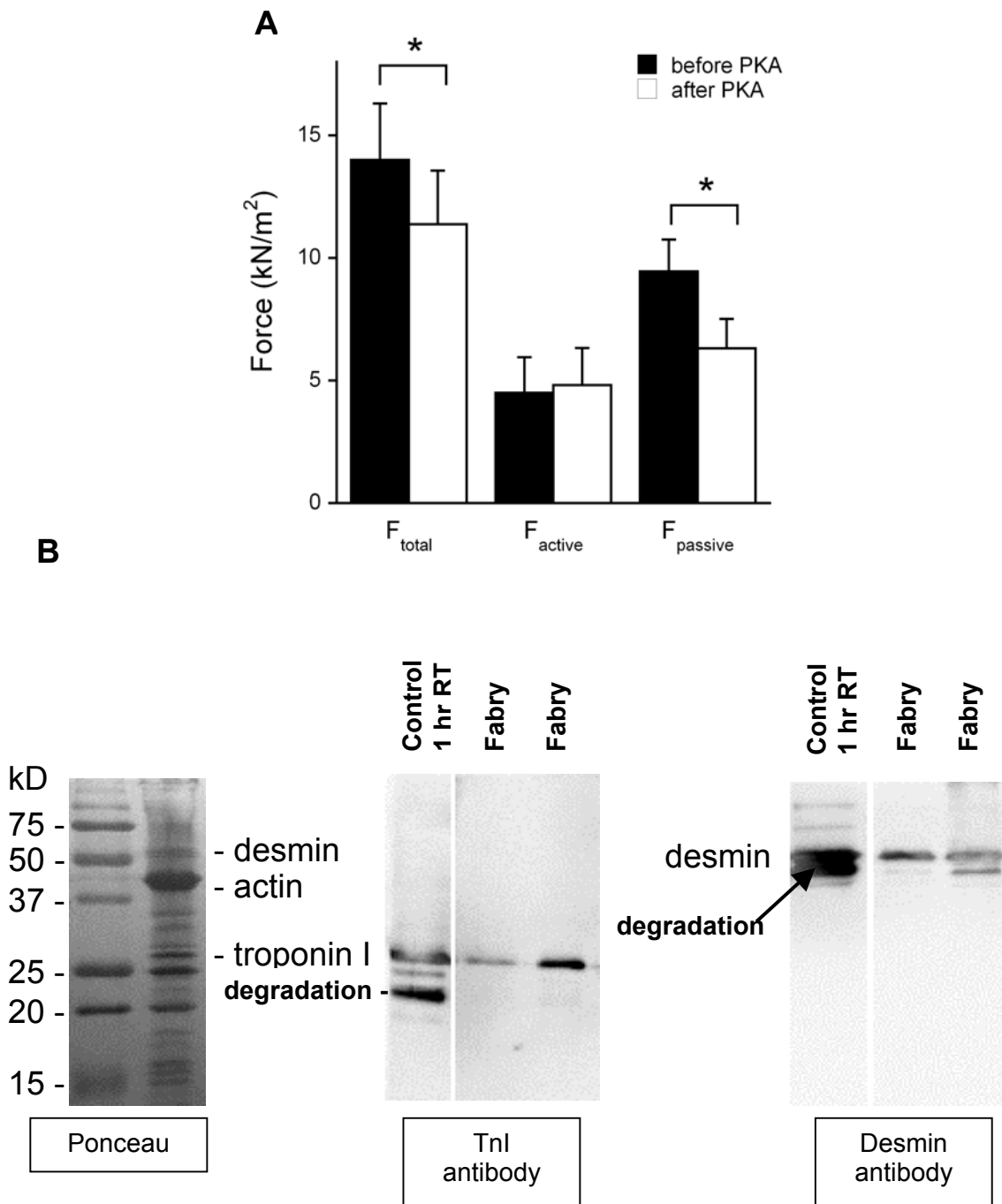


Figure 4. A. Graph showing total (F_{total}), active (F_{active}) and passive ($F_{passive}$) force before and after PKA in FD cardiomyocytes ($p=0.02$ total force before vs after, $p=0.4$ F_{active} before vs after $p=0.004$, $F_{passive}$ before vs after. **B.** Protein analysis using one-dimensional gel electrophoresis. Degradation products of TnI (left) and desmin (right) are shown in a control sample (non-failing donor heart), which was kept at 20°C for one hour. Similar degradation products were found in FD samples.

Analysis of myofilament proteolysis revealed degradation products of TnI and desmin in FD patients (Fig 4B). No degradation products of myosin light chains or of α -actinin were observed. Degradation of TnI was found in three of six samples and amounted on average to $3.1 \pm 1.4\%$ of total TnI (Table 3). Desmin degradation products were present in four of six samples and amounted to $9.7 \pm 5.8\%$ of total desmin (Table 3).

Table 3. α -Gal A mutations, force measurements, and protein analysis in Fabry disease patients

Patient	α -Gal A mutation	Force before PKA (kN/m ²)			Force after PKA (kN/m ²)			Tnl degradation (%)	Desmin degradation (%)
		F _{total}	F _{active}	F _{passive}	F _{total}	F _{active}	F _{passive}		
1	M42fsX55 ¹⁶	14.9	1.2	13.7	11.4	1.5	9.9	0.0	28.6
2	D315fsX315 ¹⁶	12.0	1.7	10.3	11.0	1.3	9.7	0.0	0.0
3	Y216C*	9.2	2.0	7.3	9.1	3.1	6.0	7.9	2.2
4	N215S ¹⁷	15.6	5.6	10.0	13.2	6.2	6.0	5.3	27.4
5	R220X ¹⁸	10.4	2.9	7.6	7.4	3.7	3.7	0.0	0.0
6	Q279K ¹⁹	19.9	10.3	9.6	14.4	10.0	4.4	5.2	0.3

Correlation between TDI, morphometric and force measurements

To establish if alterations in cardiac systolic and diastolic function could be ascribed to changes in morphometry or myofilament function or a combination of both, in vivo measurement of cardiac function by TDI were correlated with fibrosis, cardiomyocyte area, percent area of glycosphingolipids vacuoles and myofilament F_{active} and $F_{passive}$.

The average F_{active} of each individual correlated with TDI shortening velocities at both corners of the mitral annulus (Fig 5A and B; correlation coefficient=0.99, $p<0.001$, for septal Sa and 0.90, $p<0.05$, for lateral Sa). The average of $F_{passive}$ of all cardiomyocytes of each individual correlated closely with TDI long axis lengthening velocities (Fig 5C and D; correlation coefficient=0.99, $p<0.001$, for septal E/Ea and 0.94, $p<0.05$ for lateral E/Ea).

F_{active} inversely correlated with myofibrilolysis area (Fig 5E, correlation coefficient=0.94, $p<0.05$). After PKA treatment, $F_{passive}$ closely correlated with area of glycosphingolipid deposits (Fig 5 F, correlation coefficient= 0.99, $p<0.001$).

TDI lengthening and shortening velocities did not correlate with cardiomyocyte area, percent area occupied by glycosphingolipids vacuoles and extent of fibrosis.

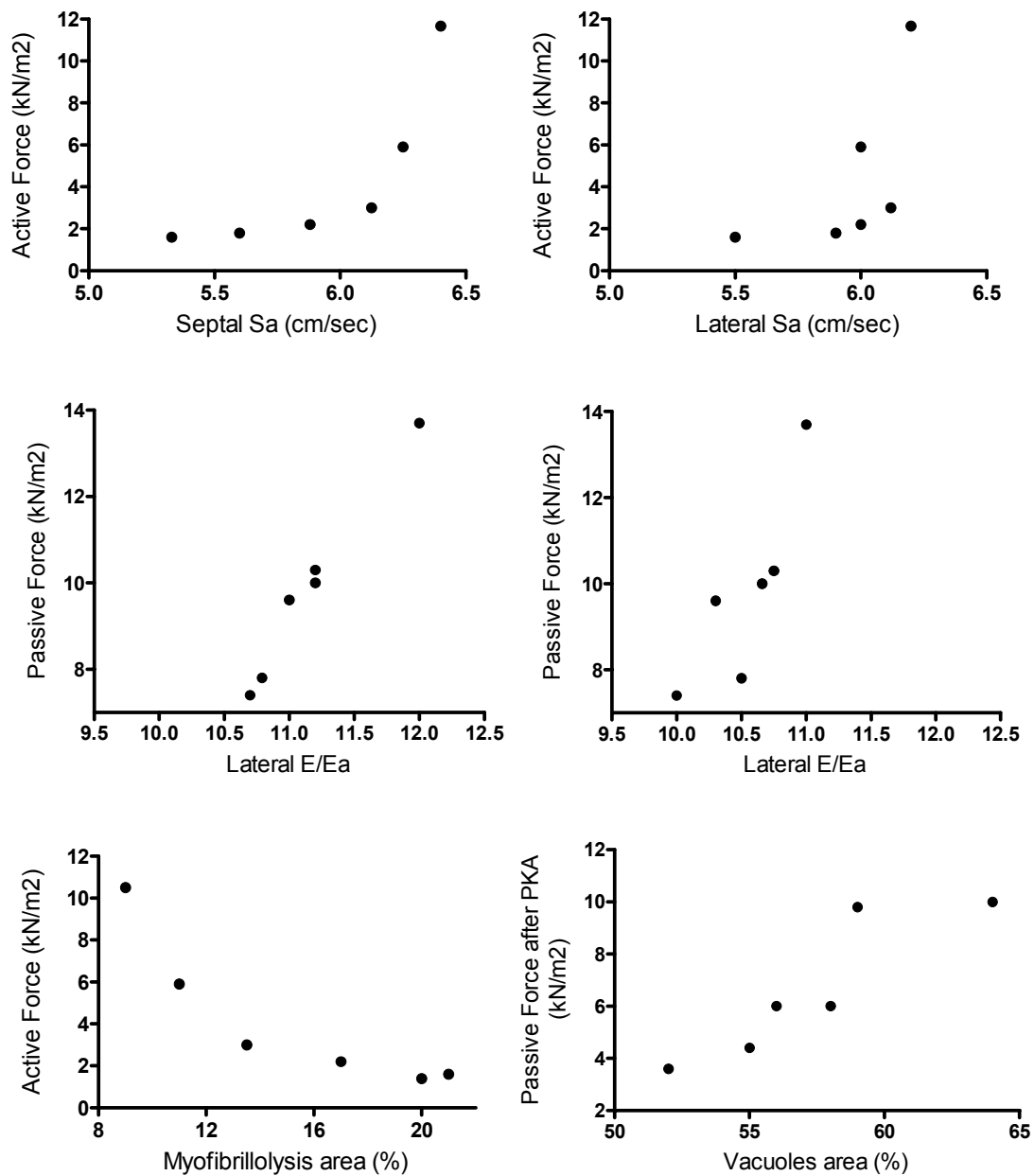


Figure 5. Scatter plot of the correlations between active force and septal Sa (**A**, correlation coefficient=0.99, $p<0.001$), active force and lateral Sa (**B**, correlation coefficient 0.90, $p<0.05$), passive force and septal E/Ea (**C**, correlation coefficient=0.99, $p<0.001$), passive force and lateral E/Ea (**D**, correlation coefficient=0.94, $p<0.05$), active force and myofibrilolysis area (**E**, correlation coefficient=0.94, $p<0.05$), passive force after PKA treatment and area of glycosphingolipid vacuoles (**F**, correlation coefficient=0.99, $p>0.001$).

Discussion

Recent studies^{5,20} using TDI imaging provided evidence for diastolic and systolic LV dysfunction in FD patients even before the development of wall thickening. The basis of these functional abnormalities, which become more prominent as LV hypertrophy progresses, is still unclear. Especially the relative contribution of myocardial fibrosis and cardiomyocyte dysfunction remains uncertain. The present study therefore analyzed mechanical properties of isolated cardiomyocytes, degree of glycosphingolipid accumulation, and myocardial fibrosis in endomyocardial biopsy samples of FD patients and correlated these parameters with TDI evaluation of LV function. Altered cardiomyocyte relaxation and contraction, derived mainly from myofilament degradation and dysfunction, was found to be a major determinant of FD cardiomyopathy. These preliminary data, obtained in a limited number of patients, generate new hypotheses on myocardial dysfunction of FD and open new areas of research for possible additional therapeutic strategies.

Compromise of cardiomyocyte contractility in fabry cardiomyopathy

Despite a normal LV ejection fraction on routine echocardiography, TDI and strain rate echocardiography^{5,20} demonstrated reduced contractility in FD cardiomyopathy and suggested an early global and regional systolic function deficit, progressively deteriorating in untreated patients. To clarify the mechanism of the contractile deficit we evaluated the maximal isometric tension of single cardiomyocytes and demonstrated that it was reduced. Moreover it correlated with the decreased TDI systolic velocities and with the ultrastructural evidence of myofibrillolysis.

In addition, myofibrillolysis was associated with degradation of myofilament proteins. In several models of ischemia/reperfusion the decrease in maximal force of the myofilaments has been ascribed to degradation of TnI. TnI degradation may be triggered by activation of the calcium-dependent protease calpain-121 or by increased preload²² and has been observed in human ischemic cardiac disease.²³ Moreover, degradation of desmin was shown to play a significant role in calpain-1-induced myofilament dysfunction²⁴ and desmin degradation has been demonstrated to correlate with reduced cardiac function in ischemic human heart failure.²⁵ Because degradation products of both TnI and desmin were observed in FD biopsies, and were paralleled by ultrastructural evidence of myofibrillolysis, part of the reduction in cardiomyocyte contractility may be explained by proteolysis. An additional obstacle to cell contraction is represented by myofilament derangement

resulting from intracellular glycosphingolipid storage that causes loss of vectorial orientation and a detrimental functional effect. Whatever the mechanism of myofilament and cell dysfunction, they can trigger at the end, similarly to hypertrophic cardiomyopathy,²⁶ trophic stimuli leading to cell hypertrophy. Indeed, it has been recently shown in FD patients the presence of circulating growth-promoting factors²⁷ able to induce in vitro a hypertrophic response of cardiomyocytes. In substance, opposite biological events of myofilament degradation/dysfunction and synthesis, in attempt of structural and functional cell repair, occur in human cardiomyocytes with FD. In this regard, the elevation of electrocardiography voltages associated to disease progression is partially attributable to synthesis of contractile elements and possibly to the accumulation of glycosphingolipids intracellularly and on the plasma membrane,²⁸ affecting the intracellular resistivity to the activation wave front and the conduction velocity.

Increased cardiomyocyte stiffness in fabry cardiomyopathy

The present study showed F_{passive} of isolated cardiomyocytes to be six times higher in FD patients than in controls. In vivo measures of LV diastolic function, such as TDI long axis lengthening velocity correlated with the in vitro measurements of F_{passive} . This indicated that in Fabry cardiomyopathy diastolic LV dysfunction is related to cardiomyocyte stiffening. These data are in agreement with recent studies on diastolic heart failure, which reported involvement of cardiomyocyte stiffness in the pathogenesis of diastolic LV dysfunction.^{13,29} Because the endomyial collagen structure was removed and the integrity of sarcolemmal and sarcoplasmic membranes was disrupted during cardiomyocyte isolation and permeabilization, the increased F_{passive} cannot be related to modifications of sarcoplasmic proteins and/or channels, but should be ascribed to alterations in myofilament or cytoskeletal proteins.

Modifications of contractile and cytoskeletal proteins may be posttranslational and involve altered phosphorylation, oxidative changes, and proteolysis. Cardiac relaxation is enhanced via β -adrenergic activation of PKA and subsequent phosphorylation of myofilament proteins including Tnl, myosin binding protein C, and titin. Partial correction of F_{passive} after PKA treatment suggests hypophosphorylation of these PKA target proteins, but the incomplete recovery of F_{passive} after PKA treatment implied additional intracellular mechanisms to account for the altered passive properties of the cardiomyocytes. Because glycosphingolipid deposits occupied more than half of the cardiomyocyte area and because they were organized in structurally

complex concentric lamellar bodies, they probably hinder cardiomyocyte relaxation. The percent area occupied by glycosphingolipid vacuoles indeed closely correlated with increased F_{passive} after PKA treatment. Thus, our results suggest that increased stiffness of cardiomyocytes contributes to diastolic dysfunction in FD cardiomyopathy. This increased stiffness is explained both by mechanical hindrance because of the glycosphingolipid storage material and by hypophosphorylation of myofilament and/or cytoskeletal proteins.

Role of fibrosis

Although fibrosis in endomyocardial tissue increased with progression of FD cardiomyopathy and was paralleled by expansion of cardiomyocyte area and glycosphingolipid vacuoles, its extent was only slightly increased compared with controls and did not correlate with TDI measurements of systolic or diastolic LV function. In addition, late myocardial MRI gadolinium enhancement, which is ascribed to focal fibrosis,³⁰ was mild and typically localized in the infero-lateral region of the left ventricle, with little involvement of the remaining LV segments. However, because fibrosis is unequally distributed along the LV wall, the percent detected in the endomyocardium is compatible with the presence of different, yet limited, amounts in the middle and subepicardial layers.

In summary, myocardial fibrosis does not appear to be the predominant mechanism causing diastolic dysfunction in FD cardiomyopathy with preserved LV contractility. Nevertheless, the limited number of patients studied requires to be cautious in the interpretation of these negative results and do not exclude a prominent role of myocardial fibrosis in the more advanced stages of the disease.

Clinical implications and conclusions

Cardiomyocyte dysfunction and structural alterations of myofilaments seem to significantly contribute to the LV dysfunction observed in FD cardiomyopathy. Prospective studies using sequential endomyocardial biopsies during enzyme replacement therapy could establish the reversibility of cardiomyocyte dysfunction and structural myofilament alteration. Partial reversal of the high cardiomyocyte resting tension after PKA could provide an inroad for pharmacological correction of the diastolic LV dysfunction observed in FD.

References

1. Desnick RJ, Ioannou YA, Eng CM. Alpha-Galactosidase A deficiency: Fabry disease. In: Scriver CR, Beaudet AL, Sly WS, Valle D, Kinzler KE, Vogelstein B, eds. *The Metabolic and Molecular Bases of Inherited Disease*. New York: McGraw-Hill; 2001. p. 3733-3774.
2. Sachdev B, Takenaka T, Teraguchi H, Tei C, Lee P, McKenna WJ, Elliott PM. Prevalence of Anderson-Fabry disease in male patients with late onset hypertrophic cardiomyopathy. *Circulation* 2002; 105:1407-1411.
3. Chimenti C, Pieroni M, Morgante E, Antuzzi D, Russo A, Russo MA, Maseri A, Frustaci A. Prevalence of Fabry disease in female patients with late-onset hypertrophic cardiomyopathy. *Circulation* 2004; 110:1047-1053.
4. Weidemann F, Breunig F, Beer M, Sandstede J, Stork S, Voelker W, Ertl G, Knoll A, Wanner C, Strotmann JM. The variation of morphological and functional cardiac manifestation in Fabry disease: potential implications for the time course of the disease. *Eur Heart J* 2005; 26:1221-1227.
5. Pieroni M, Chimenti C, Ricci R, Sale P, Russo MA, Frustaci A. Early detection of Fabry cardiomyopathy by Tissue Doppler imaging. *Circulation* 2003;107:1978–1984.
6. Frustaci A, Chimenti C, Ricci R, Natale L, Russo MA, Pieroni M, Eng CM, Desnick RJ. Improvement in cardiac function in the cardiac variant of Fabry's disease with galactose-infusion therapy. *N Engl J Med* 2001; 345:25–32.
7. Pieroni M, Chimenti C, F DeCobelli, E Morgante, Gaudio C, M A Russo, Frustaci A. Fabry cardiomyopathy: echocardiographic detection of endomyocardial glycosphingolipids compartmentalization. *JACC* 2006; 47:1663-1671.
8. Olivetti G, Melissari M, Capasso JM, Anversa P. Cardiomyopathy of the aging human heart: myocyte loss and reactive cellular hypertrophy. *Circ Res* 1991; 68:1560-1568.
9. Anversa P, Olivetti G. Cellular basis of physiological and pathological myocardial growth. In: Page E, Fozzard HA, Solaro RJ, editors. *Handbook of Physiology. The cardiovascular system. The heart*. Oxford University Press; 2002. p.75-144.
10. Frustaci A, Perrone GA, Gentiloni N, Russo MA. Morphometry and GH/IGF-1 axis deficiency may identify a form of dilated cardiomyopathy which is corrected by recombinant human growth hormone (rHGH). Reversible dilated cardiomyopathy due to growth hormone deficiency. *Am J Clin Pathol* 1992; 97:503-511.
11. Van der Velden J, Klein LJ, Zaremba R, Boontje NM, Huybregts MA, Stoker W, Eijssman L, de Jong JW, Visser CA, Visser FC, Stienen GJM. Effects of calcium, inorganic phosphate, and pH on isometric force in single skinned cardiomyocytes from donor and failing human hearts. *Circulation* 2001; 104:1140-1146.
12. Van der Velden J, Klein LJ, van der Bijl M, Huybregts MAJM, Stoker W, Witkop J, Eijssman L, Visser CA, Visser FC, Stienen GJM. Force production in mechanically isolated cardiac myocytes from human ventricular muscle tissue. *Cardiovasc Res* 1998; 38: 414-423.
13. Borbély A, van der Velden J, Papp Z, Papp Z, Édes I, Stienen GJM, Paulus WJ. Cardiomyocyte stiffness in diastolic heart failure. *Circulation* 2005; 111:774–781.
14. Papp Z, Szabo A, Barends JP, Stienen GJM. The mechanism of the force enhancement by MgADP under simulated ischaemic conditions in rat cardiac myocytes. *J Physiol* 2002; 543:177-189.

15. van der Velden J, Merkus D, Klarenbeek BR, James AT, Boontje NM, Dekkers DH, Stienen GJM, Lamers JM, Duncker DJ: Alterations in myofilament function contribute to left ventricular dysfunction in pigs early after myocardial infarction. *Circ Res* 2004, 95:e85–e95
16. Morrone A, Cavicchi C, Bardelli T, Antuzzi D, Parini R, Di Rocco M, Feriozzi S, Gabrielli O, Barone R, Pistone G, Spisni C, Ricci R, Zammarchi E: Fabry disease: molecular studies in Italian patients and X inactivation analysis in manifesting carriers. *J Med Genet* 2003, 40:e103
17. Eng CM, Resnick-Silverman LA, Niehaus DJ, Astrin KH, Desnick RJ: Nature and frequency of mutations in the alpha-galactosidase A gene that cause Fabry disease. *Am J Hum Genet* 1993, 53:1186–1197
18. Meaney C, Blanch LC, Morris CP. A nonsense mutation (R220X) in the alpha-galactosidase A gene detected in a female carrier of Fabry disease. *Hum Mol Genet* 1994; 3:1019-1020.
19. Dominissini S, Cariati R, NevvjelM, Guerci V, Ciana G, Bembi B, Pittis MG. Comparative in vitro expression study of four Fabry disease causing mutations at glutamine 279 of the alpha-galactosidase A protein. *Hum Hered* 2004; 57:138-41.
20. Weidemann F, Breunig F, Beer M, Sandstede J, Turschner O, Voelker W, Ertl G, Knoll A, Wanner C, Strotmann JM. Improvement of cardiac function during enzyme replacement therapy in patients with Fabry disease: a prospective strain rate imaging study. *Circulation* 2003; 108:1299-1301.
21. Di Lisa F, De Tullio R, Salamino F, Barbato R, Melloni E, Siliprandi N, Schiaffino S, Pontremoli S. Specific degradation of troponin T and I by mu-calpain and its modulation by substrate phosphorylation. *Biochem J* 1995; 308:57-61.
22. Feng J, Schaus BJ, Fallavollita JA, Lee TC, Canty JM, Jr. Preload induces troponin I degradation independently of myocardial ischemia. *Circulation* 2001; 103:2035-2037.
23. McDonough JL, Labugger R, Pickett W, Tse MY, MacKenzie S, Pang SC, Atar D, Ropchan G, Van Eyk JE. Cardiac troponin I is modified in the myocardium of bypass patients. *Circulation* 2001; 103:58-64.
24. Papp Z, van der Velden J, Stienen GJM. Calpain-I induced alterations in the cytoskeletal structure and impaired mechanical properties of single myocytes of rat heart. *Cardiovasc Res* 2000; 45:981-993.
25. Di Somma S, Di Benedetto MP, Salvatore G, Agozzino L, Ferranti F, Esposito S, La Dogana P, Scarano MI, Caputo G, Cotrufo M, Santo LD, de Divitiis O. Desmin-free cardiomyocytes and myocardial dysfunction in end stage heart failure. *Eur J Heart Fail* 2004; 6:389-398.
26. Marian AJ. Pathogenesis of diverse clinical and pathological phenotypes in hypertrophic cardiomyopathy. *Lancet* 2000; 355:58-60.
27. Barbey F, Brakch N, Linhart A, Rosenblatt-Velin N, Jeanrenaud X, Oanadli S, Steinmann B, Burnier M, Palecek T, Bultas J, Hayoz D. Cardiac and vascular hypertrophy in Fabry disease: evidence for a new mechanism independent of blood pressure and glycosphingolipid deposition. *Arterioscler Thromb Vasc Biol* 2006; 26:839-844.
28. Askari H, Kaneski CR, Semino-Mora C, Desai P, Ang A, Kleiner DE, Perlee LT, Quezado M, Spollen LE, Wustman BA, Schiffmann R: Cellular and tissue localization of globotriaosylceramide in Fabry disease. *Virchows Arch* 2007, 451:823–834

29. van Heerebeek L, Borbely A, Niessen HW, Bronzwaer JG, van der Velden J, Stienen GJM, Linke WA, Laarman GJ, Paulus WJ. Myocardial structure and function differ in systolic and diastolic heart failure. *Circulation* 2006; 113:1966-1973.
30. Moon JC, Sachdev B, Elkington AG, McKenna WJ, Mehta A, Pennell DJ, Leed PJ, Elliott PM. Gadolinium enhanced cardiovascular magnetic resonance in Anderson-Fabry disease. Evidence for a disease specific abnormality of the myocardial interstitium. *Eur Heart J* 2003; 24:2151-2155.

5

Distinct Myocardial Effects of Beta-Blocker Therapy in Heart Failure with Normal and Reduced Left Ventricular Ejection Fraction

Nazha Hamdani, Walter J Paulus, Loek van Heerebeek, Attila Borbély, Nicky
M. Boontje, Marian J. Zuidwijk, Jean G.F. Bronzwaer, Warner S. Simonides,
Hans W. M. Niessen, Ger J. M. Stienen, Jolanda van der Velden

Abstract

Left ventricular (LV) myocardial structure and function differ in heart failure (HF) with normal (N) and reduced (R) LV ejection fraction (EF). This difference could underlie the unequal outcome of trials with β -blockers in HFNEF and HFREF with mixed results observed in HFNEF and positive results in HFREF. To investigate if β -blockers have distinct myocardial effects in HFNEF and HFREF, myocardial structure, cardiomyocyte function and myocardial protein composition were compared in HFNEF and HFREF patients without or with β -blockers.

Patients, free of coronary artery disease, were divided into β ⁻_{HFNEF} (n=16), β ⁺_{HFNEF} (n=16), β ⁻_{HFREF} (n=17) and β ⁺_{HFREF} (n=22) groups. Using LV endomyocardial biopsies, we assessed collagen volume fraction (CVF) and cardiomyocyte diameter (MyD) by histomorphometry, phosphorylation of myofilamentary proteins by ProQ-Diamond phosphostained 1D-gels and expression of β -adrenergic signaling and calcium handling proteins by Western immunoblotting. Cardiomyocytes were also isolated from the biopsies to measure active force (F_{active}), resting force ($F_{passive}$) and calcium sensitivity (pCa_{50}).

Myocardial effects of β -blocker therapy were either shared by HFNEF and HFREF, unique to HFNEF or unique to HFREF. Higher F_{active} , higher pCa_{50} , lower phosphorylation of troponin I and myosin-binding protein C, and lower β_2 -adrenergic receptor expression were shared. Higher $F_{passive}$, lower CVF, lower MyD and lower expression of stimulatory G protein were unique to HFNEF and lower expression of inhibitory G protein was unique to HFREF.

Myocardial effects unique to either HFNEF or HFREF could contribute to the dissimilar outcome of β -blocker therapy in both HF phenotypes.

Introduction

Over the last two decades it became evident that more than 50% of all heart failure patients suffer of heart failure with normal left ventricular (LV) ejection fraction (EF).¹ In heart failure with normal LVEF (HFNEF) and in heart failure with reduced LVEF (HFREF), LV structure adapts differently with concentric LV remodeling in HFNEF and eccentric LV remodeling in HFREF.²⁻⁴ Corresponding differences were observed at the myocardial ultrastructural level with prominent cardiomyocyte hypertrophy in HFNEF and low myofibrillar density in HFREF.⁴ When cardiomyocytes were isolated from LV myocardium, cardiomyocyte resting tension (F_{passive}) was also higher in HFNEF than in HFREF.⁴⁻⁶ These structural and functional differences between LV myocardium in HFNEF and HFREF could underlie the unequal outcome of trials using β -blockers, angiotensin converting enzyme inhibitors (ACE-I) or angiotensin II receptor blockers (ARB) which usually yielded positive results in HFREF and mixed results in HFNEF. In line with this unequal outcome of trials, prognosis of HFREF patients improved over the last two decennia whereas no such trend was observed in HFNEF patients.¹ Large clinical trials have convincingly shown that β -blocker therapy reduces mortality and improves LV function in HFREF patients.⁷⁻⁹ In HFNEF patients, favourable effects of β -blocker therapy on mortality and LV function have not been convincingly demonstrated. After hospital discharge, HFNEF patients had improved survival when using β -blockers¹⁰ and in a community-based registry, carvedilol use was accompanied by similar 1 year mortality in HFNEF and HFREF patients but less reduction in hospitalizations in HFNEF patients.¹¹ In the SWEDIC trial, carvedilol had no effect on mortality or hospitalizations but ameliorated E/A ratio of HFNEF patients.¹² In a similar study however, 6 months of atenolol use had no effect on diastolic LV function of HFNEF patients with unchanged pulmonary capillary wedge pressure.¹³ Because of these inconsistent results, the use of β -blockers in

HFNEF patients is further evaluated in clinical trials such as the Japanese DHF study.¹⁴ To investigate if heart failure therapy has indeed disparate effects on LV myocardial structure and function in HFNEF and HFREF, the present study compared LV myocardial structure, function and protein composition in HFNEF and HFREF patients with and without β -blockers. The current widespread use of ACE-I precluded a similar comparison in patients with and without ACE-I. Endomyocardial biopsies procured in the four patient groups were used for: 1) histomorphometry of light and electron microscopic images to determine cardiomyocyte diameter, collagen volume fraction and myofibrillar density; 2) isolation of single cardiomyocytes to

measure active force (F_{active}), resting force (F_{passive}) and Ca^{2+} -sensitivity (pCa_{50}) and 3) protein analysis to assess phosphorylation of myofibrillar proteins and expression of proteins involved in β -adrenergic signaling and in Ca^{2+} -handling.

Material and Methods

Patients

All patients included in the study ($n=71$) had been hospitalized for worsening heart failure and were referred for cardiac catheterization and LV biopsy procurement because of suspicion of infiltrative or inflammatory myocardial disease. No patient had significant ($>50\%$) coronary artery stenoses, a history of myocardial infarction, percutaneous coronary intervention or coronary bypass surgery. Histological analysis of the biopsies showed no myocardial infiltration or inflammation. Patients were classified as HFREF if $\text{LVEF}<40\%$ and as HFNEF if $\text{LVEF}>50\%$ and $\text{LVEDP}>16$ mmHg.¹ Patients with a $\text{LVEF}>40\%$ but $<50\%$ were not included. Patients were considered as being on chronic β -blocker therapy if therapy was initiated at least 1 month prior to biopsy procurement. The mean duration of β -blocker therapy was similar in both groups (HFNEF: 12 ± 3 months; HFREF: 12 ± 4 months). Half of the patients on β -blocker therapy were using a non-selective β -blocker (carvedilol) and half were using a selective β -blocker (metoprolol, bisoprolol). Characteristics of the $\beta_{\text{-HFNEF}}$, $\beta_{\text{+HFNEF}}$, $\beta_{\text{-HFREF}}$, and $\beta_{\text{+HFREF}}$ groups are given in Table 1. Indications for β -blocker therapy in the HFNEF patients were control of arterial hypertension ($n=14$) and/or a history of atrial tachyarrhythmias ($n=4$). Most of the $\beta_{\text{-HFREF}}$ patients ($14/17$) were started on β -blocker therapy after the study. At the time of study all patients were in normal sinus rhythm. Hemodynamic data were derived from LV angiograms (LVEDVI , LVEF) and high-fidelity LV pressure catheters (LVPSP , LVEDP , $\text{LVdP/dt}_{\text{max}}$, $\text{LVdP/dt}_{\text{min}}$). LV wall thickness was derived from 2D-echocardiograms. Hemodynamic and echocardiographic data were combined to determine LV Mass Index (LVMI). After procurement, LV endomyocardial biopsies ($n=6$ per patient; ± 3.5 mg wet weight each) were fixated in formalin or stored in liquid nitrogen. The local ethics committee approved the study protocol of Vrij Universiteit medical center (Vumc). Written informed consent was obtained from all patients, and there were no complications related to catheterization or biopsy procurement. The investigation conforms with the principles outlined in the Declaration of Helsinki [Cardiovasc Res 1997;35:2–4].

Table 1. Clinical, hemodynamic and echocardiographic characteristics.

	β^-_{HFNEF}	β^+_{HFNEF}	β^-_{HFREF}	β^+_{HFREF}	<i>P</i>		
					β^- vs β^+	HFNEF vs HFREF	Interaction
N	16	16	17	22			
Age (y)	66±3	68±4	54±5	60±3	NS	0.01	NS
Sex (M/F)	11/5	8/8	10/7	17/5	NS	NS	NS
Hypertension	11/16	11/16	4/17	1/22	NS	<0.0001	NS
Diabetes Mellitus	8/16	3/16	6/17	8/22	NS	NS	NS
Obesity (BMI > 30 kg/m ²)	6/16	4/16	4/17	2/22	NS	NS	NS
Medication							
ACE-I	9	7	12	15	NS	NS	NS
Diuretic	12	9	14	18	NS	NS	NS
CCB	5	3	0	3	NS	0.04	NS
ARB	3	4	0	1	NS	0.03	NS
Digoxin	1	4	4	8	NS	NS	NS
Amiodarone	3	2	1	4	NS	NS	NS
Statin	4	6	2	5	NS	NS	NS
Nitrate	2	0	0	1	NS	NS	NS
Hemodynamics							
Heart rate (bpm)	77±3	70±3	89±5	72±5	0.008	NS	NS
LVPSP (mmHg)	169±7	168±10	120±4	116±5	NS	<0.0001	NS
LVEDP (mmHg)	29± 2	25±2	25±2	20±2	0.02	0.01	NS
LVEDVI (mL/m ²)	81±5	79±4	127±8	133±7	NS	<0.0001	NS
LVEF (%)	53±4	63±3	31±2	30±2	NS	<0.0001	NS
LVdP/dt _{max} (mmHg/s)	1547±111	1480±110	938±200	902±100	NS	0.0005	NS
LVdP/dt _{min} (mmHg/s)	1655±171	1752±67	1058±229	1000±116	NS	0.0007	NS
Echocardiography							
LVWT (mm)	11.4±0.6	11.3±0.2	9.5±0.4	8.8±0.4	NS	<0.0001	NS
LVMi/LVEDVI ratio	1.8±0.1	1.7±0.1	1.1±0.1	1.1±0.1	NS	<0.0001	NS

Abbreviations: n, number of patients; M, male; F, female; BMI, Body Mass Index; ACE-I, angiotensin-converting-enzyme-inhibitors; CCB, calcium channel blockers; ARB, angiotensin II receptor blockers; bpm, beats per minute; LVPSP: LV peak systolic pressure; LVEDP: LV end-diastolic pressure; LVEDVI: LV end-diastolic volume index; LVWT: LV wall thickness; LVMI: LV mass index.

Quantitative histomorphometry

Light microscopy

Histomorphological analysis of biopsies was performed on elastica-von-Giesson and hematoxylin-eosin stained, 4 μm thick, sections of tissue placed in 4% buffered formaldehyde solution.^{2,3} Images of these sections were acquired using a projection microscope (x50). Subsequent image analysis, using Slidebook™ 4.0 software (3I, Denver, Co), was performed to determine cardiomyocyte diameter (MyD, μm) and extent of reactive interstitial fibrosis, which was expressed as collagen volume fraction (CVF, %). Areas of reparative and perivascular fibrosis were excluded. As previously validated,^{2,4} MyD was determined perpendicularly to the outer contour of the cell membrane at nucleus level in 15 representative myocytes of the section, and CVF was calculated as the sum of all connective tissue areas divided by the sum of all connective tissue and muscle areas averaged over 4-6 representative fields of the section.^{2,4} In our laboratory, normal values of MyD and CVF for LV endomyocardial biopsy material are $13.1 \pm 0.3 \mu\text{m}$ and $5.4 \pm 2.2 \%$ respectively.

Electron microscopy

Endomyocardial biopsies were fixed in 2% (v/v) gluteraldehyde for 30 min and 1.5% (w/v) osmium tetroxide for 10 min, dehydrated with acetone and embedded in Epon812. Ultrathin sections were collected on 300-mesh Formavar-coated Nickel-grids. The sections were contrasted with uranyl acetate and lead citrate and were examined in a Jeol-1200EX electron microscope. Quantitative analysis was performed with the above mentioned automated image analyzer. Cardiomyocyte myofibrillar density (FibD) was calculated as the sum of myofibrillar areas related to total cellular area in 4-6 representative myocytes, and expressed as a percentage.

Force measurements in isolated cardiomyocytes

Force measurements were performed in single, mechanically isolated cardiomyocytes as described previously.²⁻⁴ Biopsy samples were defrosted in relaxing solution (in mmol/L: free Mg, 1; KCl, 100; EGTA, 2; MgATP, 4; imidazole, 10; pH7.0), mechanically disrupted and incubated for 5 minutes in relaxing solution

supplemented with 0.5% Triton X-100 to remove all membrane structures. Subsequently, cells were washed twice in relaxing solution, after which single cardiomyocytes were attached with silicone adhesive between a force transducer and a motor (2.7 ± 0.2 cardiomyocytes per patient). Sarcomere length of isolated cardiomyocytes was adjusted to $2.2 \mu\text{m}$ and myocytes were subjected to both relaxing and activating solutions (Fig 2A). Their pCa ($-\log_{10}[\text{Ca}^{2+}]$) ranged from 9.0 (relaxing) to 4.5 (maximal activation), which was used to calculate maximal calcium-activated isometric force. All force values were normalized for cardiomyocyte cross-sectional area. Exposure to a series of solutions with intermediate pCa yielded the baseline force-pCa relation. On transfer of the myocyte from relaxing to activating solution, isometric force started to develop. Once a steady force level was reached, the cell was shortened within 1 ms to 80% of its original length (slack test) to determine the baseline of the force transducer. The distance between the baseline and the steady force level is the total force (F_{total}) (Fig 2B). After 20 ms, the cell was restretched and returned to the relaxing solution, in which a second slack test of 10-seconds' duration was performed to determine passive F_{passive} . The difference between F_{total} and F_{passive} equalled F_{active} . Ca^{2+} -sensitivity of the contractile apparatus (pCa_{50}) corresponded to the pCa, at which F_{active} reached 50% of the value observed at maximal activation. After measurement of the baseline force-pCa relation, myocytes were incubated for 40 minutes in relaxing solution supplemented with the catalytic subunit of protein kinase A (PKA, 100 U/mL; Sigma, batch-12K7495) and 6 mmol/L dithiothreitol (DTT, MP-Biochemicals). Subsequently, a second force-pCa relation was determined. In our laboratory, F_{passive} , F_{active} and pCa_{50} of normal human cardiomyocytes are $3.5 \pm 0.4 \text{ kN/m}^2$, $20.7 \pm 3.1 \text{ kN/m}^2$ and 5.82 ± 0.02 respectively.

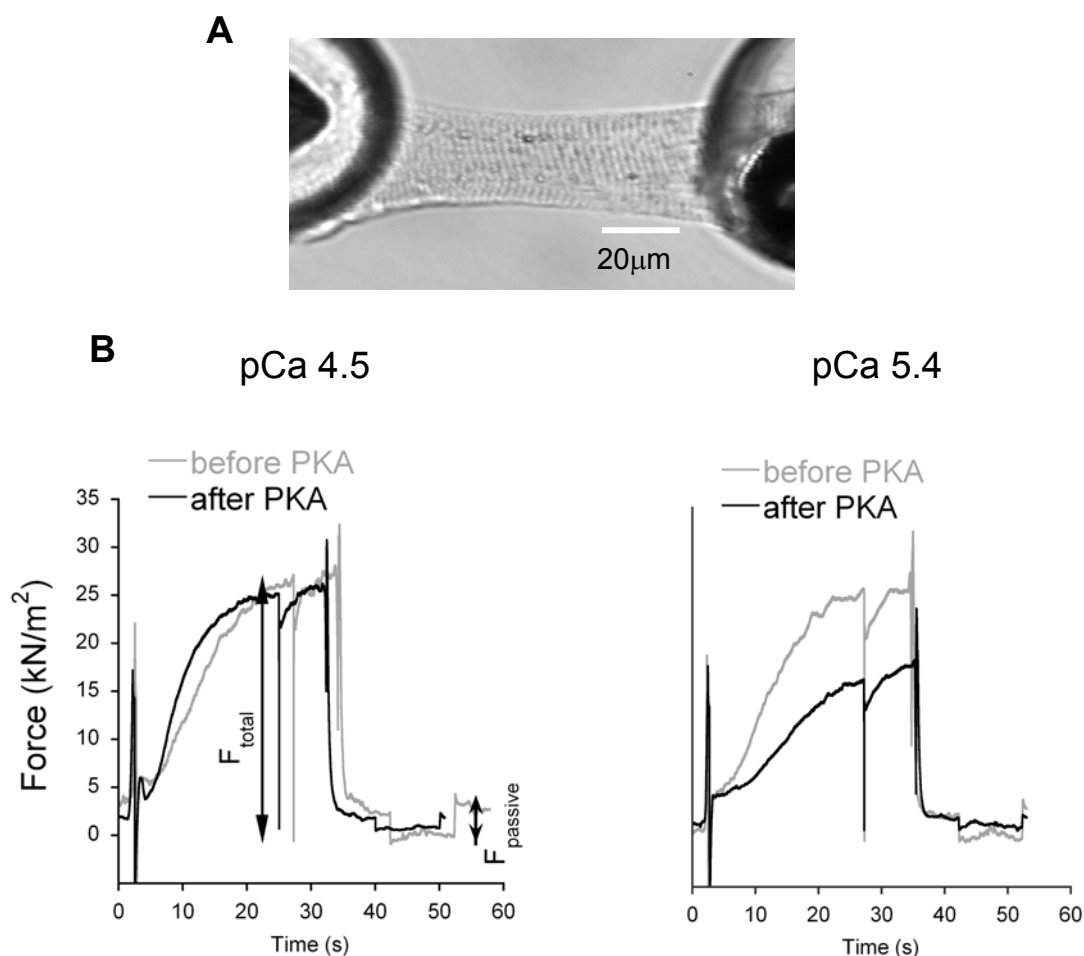


Figure 2. **A.** Single cardiomyocyte from a HFREF patient glued between a force transducer and a piezoelectric motor; **B.** Contraction-relaxation sequence recorded in a single cardiomyocyte of a HFREF patient before (black line) and after (grey line) treatment with PKA, during maximal activation (pCa 4.5) and submaximal activation (pCa 5.4).

Protein analysis

Myofilament protein phosphorylation

Myofilament protein phosphorylation was determined using Pro-Q Diamond Phosphoprotein Stain.⁵ To preserve the endogenous phosphorylation status, frozen biopsies were homogenized in liquid nitrogen and resuspended in 1 mL cold 10% trichloroacetic acid solution (TCA; dissolved in acetone containing 0.1% (w/v) dithiothreitol (DTT)). TCA-treated tissue pellets were homogenized in sample buffer containing 15% glycerol, 62.5 mmol/L Tris (pH 6.8), 1% (w/v) SDS and 2% (w/v) DTT (final concentration 2.5 μg dry weight/ μL). Tissue samples (20 μg dry weight/lane) were separated on gradient gels (Criterion tris-HCl 4-15% gel, BioRad) and proteins were stained for one hour with Pro-Q Diamond Phosphoprotein Stain. Fixation,

washing and de-staining were performed according to the manufacturer's guidelines (Molecular Probes). Subsequently gels were stained overnight with SYPRO Ruby stain (Molecular Probes). Phosphorylation status of myofilament proteins was expressed relative to the SYPRO-stained myosin binding protein-C (MyBP-C) band to correct for differences in sample loading and expressed in arbitrary units (a.u.). Staining was visualized using the LAS-3000 Image Reader (FUJI; 460 nm/605 nm Ex/Em) and signals were analyzed with AIDA.

β-Adrenergic signaling proteins

Protein expression levels of β_1 adrenoreceptor (AR), β_2 AR, G-protein-coupled receptor kinases (GRK2 and GRK5), stimulatory G protein (G_s) and inhibitory G protein (G_i) were analyzed by one-dimensional 15% SDS-polyacrylamide gel electrophoresis (1D-PAGE) and subsequent Western immunoblotting. Samples (dry weight) were applied in a concentration, which was within the linear range of detection: 25 μ g for β_1 AR and β_2 AR, 20 μ g for GRK2, GRK5, and G_i and 10 μ g for G_s . After 1D separation proteins were transferred to Hybond-ECL nitrocellulose membranes. Blots were pre-incubated with 0.5% milk powder in TTBS (Tween-tris-buffered-saline; 10 mmol/L Tris-HCl pH 7.6, 75 mmol/L NaCl, 0.1% Tween) for one hour at room temperature. The blots were incubated overnight at 4°C with primary rabbit polyclonal antibodies (Santa Cruz) against β_1 AR (dilution 1:200; sc-568), β_2 AR (dilution 1:200; sc-9042), GRK2 (dilution 1:1000; sc-562), GRK5 (dilution 1:1000; sc-565), G_s ($G_{\alpha s/olf}$; dilution 1:1000; sc-383) and against G_i ($G_{\alpha i-3}$; dilution 1:1000; sc-262). After washing with TTBS, primary antibody binding was visualized using a secondary horseradish peroxidase-labeled goat-anti-mouse antibody (dilution 1:2000; DakoCytomation) and enhanced chemiluminescence (ECL plus Western blotting detection, Amersham Biosciences). All signals were normalized to actin (dilution 1:1000; clone KJ43A; Sigma) stained on the same blots

Calcium handling proteins

Sarcoplasmic reticular Ca^{2+} -ATPase (SERCA2a) protein levels were determined immunochemically by dot-blot analysis. Briefly, homogenate tissue samples (typically 0.5 μ g total protein) and standard SERCA2a protein samples were spotted onto a nitrocellulose membrane. The blot was then incubated with a 1:2500 dilution of a polyclonal antiserum to SERCA2a and subsequently with ^{125}I -labeled anti-rabbit immunoglobulin G (0.05 μ g/ml, specific activity 7 μ Ci/ μ g). To detect phospholamban (PLB), expression blots were incubated with a 1:2500 dilution of a monoclonal mouse

antibody (Affinity Bioreagents) and subsequently with ^{125}I -labeled anti-mouse immunoglobulin G. Blots were exposed to Phosphor Imager screens, which were then scanned and spots were quantified using ImageQuant software (Molecular Dynamics).

Data analysis

Values are given as mean \pm SEM of the observations in each patient group. Data of the β ⁻_{HFNEF}, β ⁺_{HFNEF}, β ⁻_{HFREF}, and β ⁺_{HFREF} groups were compared by 2-factor ANOVA testing for β -blocker use, HFNEF/HFREF status, and their interaction (Tables 1-2). Subsequent comparisons (β ⁻_{HFREF} versus β ⁺_{HFREF} and β ⁻_{HFNEF} versus β ⁺_{HFNEF}) were performed with a Bonferroni adjusted *t* test.

Results

Clinical and hemodynamic characteristics

Clinical, hemodynamic and echocardiographic data are presented in Table 1. Patients on β -blocker therapy had lower heart rate and LVEDP in both HFNEF and HFREF groups. HFNEF patients were older and more frequently suffered of arterial hypertension with a concomitant higher use of calcium channel and angiotensin II receptor blockers. HFNEF patients also had higher LVPSP, LVEDP, LVEF, LVdP/dt_{max}, LVdP/dt_{min}, LVWT, LVMI/LVEDVI ratio and smaller LVEDVI.

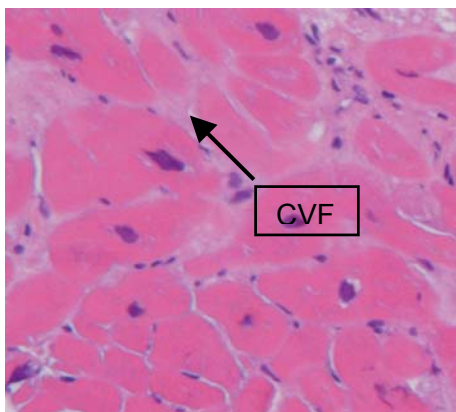
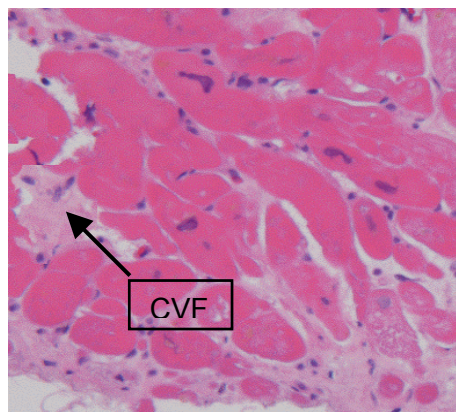
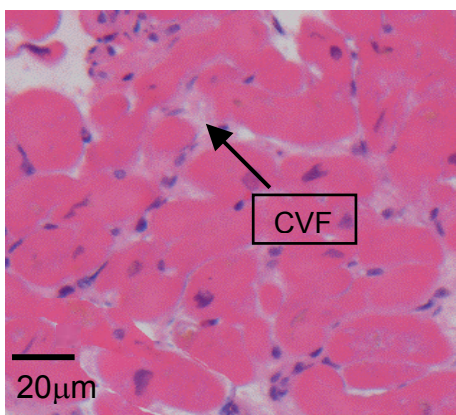
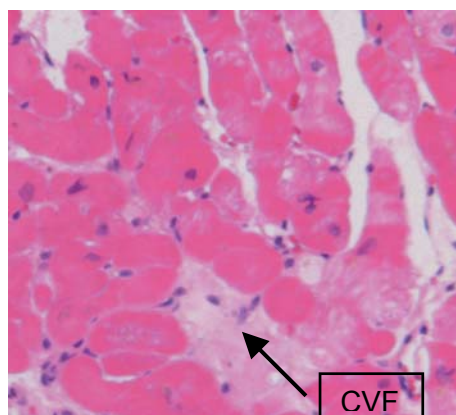
Table 2. Histomorphometry, cardiomyocyte force measurements, and protein analysis.

Abbreviations: pTnI, Phosphorylated Troponin I; pTnT, Phosphorylated Troponin T; pMyBP-C, Phosphorylated myosin-binding protein C; pDesmin, Phosphorylated Desmin; pMLC-2, Phosphorylated myosin light chain-2.

Histomorphometry							
	β^-_{HFNEF}	β^+_{HFNEF}	β^-_{HFREF}	β^+_{HFREF}	β^- vs β^+	HFNEF vs HFREF	Interaction
CVF (%)	13.2±0.3	10.8±0.2	15.9±0.2	16.7±0.3	0.0007	<0.0001	<0.0001
MyD (μm)	20.7±0.5	18.7±0.3	16.5±0.3	16.0±0.3	<0.0001	<0.0001	0.04
FibD (%)	43.2±1.2	42.8±1.4	34.1±1.0	34.2±1.0	NS	<0.0001	NS
Cardiomyocyte Force Measurements							
Before PKA							
F_{active} (kN/m ²)	13.2±1.7	17.7±1.2	15.1±2.0	17.0±1.7	0.01	NS	NS
F_{passive} (kN/m ²)	5.6±0.8	8.0±0.7	4.7±0.3	4.8±0.3	0.03	0.0006	0.02
pCa ₅₀	5.83±0.02	5.86±0.02	5.82±0.01	5.87±0.01	0.01	NS	NS
<i>After PKA</i>							
F_{active} (kN/m ²)	15.5±1.6	18.2±1.4	17.4±2.2	19.9±2.1	NS	NS	NS
F_{passive} (kN/m ²)	3.0±0.4	5.1±0.6	2.7±0.2	3.0±0.3	0.001	0.0007	0.01
pCa ₅₀	5.54±0.04	5.66±0.03	5.54±0.02	5.54±0.02	0.007	0.01	0.009
Phosphorylation of Myofilament Proteins							
pTnl (a.u.)	0.20±0.03	0.15±0.01	0.39±0.09	0.18±0.06	0.02	NS	NS
pTnT (a.u.)	1.03±0.13	1.15±0.13	1.14±0.13	0.90±0.11	NS	NS	NS
pMyBP-C (a.u.)	0.26±0.02	0.23±0.01	0.26±0.02	0.21±0.02	0.01	NS	NS
pDesmin (a.u.)	0.86±0.10	1.01±0.07	1.06±0.10	0.79±0.09	NS	NS	0.046
pMLC-2 (a.u.)	0.34±0.04	0.38±0.04	0.37±0.10	0.41±0.08	NS	NS	NS
Expression of the β-Adrenergic Signaling Proteins							
β_1 AR (a.u.)	0.45±0.09	0.35±0.06	0.9±0.18	0.8±0.2	NS	0.01	NS
β_2 AR (a.u.)	0.32±0.15	0.28±0.13	0.33±0.05	0.18±0.02	0.01	NS	NS
GRK2 (a.u.)	0.89±0.25	0.84±0.20	3.6±1.2	3.2±0.9	NS	0.004	NS
GRK5 (a.u.)	9.4±1.8	9.3±2.3	40.0±8.3	29.9±9.0	NS	0.0006	NS
Gs (a.u.)	4.0±0.9	1.5±0.2	1.4±0.3	1.1±0.2	0.03	0.03	0.09
Gi (a.u.)	0.80±0.20	0.70±0.16	1.75±0.20	1.02±0.25	0.04	0.001	0.1
Expression of Calcium Handling Proteins							
SERCA2a	10.2±1.7	8.8±1.9	10.1±3.2	7.5±1.9	NS	NS	NS
PLB	19.3±2.6	22.6±2.9	15.3±3.5	18.8±6.9	NS	NS	NS

Histomorphometry

Histomorphometric data are summarized in Table 2 and Figure 1. Myocardial CVF was significantly lower in HFNEF than in HFREF ($p < 0.0001$) and only in HFNEF was β -blocker therapy associated with lower myocardial CVF ($p = 0.0007$). MyD was significantly higher in HFNEF than in HFREF ($p < 0.0001$) and only in HFNEF was β -blocker therapy associated with reduced MyD ($p < 0.0001$). FibD was also higher in HFNEF than HFREF ($p < 0.0001$) but was unrelated to β -blocker therapy.

A β^- HFNEF β^- HFREF β^+ HFNEF β^+ HFREF

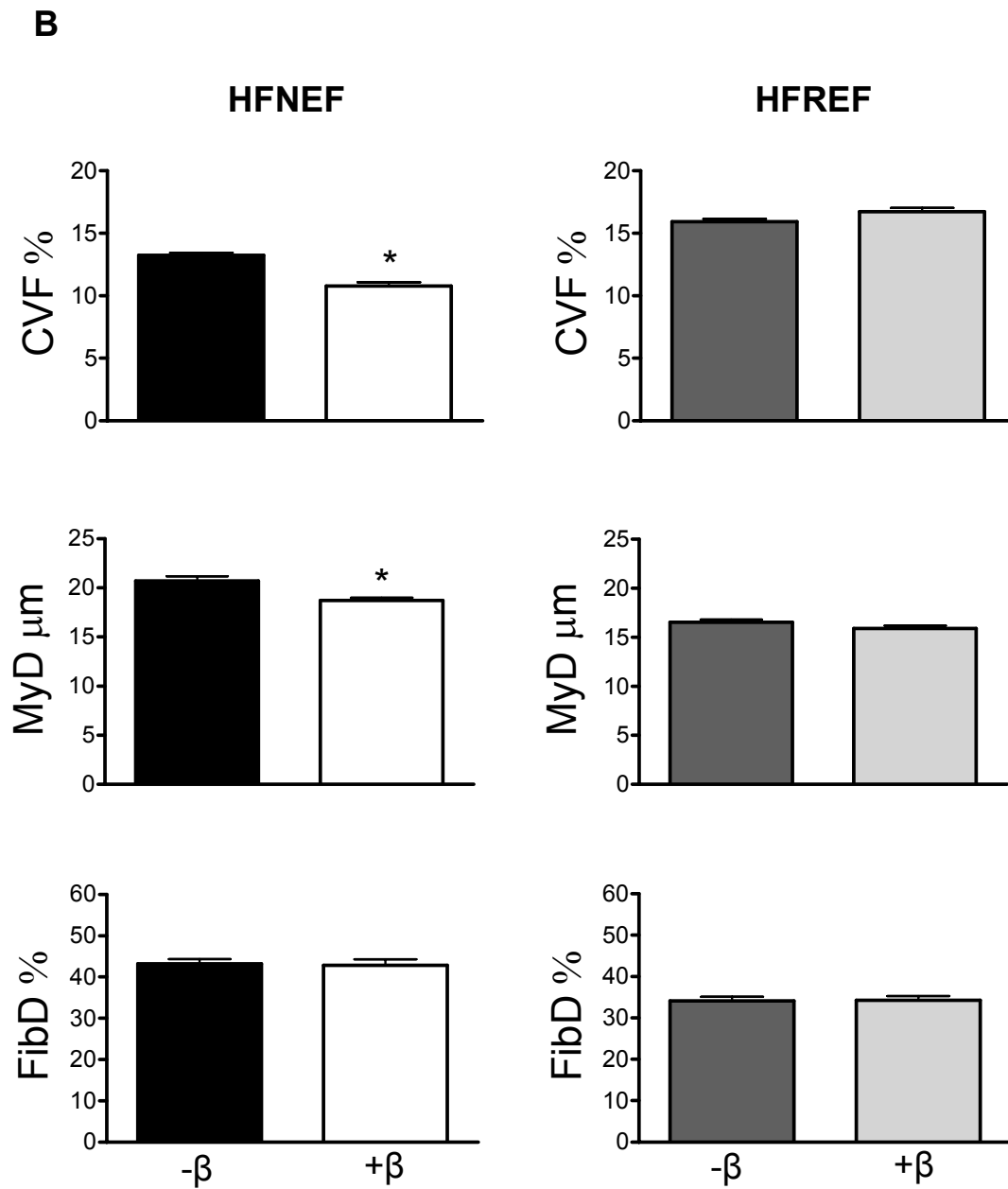


Figure 1. A. Representative examples of LV myocardial histology in the four patient groups; **B.** Bar graphs showing effects of β -blocker therapy on CVF, MyD and FibD in HFNEF and HFREF patients. Only in HFNEF patients, did β -blocker therapy reduce CVF and MyD. (* $P < 0.001$, $-\beta$ versus $+\beta$)

Force measurements in isolated cardiomyocytes

Single cardiomyocytes were attached between a force transducer and a motor (Fig 2A,B) and their sarcomere length was adjusted to $2.2\mu\text{m}$. Force measurements are summarized in Table 2 and Figure 2C. F_{active} and $p\text{Ca}_{50}$ were similar in HFNEF and HFREF but F_{passive} was higher in HFNEF ($p=0.0006$). In both HFNEF and HFREF patients, β -blocker therapy resulted in a significant increase in F_{active} ($p=0.01$) and $p\text{Ca}_{50}$ ($p=0.01$). Only in HFNEF patients did β -blocker therapy raise F_{passive} ($p=0.03$). After PKA administration to the cardiomyocytes, F_{active} was comparable in all four patient groups. After PKA, F_{passive} fell in all 4 groups but remained significantly higher in HFNEF patients with β -blockers ($p=0.001$)(Fig 3A). $p\text{Ca}_{50}$ followed a trend similar to F_{passive} by decreasing in all 4 groups and by remaining higher in HFNEF patients with β -blockers ($p=0.007$)(Fig 3B). Hence, in-vivo β -blocker therapy was associated with multiple in-vitro changes in baseline and PKA-stimulated contractile function of isolated cardiomyocytes, which differed between HFNEF and HFREF groups.

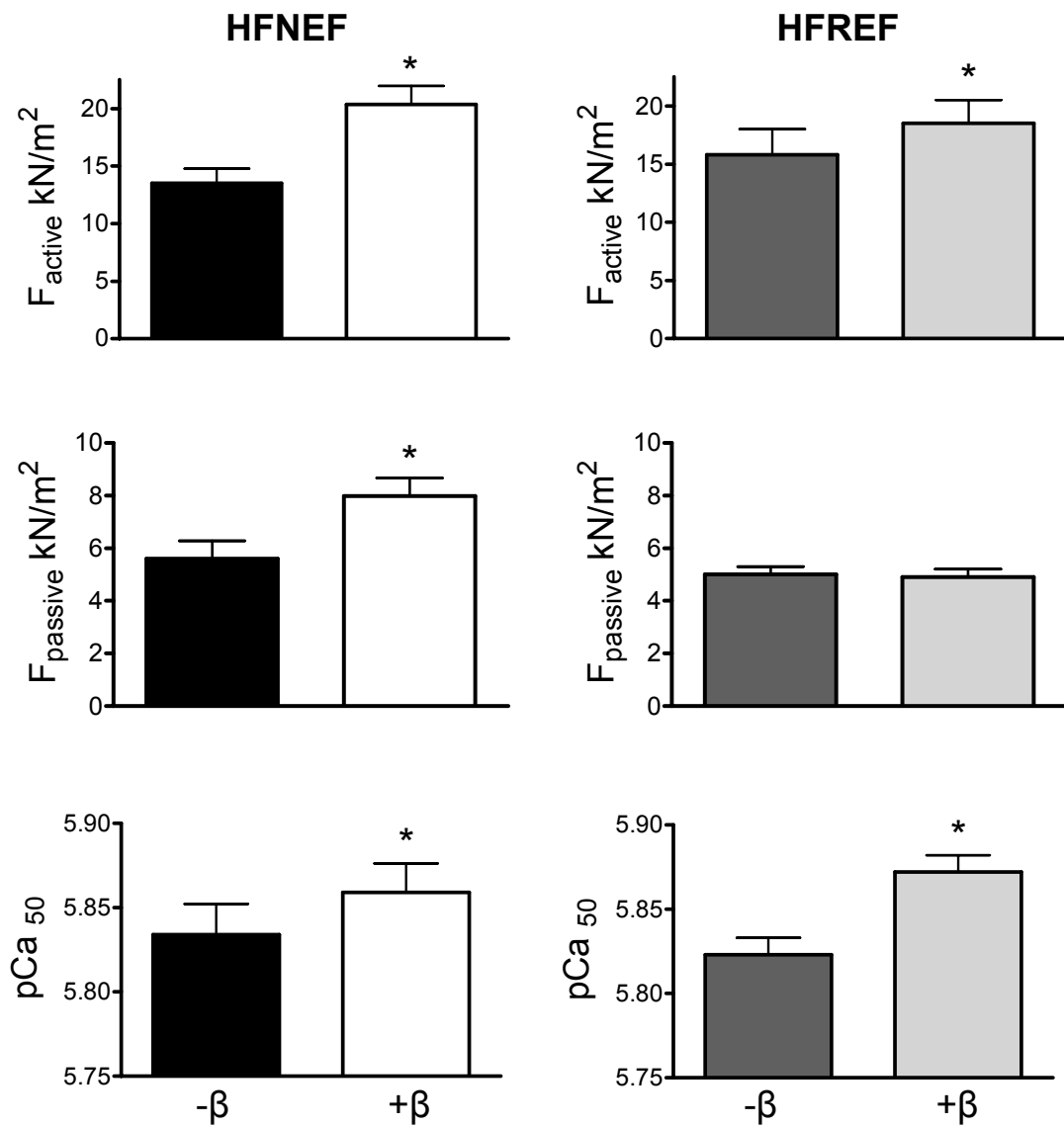


Figure 2. Bar graphs showing effects of β -blocker therapy on F_{active} , $F_{passive}$ and pCa_{50} of single cardiomyocytes. β -blocker therapy increased F_{active} and pCa_{50} in both HFNEF and HFREF and increased $F_{passive}$ only in HFNEF. (* $P < 0.05$, - β versus + β)

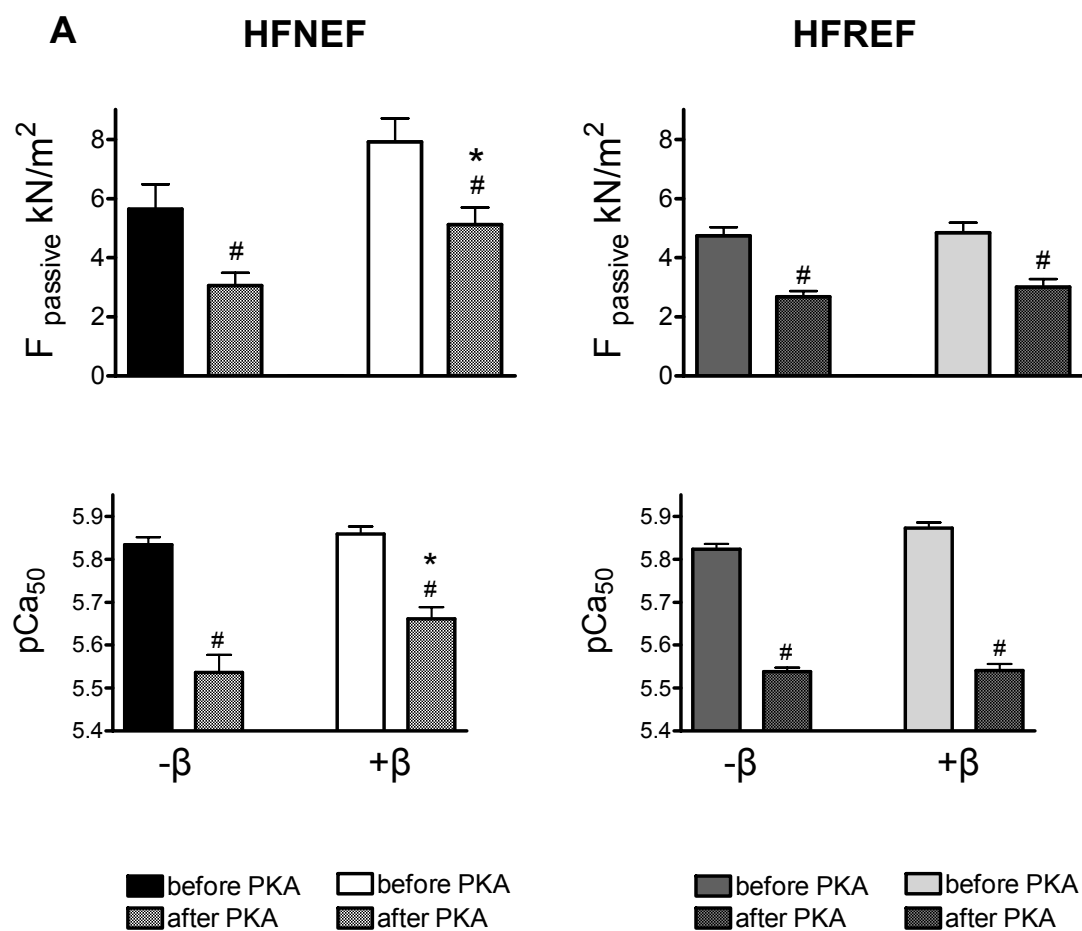


Figure 3. A. PKA treatment significantly reduced F_{passive} in all groups but F_{passive} remained higher in the β^+_{HFNEF} patients; **B.** PKA treatment significantly reduced pCa_{50} in all groups but pCa_{50} remained higher in the β^+_{HFNEF} patients. (* $P < 0.01$, $-\beta$ versus $+\beta$; # $P < 0.01$, before PKA versus after PKA)

Protein analysis

Myofilament protein phosphorylation

To explore changes in myofilamentary protein phosphorylation related to β -blocker therapy, Pro-Q Diamond-stained gels of biopsies were obtained as shown in Figure 4A. Phosphorylation status of myofilamentary proteins did not differ between HFNEF and HFREF groups. β -blocker therapy was associated with lower phosphorylation of troponin I (TnI) and of myosin-binding protein C (MyBP-C) in both HFNEF and HFREF patients (Fig 4B) and had no effect on phosphorylation status of other myofilamentary proteins (Table 2). Effect of β -blocker therapy on phosphorylation status of desmin differed with opposite changes in HFNEF and HFREF patients ($p < 0.05$).

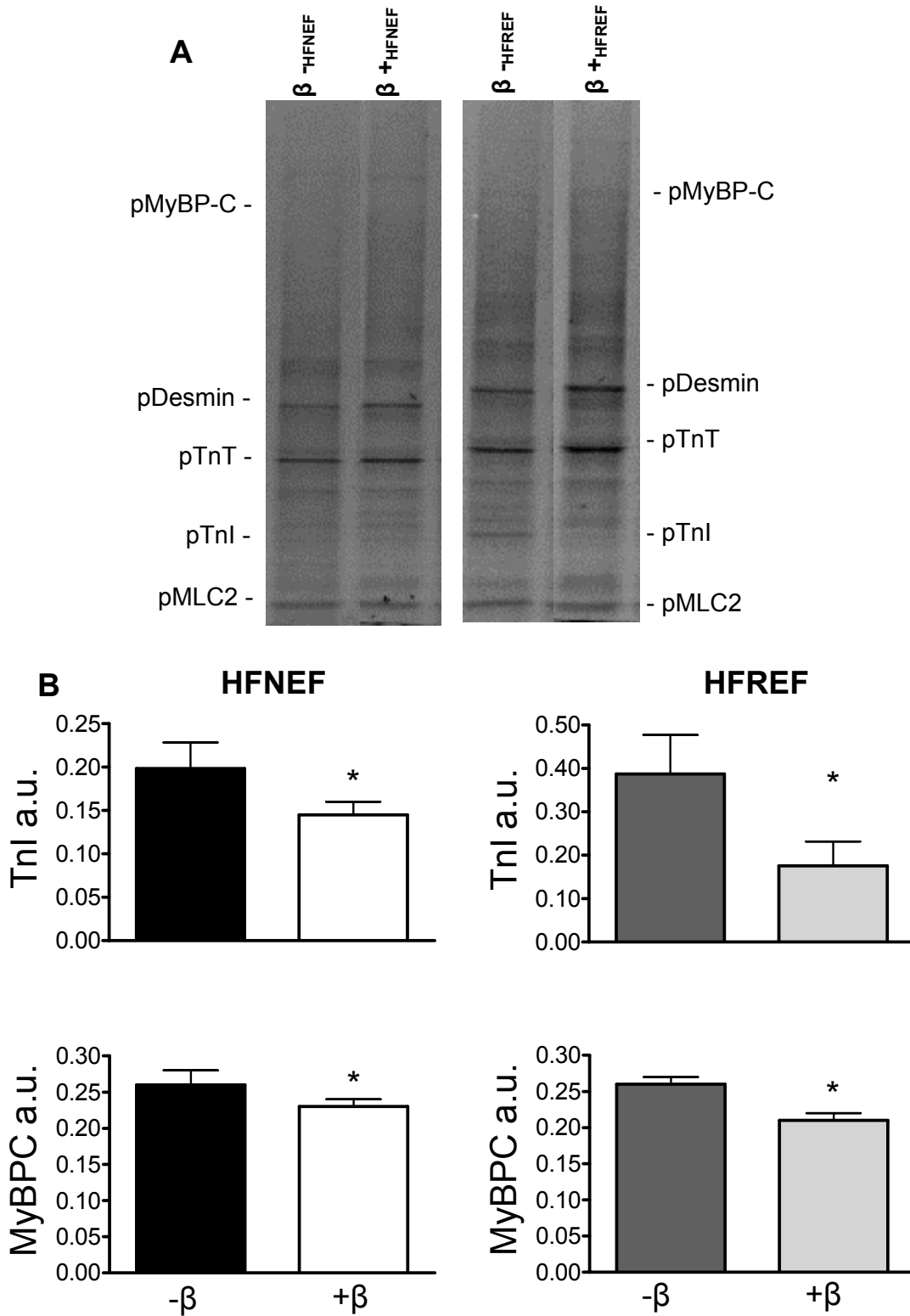


Figure 4. A. Representative Pro-Q Diamond-stained gels of a β^{-}_{HFNEF} , β^{+}_{HFNEF} , β^{-}_{HFREF} and β^{+}_{HFREF} myocardial sample; **B.** Phosphorylation status of TnI and of MyBP-C were significantly lower in β^{+}_{HFNEF} and β^{+}_{HFREF} patients compared to respectively β^{-}_{HFNEF} and β^{-}_{HFREF} patients. (* $P < 0.05$, - β versus + β)

β -Adrenergic Signaling Proteins

Expression levels of proteins involved in β -adrenergic receptor signaling were determined by Western immunoblotting (Table 2). Expression of β_1 AR, GRK2 and GRK5 were higher in HFREF than in HFNEF but unaffected by β -blocker therapy. β -blocker therapy related to downregulated expression of β_2 AR in HFREF and HFNEF. Effects of β -blocker therapy on expression of Gs and Gi differed in HFNEF and HFREF with Gs downregulated in HFNEF and Gi downregulated in HFREF.

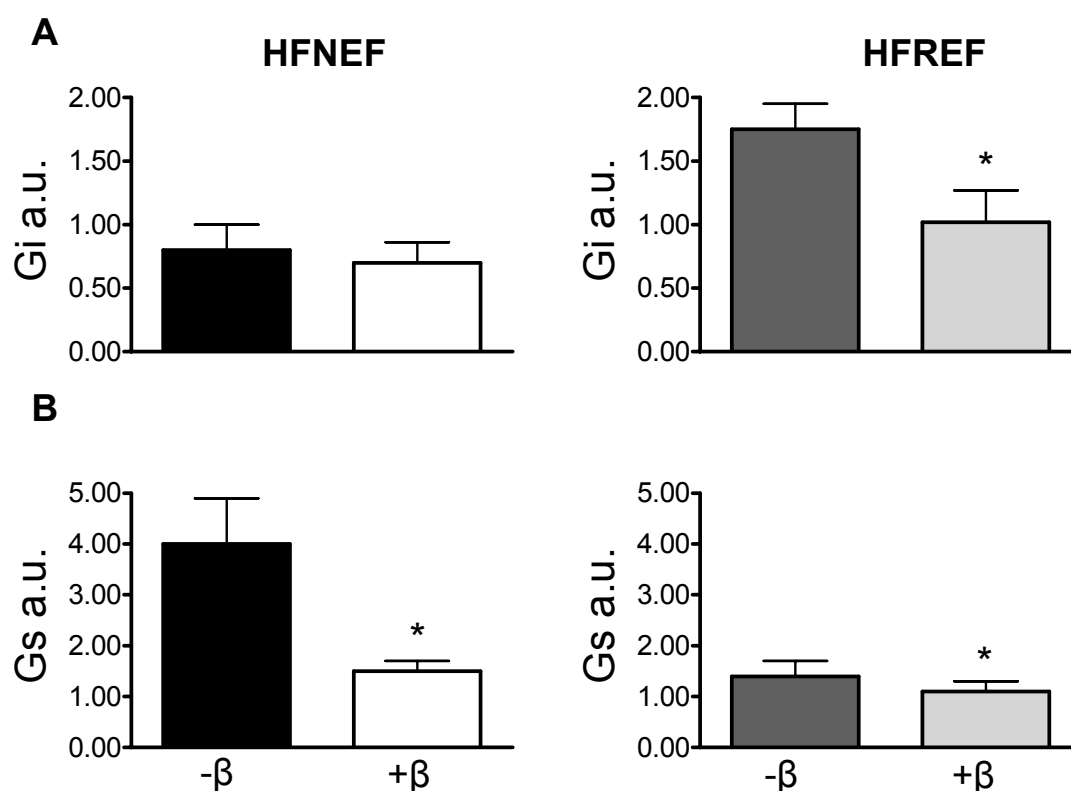


Figure 5. A and B. Represent Gi and Gs expression of a β^-_{HFNEF} , β^+_{HFNEF} , β^-_{HFREF} and β^+_{HFREF} myocardial sample. Gi expression was significantly lower in β^+_{HFREF} and Gs was significantly lower in β^+_{HFNEF} patients compared to respectively β^-_{HFREF} and β^-_{HFNEF} patients. (* $P < 0.05$, - β versus + β)

Calcium handling proteins

Expression levels of SERCA2a and PLB were determined by Western immunoblotting (Table 2). No differences related to HFNEF-HFREF status or to β -blocker therapy were observed. The ratio of SERCA2a/PLB was higher in HFREF (1.0 ± 0.2) than in HFNEF (0.5 ± 0.08 ; $p = 0.02$) and unaffected by β -blocker therapy in both groups.

Discussion

In endomyocardial biopsies of HFNEF or HFREF patients, β -blocker therapy was associated not only with structural and functional myocardial changes shared by both heart failure phenotypes but also by changes unique to each heart failure phenotype. The shared effects of β -blocker therapy consisted of enhanced pCa_{50} , higher F_{active} at saturated $[Ca^{2+}]$, lower phosphorylation status of TnI and MyBP-C and lower expression of β_2AR . Effects of β -blocker therapy unique to HFNEF were reduced interstitial fibrosis, regression of cardiomyocyte hypertrophy, elevated $F_{passive}$ before and after PKA, elevated pCa_{50} after PKA and reduced expression of Gs. An effect of β -blocker therapy unique to HFREF was the reduced expression of Gi. Effect of β -blocker therapy on phosphorylation status of desmin also differed between HFNEF and HFREF with opposite changes in both groups.

Myocardial effects of β -blocker therapy present in both HFNEF and HFREF

Chronic β -blocker therapy was associated with increased pCa_{50} of cardiomyocytes isolated from biopsies of both HFNEF and HFREF patients. Increased pCa_{50} implies improved cardiomyocyte contractile performance within the physiological range of Ca^{2+} concentrations and could be explained by the observed fall in phosphorylation status of TnI.¹⁵ Chronic β -blocker therapy increased F_{active} at saturated $[Ca^{2+}]$. Although this Ca^{2+} concentration is outside the physiological range, higher F_{active} also reflects an increased cardiomyocyte force generating capacity. The present study observed reduced phosphorylation of MyBP-C in both β -blocker therapy groups. This reduction could relate to the lack of preload dependence of LV dP/dt_{max} , which was evident in both β -blocker therapy groups from the unchanged LV dP/dt_{max} despite lower LVEDP. Preload dependence of early LV pressure rise was recently demonstrated in transgenic mice to derive from phosphorylation of MyBP-C.^{16,17} Reduced phosphorylation of MyBP-C during chronic β -blocker therapy could have resulted both from lower PKA activity and from lower activity of Ca^{2+} -calmodulin-dependent kinase (CaM-kinase). CaM-kinase can phosphorylate MyBP-C and its activity is also enhanced by β -adrenergic receptor stimulation.¹⁸⁻²⁰

In longitudinal studies performing serial hemodynamic investigations in HFREF patients, before and during chronic β -blocker therapy, improved myocardial contractile performance was evident from higher LVEF and lower LV filling pressures.²¹⁻²⁵ The present study confirmed lower LVEDP with β -blocker therapy in both HFNEF and HFREF groups. The enhanced pCa_{50} and increased F_{active} observed

in isolated cardiomyocytes of β -blocker treated patients suggested improved cardiomyocyte contractile performance to contribute to the in-vivo lowering of LVEDP induced by β -blocker therapy. The enhanced pCa_{50} and increased F_{active} could also have contributed to the lower LVEDP in the HFNEF patient group despite the increased $F_{passive}$ of the β_{+HFNEF} cardiomyocytes.

In sequential right ventricular biopsies of patients with dilated cardiomyopathy, cardiac β -receptor density increased during metoprolol²² and carvedilol therapy.²⁴ A subsequent study using explanted hearts corroborated these findings and also observed restoration of cardiac β -receptor density by carvedilol treatment.²⁶ In the present study, which used LV biopsies, chronic β -blocker therapy had no effect on β_1AR expression but downregulated β_2AR expression. The present study however did not look at βAR density in membrane fractions but at βAR protein expression in homogenates. Downregulation of β_2AR is beneficial for cardiac contractile performance because of less negative inotropy resulting from coupling of β_2AR to Gi proteins.²⁷ Coupling of β_2AR to Gi was recently also suggested to cause the apical LV dysfunction in patients with Takotsubo cardiomyopathy.²⁸

Previous investigations²⁴ demonstrated that β -blocker therapy induced LV functional improvement in HFREF patients by altering expression of genes responsible for cardiomyocyte contractility. The present study also related LV functional amelioration during β -blocker therapy to improved cardiomyocyte contractility and did so in both HFREF and HFNEF patient groups. In contrast to previous studies, contractility of single cardiomyocytes was directly assessed and its improvement was evident from both higher pCa_{50} and F_{active} and linked to lower phosphorylation of TnI and MyBP-C and to reduced expression of β_2AR .

Myocardial effects of β -blocker therapy unique to HFNEF.

Only in HFNEF patients CVF was lower in the group with β -blockers. The absence of an effect of β -blockers on CVF in HFREF patients supports previous studies, which identified high myocardial fibrosis as an important predictor for poor outcome on β -blocker therapy in HFREF.^{29,30} The lower CVF observed in β_{+HFNEF} patients was paralleled by a reduction of cardiomyocyte hypertrophy evident from lower MyD. In spontaneously hypertensive rats, the β -blocker bisoprolol did not reverse cardiomyocyte hypertrophy in contrast to the ACE-I perindopril.³¹ This study suggests that reduced renin-angiotensin system activity could possibly be involved in the observed regression of cardiomyocyte hypertrophy in the β_{+HFNEF} patients.

Previous longitudinal studies showed LV mass to decrease in both HFNEF¹³

and HFREF patients^{21,23,25} as a result of β -blocker therapy. Because of smaller LVEDVI, reduction of LV mass resulted in unaltered relative wall thickness in HFREF patients. In HFNEF patients, LV volumes remained unchanged and reduction of LV mass resulted in decreased relative wall thickness. The present study also observed unchanged LVMI/LVEDVI ratio in the HFREF group and a trend for reduced LVMI/LVEDVI ratio in the HFNEF group. The reversal of LV remodeling with β -blocker therapy therefore parallels the regression of cardiomyocyte hypertrophy observed in the present study with unchanged MyD in HFREF and decreased MyD in HFNEF.

Skinned cardiomyocytes isolated from biopsies of HFNEF patients have an elevated F_{passive} , which was higher than F_{passive} of HFREF cardiomyocytes⁴ or of normal cells.⁵ In-vitro administration of PKA corrected the high F_{passive} of HFNEF cardiomyocytes, which was therefore attributed to phosphorylatable myofilamentary proteins.⁴ Within the HFNEF patient group, the present study observed higher F_{passive} in β^+_{HFNEF} patients than in β^-_{HFNEF} patients. After in-vitro administration of PKA, F_{passive} was still higher in β^+_{HFNEF} patients. This finding suggests the effect of β -blocker therapy on cardiomyocyte F_{passive} in HFNEF relates not only to hypophosphorylation but also to structural or other posttranslational modifications of myofilamentary proteins. The persistent elevation of $p\text{Ca}_{50}$ after PKA observed in β^+_{HFNEF} cardiomyocytes also supports β -blocker therapy to induce additional modifications of myofilamentary proteins.

HFREF is usually associated with reduced $\beta_1\text{AR}$ density and translocation of GRK2 to the plasma membrane. These changes in β -adrenergic signaling were not observed in a recently published HFNEF rat model.³² Although the present study did not look at βAR density in membrane fractions but at βAR protein expression in homogenates, it found important differences in expression of $\beta_1\text{AR}$ and GRK2 proteins between patient groups with higher myocardial expression of both proteins in HFREF than in HFNEF irrespective of the use of β -blockers. This unequal expression of β -adrenergic signaling proteins in both heart failure phenotypes could explain changes in other components of the β -adrenergic system by β -blocker therapy unique for each heart failure phenotype. Of the different components of the β -adrenergic system, Gs protein was significantly lower in HFNEF patients with β -blockers. Downregulation of $\beta_2\text{AR}$ -Gs signalling could be beneficial as it would favor $\beta_2\text{AR}$ -Gi signalling, which is known to exert antiapoptotic effects.³³ Because of normal contractile LV function, potential negative inotropic effects resulting from increased $\beta_2\text{AR}$ -Gi signalling are less important for HFNEF patients.

Myocardial effects of β -blocker therapy unique to HFREF

The reduced expression of Gi in HFREF patients treated with β -blockers could be beneficial, because Gi is upregulated in HFREF patients with a dilated hypocontractile LV and contributes to the blunted inotropic response to adrenergic stimulation observed in these patients.^{34,35} Desmin phosphorylation responded differently to β -blocker therapy with increased phosphorylation in HFNEF and decreased phosphorylation in HFREF. Most previous studies on myofilamentary proteins looked at desmin expression and not at desmin phosphorylation. Desmin loss has been observed in ischaemic cardiomyopathy,³⁶ disrupted desmin in doxorubicin induced cardiotoxicity³⁷ and desmin accumulation in restrictive cardiomyopathy.³⁸ Only one study reported on desmin phosphorylation and linked desmin phosphorylation to myofibrillar disarray in cardiomyopathic hamster hearts.³⁹ Based on this study, the reduced desmin phosphorylation in β^+_{HFREF} could be beneficial as it would limit myofibrillar disarray in HFREF hearts.

Limitations

Patient recruitment of the present study was based on referral for diagnostic endomyocardial biopsy procurement. This resulted in a cross-sectional, non-randomised study design. Ethical restrictions only allowed for diagnostic biopsy procurement. This prevented a serial, randomised study design because follow-up biopsies would no longer serve diagnostic purposes. The cross-sectional, non-randomised study design could cause untreated patients to systematically differ from treated patients because of presence of certain comorbidities for which β -blockers were contraindicated. Such comorbidities, that could have significantly confounded the study results, were however unlikely. Failure to use β -blockers in the β^-_{HFREF} group resulted mainly from the referring physician non-adhering to current guidelines as the majority of these patients (14/17) were started on β -blocker therapy during the same hospitalization. Furthermore, β -blockers were used in the β^+_{HFNEF} group for control of arterial hypertension (14/16) and/or previous atrial tachyarrhythmias (4/16). Prevalence of arterial hypertension was however similar in the β^+_{HFNEF} and β^-_{HFNEF} groups (Table 1) and at the time of study all patients were in regular sinus rhythm. The comparable LVEF in the β^-_{HFREF} and β^+_{HFREF} groups probably also resulted from patient recruitment based on referral for diagnostic endomyocardial biopsy procurement. This recruitment procedure introduced a bias consisting of more frequent referral for endomyocardial biopsy procurement in patients with a poor functional response to β -blocker therapy.

Conclusions

Myocardial effects associated with β -blocker therapy are either shared by HFNEF and HFREF groups, unique to HFNEF or unique to HFREF. Higher pCa_{50} , higher F_{active} , lower Tnl phosphorylation and lower β_2AR expression are shared and beneficial for cardiomyocyte contractile performance. Lower MyD and higher $F_{passive}$ are unique to HFNEF and probably relate to the hypertrophied and stiff cardiomyocytes characteristic of HFNEF. Unchanged CVF in HFREF confirms poor clinical outcome of β -blocker therapy in HFREF patients with intense myocardial fibrosis whereas lower G_i in HFREF contributes to improve myocardial contractile performance. Unequal outcome of β -blocker therapy in HFNEF and HFREF could relate to myocardial effects of β -blocker therapy, which are unique to either HFNEF or HFREF.

References

1. Owan TE, Hodge DO, Herges RM, Jacobsen SJ, Roger VL, Redfield MM. Trends in prevalence and outcome of heart failure with preserved ejection fraction. *N Engl J Med* 2006;355:251-259.
2. Kitzman DW, Little WC, Brubaker PH, Anderson RT, Hundley WG, Marburger CT, Brosnihan B, Morgan TM, Stewart KP. Pathophysiological characterization of isolated diastolic heart failure in comparison to systolic heart failure. *JAMA* 2002;288:2144-2150.
3. Zile MR, Gaasch WH, Carroll JD, Feldman MD, Aurigemma GP, Schaer GL, Ghali JK, Liebson PR. Heart failure with a normal ejection fraction: is measurement of diastolic function necessary to make the diagnosis of diastolic heart failure? *Circulation* 2001;104:779-782.
4. van Heerebeek L, Borbély A, Niessen HW, Bronzwaer JG, van der Velden J, Stienen GJ, Linke WA, Laarman GJ, Paulus WJ. Myocardial structure and function differ in systolic and diastolic heart failure. *Circulation* 2006;113:1966-1973.
5. Borbely A, van der Velden J, Papp Z, Bronzwaer JG, Edes I, Stienen GJ, Paulus WJ. Cardiomyocyte stiffness in diastolic heart failure. *Circulation* 2005;111:774-781.
6. van Heerebeek L, Hamdani N, Handoko ML, Falcao-Pires I, Musters RJ, Kupreishvili K, Ijsselmuiden AJ, Schalkwijk CG, Bronzwaer JG, Diamant M, Borbely A, van der Velden J, Stienen GJ, Laarman GJ, Niessen HW, Paulus WJ. Diastolic stiffness of the failing diabetic heart: importance of fibrosis, advanced glycation end products, and myocyte resting tension. *Circulation* 2008;117:43-51.
7. MERIT-HF Study group. Effect of metoprolol CR/XL in chronic heart failure: Metoprolol CR/XL Randomised Intervention Trial in Congestive Heart Failure (MERIT-HF). *Lancet* 1999;353:2001-2007.
8. CIBIS-II Investigators and Committees. The Cardiac Insufficiency Bisoprolol Study II (CIBIS-II): a randomised trial. *Lancet* 1999;353:9-13.
9. Packer M, Coats AJ, Fowler MB, Katus HA, Krum H, Mohacsi P, Rouleau JL, Tendera M, Castaigne A, Roecker EB, Schultz MK, DeMets DL, for the Carvedilol Prospective Randomized Cumulative Survival Study Group. Effect of carvedilol on survival in severe chronic heart failure. *N Engl J Med* 2001; 344:1651-1658.
10. Dobre D, van Veldhuisen DJ, DeJongste MJ, Lucas C, Cleuren G, Sanderman R, Ranchor AV, Haaijer-Ruskamp FM. Prescription of beta-blockers in patients with advanced heart failure and preserved left ventricular ejection fraction. Clinical implications and survival. *Eur J Heart Fail* 2007;9:280-286.
11. Massie BM, Nelson JJ, Lukas MA, Greenberg B, Fowler MB, Gilbert EM, Abraham WT, Lottes SR, Franciosa JA. Comparison of outcomes and usefulness of carvedilol across a spectrum of left ventricular ejection fractions in patients with heart failure in clinical practice. *Am J Cardiol* 2007;99:1263-1268.
12. Bergström A, Andersson B, Edner M, Nylander E, Persson H, Dahlström U. Effect of carvedilol on diastolic function in patients with diastolic heart failure and preserved systolic function. Results of the Swedish Doppler-echocardiographic study (SWEDIC). *Eur J Heart Fail* 2004;6:453-461.
13. Nodari S, Metra M, Dei Cas L. Beta-blocker treatment of patients with diastolic heart failure and arterial hypertension. A prospective, randomized, comparison of the long-term effects of atenolol vs. nebivolol. *Eur J Heart Fail* 2003;5:621-627.

14. Hori M, Kitabatake A, Tsutsui H, Okamoto H, Shirato K, Nagai R, Izumi T, Yokoyama H, Yasumura Y, Ishida Y, Matsuzaki M, Oki T, Sekiya M. Rationale and design of a randomized trial to assess the effects of beta-blocker in diastolic heart failure; Japanese Diastolic Heart Failure Study (J-DHF). *J Card Fail* 2005;11:542-547.
15. Kranias EG, Garvey JL, Srivastava RD, Solaro RJ. Phosphorylation and functional modifications of sarcoplasmic reticulum and myofibrils in isolated rabbit hearts stimulated with isoprenaline. *Biochem J* 1985;226:113-121.
16. Stelzer JE, Patel JR, Walker JW, Moss RL. Differential roles of cardiac myosin-binding protein C and cardiac troponin I in the myofibrillar force responses to protein kinase A phosphorylation. *Circ Res.* 2007;101:503-511.
17. Nagayama T, Takimoto E, Sadayappan S, Mudd JO, Seidman JG, Robbins J, Kass DA. Control of in vivo left ventricular contraction/relaxation kinetics by myosin binding protein C: protein kinase A phosphorylation-dependent and -independent regulation. *Circulation* 2007;116:2399-2408.
18. Zhang R, Khoo MS, Wu Y, Yang Y, Grueter CE, Ni G, Price EE Jr, Thiel W, Guatimosim S, Song LS, Madu EC, Shah AN, Vishnivetskaya TA, Atkinson JB, Gurevich VV, Salama G, Lederer WJ, Colbran RJ, Anderson ME. Calmodulin kinase II inhibition protects against structural heart disease. *Nat Med* 2005;11:409-417.
19. Curran J, Hinton MJ, Ríos E, Bers DM, Shannon TR. Beta-adrenergic enhancement of sarcoplasmic reticulum calcium leak in cardiac myocytes is mediated by calcium/calmodulin-dependent protein kinase. *Circ Res* 2007;100:391-398.
20. Sipido KR. CaM or cAMP: linking beta-adrenergic stimulation to 'leaky' RyRs. *Circ Res* 2007;100:296-298
21. Hall SA, Cigarroa CG, Marcoux L, Risser RC, Grayburn PA, Eichhorn EJ. Time course of improvement in left ventricular function, mass and geometry in patients with congestive heart failure treated with beta-adrenergic blockade. *J Am Coll Cardiol* 1995;25:1154-1161.
22. Gilbert EM, Abraham WT, Olsen S, Hattler B, White M, Mealy P, Larrabee P, Bristow MR. Comparative hemodynamic, left ventricular functional, and antiadrenergic effects of chronic treatment with metoprolol versus carvedilol in the failing heart. *Circulation* 1996;94:2817-2825.
23. Lowes BD, Gill EA, Abraham WT, Larrain JR, Robertson AD, Bristow MR, Gilbert EM. Effects of carvedilol on left ventricular mass, chamber geometry, and mitral regurgitation in chronic heart failure. *Am J Cardiol* 1999;83:1201-1205.
24. Lowes BD, Gilbert EM, Abraham WT, Minobe WA, Larrabee P, Ferguson D, Wolfel EE, Lindenfeld JA, Tsvetkova T, Robertson AD, Quaife RA, Bristow MR. Myocardial gene expression in dilated cardiomyopathy treated with beta-blocking agents. *N Engl J Med* 2002;346:1357-1365.
25. Palazzuoli A, Bruni F, Puccetti L, Pastorelli M, Angori P, Pasqui AL, Auteri A. Effects of carvedilol on left ventricular remodeling and systolic function in elderly patients with heart failure. *Eur J Heart Fail* 2002;4:765-770.
26. Reiken S, Wehrens XH, Vest JA, Barbone A, Klotz S, Mancini D, Burkhoff D, Marks AR. Beta-blockers restore calcium release channel function and improve cardiac muscle performance in human heart failure. *Circulation* 2003;107:2459-2466.
27. Xiao RP, Zhang SJ, Chakir K, Avdonin P, Zhu W, Bond RA, Balke CW, Lakatta EG, Cheng H. Enhanced G(i) signaling selectively negates beta2-adrenergic receptor (AR)--but not beta1-AR-mediated positive inotropic effect in myocytes from failing rat

- hearts. *Circulation* 2003;108:1633-1639.
28. Lyon AR, Rees PS, Prasad S, Poole-Wilson PA, Harding SE. Stress (Takotsubo) cardiomyopathy--a novel pathophysiological hypothesis to explain catecholamine-induced acute myocardial stunning. *Nat Clin Pract Cardiovasc Med* 2008;5:22-29.
 29. Yamada T, Fukunami M, Ohmori M, Iwakura K, Kumagai K, Kondoh N, Minamino T, Tsujimura E, Nagareda T, Kotoh K. Which subgroup of patients with dilated cardiomyopathy would benefit from long-term beta-blocker therapy? A histologic viewpoint. *J Am Coll Cardiol* 1993;21:628-633.
 30. Suwa M, Ito T, Kobashi A, Yagi H, Terasaki F, Hirota Y, Kawamura K. Myocardial integrated ultrasonic backscatter in patients with dilated cardiomyopathy: prediction of response to beta-blocker therapy. *Am Heart J*. 2000;139:905-912.
 31. Onodera T, Okazaki F, Miyazaki H, Minami S, Ito T, Seki S, Taniguchi M, Taniguchi I, Mochizuki S. Perindopril reverses myocyte remodeling in the hypertensive heart. *Hypertens Res* 2002;25:85-90.
 32. Nishio M, Sakata Y, Mano T, Ohtani T, Takeda Y, Miwa T, Hori M, Masuyama T, Kondo T, Yamamoto K. Beneficial effects of bisoprolol on the survival of hypertensive diastolic heart failure model rats. *Eur J Heart Fail* 2008;10:446-453.
 33. Communal C, Singh K, Sawyer DB, Colucci WS. Opposing effects of beta(1)- and beta(2)-adrenergic receptors on cardiac myocyte apoptosis : role of a pertussis toxin-sensitive G protein. *Circulation* 1999;100:2210-2212.
 34. Eschenhagen T, Mende U, Nose M, Schmitz W, Scholz H, Haverich A, Hirt S, Doring V, Kalmar P, Hoppner W. Increased messenger RNA level of the inhibitory G protein alpha subunit Gi alpha-2 in human end-stage heart failure. *Circ Res*. 1992;70:688-696.
 35. Bohm M, Eschenhagen T, Gierschik P, Larisch K, Lensche H, Mende U, Schmitz W, Schnabel P, Scholz H, Steinfath M, Erdmann E. Radioimmunochemical quantification of Gi alpha in right and left ventricles from patients with ischaemic and dilated cardiomyopathy and predominant left ventricular failure. *J Mol Cell Cardiol* 1994;26:133-149.
 36. Di Somma S, Di Benedetto MP, Salvatore G, Agozzino L, Ferranti F, Esposito S, La Dogana P, Scarano MI, Caputo G, Cotrufo M, Santo LD, de Divitiis O. Desmin-free cardiomyocytes and myocardial dysfunction in end stage heart failure. *Eur J Heart Fail* 2004;6:389-398.
 37. Fisher PW, Salloum F, Das A, Hyder H, Kukreja RC. Phosphodiesterase-5 inhibition with sildenafil attenuates cardiomyocyte apoptosis and left ventricular dysfunction in a chronic model of doxorubicin cardiotoxicity. *Circulation* 2005;111:1601-1610.
 38. Zhang J, Kumar A, Stalker HJ, Viridi G, Ferrans VJ, Horiba K, Fricker FJ, Wallace MR. Clinical and molecular studies of a large family with desmin-associated restrictive cardiomyopathy. *Clin Genet* 2001;59:248-256.
 39. Huang X, Li J, Foster D, Lemanski SL, Dube DK, Zhang C, Lemanski LF. Protein kinase C-mediated desmin phosphorylation is related to myofibril disarray in cardiomyopathic hamster heart. *Exp Biol Med (Maywood)* 2002;227:1039-1046.

6

Diastolic stiffness of the failing diabetic heart: Importance of fibrosis, advanced glycation end products, and myocyte resting tension

Loek van Heerebeek, Nazha Hamdani, Martin L Handoko, Ines Falcao-Pires,
Rene J Musters, Koba Kupreishvili, Alexander J Ijsselmuiden, Casper G
Schalkwijk, Jean GF Bronzwaer, Michaela Diamant, Attila Borbely,
Jolanda van der Velden, Ger J M Stienen, Gerrit J Laarman,
Hans WM Niessen, Walter J Paulus

Abstract

High diastolic left ventricular (LV) stiffness is an important contributor to heart failure in patients with diabetes. Diabetes is presumed to increase stiffness through myocardial deposition of collagen and advanced glycation endproducts (AGEs). Cardiomyocyte resting tension also elevates stiffness especially in heart failure with normal LV ejection fraction (EF). The contribution to diastolic stiffness of fibrosis, AGEs and cardiomyocyte resting tension was assessed in diabetic heart failure patients with normal or reduced LVEF.

LV endomyocardial biopsies were procured in 28 patients with normal and 36 patients with reduced LVEF, all without coronary artery disease. Sixteen patients with normal and 10 patients with reduced LVEF had diabetes. Biopsies were used for quantification of collagen and AGEs and for isolation of cardiomyocytes to measure resting tension.

Diabetic heart failure patients had higher diastolic LV stiffness irrespective of LVEF. Diabetes raised myocardial collagen volume fraction only in patients with reduced LVEF (from 14.6 ± 1.0 to $22.4 \pm 2.2\%$; $p < 0.001$) and raised cardiomyocyte resting tension only in patients with normal LVEF (from 5.1 ± 0.7 to 8.5 ± 0.9 kN/m²; $p = 0.006$). Diabetes increased myocardial AGEs deposition in patients with reduced LVEF (from 8.8 ± 2.5 to 24.1 ± 3.8 score/mm²; $p = 0.005$) and less so in patients with normal LVEF (from 8.2 ± 2.5 to 15.7 ± 2.7 score/mm²; NS).

Mechanisms responsible for the increased diastolic stiffness of the diabetic heart differ in heart failure with reduced and normal LVEF: fibrosis and AGEs are more important when LVEF is reduced while cardiomyocyte resting tension is more important when LVEF is normal.

Introduction

High diastolic left ventricular (LV) stiffness is recognized as the earliest manifestation of LV dysfunction induced by diabetes mellitus (DM)¹⁻⁵ and frequently becomes the main functional deficit of the diabetic heart as many diabetic patients present with heart failure (HF) and normal LV ejection fraction (EF)^{6,7}. This high diastolic LV stiffness also modifies ischemic LV dysfunction as evident from the reduced LV remodeling and the raised incidence of HF after acute myocardial infarction^{8,9}.

In the absence of coronary artery disease (CAD), the high diastolic LV stiffness of the diabetic heart has been related to myocardial fibrosis¹⁰ and to circulating advanced glycation end products (AGEs)¹¹ although associations of histological and biochemical data with in-vivo LV function are largely lacking. Furthermore, a contribution to this high diastolic LV stiffness of an elevated cardiomyocyte resting tension (F_{passive}) has so far not been assessed. In patients with HF and normal LVEF (HFNEF), F_{passive} of cardiomyocytes isolated from LV endomyocardial biopsies was recently demonstrated to be elevated and an important determinant of LV stiffness¹². In patients with HF and reduced LVEF (HFREF), F_{passive} was lower and failed to correlate with LV stiffness¹³. The high F_{passive} in HFNEF was paralleled by cardiomyocyte hypertrophy and concentric LV remodeling^{12,13}. As myocardial hypertrophy is associated with insulin resistance¹⁴ and as HFNEF is common in type 2 DM patients⁷, high F_{passive} could be an important contributor to the high diastolic LV stiffness of the diabetic heart.

Using LV endomyocardial biopsies, the present study therefore compared myocardial fibrosis, AGEs deposition and F_{passive} of isolated cardiomyocytes between diabetic (DM^+) and non-diabetic (DM^-) HFNEF patients (DM^+_{HFNEF} ; DM^-_{HFNEF}) and between DM^+ and DM^- HFREF patients (DM^+_{HFREF} ; DM^-_{HFREF}). All patients had been hospitalized for worsening HF and had no evidence of CAD on their coronary angiogram or of myocardial infiltration or active inflammation in their LV endomyocardial biopsies.

Methods

Patients

The study population consisted of 90 patients hospitalized for worsening HF between October 2003 and December 2006. Patients were referred for cardiac catheterization and LV endomyocardial biopsy procurement because of suspicion of infiltrative or inflammatory myocardial disease. Fifty-eight patients suffered of new onset HF and 32 of acute decompensation superimposed on chronic HF. Modes of presentation were similar in HFNEF versus HFREF patients and in DM⁺ versus DM⁻ patients. Patients were studied following medical recompensation. No patient had undergone cardiac transplantation. Coronary angiography showed epicardial coronary artery stenoses in 20 patients. These patients were excluded. Histological analysis of the biopsies revealed active inflammatory infiltration or myocardial deposits in 6 patients. A histologically positive biopsy in 8.6% of the study population is comparable to previous studies, which reported active lymphocytic infiltration in 8.3% of patients with dilated cardiomyopathy¹⁵ and amyloid deposits in 6.3% of patients with LV restrictive physiology¹⁶ of hemodynamic severity comparable to the present study population. Patients with a positive biopsy were also excluded. The final study cohort therefore consisted of 64 patients. From 44 of these 64 patients, myocardial collagen volume fraction (CVF) and cardiomyocyte F_{passive} were included in previous studies^{12,13}.

In accordance to a recent consensus document on the diagnosis of HFNEF¹⁷, patients had HFNEF (n=28) if LVEF > 50 %, if left ventricular end-diastolic volume index (LVEDVI) < 97 ml/m² and if LV end-diastolic pressure (LVEDP) > 16 mmHg¹⁷. Patients had HFREF (n=36) if LVEF < 45%. A patient had DM, if a history of DM was evident from use of glucose-lowering medications and/or insulin, or if fasting plasma glucose ≥ 7.0 mmol/L¹⁸. No patient was using thiazolidinediones. Three HFREF patients had type 1 DM, 7 HFREF and all 16 HFNEF patients had type 2 DM. In DM⁺_{HFREF} and DM⁺_{HFNEF} patients, which were not on insulin therapy, fasting insulin plasma levels were elevated and equalled respectively 20.1 \pm 4.3 μ U/ml and 22.4 \pm 3.0 μ U/ml. The local ethics committee approved the study protocol. Written, informed consent was obtained from all patients.

Quantitative histomorphometry – light and electron microscopy

Light microscopic quantification of cardiomyocyte diameter and CVF has previously been described and validated^{12,13}. Biopsy samples used for CVF averaged 2.8 \pm 0.2 samples per patient. The same automated image analyzer was also used for electron microscopic quantification¹³ of sarcomeric Z-disc thickness of cardiomyocytes. For

each patient, 30 Z-disc thickness measurements were averaged.

Quantitative histomorphometry - immunohistochemistry

Deposition of AGEs was inferred from measurement of the AGE, N^ε-(carboxymethyl)lysine (CML). Development of the used anti-CML monoclonal antibody and immunohistochemical staining techniques for CML and E-selectin have previously been described^{19,20}. AGE and E-selectin positivity was scored for intensity. The sum of all positivities times their score was subsequently divided by the area of the slide to yield an immunohistochemical score/mm².

Quantitative histomorphometry - immunofluorescence light microscopy

For analysis of Z-line thickness, fixed slides with isolated cardiomyocytes were stained with anti- α -actinin for 60 min at room temperature (1:50, mAb, Monosan, Uden, The Netherlands). After washing in phosphate buffered saline tween (PBST), the cells were subsequently incubated for 30 min with rabbit-anti-mouse AlexaFluor 488 secondary antibody (1:40, Molecular Probes, Invitrogen) and again washed in PBST. Slides were covered and sealed by mounting medium and ultrathin glass cover slips. Z-disc thickness analysis was performed under a 3D MarianasTM widefield deconvolution microscopy workstation (Intelligent Imaging Innovations, Denver, CO, USA). For each patient, 3D stacks (stepsize in z = 0.2 μ m) of isolated cardiomyocytes were made and 30 Z-disc thickness measurements were averaged.

Force measurements in isolated cardiomyocytes

Force measurements were performed in single, mechanically isolated cardiomyocytes as described previously^{12,13}. Biopsy samples (5 mg wet weight) were defrosted in relaxing solution, mechanically disrupted and incubated for 5 minutes in relaxing solution supplemented with 0.2 % TritonX-100 to remove all membrane structures. Single cardiomyocytes were subsequently attached with silicone adhesive between a force transducer and a piezoelectric motor (2.7 \pm 0.4 cardiomyocytes per patient). Sarcomere length of isolated cardiomyocytes was adjusted to 2.2 μ m. To assess reversibility of elevated F_{passive} , myocytes were also incubated in relaxing solution supplemented with the catalytic subunit of protein kinase A (PKA, 100 U/mL; Sigma, batch-12K7495). After 40 minutes incubation with PKA, F_{passive} measurements were repeated. Force values were normalized for myocyte cross-sectional area.

Data analysis

LVEDV, LVEDVI, LV stroke volume (LVSV) and LVEF were derived from biplane LV angiograms. Effective arterial elastance (Ea) equalled LV end-systolic pressure divided by angiographic LVSV. Total arterial compliance (Art Compl) equalled angiographic LVSV divided by aortic pulse pressure (PP).

LV diastolic internal diameter (LVIDd), diastolic septal and posterior wall thicknesses (SWTd, PWTd), relative wall thickness (RWT), LV mass (LVM) and LV mass index (LVMI) were derived from 2D-echocardiograms. LV mass and RWT were calculated in accordance to the recent recommendations for cardiac chamber quantification²¹:

$$\text{LVM} = 0.8 \times \{1.04 [(LVIDd + PWTd + SWTd)^3 - LVIDd^3]\} + 0.6 \text{ g}$$

$$\text{RWT} = 2 \times \text{PWTd}/\text{LVIDd}.$$

To calculate LV peak systolic wall stress (LVPSs) and LV myocardial stiffness modulus (Stiff Mod), hemodynamic, angiographic and 2D-echocardiographic data were combined. Circumferential LVPSs was computed using a thick wall ellipsoid model of the left ventricle as follows²²:

LVPSs = LVPSP x D/(2 PWTs) x [1 - (PWTs/D) - (D²/2L²)] x 1.332 dyne/cm² where LVPSP is LV peak systolic pressure, PWTs is corresponding systolic echocardiographic posterior wall thickness and D and L are corresponding angiographic LV systolic diameter and length.

To assess diastolic LV material properties, a radial LV Stiff Mod was derived²³. Stiff Mod was defined as the increment of radial stress ($\Delta\sigma$) divided by the increment of radial strain ($\Delta\varepsilon$) (Stiff Mod = $\Delta\sigma/\Delta\varepsilon$). $\Delta\sigma$ is equal but opposite in sign to the increment of LV pressure (P) at the endocardium ($-\Delta\text{LVP}$) and $\Delta\varepsilon$ equals the increment in 2D-echocardiographic PWT relative to the instantaneous PWT ($\Delta\text{PWT}/\text{PWT}$). Early diastolic LV relaxation pressure was extrapolated from the exponential curve fit to isovolumic LV pressure decay, which was used to calculate Tau, the time constant of isovolumic LV pressure decay. Early diastolic LV relaxation pressure was subtracted from measured LVP to yield residual LV diastolic pressure (LVP_{res}). Substitution of LVP by LVP_{res} allowed Stiff Mod to be calculated also in early diastole, when LVP is still declining²³. As $\Delta\text{PWT}/\text{PWT} = \Delta\ln\text{PWT}$, Stiff Mod equals the slope of a plot of LVP_{res} against corresponding $\Delta\ln\text{PWT}$ data points.

Values are given as mean \pm SEM. Data of the $\text{DM}^-_{\text{HFREF}}$, $\text{DM}^+_{\text{HFREF}}$, $\text{DM}^-_{\text{HFNEF}}$ and $\text{DM}^+_{\text{HFNEF}}$ groups were analysed by two-factor ANOVA testing for DM status, HFREF-HFNEF status and their interaction. Subsequent comparisons ($\text{DM}^-_{\text{HFREF}}$ vs. $\text{DM}^+_{\text{HFREF}}$ and $\text{DM}^-_{\text{HFNEF}}$ vs. $\text{DM}^+_{\text{HFNEF}}$) were performed using a Bonferroni adjusted *t*

test. Single comparisons were assessed by an unpaired Student's *t* test. Relations between two continuous variables were assessed with linear regression analysis. Statistical analysis was performed using SPSS (version 9.0).

Table 1. Clinical and hemodynamic characteristics

	DM ⁻ _{HFREF} (n=26)	DM ⁺ _{HFREF} (n=10)	DM ⁻ _{HFNEF} (n=12)	DM ⁺ _{HFNEF} (n=16)	p value	
					DM ⁻ vs DM ⁺	HFREF vs HFNEF
Age (y)	60.2±3.4	62.4±4.1	63.2±4.1	65.3±2.7	NS	NS
Sex (M/F)	10/16	7/3	6/6	9/7	NS	NS
Hypertension	3/26	1/10	10/12	13/16	NS	<0.001
DM1/DM2		3/7		0/16		
Fasting Glucose (mmol/L)	4.97±0.23	7.10±0.56*	5.78±0.28	8.64±0.94§	<0.001	0.048
Glycated hemoglobin (%)	5.54±0.20	7.04±0.58*	5.50±0.04	7.26±0.51§	<0.001	NS
Body Mass Index (kg/m ²)	26.4±0.95	28.9±1.71	25.9±1.86	32.6±1.98‡	0.007	NS
DM duration (y)		6.9±0.7		6.4±0.4		
Creatinine (μmol/L)	94.3±4.0	101.0±3.0	94.8±4.0	96.2±3.0	NS	NS
GFR (mL/min/1.73m ²)	75±3.0	69±1.5	74±3.0	72±1.7	NS	NS
Microalbuminuria		3/10		3/16		
Medication						
ACEI	20/26	9/10	9/12	13/16	NS	NS
β-blocker	14/26	4/10	5/12	8/16	NS	NS
Diuretic	24/26	10/10	11/12	16/16	NS	NS
CCB	1/26	2/10	3/12	5/16	NS	NS
ARB	3/26	0/10	2/12	3/16	NS	NS
Digoxin	10/26	5/10	3/12	2/16	NS	0.035
Amiodarone	2/26	1/10	2/12	3/16	NS	NS
Statin	4/26	5/10	6/12	10/16	NS	NS
Insulin		3/10		5/16		

	DM ⁻ _{HFREF} (n=26)	DM ⁺ _{HFREF} (n=10)	DM ⁻ _{HFNEF} (n=12)	DM ⁺ _{HFNEF} (n=16)	p value	
					DM ⁻ vs DM ⁺	HFREF vs HFNEF
LVPSP (mmHg)	117.4±3.4	126.4±8.2	166.0±8.5	172.0±9.7	NS	<0.001
LVEDP (mmHg)	19.9±1.7	27.8±2.5*	22.2±1.9	28.0±1.7	0.002	NS
RAP (mmHg)	6.7±1.0	9.5±1.9	8.1±1.0	8.4±1.2	NS	NS
Tau (ms)	66.5±10	63.0±8.5	58.3±5.3	72.5±5.7	NS	NS
Ea (mmHg/mL)	2.2±0.2	2.5±0.7	2.3±0.2	2.7±0.3	NS	NS
PP (mmHg)	49.1±2.9	51.2±6.2	82.9±5.0	97.9±7.6	NS	<0.001
Art Compl(mL/mmHg)	1.7±0.2	1.4±0.2	1.4±0.2	1.0±0.1	NS	NS
SVR (dyne/sec/cm ⁵)	1832±101	1963±114	1781±158	1913±263	NS	NS
LVEDV (mL)	236.6±12.5	226.1±17.6	176.3±17.8	148.0±10.9	NS	<0.001
LVEDVI (mL/m ²)	127.9±6.6	117.8±7.2	88.0±7.2	77.0±4.2	NS	<0.001
LVEF (%)	33.0±1.8	26.0±2.9	60.5±2.2	60.2±3.2	NS	<0.001
CO (L/min)	3.9±0.2	3.6±0.2	5.3±0.6	5.1±0.1	NS	<0.001
CI (L/min/m ²)	2.1±0.1	1.9±0.1	2.7±0.3	2.7±0.1	NS	<0.001
LVIDd (cm)	7.1±0.1	6.9±0.2	5.4±0.2	5.1±0.1	NS	<0.001
PWTd (mm)	9.0±0.3	10.3±0.4*	10.3±0.4	11.4±0.3	0.002	0.002
RWT	0.25±0.01	0.30±0.02*	0.40±0.02	0.45±0.02‡	0.005	<0.001
LVM (g)	298.8±18.1	338.6±16.3	227.9±14.6	231.0±10.6	NS	<0.001
LVMI (g/m ²)	163.1±10.1	181.2±11.1	114.6±5.5	121.3±4.4	NS	<0.001
LVMI/LVEDVI (g/mL)	1.3±0.1	1.4±0.1	1.4±0.1	1.6±0.1	NS	NS
LVPSSs (dyne/cm ²)	243.4±8.0	255.0±7.0	137.8±8.4	130.3±9.9	NS	<0.001
Stiff Mod (kN/m ²)	2.5±0.2	6.3±2.0†	4.5±0.8	7.4±0.7	<0.001	<0.001

M, male; F, female; DM1, type 1 DM; DM2, type 2 DM; GFR, glomerular filtration rate; ACEI, ACE inhibitors; CCB, calcium channel blockers; ARB, angiotensin II receptor blockers; RAP, right atrial pressure; SVR, systemic vascular resistance; CO, cardiac output; CI, cardiac index. * p < 0.05 vs. DM⁻_{HFREF}; † p < 0.001 vs. DM⁻_{HFREF}; ‡ p < 0.05 vs. DM⁻_{HFNEF}; § p < 0.01 vs. DM⁻_{HFNEF}; || p < 0.001 vs. DM⁻_{HFNEF}. For all variables listed, two-factor ANOVA showed no significant interaction between DM status and HFNEF-HFREF status.

Results

DM and LV function

As evident from the higher LVEDP at similar LVEDVI, LV end-diastolic distensibility was reduced in DM^+_{HFREF} and DM^+_{HFNEF} patients (Fig 1A). Stiff Mod was also higher in DM^+_{HFREF} and DM^+_{HFNEF} patients when compared respectively to DM^-_{HFREF} and DM^-_{HFNEF} patients (Table, Fig 1B).

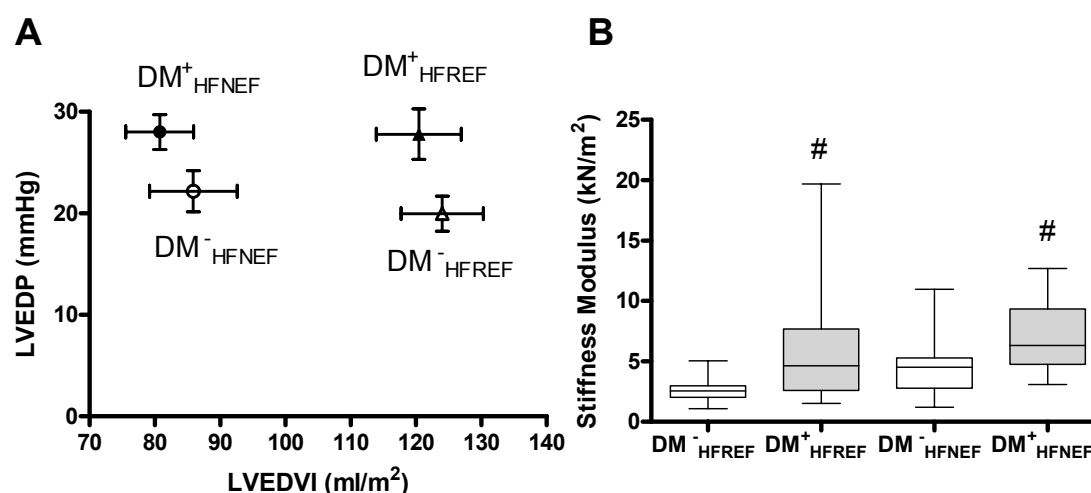


Figure 1. **A.** LVEDP-LVEDVI relations in DM^-_{HFREF} , DM^+_{HFREF} , DM^-_{HFNEF} and DM^+_{HFNEF} patients. Reduced LV end-diastolic distensibility in DM^+_{HFREF} and DM^+_{HFNEF} patients is evident from higher LVEDP at similar LVEDVI. **B.** Higher LV stiffness modulus in DM^+_{HFREF} and DM^+_{HFNEF} patients (# $p < 0.001$).

Myocardial AGEs deposition and fibrosis

AGEs deposition was inferred from CML immunostaining and occurred mainly in the wall of small intramyocardial vessels (Fig 2A). In two-factor ANOVA, CML deposition depended on presence of DM ($p < 0.001$) but not on HFNEF-HFREF status. CML deposition was especially evident when DM^+_{HFREF} patients were compared to DM^-_{HFREF} patients (24.1 ± 3.8 vs. 8.8 ± 2.5 score/mm²; $p = 0.005$) and less so when DM^+_{HFNEF} patients were compared to DM^-_{HFNEF} patients (15.7 ± 2.7 vs. 8.2 ± 2.5 score/mm²; NS) (Fig 2B). CML deposition correlated with the myocardial stiffness modulus in HFREF ($r = 0.48$; $p = 0.014$). The DM-induced rise in myocardial CML deposition in HFREF was paralleled by a rise in E-selectin expression from 3.6 ± 0.9 score/mm² to 9.2 ± 1.9 score/mm² ($p = 0.022$). E-selectin is a marker of inflammatory endothelial activation (Fig 2C).

In two-factor ANOVA, myocardial CVF depended on DM ($p = 0.006$) and on

HFNEF-HFREF status ($p < 0.001$). Moreover, the effect of DM on CVF depended on HFNEF-HFREF status ($p = 0.007$). CVF was higher when DM^+_{HFREF} patients were compared to DM^-_{HFREF} patients (22.4 ± 2.2 vs. $14.6 \pm 1.0\%$; $p < 0.001$) and similar when DM^+_{HFNEF} patients were compared to DM^-_{HFNEF} patients (11.6 ± 1.1 vs. $11.7 \pm 1.1\%$; NS) (Fig 2D). In HFREF patients, CVF correlated with Stiff Mod ($r = 0.37$; $p = 0.039$) and with plasma glycated hemoglobin ($r = 0.61$; $p = 0.0014$).

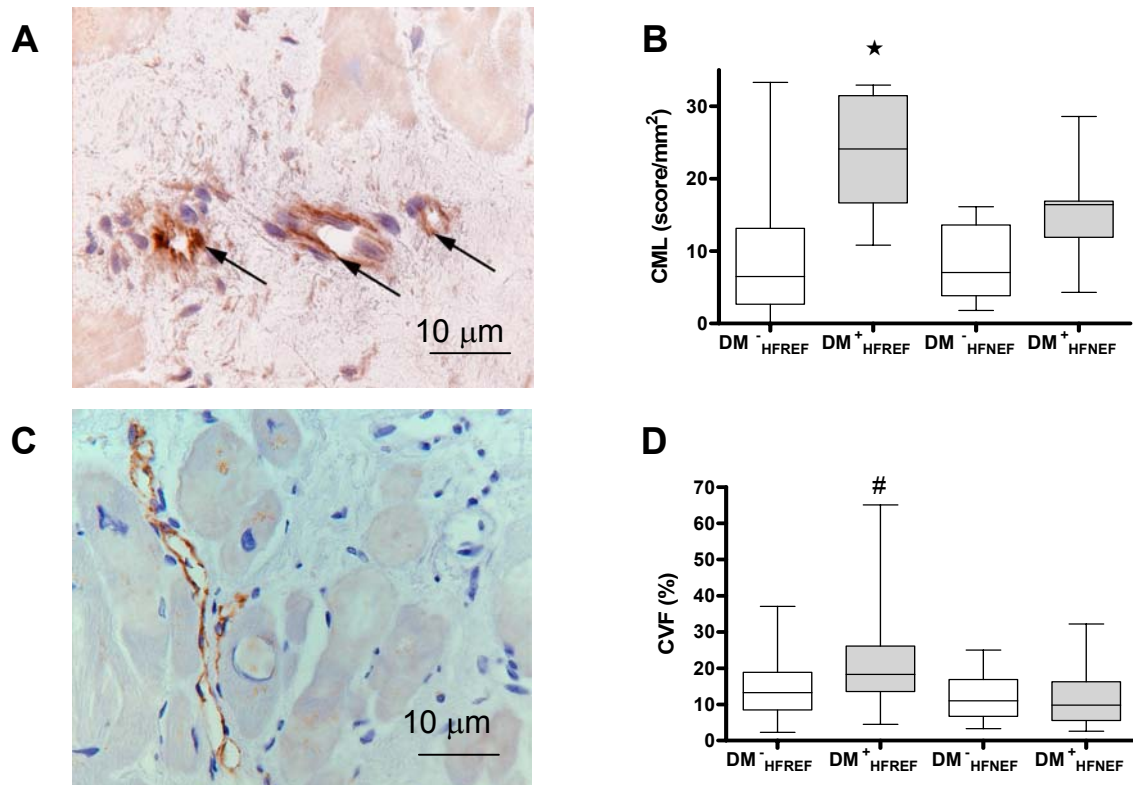


Figure 2. **A.** Representative example of CML deposition in small myocardial vessels (arrows) of DM^+_{HFREF} patients. **B.** Higher CML deposition score in DM^+_{HFREF} patients (* $p < 0.01$). **C.** Representative example of endothelial (arrows) E-selectin expression in DM^+_{HFREF} patients. **D.** Higher CVF in DM^+_{HFREF} patients (# $p < 0.001$).

Myocyte $F_{passive}$, myocyte hypertrophy and LV remodeling

In all cardiomyocytes, $F_{passive}$ was measured at the same sarcomere length of $2.2\mu\text{m}$ (Fig 3A). In two-factor ANOVA, $F_{passive}$ depended on DM ($p=0.009$) and on HFNEF-HFREF status ($p<0.001$). Similar to myocardial CVF, the effect of DM on $F_{passive}$ was depended on HFNEF-HFREF status ($p=0.021$). $F_{passive}$ of $\text{DM}^+_{\text{HFNEF}}$ cardiomyocytes was higher than $F_{passive}$ of $\text{DM}^-_{\text{HFNEF}}$ cardiomyocytes (8.5 ± 0.9 vs. 5.1 ± 0.7 kN/m^2 ; $p=0.006$) while $F_{passive}$ of $\text{DM}^+_{\text{HFREF}}$ cardiomyocytes was comparable to $F_{passive}$ of $\text{DM}^-_{\text{HFREF}}$ cardiomyocytes (3.9 ± 0.5 vs. 3.7 ± 0.4 kN/m^2 ; NS) (Fig 3B). Higher $F_{passive}$ of $\text{DM}^+_{\text{HFNEF}}$ cardiomyocytes was unrelated to isolation-associated cell damage, because active force development at saturating calcium concentration ($p\text{Ca}=4.5$) was comparable in $\text{DM}^+_{\text{HFNEF}}$ (14.7 ± 1.3 kN/m^2) and $\text{DM}^-_{\text{HFNEF}}$ (16.9 ± 1.9 kN/m^2) cardiomyocytes. After administration of PKA, $F_{passive}$ fell especially in $\text{DM}^+_{\text{HFNEF}}$ cardiomyocytes (from 8.5 ± 0.9 to 4.0 ± 0.3 kN/m^2 ; $p<0.001$) and the values of $F_{passive}$ became comparable in all patient groups (Fig 3C). The higher $F_{passive}$ in $\text{DM}^+_{\text{HFNEF}}$ compared to $\text{DM}^-_{\text{HFNEF}}$ cardiomyocytes was paralleled by widening of the sarcomeric Z-disc, which was significantly larger in $\text{DM}^+_{\text{HFNEF}}$ than in $\text{DM}^-_{\text{HFNEF}}$ both on immunofluorescent images stained for α -actinin ($+16.9\%$; $p=0.045$; Fig 3D) and on electronmicroscopy images ($+15.2\%$; $p<0.001$; Fig 3E). In HFNEF patients, $F_{passive}$ correlated with Stiff Mod ($r=0.55$; $p=0.022$) and with the DM duration ($r=0.35$; $p=0.04$).

In control conditions, $F_{passive}$ rose progressively from HFREF to $\text{DM}^-_{\text{HFNEF}}$ and to $\text{DM}^+_{\text{HFNEF}}$ (Fig 3B). This trend was paralleled by the rise of cardiomyocyte diameter (MyD), PWTd and RWT. MyD rose from 16.0 ± 1.5 μm in HFREF, to 19.8 ± 1.7 μm in $\text{DM}^-_{\text{HFNEF}}$ and to 22.4 ± 0.9 μm in $\text{DM}^+_{\text{HFNEF}}$ cardiomyocytes ($r=0.98$; $p<0.001$). PWTd rose from 9.4 ± 0.3 mm in HFREF, to 10.3 ± 0.4 mm in $\text{DM}^-_{\text{HFNEF}}$ and to 11.4 ± 0.3 mm in $\text{DM}^+_{\text{HFNEF}}$ ($r=0.98$; $p=0.037$). RWT rose from 0.27 ± 0.01 in HFREF, to 0.40 ± 0.02 in $\text{DM}^-_{\text{HFNEF}}$ and to 0.45 ± 0.02 in $\text{DM}^+_{\text{HFNEF}}$ ($r=0.97$; $p=0.03$). The progressive rise in RWT indicates a shift from eccentric to concentric LV remodeling.

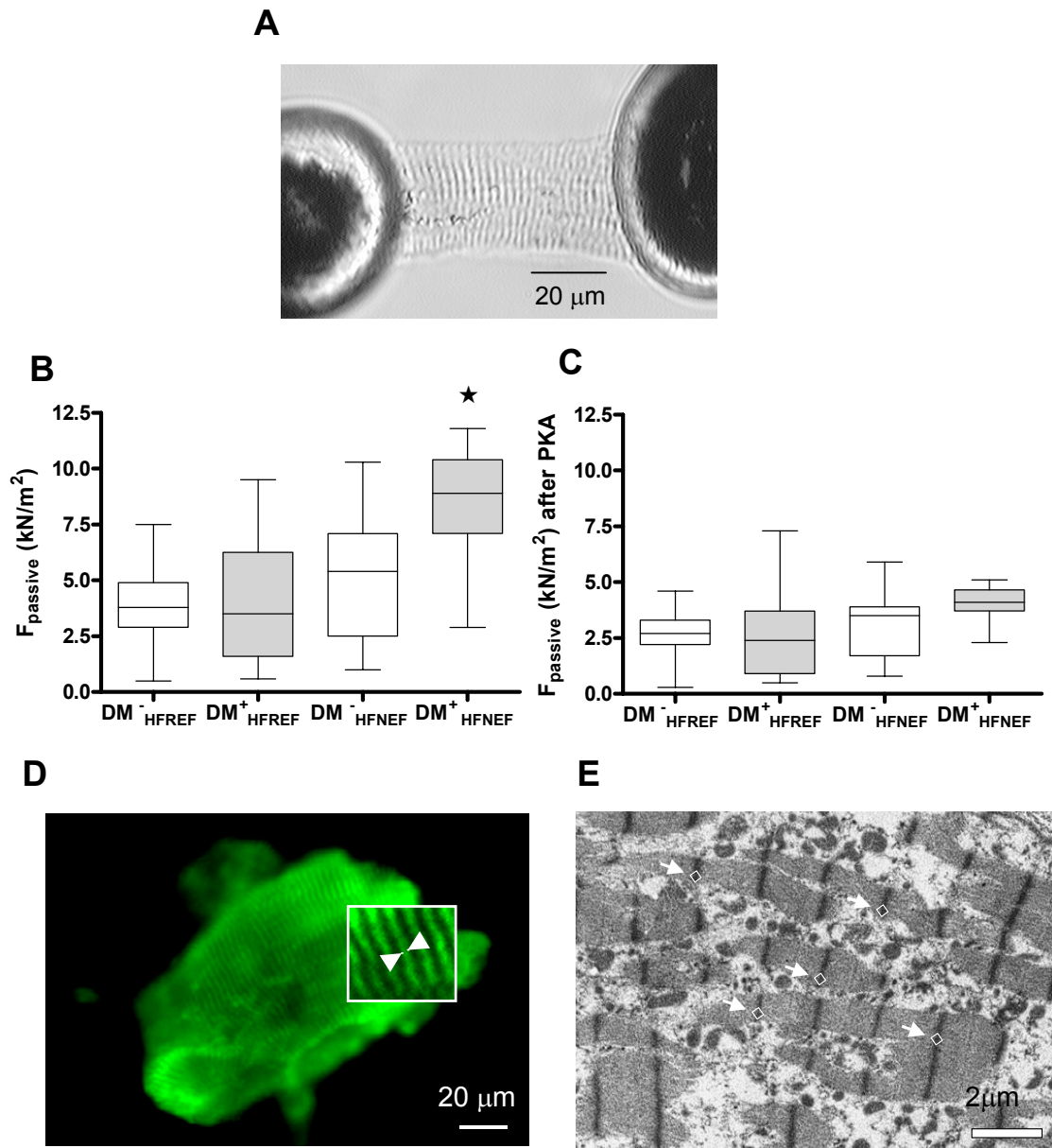


Figure 3. A. Cardiomyocyte mounted between force transducer and piezoelectric motor to measure F_{passive} . **B.** F_{passive} is higher in $\text{DM}^+_{\text{HFNEF}}$ patients (* $p < 0.01$). **C.** After PKA administration, F_{passive} is comparable in all patient groups; **D.** Representative example of immunofluorescent image of cardiomyocytes, stained for α -actinin and used for Z-disc thickness measurement (arrows indicate Z discs); **E.** Representative example of electronmicroscopic Z-disc thickness measurement (arrows indicate Z discs).

Discussion

The prevalence of DM in heart failure is increasing^{24,25} and mortality or hospitalization rates in diabetic patients with heart failure remain particularly high²⁶⁻²⁸. Although CAD is the most important contributor to the myocardial dysfunction observed in DM, DM-related disturbances, such as hyperglycemia, insulin resistance and hyperlipidemia can also directly act on the myocardium²⁹ and induce myocardial dysfunction because of a shift in myocardial energy production from glucose utilization to fatty acid oxidation³⁰⁻³². In the first clinical description of DM-induced myocardial dysfunction, LV dilatation and systolic LV dysfunction were prominent features³³ and DM-induced myocardial dysfunction was therefore classified as a dilated cardiomyopathy. Subsequently, diastolic LV dysfunction was recognized as an earlier manifestation of DM-induced myocardial dysfunction¹⁻⁵. The present study confirmed diastolic LV stiffness to be higher in failing hearts of diabetic patients in the absence of significant CAD. Mechanisms responsible for this DM-induced diastolic myocardial stiffening were identified in endomyocardial biopsies of these patients. The main finding of the study is that DM elevated diastolic LV stiffness by different mechanisms in HFREF and HFNEF patients. In HFREF, DM elevated diastolic LV stiffness through myocardial AGEs deposition and fibrosis whereas in HFNEF, DM raised diastolic LV stiffness mainly through higher F_{passive} of hypertrophied cardiomyocytes.

Myocardial AGEs deposition and fibrosis

DM⁺_{HFREF} patients had higher diastolic LV stiffness than DM⁻_{HFREF} patients. This higher diastolic LV stiffness was related both to AGEs deposition and interstitial fibrosis. AGEs deposition results from longstanding hyperglycemia and affects diastolic LV stiffness by direct and indirect mechanisms^{29,34,35}. AGE crosslinking of collagen increases its tensile strength and this altered biophysical property of collagen raises diastolic LV stiffness. AGEs deposition can also indirectly augment diastolic LV stiffness through enhanced collagen formation and reduced NO bioavailability. Enhanced collagen formation in the presence of AGEs was observed in the present study. AGEs quench endothelially produced NO and low myocardial NO bioavailability was previously demonstrated to raise diastolic LV stiffness in HFREF patients³⁶.

Previous myocarditis and not DM is the most likely cause for the dilated cardiomyopathy in the majority of the DM⁺_{HFREF} patients because fasting glucose, glycated hemoglobin and DM duration were all similar in the DM⁺_{HFREF} and DM⁺_{HFNEF} groups. Even in the absence of cellular infiltration, patients with post myocarditis

HFREF frequently have persistent myocardial microvascular inflammation³⁷. Inflammation facilitates AGEs deposition^{20,38} and persistent microvascular inflammation could therefore explain the preferential CML deposition in small intramyocardial vessels of the DM⁺_{HFREF} patients. In rodent DM animal models, AGEs deposition occurs also in the myocardial interstitium³⁹. Failure to observe interstitial CML deposition in the present study probably relates to better glycemia control in patients treated with glucose lowering medication or insulin than in untreated rodent animal models. The clinical importance of endothelial AGEs deposition was recently confirmed in hypertensive patients in whom a crosslink breaker improved endothelial function⁴⁰.

The present study observed a higher CVF in DM⁺_{HFREF} than in DM⁻_{HFREF} patients. Activation of fibroblasts in DM⁺_{HFREF} patients may have resulted from the aforementioned AGEs deposition, from protein kinase C activation or from high intracellular glucose concentrations^{35,41}.

Cardiomyocyte resting tension

DM⁺_{HFNEF} patients had a higher Stiff Mod than DM⁻_{HFNEF} patients. The higher Stiff Mod related to cardiomyocyte F_{passive} and less to AGEs deposition. Correction of high cardiomyocyte F_{passive} by PKA suggests a phosphorylation deficit of myofilamentary or cytoskeletal proteins^{12,13} because the cardiomyocytes had been pretreated with Triton X-100 to remove all membranes. High F_{passive} of DM⁺_{HFNEF} cardiomyocytes was accompanied by Z-disc widening. Z-disc widening has been observed in transgenic mice after nebulin or muscle LIM protein knock-out^{42,43}. The present study is the first to report Z-disc widening in humans and because of the simultaneous elevation of F_{passive} , suggests Z-disc widening to result from altered elastic properties of cytoskeletal proteins, which pull at and open up adjacent Z-discs. In a previous study comparing HFREF to HFNEF¹³, a significant correlation was observed between cardiomyocyte hypertrophy and F_{passive} . In the present study, F_{passive} rose progressively from HFREF to DM⁻_{HFNEF} and to DM⁺_{HFNEF} and this rise was again paralleled by a rise in MyD and by a shift from eccentric to concentric LV remodeling. As LVPSP and LVPSs were similar in DM⁺_{HFNEF} and DM⁻_{HFNEF}, excess cardiomyocyte hypertrophy in DM⁺_{HFNEF} was unrelated to pressure overload and probably induced by insulin resistance¹⁴. All DM⁺_{HFNEF} patients indeed had type 2 DM and elevated fasting insulin plasma level. Furthermore, hyperinsulinemia is known to stimulate prohypertrophic signaling in insulin responsive tissues, such as the myocardium²⁹.

Limitations

The clinical characteristics of the HFNEF patients differed from clinical characteristics observed in epidemiological studies. In the present study, HFNEF patients were younger (mean age: 64 years) and less often female (46%) in contrast to epidemiological studies⁴⁴ where patients are typically older (mean age: 76 years) and more often female (55%). Patient recruitment from tertiary referral because of suspicion of inflammatory or infiltrative myocardial disease explains this discrepancy.

In the present study, diastolic LV material properties were analyzed by a radial LV stiffness modulus. Use of a radial LV stiffness modulus avoids geometrical assumptions on LV shape. Furthermore, substitution of measured LVP by LVP_{res} allows early diastole to be included in the LV stiffness analysis as it corrects for the upward displacement of the early diastolic LV pressure-volume relation⁴⁵. In a previous study⁴⁶ of HFREF patients, close agreement was observed between the radial LV stiffness modulus and the LV chamber stiffness constant derived from a curve fit to multiple LV end-diastolic pressure-volume points during balloon caval occlusion.

Higher LVEDP at similar or smaller LVEDV can result from altered myocardial material properties and from external constraints on the left ventricle by the right ventricle or by the pericardium⁴⁷. Right ventricular constraints because of the shared interventricular septum are prominent in patients with hypertrophic cardiomyopathy but not in patients with HFNEF who usually have hypertensive heart disease⁴⁷. Right atrial pressure (RAP) was determined as a measure of intrapericardial pressure or pericardial constraint and was comparable in all patient groups.

Because of microvascular CML deposition, relative reduction of the number of microvessels in hypertrophied myocardium could have lowered the CML score in the DM^+_{HFNEF} patients. A similar CML score in DM^-_{HFNEF} and DM^-_{HFREF} patients however argues against such an artifact. Isolation of cardiomyocytes and assessment of myocardial tissue properties was performed on a limited number of samples procured by endomyocardial biopsy technique and potentially overlooks tissue heterogeneity. Extent of tissue heterogeneity was assessed in the present and previous^{12,48} studies. Sampling related variability was < 5% for cardiomyocyte force measurements and < 15% for histomorphometric data.

Development of HFNEF results from diastolic LV dysfunction⁴⁴, deficient chronotropic or vasomotor responses^{49,50} and arterial stiffening⁴⁵. In DM, not only diastolic LV dysfunction but also arterial stiffness becomes a more important contributor to HFNEF.

Conclusions

In the absence of CAD, the failing diabetic heart has an elevated diastolic LV stiffness. Mechanisms responsible for this increase in diastolic LV stiffness differ between HFREF and HFNEF patients. Deposition of AGEs and collagen are important determinants of the increased LV stiffness in diabetic patients with HFREF, while high cardiomyocyte F_{passive} is the main determinant of the increased LV stiffness in diabetic patients with HFNEF.

References

1. Zarich SW, Arbuckle BE, Cohen LR, Roberts M, Nesto RW. Diastolic abnormalities in young asymptomatic diabetic patients assessed by pulsed Doppler echocardiography. *J Am Coll Cardiol* 1988;12:114-120.
2. Avendano G, Dharamsey S, Dasmahapatra A, Agarwal R, Reddi A, Regan T. Left ventricular diastolic function in hypertension and role of plasma glucose and insulin. Comparison with diabetic heart. *Circulation* 1996;93:1396-1402.
3. Diamant M, Lamb HJ, Groeneveld Y, Endert EL, Smit JW, Bax JJ, Romijn JA, de Roos A, Radder JK. Diastolic dysfunction is associated with altered myocardial metabolism in asymptomatic normotensive patients with well-controlled type 2 diabetes mellitus. *J Am Coll Cardiol* 2003;42:328-335.
4. Rutter MK, Parise H, Benjamin EJ, Levy D, Larson MG, Meigs JB, Nesto RW, Wilson PWF, Vasan RS. Impact of glucose intolerance and insulin resistance on cardiac structure and function. Sex-related differences in the Framingham Heart Study. *Circulation* 2003;107:448-454.
5. Fang ZY, Prins JB, Marwick TH. Diabetic cardiomyopathy: evidence, mechanisms, and therapeutic implications. *Endocrine Rev* 2004;25:543-567.
6. Kitzman DW, Gardin JM, Gottdiener JS, Arnold A, Boineau R, Aurigemma G, Marino EK, Lyles M, Cushman M, Enright PL; Cardiovascular Health Research Group. Importance of heart failure with preserved systolic function in patients > or = 65 years of age. CHS Research Group. Cardiovascular Health Study. *Am J Cardiol* 2001;87:413-419.
7. M. Klapholz, M. Maurer, A. M. Lowe, F. Messineo, J. S. Meisner, J. Mitchell, J. Kalman, R. A. Phillips, R. Steingart, E. J. Brown Jr, R. Berkowitz, R. Moskowitz, A. Soni, D. Mancini, R. Bijou, K. Sehhat, N. Varshneya, M. Kukin, S. D. Katz, L. A. Sleeper, T. H. Le Jemtel, and New York Heart Failure Consortium. Hospitalization for heart failure in the presence of a normal left ventricular ejection fraction: Results of the New York heart failure registry. *J Am Coll Cardiol* 2004;43:1432-1438.
8. Stone PH, Muller JE, Hartwell T, York BJ, Rutherford JD, Parker CB, Turi ZG, Strauss HW, Willerson JT, Robertson T. The effect of diabetes mellitus on prognosis and serial left ventricular function after acute myocardial infarction: contribution of both coronary disease and diastolic left ventricular dysfunction to the adverse prognosis. The MILIS Study Group. *J Am Coll Cardiol* 1989;14:49-57.
9. Solomon SD, St John SM, Lamas GA, Plappert T, Rouleau JL, Skali H, Moya L, Braunwald E, Pfeffer MA, Survival and Ventricular Enlargement (SAVE) Investigators. Ventricular remodeling does not accompany the development of heart failure in diabetic patients after myocardial infarction. *Circulation* 2002;106:1251-5.
10. Van Hoesen KH, Factor SM. A comparison of the pathological spectrum of hypertensive, diabetic, and hypertensive-diabetic heart disease. *Circulation* 1990;82:848-855.
11. Berg TJ, Snorgaard O, Faber J, Torjesen PA, Hildebrandt P, Mehlsen J, Hanssen KF. Serum levels of advanced glycation end products are associated with left ventricular diastolic function in patients with type 1 diabetes. *Diabetes Care* 1999;22:1186.
12. Borbély A, van der Velden J, Papp Z, Bronzwaer JGF, Edes I, Stienen GJ, Paulus WJ. Cardiomyocyte Stiffness in Diastolic Heart Failure. *Circulation* 2005;111:774-781.

13. van Heerebeek L, Borbely A, Niessen HW, Bronzwaer JGF, van der Velden J, Stienen GJ, Linke WA, Laarman GJ, Paulus WJ. Myocardial structure and function differ in systolic and diastolic heart failure. *Circulation* 2006;113:1966-73.
14. Ilercil A, Devereux RB, Roman MJ, Paranicas M, O'Grady MJ, Lee ET, Welty TK, Fabsitz RR, Howard BV. Associations of insulin levels with left ventricular structure and function in American Indians: the strong heart study. *Diabetes* 2002;51:1543-1547.
15. Wojnicz R, Nowalany-Kozielska E, Wojciechowska C, Glanowska G, Wilczewski P, Niklewski T, Zembala M, Polonski L, Rozek MM, Wodniecki J. Randomised, placebo-controlled study for immunosuppressive treatment of inflammatory dilated cardiomyopathy: two year follow-up results. *Circulation* 2001;104:39-45.
16. Schoenfeld MH, Supple EW, Dec GW Jr, Fallon JT, Palacios IF. Restrictive cardiomyopathy versus constrictive pericarditis: role of endomyocardial biopsy in avoiding unnecessary thoracotomy. *Circulation* 1987;75:1012-1017.
17. Paulus WJ, Tschöpe C, Sanderson JE, Rusconi C, Flachskampf FA, Rademakers FE, Marino P, Smiseth OA, De Keulenaer G, Leite-Moreira AF, Borbely A, Édes I, Handoko ML, Heymans S, Pezzali N, Pieske B, Dickstein K, Fraser AG, Brutsaert DL. How to diagnose diastolic heart failure ? A consensus statement on the diagnosis of heart failure with normal left ventricular ejection fraction (HFNEF) by the Heart Failure and Echocardiography Associations of the European Society of Cardiology. *Eur Heart J* 2007;28:2539-2550
18. The Expert Committee on the Diagnosis and Classification of Diabetes Mellitus. Follow-up report on the Diagnosis of Diabetes Mellitus. *Diabetes Care* 2003;26:3160-3167.
19. Schalkwijk CG, Baidoshvili A, Stehouwer CD, van Hinsbergh VW, Niessen HW. Increased accumulation of the glycoxidation product N epsilon-(carboxymethyl)lysine in hearts of diabetic patients: generation and characterisation of a monoclonal anti-CML antibody. *Biochim Biophys Acta*. 2004;1636:82-9.
20. Baidoshvili A, Krijnen PAJ, Kupreishvili K, Ciurana C, Bleeker W, Nijmeijer R, Visser CA, Visser FC, Meijer CJLM, Stooker W, Eijnsman L, Van Hinsbergh VWM, Hack CE, Niessen HWM, Schalkwijk CG. N^ε-(carboxymethyl)lysine depositions in intramyocardial arteries in human acute myocardial infarction. A predictor or reflection of infarction ? *Arterioscl Thromb Vasc Biol* 2006;26:2497-2503.
21. Lang RM, Bierig M, Devereux RB, Flachskampf FA, Foster E, Pellikka PA, Picard MH, Roman MJ, Seward J, Shanewise J, Solomon S, Spencer KT, St John Sutton M, Stewart W. Recommendations for chamber quantification. *Eur J Echocardiography* 2006;7:79-108.
22. Paulus WJ, Heyndrickx GR, Buyl P, Goethals MA, Andries E. Wide-range load shift of combined aortic valvuloplasty-arterial vasodilation slows isovolumic relaxation of the hypertrophied left ventricle. *Circulation* 1990;81:886-898.
23. Paulus WJ, Grossman W, Serizawa T, Bourdillon PD, Pasipoularides A, Mirsky I. Different effects of two types of ischemia on myocardial systolic and diastolic function. *Am J Physiol Heart Circ Physiol*. 1985;248:H719-H728.
24. Kamalesh M, Nair G. Disproportionate increase in prevalence of diabetes among patients with congestive heart failure due to systolic dysfunction. *Int J Cardiol* 2005;99:125-127.
25. Owan TE, Hodge DO, Herges RM, Jacobsen SJ, Roger VL, Redfield MM. Trends in prevalence and outcome of heart failure with preserved ejection fraction. *N Engl J Med*

- 2006;355:251-259.
26. Bertoni AG, Hundley WG, Massing MW, Bonds DE, Burke GL, Goff DC Jr. Heart failure prevalence, incidence and mortality in the elderly with diabetes. *Diabetes Care* 2004;27:699-703.
 27. Murcia AM, Hennekens CH, Lamas GA, Jimenez-Navarro M, Rouleau JL, Flaker GC, Goldman S, Skali H, Braunwald E, Pfeffer MA. Impact of diabetes on mortality in patients with myocardial infarction and left ventricular dysfunction. *Arch Intern Med* 2004;164:2273-2279.
 28. Held C, Gerstein HC, Yusuf S, Zhao F, Hilbrich L, Anderson C, Sleight P, Teo K for the ONTARGET/TRANSCEND investigators. Glucose levels predict hospitalization for congestive heart failure in patients at high cardiovascular risk. *Circulation* 2007;115:1371-1375.
 29. Poornima IG, Parikh P, Shannon RP. Diabetic cardiomyopathy: the search for a unifying hypothesis. *Circ Res* 2006;98:596-605.
 30. Taegtmeyer H, McNulty P, Young ME. Adaptation and maladaptation of the heart in diabetes: Part 1. *Circulation* 2002;105:1727-1733.
 31. Lopaschuk GD. Metabolic abnormalities in the diabetic heart. *Heart Failure Reviews* 2002;7:149-159.
 32. Boudina S, Abel ED. Diabetic cardiomyopathy revisited. *Circulation* 2007;115:3213-3223.
 33. Rubler S, Dlugash J, Yuceoglu YZ, Kumral T, Branwood AW, Grishman A. New type of cardiomyopathy associated with diabetic glomerulosclerosis. *Am J Cardiol* 1972;30:595-602.
 34. Kass DA, Bronzwaer JGF, Paulus WJ. What Mechanisms Underlie Diastolic Dysfunction in Heart Failure? *Circ Res* 2004;94:1533-1542.
 35. Asbun J, Villarreal FJ. The pathogenesis of myocardial fibrosis in the setting of diabetic cardiomyopathy. *J Am Coll Cardiol* 2006;47:693-700.
 36. Heymes C, Vanderheyden M, Bronzwaer JGF, Shah AM, Paulus WJ. Endomyocardial nitric oxide synthase and left ventricular preload reserve in dilated cardiomyopathy. *Circulation* 1999;99:3009-3016.
 37. Vallbracht KB, Schwimmbeck PL, Kühl U, Rauch U, Seeberg B, Schultheiss HP. Differential aspects of endothelial function of the coronary microcirculation considering myocardial virus persistence, endothelial activation, and myocardial leukocyte infiltrates. *Circulation* 2005;111:1784-1791.
 38. Anderson MM, Requena JR, Crowley JR, Thorpe SR, Heinecke JW. The myeloperoxidase system of human phagocytes generates N-epsilon-(carboxymethyl)lysine on proteins: a mechanism for producing advanced glycation end products at sites of inflammation. *J Clin Invest* 1999;104:103-113.
 39. Candido R, Forbes JM, Thomas MC, Thallas V, Dean RG, Burns WC, Tikellis C, Ritchie RH, Twigg SM, Cooper ME, Burrell LM. A breaker of advanced glycation end products attenuates diabetes-induced myocardial structural changes. *Circulation Research* 2003;92:785-792.
 40. Zieman SJ, Melenovsky V, Clattenburg L, Corretti MC, Capriotti A, Gerstenblith G, Kass DA. Advanced glycation endproduct crosslink breaker (alagebrium) improves endothelial function in patients with isolated systolic hypertension. *J Hypertens*.

- 2007;25:577-583.
41. Brownlee M. The pathobiology of diabetic complications. *Diabetes* 2005;54:1615-1625.
 42. Witt CC, Burkart C, Labeit D, McNabb M, Wu Y, Granzier H, Labeit S. Nebulin regulates thin filament length, contractility, and Z-disk structure in vivo. *The EMBO Journal* 2006;25:3843-3855.
 43. Hoshijima M. Mechanical stress-strain sensors embedded in cardiac cytoskeleton: Z disk, titin and associated structures. *Am J Physiol* 2006;290:H1313-H1325.
 44. Lam CS, Roger VL, Rodeheffer RJ, Bursi F, Borlaug BA, Ommen SR, Kass DA, Redfield MM. Cardiac structure and ventricular-vascular function in persons with heart failure and preserved ejection fraction from Olmsted County, Minnesota. *Circulation*. 2007;115:1982-90.
 45. Kawaguchi M, Hay I, Fetcs B, Kass DA. Combined ventricular systolic and arterial stiffening in patients with heart failure and preserved ejection fraction: implications for systolic and diastolic reserve limitations. *Circulation* 2003;107:714-720.
 46. Bronzwaer JGF, Zeitz C, Visser CA, Paulus WJ. Endomyocardial nitric oxide synthase and the hemodynamic phenotypes of human dilated cardiomyopathy and of athlete's heart. *Cardiovasc Res* 2002;55:270-278.
 47. Pak PH, Maughan L, Baughman KL, Kass DA. Marked discordance between dynamic and passive diastolic pressure-volume relations in idiopathic hypertrophic cardiomyopathy. *Circulation* 1996;94:52-60.
 48. Bronzwaer JGF, Heymes C, Visser CA, Paulus WJ. Myocardial fibrosis blunts nitric oxide synthase-related preload reserve in human dilated cardiomyopathy. *Am J Physiol*. 2003;284:H10-H16.
 49. Melenovsky V, Borlaug BA, Rosen B, Hay I, Ferruci L, Morell CH, Lakatta EG, Najjar SS, Kass DA. Cardiovascular features of heart failure with preserved ejection fraction versus nonfailing hypertensive left ventricular hypertrophy in the urban Baltimore community: the role of atrial remodeling/dysfunction. *J Am Coll Cardiol* 2007;49:198-207.
 50. Borlaug BA, Melenovsky V, Russell SD, Kessler K, Pacak K, Becker LC, Kass DA. Impaired chronotropic and vasodilator reserves limit exercise capacity in patients with heart failure and a preserved ejection fraction. *Circulation* 2006;114:2138-214.

7

Lack of Specificity of Antibodies Directed Against Human Beta-Adrenergic Receptors

Nazha Hamdani, Jolanda van der Velden

Abstract

The present study was designed to investigate if antibodies against β -adrenergic receptors (β ARs) can be used to determine expression of β AR in human myocardium.

Western blotting was performed to investigate the specificity of antibodies directed against β_1 AR and β_2 AR in human left ventricular (LV) tissue. A comparison was made between cardiac tissue from patients with idiopathic dilated cardiomyopathy (IDCM) and ischemic heart disease (ISHD), and non-failing donors.

The antibodies directed against β_1 AR and β_2 AR recognized several protein bands at different molecular weights. Moreover, both antibodies also recognized multiple proteins in Chinese hamster ovary (CHO) cells expressing β_1 AR, β_2 AR and even β_3 AR.

β AR antibodies are not specific and are not suited to study expression of β AR in human myocardium.

Introduction

The β -adrenergic pathway is activated upon an increase in catecholamine levels. Binding of catecholamines to the β ARs increases contractility of the cardiomyocytes via protein kinase A-mediated phosphorylation of down-stream target proteins involved in calcium handling¹ and myofilament contraction.² In the human myocardium at least three types of β ARs are present, including β_1 AR, β_2 AR and β_3 AR.³ Analysis of β ARs in crude membrane fractions using radioligand binding studies revealed a ratio of 80:20 for β_1 AR and β_2 AR in non-failing human donor tissue,³ with β_1 AR as the predominant receptor. In failing idiopathic dilated cardiomyopathy (IDCM) myocardium a down-regulation of β_1 AR has been observed, leading to a relative increase in β_2 AR, as illustrated by the altered ratio of β_1 AR and β_2 AR to 60:40 in the failing heart.³⁻⁵ Diverse alterations in myocardial β AR density have been reported in IDCM and ischemic heart disease (ISHD) patients.^{6,7} In failing IDCM myocardium a down-regulation of β_1 AR has been observed,⁶ while β_2 AR remained unchanged.⁷ In contrast, a reduction of both β_1 AR and β_2 AR was reported in ISHD patients.^{4,5,7}

Apart from radioligand binding studies, Western blotting is often used to determine expression levels of β AR. The present study was designed to investigate specific binding of antibodies directed against β_1 AR and β_2 AR in different human heart samples. LV tissue from patients with IDCM and ISHD was compared with non-failing donor myocardium. Moreover, specific binding of β AR antibodies was investigated in CHO cells expressing human β ARs.⁸

Methods and Materials

Human ventricular tissue

LV transmural tissue samples were obtained during heart transplantation surgery from end-stage heart failure patients (NYHA III-IV) with IDCM (n=21) and ISHD (n=19). LV tissue from donor hearts (n=10) served as reference for non-failing myocardium. Tissue was collected in cardioplegic solution and stored in liquid nitrogen. Samples were obtained after informed consent and with approval of the local Ethical Committee (St Vincents' Hospital Human Research Ethics Committee: File number: H03/118; Title: Molecular Analysis of Human heart Failure).

Cell culture

Our experiments are based on CHO cells expressing either the human β_1 AR, β_2 AR or β_3 AR at densities (B_{max}) of 118 ± 28 , 202 ± 27 and 199 ± 59 fmol/mg proteins as previously described (Niclauss et al. 2006).⁸ CHO cells were stably transfected with human β AR subtypes using a pSW104 vector and grown in an atmosphere of 5% CO₂/95% air at 37°C in F-12 HAM medium supplemented with 10% heat-inactivated fetal calf serum, 1 mM glutamine, 100 U/ml penicillin and 0.1 mg/ml streptomycin. Subconfluent cells were subcultured every 3–4 days with a 2.5 g/liter trypsin and 0.2 g/liter Na⁴EDTA solution. To maintain selection pressure the antibiotic G418 (400 mg/ml) was added to all growing cells in regular intervals, but was not present during the experiments. For all experiments the cells were cultured in the absence of serum for 24 h preceding the experiments to avoid interference of serum factors with cell growth and related signal transduction.

Detection of β ARs

Antibodies against β_1 AR and β_2 AR

Two different primary rabbit polyclonal antibodies directed against the β_1 AR and β_2 AR were used for Western blotting. Both antibodies were from Santa Cruz (β_1 AR (V-19): catalogue: sc-568; β_2 AR (H-73): catalogue: sc-9042). The antibody directed against β_1 AR was raised against amino acids 420-470 at the C-terminus of β_1 AR of mouse origin, while the β_2 AR antibody was raised against amino acids 338-413 mapping at the C-terminus of the β_2 AR of human origin.

Western blotting

Protein expression levels of β_1 AR and β_2 AR were analyzed by one-dimensional 15% SDS-polyacrylamide gel electrophoresis (1D-PAGE) and subsequent Western blotting. Cardiac tissue homogenates (in sample buffer containing 15% glycerol, 62.5 mmol/l Tris (pH 6.8), 1% (w/v) SDS and 2% (w/v) DTT) were applied in a concentration, which was within the linear range of detection: 20 μ g protein/lane for β_1 AR and β_2 AR. After 1D separation proteins were transferred to Hybond-ECL nitrocellulose membranes. Blots were pre-incubated with 0.5% milk powder in TTBS (Tween-tris-buffered-saline; 10 mmol/L Tris-HCl pH 7.6, 75 mmol/L NaCl, 0.1% Tween) for one hour at room temperature. The blots were incubated overnight at 4°C with primary rabbit polyclonal antibodies against β_1 AR (dilution 1:200) and β_2 AR (dilution 1:200). After washing with TTBS, primary antibody binding was visualized using a secondary horseradish peroxidase-labeled goat-anti-rabbit antibody (dilution

1:2000; DakoCytomation) and enhanced chemiluminescence (ECL plus Western blotting detection, Amersham Biosciences). All signals were normalized to actin (dilution 1:1000; clone KJ43A; Sigma) stained on the same blots.

Results

Detection of β ARs in human myocardium

Figure 1A shows Western blots of failing and non-failing cardiac samples. The antibodies against β_1 AR and β_2 AR recognized multiple bands at different molecular weights (mw) (Fig 1A). A similar pattern of protein bands was obtained when we replaced milk by albumin (BSA, bovine serum albumin 2%) as blocking agent. The molecular weight of the detected protein bands was calculated on the basis of the molecular weight marker (Precision Plus Protein Standards Dual Color).

The most prominent band visualized upon β_1 AR labeling was observed at 33 kDa, and two more faint bands of higher molecular weight were found. All of these were no longer visible in the presence of blocking peptide against β_1 AR (dilution 1:200; sc-568p; Santa Cruz) (Fig 1B).

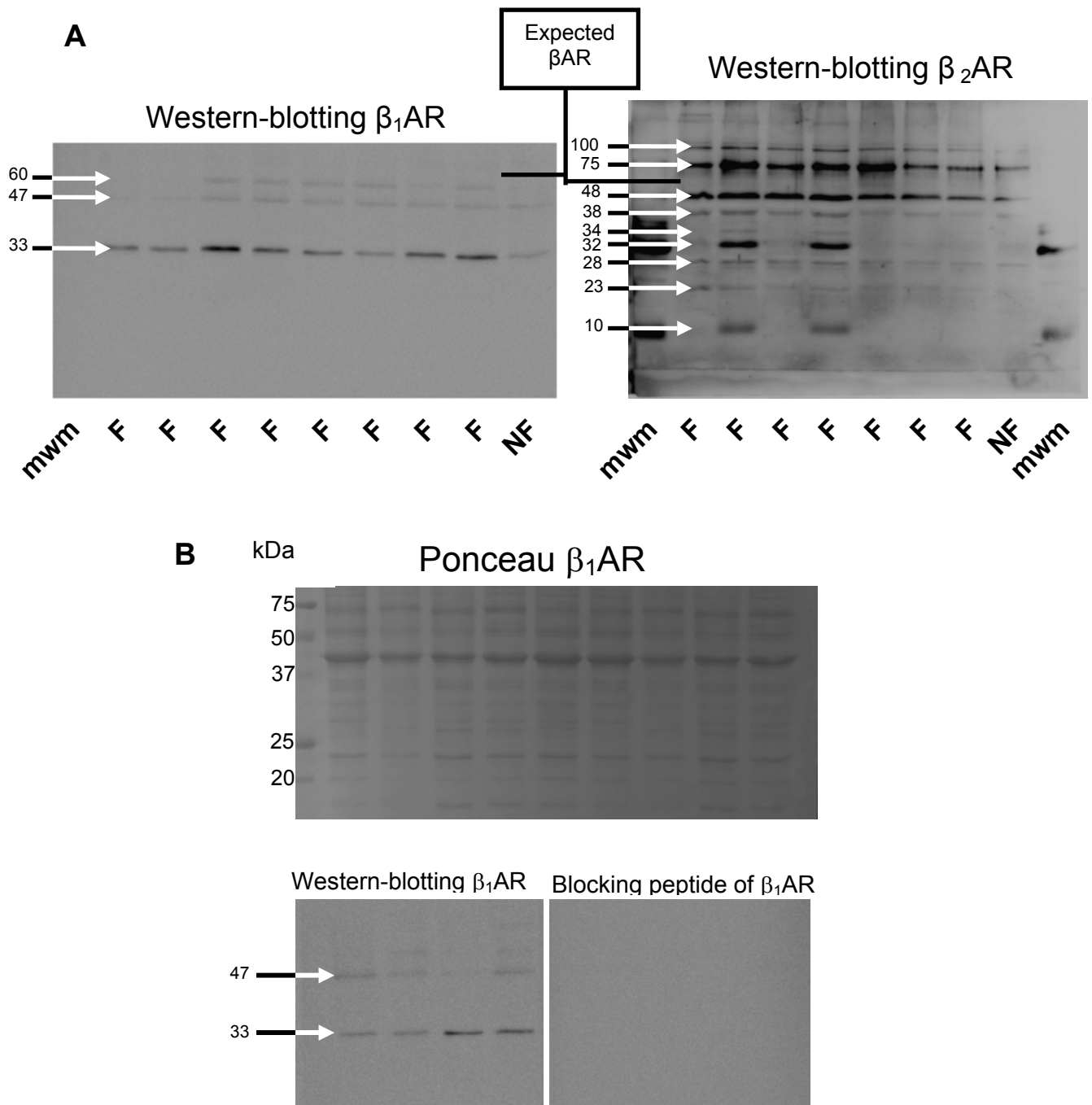


Figure 1. Western blot staining of a failing (F) and nonfailing (NF) cardiac samples separated by 1D-PAGE. **A** illustrates protein bands (indicated by arrows) detected by antibodies against β_1 AR and β_2 AR. Molecular weight of the protein bands was calculated on the basis of the molecular weight marker (mwm). The predicted molecular weight for the β ARs is shown in bold. **B.** Western blots incubated with β_1 AR antibody without blocking peptide (left panel) and with blocking peptide (right panel) of F and NF samples.

The β_2 AR antiserum recognized a large number of bands among which those at 32, 48 and 75 kDa were most prominent. None of the detected protein bands corresponded with the predicted molecular weight of the β_2 AR, which is ~65 kDa.

Immunoreactivity levels of different protein bands detected by the β AR antibodies were expressed relative to actin expression. Bar graphs are shown in Figure 1C for the mean data (sum of all signals obtained with antibodies directed against β AR) obtained in IDCM and ISHD samples in comparison to donor myocardium, which was set to 1. One-way ANOVA revealed no significant differences in the immunoreactivity of β_1 AR and β_2 AR between all groups.

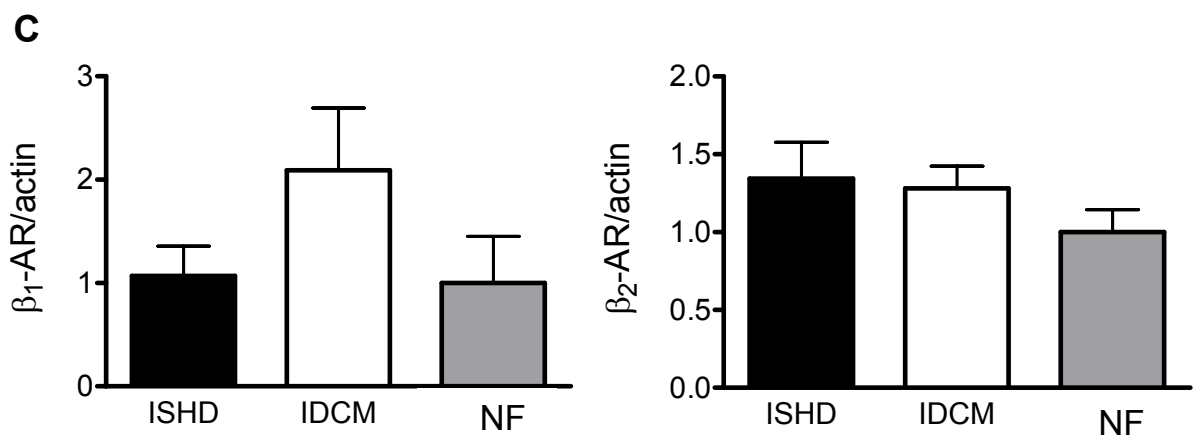


Figure 1. C. Analysis of β ARs revealed no significant differences between IDCM, ISHD, and NF donor myocardium

Analysis of β ARs in CHO cells

Subsequently, specificity of antibodies directly against β_1 AR and β_2 AR was tested in CHO cells expressing β_1 AR, β_2 AR and β_3 AR (Fig 2). In addition failing and non-failing samples were used as controls. The antibodies directed against β_1 AR and β_2 AR all recognized several protein bands with molecular weights ranging between 25 and 120 kDa in CHO cells expressing β_1 AR, β_2 AR, and even β_3 AR, while no band was observed at the expected molecular weight of ~65 kDa. All protein bands stained with the β_1 AR antibody disappeared in the presence of the blocking peptide against β_1 AR (Fig 3).

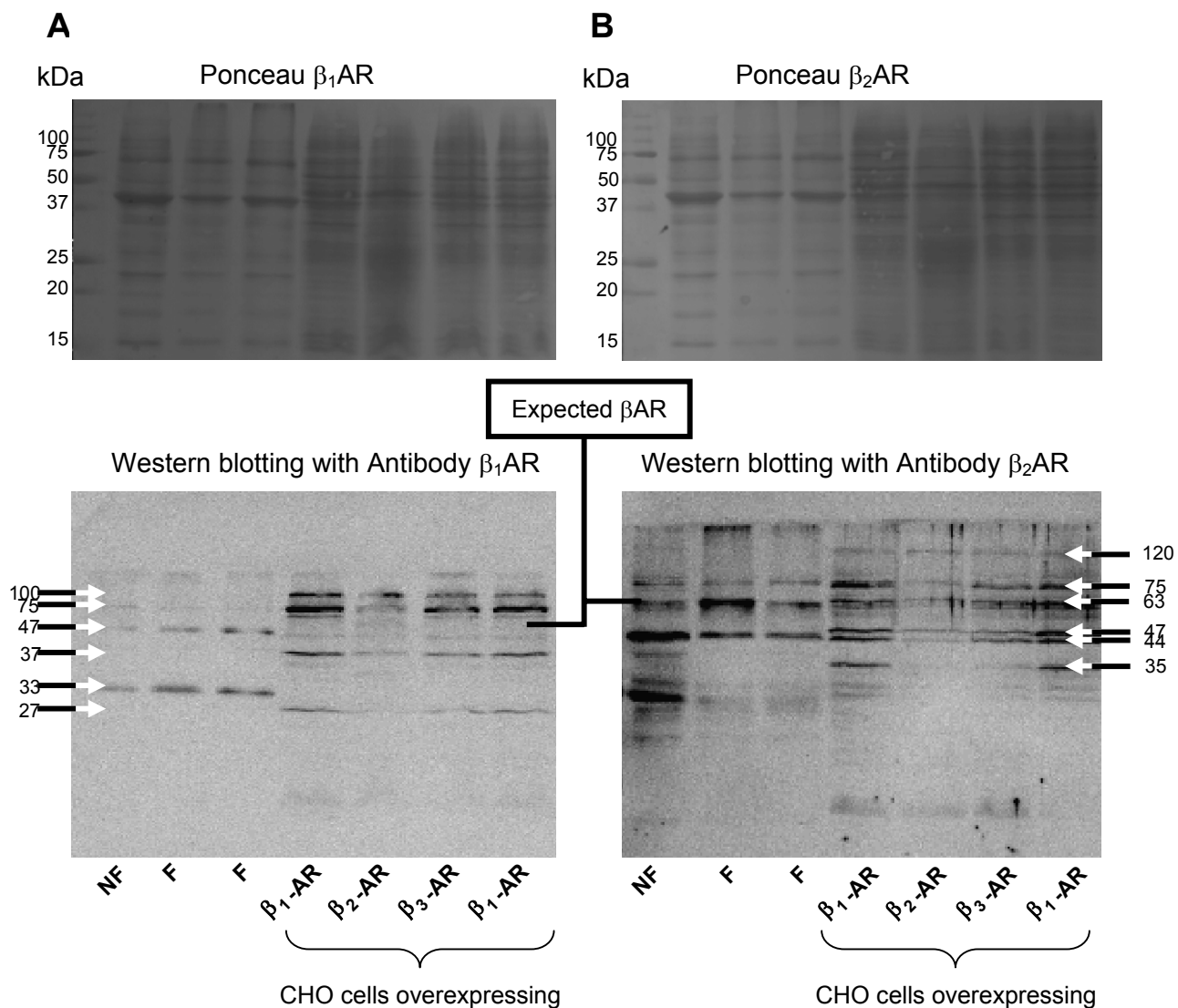


Figure 2. Western blots illustrating the binding of antibodies directed against β_1 AR (**A**) and β_2 AR (**B**) in failing and nonfailing human samples and CHO cells expressing β_1 AR, β_2 AR and β_3 AR.

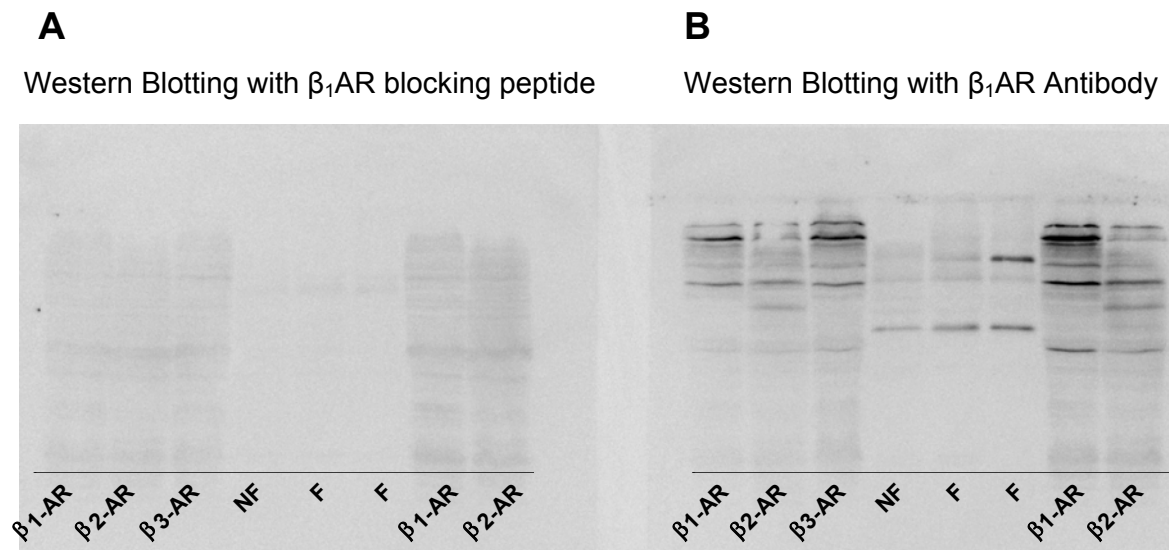


Figure 3. A. Western blots illustrating the Western blot analysis using antibodies directed against β_1 AR in combination with a blocking peptide in CHO cells, failing and non-failing donor. **B.** Western blots illustrating the binding of antibodies directed against β_1 AR in CHO cells, failing and non-failing donor. All protein bands stained with the β_1 AR antibody disappeared in the presence of the blocking peptide against β_1 AR, both in tissue and CHO cells

Discussion

Most of the antibodies known to interact with β ARs described in the literature did not exhibit subtype selectivity.⁹⁻¹¹ Moxham et al. (1986)⁹ investigated β_1 ARs and β_2 ARs in membrane preparations from rat lung and rat heart, respectively, and observed that antibodies directed against β_1 AR and β_2 AR, interacted with both receptor subtypes. In these previous studies antibodies were raised against isolated receptor subtypes, while the antibodies used in our study were directed against a peptide sequence, which might increase their selectivity.

Our study shows that antibodies directed at a specific part of the β ARs are still not specific and do not allow determination of β AR expression levels, since both antibodies detected a range of protein bands at different molecular weights in failing and non-failing human cardiac samples. Noteworthy, no bands were observed at the predicted molecular weight of 65 kDa. Several studies have shown that the 65 kDa subunit exists in a dimeric form in the cell membrane, with a molecular size of 109 kDa as determined by immunoaffinity chromatography using monoclonal autoantibodies and SDS-polyacrylamide gels.^{12,13} We did not find evidence for a dimeric form in our study using the β_1 AR and β_2 AR antibodies.

It has been proposed that the different bands detected upon β AR antibody binding represent different forms of the β ARs resulting from complex formation and/or post-translational modifications such as glycosylation as described by Rybin et al. (2000).¹⁴ Both antibodies against β_1 AR and β_2 AR detected a band with a molecular weight of 75 kDa in all samples. Glycosylation may alter molecular weight of β ARs by 8 to 11 kDa (George et al. 1986),¹⁵ and hence it is possible that the band detected at 75 kDa is the putative β AR.

Based on the assumption that all signals represent different forms of β ARs, we averaged the sum of all β AR signals for the different cardiac samples. No significant difference was observed in β AR expression level (sum of all β AR signals relative to actin) between failing and non-failing samples. It should be noted that tissue preparation might have interfered with analysis of β AR expression. In the present study, expression of β_1 AR and β_2 AR was determined in whole cardiac homogenates, and therefore lacks information about receptor density at the membranes (i.e. functionally available receptors for ligand binding). However, the fact that multiple protein bands were stained with both β_1 AR and β_2 AR antibodies in CHO cells expressing β ARs, even in cells with the β_3 AR, indicates that the antibodies are not specific. Moreover, all protein bands stained with the β_1 AR antibody disappeared in the presence of the blocking peptide against β_1 AR, both in tissue and CHO cells (Fig

3A and B), illustrating that the Western blot analysis using antibodies directed against β AR in combination with a blocking peptide is invalid and cannot be used for quantitative analysis of β AR densities.

In conclusion, Western blot analysis cannot be used for quantitative analysis of β AR receptors because they do not show specific binding to their target protein. Further investigations have to be performed to clarify the selectivity and specificity of antibodies against β AR receptor proteins.

Acknowledgements

We thank Prof Cris dos Remedios (Muscle Research Unit, Institute For Biomedical Research, the University of Sydney, Australia) for the human ventricular tissue samples. We thank Prof Martin Michel (Dept. Pharmacology & Pharmacotherapy AMC, University of Amsterdam, Amsterdam, the Netherlands) for providing the CHO cells expressing β ARs.

References

1. Hasenfuss G, Pieske B. Calcium cycling in congestive heart failure. *J Mol Cell Cardiol.* 2002;34:951-969.
2. Solaro RJ, Moir AJ, Perry SV. Phosphorylation of troponin I and the inotropic effect of adrenaline in the perfused rabbit heart. *Nature.* 1976;262:615-617
3. Brodde OE. Beta-adrenoceptor blocker treatment and the cardiac beta-adrenoceptor-G-protein(s)-adenylyl cyclase system in chronic heart failure. *Naunyn Schmiedebergs Arch Pharmacol.* 2007;374:361-72.
4. Bristow MR, Ginsburg R, Umans V, Fowler M, Minobe W, Rasmussen R, Zera P, Menlove R, Shah P, Jamieson S. Beta 1- and beta 2-adrenergic-receptor subpopulations in nonfailing and failing human ventricular myocardium: coupling of both receptor subtypes to muscle contraction and selective beta 1-receptor down-regulation in heart failure. *Circ Res.* 1986;59:297-309.
5. Bristow MR, Hershberger RE, Port JD, Minobe W, Rasmussen R. Beta 1- and beta 2-adrenergic receptor-mediated adenylyl cyclase stimulation in nonfailing and failing human ventricular myocardium. *Mol Pharmacol.* 1989;35:295-303.
6. Bristow MR, Anderson FL, Port JD, Skerl L, Hershberger RE, Larrabee P, O'Connell JB, Renlund DG, Volkman K, Murray J. Differences in beta-adrenergic neuroeffector mechanisms in ischemic versus idiopathic dilated cardiomyopathy. *Circulation.* 1991;84:1024-39.
7. Steinfath M, Geertz B, Schmitz W, Scholz H, Haverich A, Breil I, Hanrath P, Reupcke C, Sigmund M, Lo HB. Distinct down-regulation of cardiac beta 1- and beta 2-adrenoceptors in different human heart diseases. *Naunyn Schmiedebergs Arch Pharmacol.* 1991;343:217-220.
8. Niclauss N, Michel-Reher MB, Alewijnse AE, Michel MC. Comparison of three radioligands for the labelling of human β -adrenoceptor subtypes. *Naunyn-Schmiedeberg's Arch Pharmacol.* 2006;374:99-105.
9. Moxham CP, George ST, Graziano MP, Brandwein HJ, Malbon CC. Mammalian beta 1- and beta 2-adrenergic receptors. Immunological and structural comparisons. *J Biol Chem.* 1986;261:14562-14570.
10. Dixon RA, Kobilka BK, Strader DJ, Benovic JL, Dohlman HG, Frielle T, Bolanowski MA, Bennett CD, Rands E, Diehl RE, Mumford RA, Slater EE, Sigal IS, Caron MG, Lefkowitz RJ, Strader CD. Cloning of the gene and cDNA for mammalian beta-adrenergic receptor and homology with rhodopsin. *Nature.* 1986;321:75-79.
11. Kaveri SV, Cervantes-Olivier P, Delavier-Klutchko C, Strosberg AD. Monoclonal antibodies directed against the human A431 beta 2-adrenergic receptor recognize two major polypeptide chains. *Eur J Biochem.* 1987;167:449-456.
12. Boivin B, Lavoie C, Vaniotis G, Baragli A, Villeneuve LR, Ethier N, Trieu P, Allen BG, Hébert TE. Functional beta-adrenergic receptor signalling on nuclear membranes in adult rat and mouse ventricular cardiomyocytes. *Cardiovasc Res.* 2006;71:69-78.
13. Fraser CM, Venter JC. The size of the mammalian lung beta 2-adrenergic receptor as determined by target size analysis and immunoaffinity chromatography. *Biochem Biophys Res Commun.* 1982;109:21-29.
14. Rybin VO, Xu X, Lisanti MP, Steinberg SF. Differential targeting of beta -adrenergic receptor subtypes and adenylyl cyclase to cardiomyocyte caveolae: A mechanism to

functionally regulate the cAMP signaling pathway. *J Biol Chem.* 2000;275:41447-41457.

15. George ST, Ruoho AE, Malbon CC. N-Glycosylation in expression and function of β -adrenergic receptors. *J Biol Chem.* 1986;261:16559–16564.

8

Myofilament Dysfunction in Cardiac Disease From Mice to Men.

Nazha Hamdani, Monique de Waard, Andrew E Messer, Nicky M Boontje,
Viola Kooij, Sabine van Dijk, Amanda Versteilen, Regis Lamberts, Daphne
Merkus, Cris dos Remedios, Dirk J Duncker, Attila Borbely, Zoltan Papp,
Walter Paulus, Ger JM Stienen, Steven B Marston,
Jolanda van der Velden

Journal of muscle Research and Cell Motility 2008 29:189-201

Abstract

In healthy human myocardium a tight balance exists between receptor-mediated kinases and phosphatases coordinating phosphorylation of regulatory proteins involved in cardiomyocyte contractility. During heart failure, when neurohumoral stimulation increases to compensate for reduced cardiac pump function, this balance is perturbed. The imbalance between kinases and phosphatases upon chronic neurohumoral stimulation is detrimental and initiates cardiac remodelling, and phosphorylation changes of regulatory proteins, which impair cardiomyocyte function.

The main signalling pathway involved in enhanced cardiomyocyte contractility during increased cardiac load is the β -adrenergic signalling route, which becomes desensitised upon chronic stimulation. At the myofilament level, activation of protein kinase A (PKA), the down-stream kinase of the β -adrenergic receptors (β AR), phosphorylates troponin I, myosin binding protein C and titin, which all exert differential effects on myofilament function. As a consequence of β AR down-regulation and desensitization, phosphorylation of the PKA-target proteins within the cardiomyocyte may be decreased and alter myofilament function. Here we discuss involvement of altered PKA-mediated myofilament protein phosphorylation in different animal and human studies, and discuss the roles of troponin I, myosin binding protein C and titin in regulating myofilament dysfunction in cardiac disease. Data from the different animal and human studies emphasize the importance of careful biopsy procurement, and the need to investigate localization of kinases and phosphatases within the cardiomyocyte, in particular their co-localization with cardiac myofilaments upon receptor stimulation.

Introduction

In healthy humans, the sympathetic nervous system (SNS) as well as the renin-angiotensin-aldosterone system are important mechanisms to maintain adequate perfusion of vital organs via peripheral vasoconstriction, an increase in heart rate and an improvement of myocardial contractility. Although aimed at maintaining cardiac pump function, chronic neurohumoral stimulation in patients with cardiovascular disease is detrimental for cardiac function¹ illustrated by the negative correlation between noradrenaline plasma levels² and prognosis of the patient and by the improvement of symptoms and prolonged survival of patients treated with neurohumoral antagonists.³

Activation of the β -adrenergic receptors by SNS is the main signalling route responsible for increasing cardiomyocyte contractility. Beta-adrenergic receptor (β AR) stimulation induces protein kinase A (PKA)-mediated phosphorylation of L-type Ca^{2+} channels and ryanodine receptors, increasing cytosolic Ca^{2+} , and of phospholamban, increasing activity of the SR Ca^{2+} -ATPase pump and SR Ca^{2+} uptake and loading.⁴ At the myofilament level, PKA-mediated phosphorylation of troponin I (cTnI) and myosin binding protein C (cMyBP-C) decrease myofilament Ca^{2+} -sensitivity^{5,6} and contributes to an acceleration of cardiac relaxation.⁷⁻⁹ Stelzer et al. (2007)¹⁰ have proposed a dominant role for cMyBP-C phosphorylation in regulating the rate of cross-bridge cycling and force development upon β -AR stimulation.¹⁰ Moreover, several studies revealed a role for PKA-mediated phosphorylation of titin in regulating cardiomyocyte stiffness.¹¹⁻¹³

Chronic SNS activation in cardiovascular disease results in down-regulation and uncoupling of β -adrenergic receptors^{14,15} and thereby limits cardiac responsiveness during increased cardiac load as occurs during exercise. In human heart failure, down-regulation and uncoupling of the β AR pathway leads to decreased PKA-mediated phosphorylation of Ca^{2+} handling and myofilament proteins. Here we present data from different animal (mouse, rat, pig) and human heart failure models in support for reduced β AR-mediated signalling and defects in myofilament function.

Materials and methods

Cardiac tissue

All animal experiments were performed in accordance with the Guide for the Care and Use of Laboratory Animals (NIH Publication 86-23, revised 1996), and with approval of the Animal Care Committee of the VU Medical Center and of the Erasmus Medical Center. Cardiac samples from the left (LV) or right (RV) ventricular wall were obtained from control and diseased: mouse (myocardial infarction, MI), rat (pressure overload), pig (MI) and human (ischemic heart disease, ISHD; idiopathic dilated cardiomyopathy, IDCM) myocardium.

Mice: In mice (C57B1/6J of either sex) myocardial infarction (n=7) was produced by permanent ligation of the left anterior descending coronary artery as described before.¹⁶ Sham animals (n=6) underwent the operation without infarct induction. Cardiomyocyte measurements and protein analysis were performed in tissue from remodelled LV myocardium.

Rats: Animals (male, Wistar; body weight 175 g) received a single subcutaneous injection of 80 mg kg⁻¹ monocrotaline (n=10).¹⁷ During its first passage through the pulmonary circulation monocrotaline damages the pulmonary endothelium, thereby inducing pulmonary hypertension, causing right ventricular (RV) hypertrophy resulting eventually in RV heart failure.^{18,19} Sham animals (control, n=11) received a saline injection. Cardiomyocyte measurements and protein analysis were performed in isolated skinned cardiomyocytes obtained from RV tissue of quiescent control and failing hearts.

Pigs: In pigs (2-3 month old Yorkshire-Landrace pigs of either sex) the left circumflex coronary artery was permanently ligated to produce a myocardial infarction (n=6).^{20,21} In sham animals (n=7) the suture was removed. Three weeks after surgery (transmural, 0.5 mg wet weight) needle biopsies were taken from the LV anterior free wall myocardium (in MI pigs: remodelled non-infarcted tissue) and immediately frozen and stored in liquid nitrogen.²² Cardiomyocyte measurements and protein analysis were performed in the subendocardial part of the biopsies.

Human: Within the human studies LV tissue samples were obtained during heart transplantation surgery from patients with end-stage ischemic (n=10) and dilated cardiomyopathy (n=5) (NYHA class IV).^{23,24} Non-failing heart tissue was obtained

from donor hearts (n=10) when no suitable transplant recipient was found. The donors had no history of cardiac disease, a normal cardiac examination, normal ECG and normal ventricular function on echocardiography within 24 h of heart explantation. The tissue was collected in cardioplegic solution and stored in liquid nitrogen. Samples were obtained after informed consent and with approval of the local Ethical Committee (St Vincents' Hospital Human Research Ethics Committee: File number: H03/118; Title: Molecular Analysis of Human heart Failure).

Cardiomyocyte measurements

Single cardiomyocytes were obtained via mechanical isolation from left or right ventricular tissue samples, and incubated for 5 min with Triton X-100 (0.5%) to remove all membranes. Isometric force was measured at various calcium concentrations (pCa, $-\log[\text{Ca}^{2+}]$, ranged from 4.5 to 9) at 15°C and sarcomere length of 2.2 μm . Figure 1A shows a single human cardiomyocyte glued between a force transducer and a motor. After maximal activation 4 to 5 measurements were carried out at submaximal $[\text{Ca}^{2+}]$ followed by a maximal activation. Force values obtained in solutions with submaximal $[\text{Ca}^{2+}]$ were normalized to the interpolated maximal force values. In a number of cells force measurements were repeated after incubation with the catalytic subunit of protein kinase A (PKA, 40 min; 20°C; 100 U/mL, Sigma). Force registrations before and after PKA at maximal $[\text{Ca}^{2+}]$ (pCa 4.5) and submaximal $[\text{Ca}^{2+}]$ (pCa 5.6) are shown in Figure 1B. Maximal calcium activated tension (F_{active} , i.e. maximal force/cross-sectional area) was calculated by subtracting passive force (F_{passive}) from the total force (F_{total}) at saturating $[\text{Ca}^{2+}]$ (pCa 4.5) (Fig 1B). Passive tension (F_{pas}) was determined by shortening the cell in relaxation solution (pCa 9.0) by 20%. Ca^{2+} -sensitivity is denoted as pCa_{50} , i.e. pCa value at which 50% of F_{active} is reached.

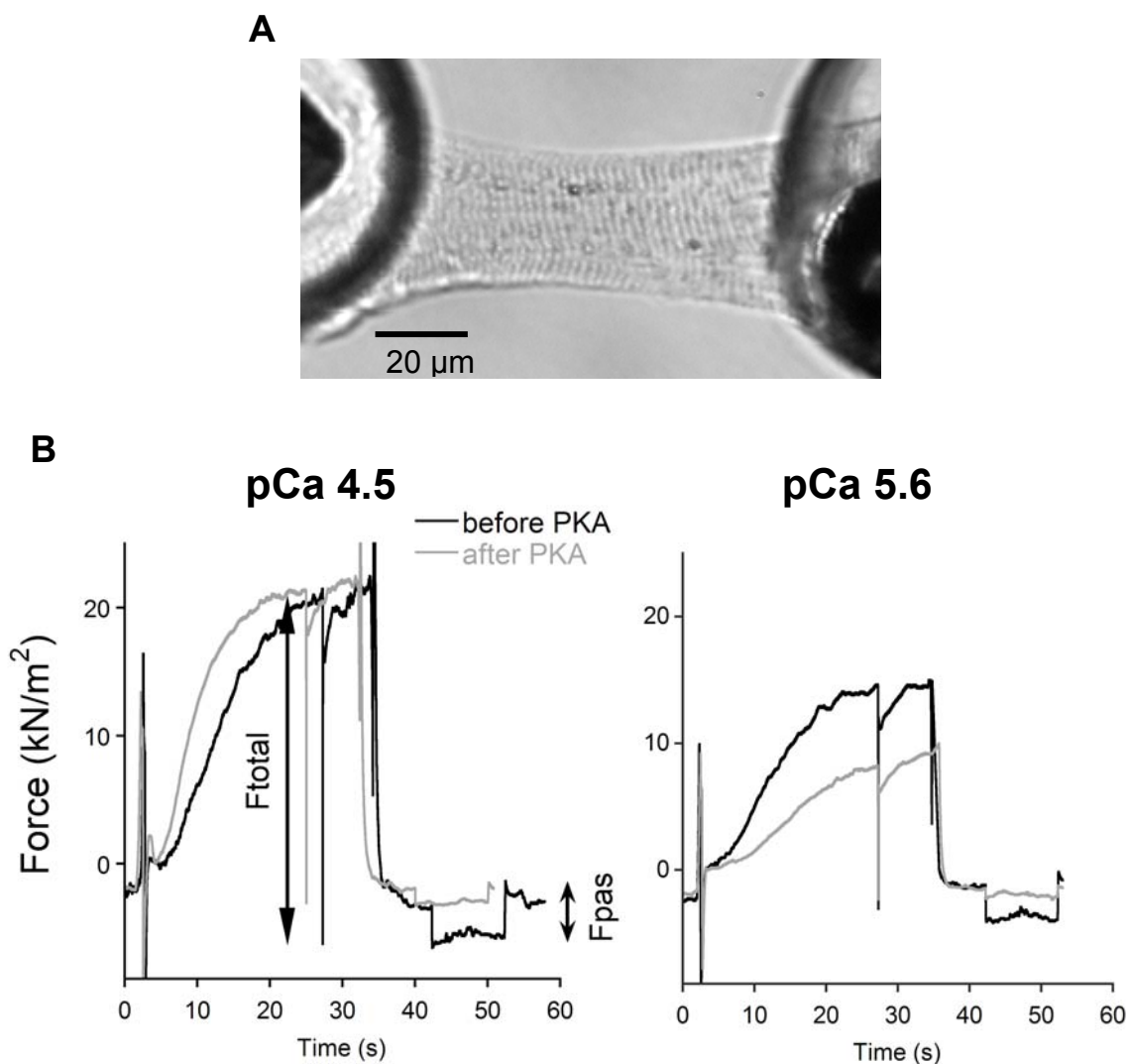


Figure 1. Force measurements in single permeabilized cardiomyocytes. A. Single human cardiomyocyte at a sarcomere length of 2.2 μm . **B.** Isometric force measured at maximal $[\text{Ca}^{2+}]$ (pCa 4.5) and submaximal $[\text{Ca}^{2+}]$ (pCa 5.6) before and after protein kinase A in a cardiomyocyte from a patient with heart failure.

In vitro motility assay

Thin filament Ca^{2+} regulatory function of human troponin was studied with the quantitative in vitro motility assay. Regulation of TRITC-Phalloidin labelled actin (actin- Φ) filaments movement over immobilised rabbit fast muscle heavy meromyosin^{23,25} was defined as fraction of filaments motile and filament sliding speed. The actomyosin was reconstituted in a flow cell, constructed from a microscope slide and a siliconised coverslip. Actin- Φ was premixed with tropomyosin and troponin at a 10x working concentration prior to dilution and infusion into the assay flow cell. Thin filament movement over a bed of immobilised rabbit fast muscle

heavy meromyosin (100 µg/ml) was performed and analysed as before.²⁶ Affinity chromatography on immobilised monoclonal anti-troponin I antibody was used for purification of the whole troponin complex from human failing (IDCM) and non-failing donor myocardium as described previously.²³

Phosphorylation status of myofilament proteins

ProQ phosphostaining

Cardiac tissue samples (~0.5-5.0 mg dry weight) were TCA (tri-chloro acetic acid)-treated as described previously.²² Phosphorylation status of β-AR target proteins, myosin binding protein C (cMyBP-C) and troponin I (cTnI), and other myofilament proteins (desmin, troponin T (cTnT) and myosin light chain 2 (MLC2)) was determined using Pro-Q Diamond phosphostaining (Molecular Probes). Samples were separated on a gradient gel (Criterion tris-HCl 4-15% gel, BioRad) and proteins were stained for one hour with Pro-Q Diamond Phosphoprotein Stain. Fixation, washing and de-staining were performed according to the manufacturers guidelines. Staining was visualized using the LAS-3000 Image Reader (FUJI; 460 nm/605 nm Ex/Em; 2 min illumination) and signals were analyzed with AIDA. All protein signals were within the linear range. Subsequently gels were stained overnight with SYPRO Ruby stain (Molecular Probes) and visualized with the LAS-3000 (460 nm/605 nm Ex/Em; 2 s illumination). The phosphorylation signals of myofilament proteins were normalized to SYPRO-stained cMyBP-C to correct for minor differences in protein loading.

Western immunoblotting

Gel electrophoresis (15% acrylamide gels) and Western immunoblotting was performed to analyze bisphosphorylation of cTnI at Ser-23/24 (i.e. PKA sites, rabbit polyclonal Ab, dilution 1:500, Cell signaling). All signals were normalized to Ponceau-stained actin to correct for differences in protein loading.

Statistical analysis

Data are given as means ± SEM. Data of control and failing animals/human were compared using unpaired Student *t*-tests. Effects of PKA were tested by paired student *t*-tests. The differences in pCa₅₀ between groups were tested with one-way analysis of variance (ANOVA). Significance was accepted when *P*<0.05. All protein signals were visualized using the LAS-3000 Image Reader (FUJI) and signals were analyzed with AIDA software (Raytest).

Results

Enhanced myofilament Ca^{2+} -sensitivity in cardiac disease

Force measurements in single cardiomyocytes revealed an increase in myofilament Ca^{2+} -sensitivity in diseased (failing) myocardium in comparison to control/sham (non-failing) hearts. Figure 2 illustrates a leftward shift of the force-pCa relationship in all failing models. The difference in pCa_{50} between failing and non-failing tissue differed significantly among groups (1-way ANOVA, $P < 0.001$) and was smallest in the mouse myocardial infarction model ($\Delta\text{pCa}_{50} = 0.05 \pm 0.01$), and amounted to 0.07 ± 0.01 in rat, 0.12 ± 0.01 in pig and 0.14 ± 0.02 in human.

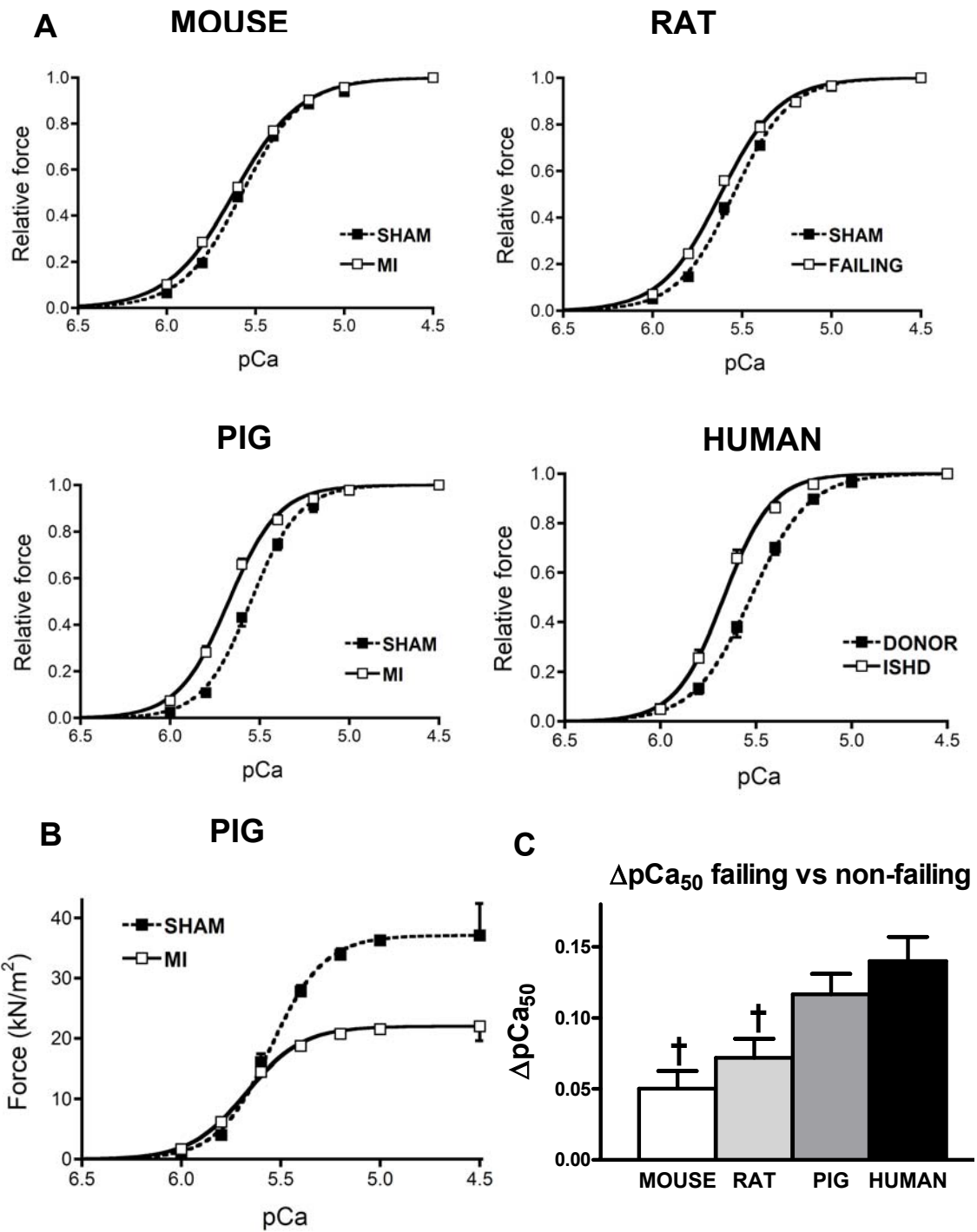


Figure 2. Ca²⁺-sensitivity of myofilaments in different species. A. Ca²⁺-sensitivity of the myofilaments was significantly higher in failing compared to non-failing controls in all studies. **B.** A reduction in maximal force generating capacity was observed in post-infarct remodeled myocardium. **C.** †P<0.05, animal vs. human in Bonferroni post-test analysis.

Correction of enhanced myofilament Ca²⁺-sensitivity by exogenous protein kinase A

Cardiomyocyte force measurements were repeated after incubation with exogenous protein kinase A. Consistent with previous studies, PKA reduced Ca²⁺-sensitivity of the myofilament in all samples.^{27,28} This is illustrated by the reduction in force development after PKA at submaximal [Ca²⁺] (pCa 5.4) in Figure 1B. Incubation with PKA abolished the difference in baseline Ca²⁺-sensitivity in all groups (Fig 3A). The reduction in pCa₅₀ was significantly larger in failing compared to non-failing hearts in all models (Fig 3B). Among the failing groups the shift in pCa₅₀ (Δ pCa₅₀) was smallest in MI mice and largest in end-stage failing human cardiomyocytes.

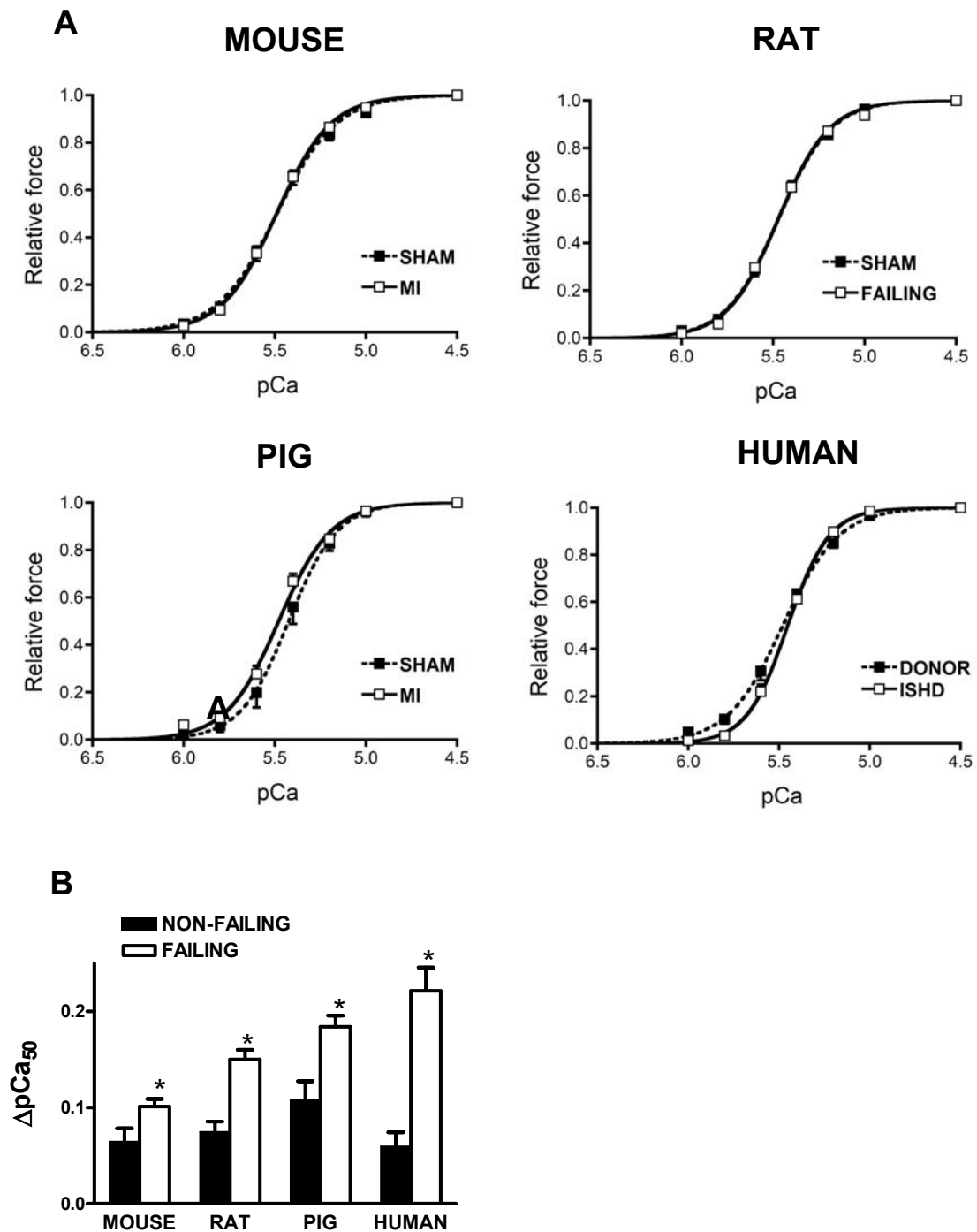


Figure 3. Effect of protein kinase A on myofilament Ca^{2+} -sensitivity. **A.** Force-pCa relations after incubation with PKA. After PKA myofilament Ca^{2+} -sensitivity did not differ between failing and non-failing cardiomyocytes. **B.** Change in pCa_{50} (ΔpCa_{50}) upon PKA in all groups. * $P < 0.05$, failing vs. non-failing in unpaired student t-test.

Altered thin filament regulation

To study if changes in troponin phosphorylation account for altered contractile function, Ca^{2+} -regulation of reconstituted thin filaments was studied using quantitative in vitro motility assay. Ca^{2+} -regulation of actin motility by troponin was studied comparing troponin from failing (IDCM) and non-failing (donor) human myocardium. In Figure 4A thin filament sliding speed and motile fraction are plotted as a function of $[\text{Ca}^{2+}]$ (i.e. pCa). Failing heart thin filament Ca^{2+} -sensitivity was always significantly higher than non-failing for both sliding speed ($\Delta\text{pCa}_{50} = 0.39$) and fraction motile ($\Delta\text{pCa}_{50} = 0.38$). Ca^{2+} -sensitivity of thin filament regulation was decreased when non-failing troponin was reconstituted with recombinant PKA-phosphorylated human cTnI (not shown).²³ When failing and non-failing donor troponin were reconstituted with recombinant human cTnI phosphorylated with PKA, Ca^{2+} -regulation of thin filaments was similar for failing and non-failing troponin (Fig 4B).

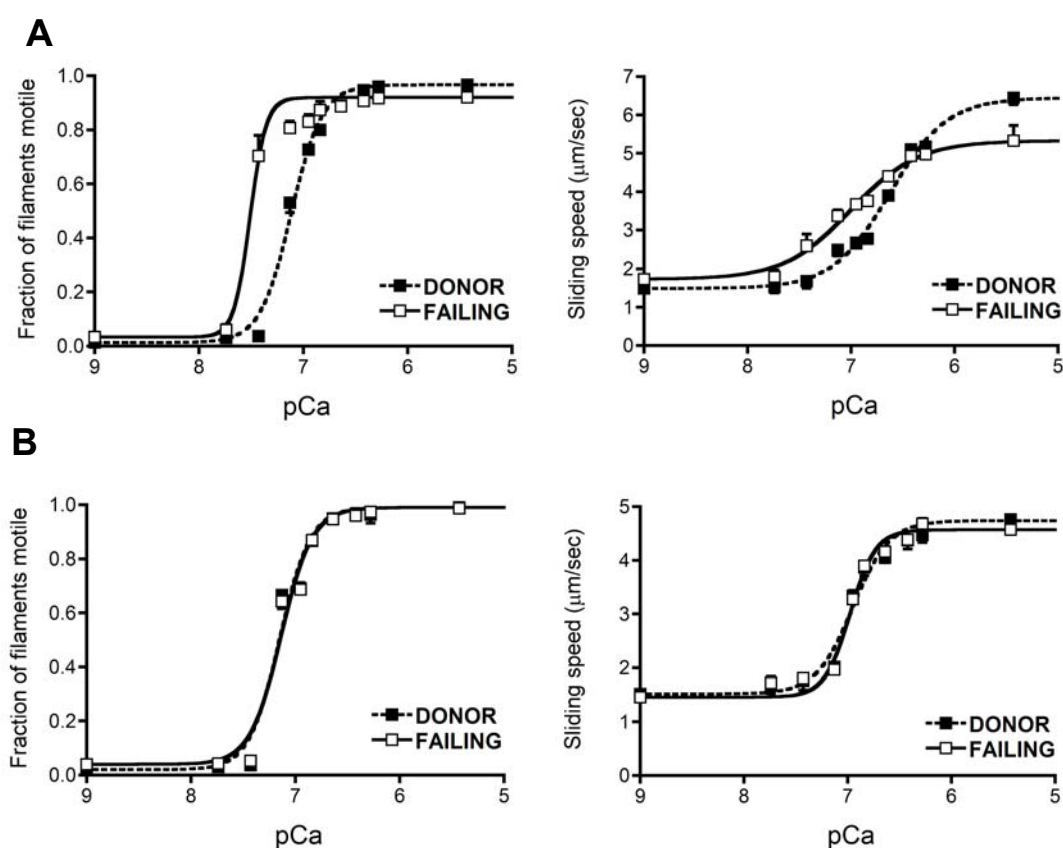


Figure 4. Ca^{2+} -regulation of thin filaments by human troponin. Ca^{2+} -regulation of thin filament motility by non-failing and failing heart troponin was compared in dual chambered motility cells. **A.** Thin filament Ca^{2+} -sensitivity was higher for failing than non-failing troponin, both for sliding speed and fraction motile. **B.** The difference was abolished when failing and non-failing troponin were reconstituted with PKA-phosphorylated recombinant human cTnI.

Reduction in maximal force generating capacity in cardiac disease

While force generation at low calcium concentrations was higher in cardiomyocytes from failing compared to non-failing hearts, the maximal force (F_{active}) generating capacity was significantly lower in the infarct mouse (sham: 18.5 ± 1.8 kN/m² and MI: 14.6 ± 1.1 kN/m²) and pig model. Figure 2B illustrates the absolute force values plotted as function of pCa in the pig model, illustrating the reduction in myofilament force development in cardiomyocytes from post-infarct remodeled myocardium. PKA did not abolish the difference in F_{active} (not shown). F_{active} did not differ in the failing rat model (control: 24.4 ± 2.6 kN/m² and failing: 29.0 ± 2.1 kN/m²) and between human ISHD (33.1 ± 3.0 kN/m²) and donor (33.8 ± 2.5 kN/m²) cardiomyocytes.

Correction of enhanced cardiomyocyte stiffness by protein kinase A

Passive force did not significantly differ between cells from failing and non-failing hearts in the mouse, rat and pig model, while cardiomyocyte stiffness was significantly lower in ISHD compared to non-failing donor (Fig 5A). PKA reduced F_{passive} in all models. Noteworthy, recent studies in cardiomyocytes isolated from human biopsies,^{12,29} which were taken during cardiac catheterization revealed enhanced cardiomyocyte stiffness in patients with heart failure. The F_{passive} was significantly lowered upon incubation with PKA. Figure 5B shows F_{passive} in cardiomyocytes from heart failure patients with reduced left ventricular ejection fraction (HFREF; NYHA II-III) in comparison to controls. In both HFREF and controls PKA significantly reduced cardiomyocyte stiffness. The reduction in F_{passive} upon PKA is also illustrated in Figure 1B.

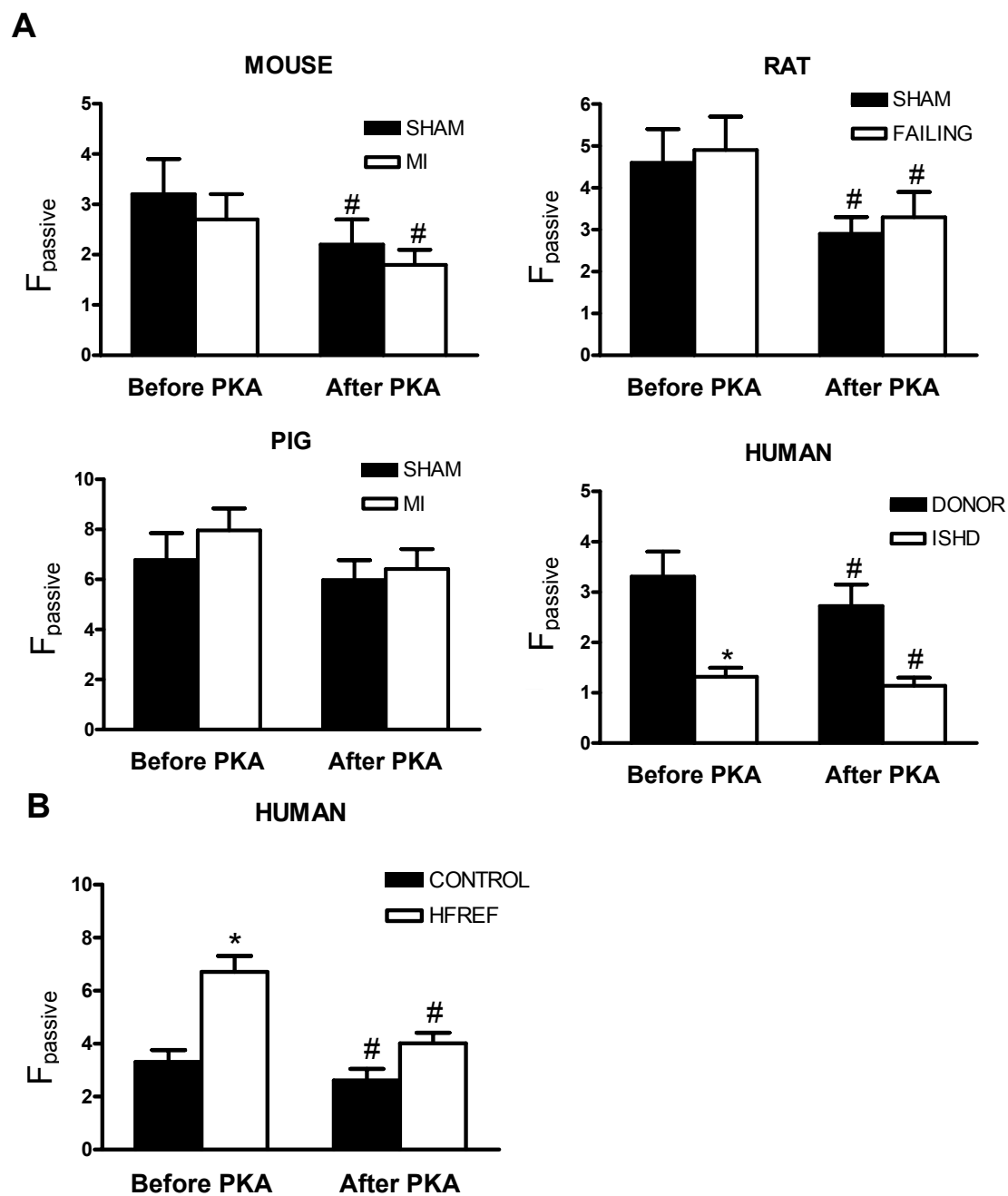


Figure 5. Cardiomyocyte stiffness. **A.** Protein kinase A (PKA) reduced cardiomyocyte passive force (F_{passive}). **B.** Force measurements in cardiomyocytes from human catheter biopsies revealed enhanced cardiomyocyte stiffness in heart failure patients with reduced left ventricular ejection fraction (HFREF) compared to controls. * $P < 0.05$, failing vs non-failing in unpaired student t-test; # $P < 0.05$, effect PKA in paired student t-test.

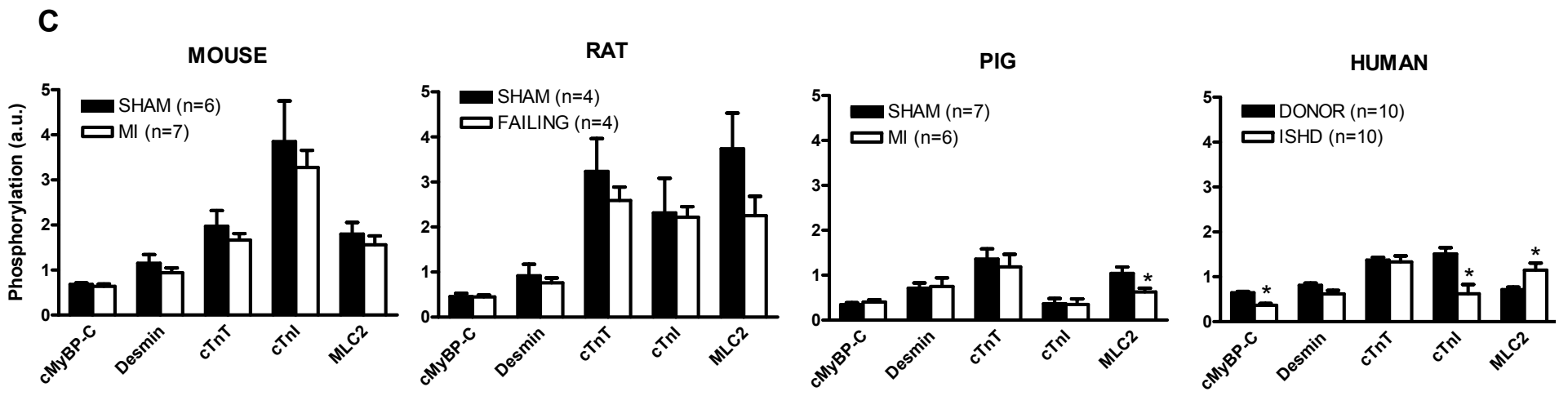
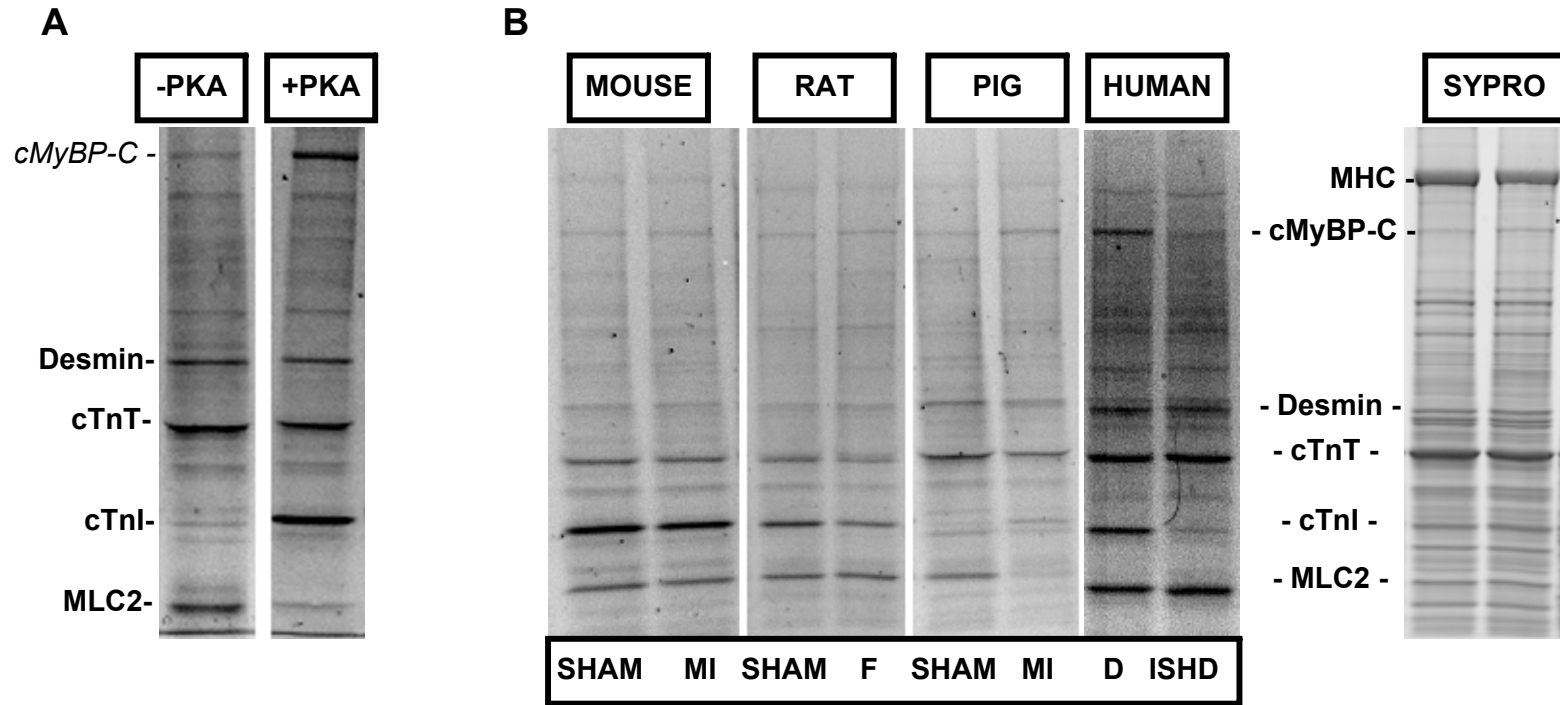
Phosphorylation status of myofilament proteins

ProQ Diamond staining of a pig sample incubated with and without PKA showed increased phosphorylation of the β -AR myofilament target proteins, cMyBP-C and cTnI, while MLC2 phosphorylation was decreased during the incubation (Fig 6A). ProQ Diamond stained samples from mouse, rat, pig and human samples are shown in Figure 6B. Phosphorylation signals were normalized to the SYPRO-stained cMyBP-C band in the same samples to correct for small differences in protein loading. Moreover, to correct for differences in staining between gels the PeppermintStick Phosphoprotein marker (PPM, Molecular Probes) was used as described previously²² (see PPM in Figure 7). This marker contains phosphorylated ovalbumin. The ProQ Diamond signal for ovalbumin is divided by the SYPRO-stained ovalbumin band, which is subsequently used as correction factor for inter-gel differences.

Analysis of the average values for myofilament protein phosphorylation, obtained after correction for protein loading and inter-gel differences, revealed reduced phosphorylation of cMyBP-C and cTnI in failing human compared to non-failing donor myocardium (Fig 6C). No significant changes in myofilament protein phosphorylation were observed between failing and non-failing mouse and rat samples. In pig myocardium, MLC2 phosphorylation was significantly lower in MI compared to sham. A similar reduction in MLC2 phosphorylation was observed in failing rat hearts compared to shams, although the difference was not significant ($P=0.08$). In contrast, MLC2 phosphorylation was significantly higher in end-stage human ISHD than in non-failing donor hearts.

Noteworthy, phosphorylation of cTnI is was much higher in mice cardiac samples in comparison to myocardium from other species, in particular pig and human. To determine if PKA is able to increase cTnI phosphorylation in human myocardium to values observed in mice myocardium, a donor and failing human sample were treated with exogenous PKA. The gels shown in Figure 7 illustrate that the effect of PKA on protein phosphorylation was only minor in the non-failing donor sample (5% increase in cMyBP-C, no effect on cTnI), while PKA increased cMyBP-C and cTnI phosphorylation in the failing sample by 27% and 130%, respectively. These data show that PKA-phosphorylation in non-failing donor myocardium is almost saturated. The relatively high phosphorylation status of cTnI observed in particular in mouse myocardium might reflect phosphorylation at other sites, possibly targeted by PKC, and may be related to differences between species and/or tissue handling.

Figure 6. ProQ-phosphostaining of myofilament proteins. A. Pig samples treated with and without PKA, stained with ProQ diamond. **B.** ProQ diamond staining of cardiac samples from mouse, rat, pig and human cardiac samples. Mean values for protein phosphorylation (relative to SYPRO-stained cMyBP-C) are given in **C.** Abbreviations: MHC, myosin heavy chain; cMyBP-C, myosin binding protein C; cTnT, troponin T; cTnI, troponin I; MLC2, myosin light chain 2; F, failing; D, donor; ISHD, ischemic heart disease. n, number of heart samples. *P<0.05, failing vs non-failing in unpaired student t-test.



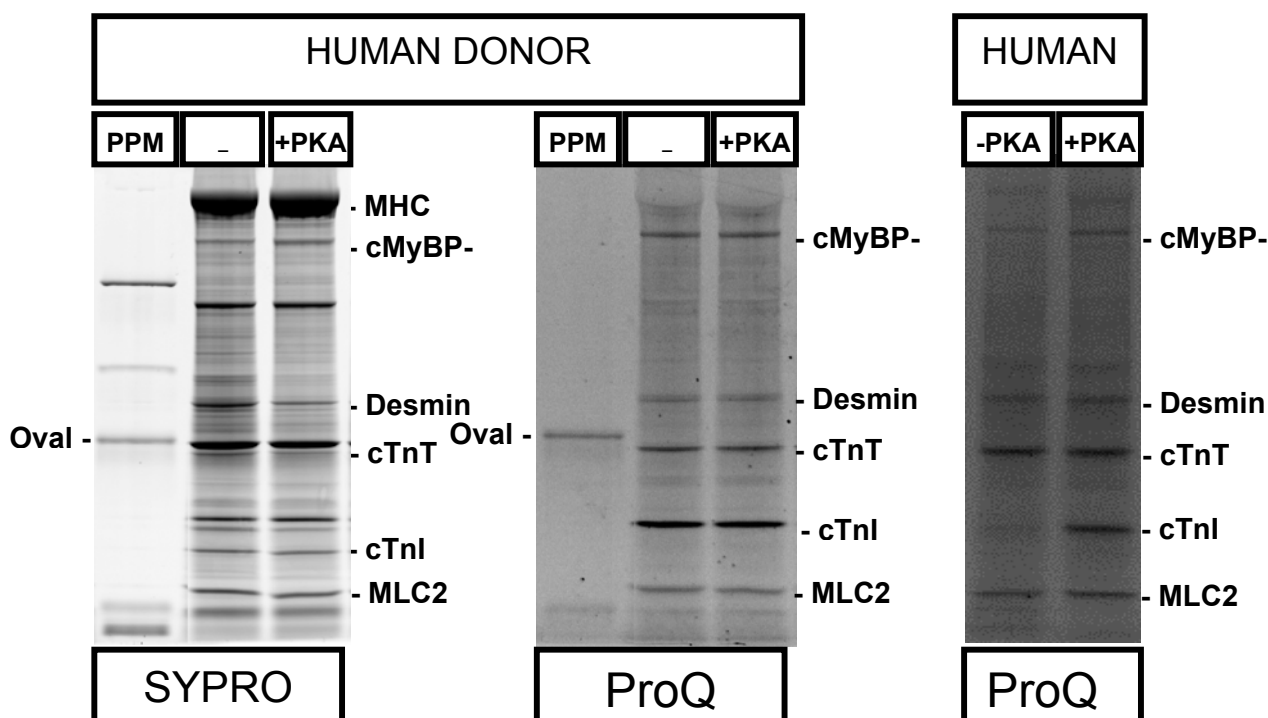


Figure 7. SYPRO and ProQ-phospho staining of human cardiac samples treated with PKA. PKA incubation of a donor sample slightly increased cMyBP-C, but did not increase cTnI phosphorylation, while an increased ProQ-staining of cMyBP-C and cTnI was observed in failing myocardium treated with PKA. Please note that MLC2 phosphorylation was preserved during PKA treatment as the specific PP1 inhibitor, calyculin A, was present during incubation. Abbreviations: PPM, PeppermintStick Phosphoprotein marker; oval, ovalbumin; MHC, myosin heavy chain; cMyBP-C, myosin binding protein C; cTnT, troponin T; cTnI, troponin I; MLC2, myosin light chain 2.

Western immunoblot analysis of cTnI phosphorylation at serines 23/24 revealed significantly lower phosphorylation at the PKA-sites of cTnI in ISHD compared to non-failing donor myocardium (Fig 8A,B), while no significant differences were observed in the animal models. It should be noted that the antibody only detects the PKA-bis-phosphorylated form of cTnI and not mono-phosphorylated cTnI forms. As our analysis cannot distinguish between mono-phosphorylation of PKA-sites, a difference in the mono-phosphorylated forms of cTnI may still be present between failing and non-failing myocardium.

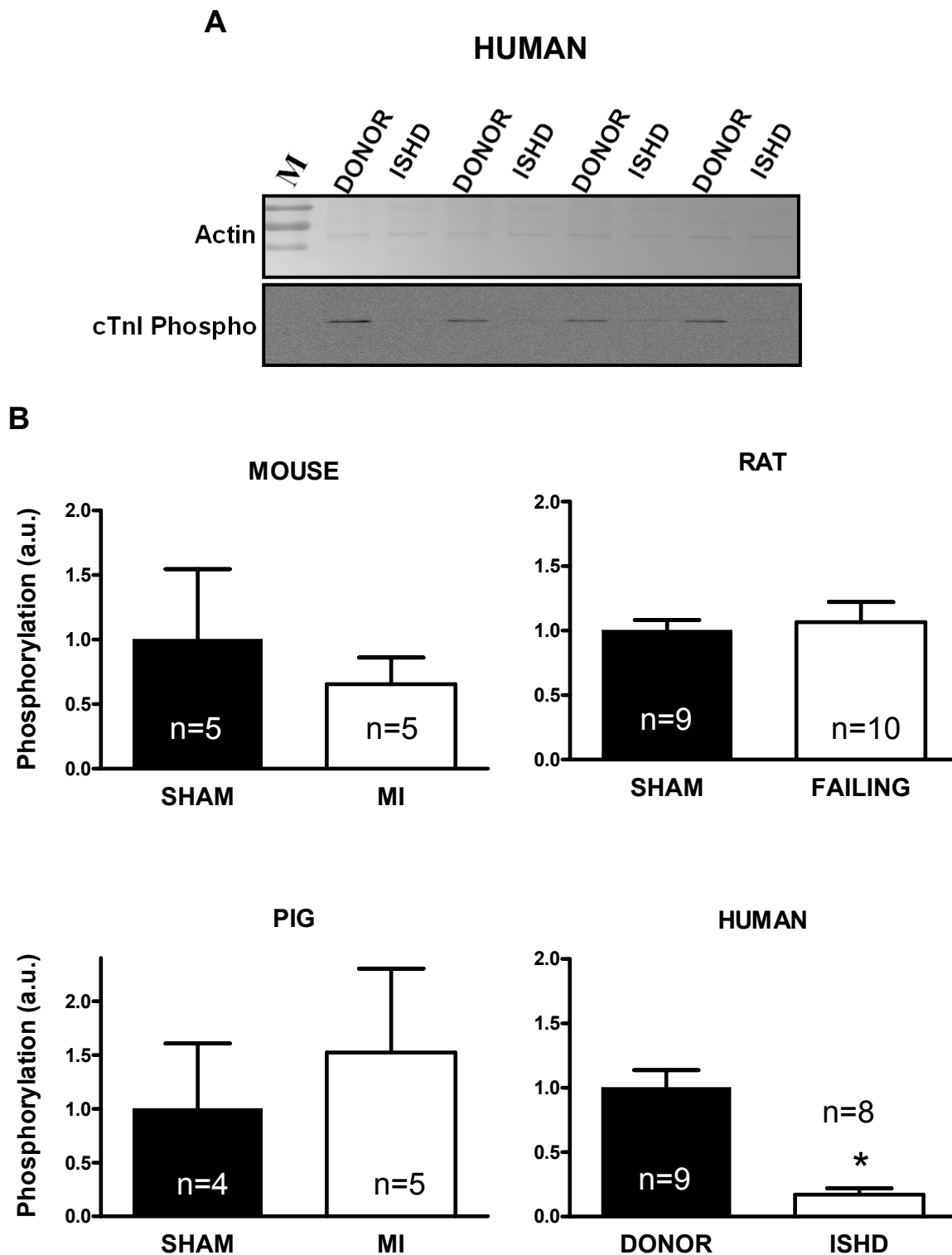


Figure 8. PKA-mediated cTnI phosphorylation. **A.** Western immunoblot analysis revealed reduced PKA-mediated phosphorylation at Ser 23/24 in cTnI in ISHD compared to non-failing human myocardium. **B.** Phosphorylation signals of cTnI were normalized to Ponceau-stained actin to correct for differences in protein loading. n, number of heart samples. *P<0.05, ISHD vs. donor in unpaired student t-test.

Discussion

Activation of the β AR pathway results in enhanced cardiac contractile performance in response to increased circulatory demand. However, reduced responsiveness to β AR stimulation in heart failure is thought to limit cardiac performance during exercise. Functional data from all our animal and human studies are in support of reduced β AR-signalling, as baseline myofilament dysfunction (i.e. enhanced Ca^{2+} -sensitivity and cardiomyocyte stiffness) was restored upon incubation with exogenous protein kinase A. However, analysis of the phosphorylation status of β AR target proteins revealed reduced PKA-mediated phosphorylation only in end-stage failing human myocardium. Moreover, the reduction in maximal force generating capacity was only observed in post-infarct remodelled myocardium early after MI (mouse and pig model), and could not be restored by PKA. The discrepancies in myofilament function and protein phosphorylation are discussed below.

Enhanced myofilament Ca^{2+} -sensitivity and stiffness

In healthy myocardium, myofilament Ca^{2+} -sensitivity is reduced upon β AR stimulation and is thought to exert a positive lusitropic effect on cardiac performance.³⁰ The reduction in myofilament Ca^{2+} -sensitivity has been ascribed to PKA-mediated phosphorylation of cTnI and cMyBP-C.^{5,6} As a consequence of reduced β AR signalling in heart failure, reduced PKA-mediated phosphorylation would result in an enhanced myofilament Ca^{2+} -sensitivity. Our functional measurements in single cardiomyocytes revealed an increase in myofilament Ca^{2+} -sensitivity in all failing heart models (Fig 2A), which could be corrected by exogenous PKA (Fig 3). In vitro motility analysis of regulation of thin filament movement by troponin from failing and non-failing human myocardium revealed a similar increase in Ca^{2+} -sensitivity in failing myocardium (Fig 4A). Moreover, troponin regulation of thin filaments was similar when failing and non-failing human troponin was reconstituted with PKA-phosphorylated recombinant human cTnI (Fig 4B). This indicates that reduced phosphorylation of the PKA-sites in cTnI (Ser 23/24) accounts for the enhanced myofilament Ca^{2+} -sensitivity observed in end-stage failing human myocardium.

The difference in Ca^{2+} -sensitivity between failing and non-failing hearts was smallest in mice and largest in human. The relatively small difference between MI and sham mice (Fig 2A) and small effects of PKA (Fig 3A) may be explained by the relatively high baseline cTnI phosphorylation status (Fig 6) in these animals. Defects in β AR signalling may be difficult to uncover in mice due to the small dynamic range in response to β AR stimulation. Although, the direction of the change in pCa_{50} was

similar in all heart failure models, Bonferroni post-test analysis revealed that the difference in pCa_{50} (ΔpCa_{50}) between failing and non-failing cardiomyocytes was significantly larger in human compared to the mouse and rat model, while ΔpCa_{50} (failing vs. non-failing) did not differ from the pig model (Fig 2C). Hence, large animal models may be more representative to investigate consequences of β AR stimulation on myofilament protein phosphorylation and function.

Alternatively, the smaller differences in pCa_{50} in rodents and absence of reduced phosphorylation of β AR target proteins in animal models in contrast to human, may be a reflection of disease progression, as the human studies involve end-stage heart failure. During earlier stages of heart failure, such as present in the animal studies, defects in β AR signalling may be less severe, and the functional and proteomic phenotype observed in less severe stages of cardiac disease may be the resultant of changes in other signalling pathways as well. Within our human studies we observed a striking difference in cardiomyocyte stiffness, which may relate to severity of cardiac disease. In agreement with previous studies³¹⁻³³ cardiomyocyte stiffness in end-stage human heart failure was lower in comparison to non-failing donors (Fig 5A). It has been proposed that the reduction in $F_{passive}$ is due to a shift in titin isoform composition, from the stiff N2B to the more compliant N2BA isoform.^{31,32} In contrast, recent measurements in cardiomyocytes isolated from catheter biopsies from patients with less severe forms of heart failure (NYHA II-III) revealed enhanced cardiomyocyte stiffness in all heart failure patients, which was largely corrected with PKA.^{12,29,34} In these samples, a similar shift in titin isoform composition was found as observed in end-stage heart failure. However, analysis of titin phosphorylation indicated differential titin isoform phosphorylation as possible cause for enhanced cardiomyocyte stiffness and may involve reduced protein kinase G-mediated phosphorylation.^{35,36}

The functional consequences of impaired PKA-mediated phosphorylation may be balanced by changes in other kinases. In congestive heart failure models in rat (pressure overload and MI), reductions in F_{max} and in Ca^{2+} -sensitivity were associated with increased protein kinase C (PKC) expression.³⁷ Increased phosphorylation of cTnI was observed in failing rat myocardium and deficits in myofilament function were corrected by phosphatase treatment. It has been proposed that the relative balance of phosphorylation of the 3 PKC-sites on cTnI (Ser 43/45 and Thr 144) is important for the regulation of its function.³⁸ Pseudophosphorylation of Ser 43/45 significantly reduced myofilament response to Ca^{2+} ³⁹ and phosphorylation of Thr 144 induced an increase in sensitivity to Ca^{2+} .⁴⁰

Increased PKC activity and isoform expression has been reported in human heart failure.⁴¹⁻⁴³ However, it remains to be investigated if PKC targets the myofilament proteins *in vivo*.⁴⁴ Recent mass spectrometry analysis revealed a novel *in vivo* phosphorylation site in human cTnI (Ser 76/Thr 77), which may be target of PKC.⁴⁵ To establish if PKC-mediated protein phosphorylation impacts myofilament function in human cardiac disease quantitative mass spectrometry should be performed in cardiac samples, which are obtained under well-defined conditions, preferably before and after *in vivo* receptor stimulation.

Reduced maximal force generating capacity

The maximal force generating capacity of cardiomyocytes from remodelled myocardium early after a myocardial infarction was reduced and, unlike pCa_{50} and $F_{passive}$, was not corrected by PKA. An important role has been assigned to PKC-mediated phosphorylation of cTnT at Thr 206,⁴⁰ and cTnI at Ser 43/45³⁹ in reducing myofilament F_{active} . However, up to date, no changes in cTnT phosphorylation have been reported in any heart failure model (Fig 6). Moreover, using an elegant troponin exchange method in failing and non-failing rat cardiomyocytes, Belin et al. (2006)⁴⁶ showed that replacement of failing troponin by non-failing troponin restored myofilament Ca^{2+} -sensitivity to values observed in non-failing cardiomyocytes, but not F_{active} . Hence, alterations in troponin phosphorylation underlie changes in myofilament Ca^{2+} -sensitivity, but are not the cause of reduced maximal force generating capacity.

In our previous study in MI mice,¹⁶ exercise prevented the reduction in F_{active} , which was associated with an increase in MLC2 phosphorylation, although MLC2 phosphorylation was not significantly reduced in MI (Fig 6B,C). A transmural gradient in MLC2 phosphorylation has been described in rodent studies.⁴⁷⁻⁴⁹ A reduction in MLC2 phosphorylation in myocardium from MI mice may have been obscured by regional differences, as a significant reduction in MLC2 phosphorylation was observed in subendocardial tissue from MI pigs (Fig 6B,C). Accordingly, a recent study in rats with ischaemic heart failure⁵⁰ revealed impaired contractile function and reduced MLC2 phosphorylation only in subendocardial cardiomyocytes, which were both restored by exercise training. It has been proposed that the overall pattern of cardiac contraction depends on a spatial gradient of MLC2 phosphorylation,⁴⁷ and loss of the MLC2 phosphorylation gradient may impair cardiac performance.^{47,49} Hence, myofilament function may be hampered by alterations in MLC2 phosphorylation. Investigation of transmural biopsies taken under well-controlled hemodynamic conditions allow careful analysis of MLC2 phosphorylation at rest and

during enhanced cardiac load (i.e. upon receptor stimulation) and would allow investigation of the importance of a transmural MLC2 phosphorylation gradient for cardiac contraction in a large animal model. As the opposite changes in MLC2 phosphorylation in animal models with ischemic heart disease (reduction) and end-stage failing human ischemic cardiomyopathy (increase) may relate to severity of cardiac disease, changes during the progression of cardiac disease should be addressed as well.

In conclusion, cardiomyocyte force measurements revealed enhanced myofilament Ca^{2+} -sensitivity and passive stiffness, which were both largely corrected with exogenous PKA indicative for hypo-phosphorylation of βAR target proteins. When translated to in vivo cardiac performance, an enhancement in myofilament Ca^{2+} -sensitivity and cardiomyocyte stiffness would both limit cardiac relaxation. This is illustrated by the positive correlation between high left ventricular end-diastolic pressures (LVEDP) in heart failure patients and high cardiomyocyte stiffness.¹² As high LVEDP could not be solely attributed to increased cardiac collagen, high LV filling pressures may be in part explained by high intrinsic stiffness of the cardiomyocytes. Though limiting relaxation, the enhanced myofilament Ca^{2+} -sensitivity might increase cardiomyocyte force development and increase cardiac contractility.

Although the enhanced myofilament Ca^{2+} -sensitivity in failing myocardium would enhance cardiomyocyte contractility, a reduction in F_{active} would counteract this. This is illustrated by the relationship between absolute force development and pCa in Figure 2B. In vivo, the impact of altered myofilament function depends on cytosolic $[\text{Ca}^{2+}]$ during the different phases of the cardiac cycle. As systolic calcium levels are reduced in failing cardiomyocytes, it may be speculated that myofilament dysfunction in remodelled myocardium after MI further deteriorates cardiac performance.

Future perspectives

Our data illustrate the need for careful tissue handling under well-defined conditions, preferably at the time of hemodynamic measurements, and careful analysis of the myofilament phosphoproteome. Research on the cellular mechanisms underlying human heart failure is hampered by the limited availability of biopsy material and, since biopsies are routinely obtained at one time point, by the lack of information on the dynamic aspects of the processes involved. The dynamic changes in cellular signalling critically depend on the phosphorylation status of a number of target

proteins. Analysis of dynamic changes in intracellular signalling pathways and the interaction between kinases and phosphatases and their specific myofilament target proteins within intact cells is essential to establish a direct relation between changes in myofilament protein phosphorylation and myofilament dysfunction in heart failure.

References

1. Packer M. Evolution of the neurohormonal hypothesis to explain the progression of chronic heart failure. *Eur Heart J* 1995;16:F4-6.
2. Cohn JN, Levine TB, Olivari MT, Garberg V, Lura D, Francis GS, Simon AB, Rector T. Plasma norepinephrine as a guide to prognosis in patients with chronic congestive heart failure. *N Engl J Med* 1984; 311:819-823.
3. Bohm M, Maack C. Treatment of heart failure with beta-blockers. *Basic Res Cardiol* 2000;95: 115-24.
4. Bers DM. Cardiac excitation-contraction coupling. *Nature* 2002;415:198-205.
5. Wolff MR, Buck SH, Stoker SW, Greaser ML, Mentzer RM. Myofibrillar calcium sensitivity of isometric tension is increased in human dilated cardiomyopathies. *J Clin Invest* 1996;98:167-176.
6. Cazorla O, Szilagyi S, Vignier N, Salazar G, Krämer E, Vassort G, Carrier L, Lacampagne A. Length and protein kinase A modulations of myocytes in cardiac myosin binding protein C-deficient mice. *Cardiovasc Res* 2006;69:370-380.
7. Solaro RJ, Moir AJ, Perry SV. Phosphorylation of troponin I and the inotropic effect of adrenaline in the perfused rabbit heart. *Nature* 1976;262:615-617.
8. Zhang R, Zhao J, Mandveno A, Potter JD. Cardiac troponin I phosphorylation increases the rate of cardiac muscle relaxation. *Circ Res* 1995;76:1028-1035
9. Kentish JC, McCloskey DT, Layland J, Palmer S, Leiden JM, Martin AF, Solaro RJ. Phosphorylation of troponin I by protein kinase A accelerates relaxation and crossbridge cycle kinetics in mouse ventricular muscle. *Circ Res* 2001;88:1059-1065.
10. Stelzer JE, Patel JR, Walker JW, Moss RL. Differential roles of cardiac myosin-binding protein C and cardiac troponin I in the myofibrillar force responses to protein kinase A phosphorylation. *Circ Res*. 2007; 101:503-511.
11. Fukuda N, Wu Y, Nair P, Granzier HL. Phosphorylation of titin modulates passive stiffness of cardiac muscle in a titin isoform-dependent manner. *J Gen Physiol* 2005;125:257-271.
12. Borbély A, van der Velden J, Papp Z, Bronzwaer JG, Edes I, Stienen GJ, Paulus WJ. Cardiomyocyte stiffness in diastolic heart failure. *Circulation* 2005;111:774-781.
13. Krüger M, Linke WA. Protein kinase-A phosphorylates titin in human heart muscle and reduces myofibrillar passive tension. *J Muscle Res Cell Motil* 2006;27:435-444.
14. Harding SE, Brown LA, Wynne DG, Davies CH, Poole-Wilson PA. Mechanisms of beta adrenoceptor desensitisation in the failing human heart. *Cardiovasc Res* 1994;28:1451-1460.
15. Bristow MR (2000). Beta-Adrenergic receptor blockade in chronic heart failure. *Circulation* 101: 558-569.
16. de Waard MC, van der Velden J, Bito V, Ozdemir S, Biesmans L, Boontje NM, Dekkers DH, Schoonderwoerd K, Schuurbijs HC, de Crom R, Stienen GJ, Sipido KR, Lamers JM, Duncker DJ. Early exercise training normalizes myofilament function and attenuates left ventricular pump dysfunction in mice with a large myocardial infarction. *Circ Res* 2007;100:1079-1088.
17. Lamberts RR, Hamdani N, Soekhoe TW, Boontje NM, Zaremba R, Walker LA, de

- Tombe PP, van der Velden J, Stienen GJ. Frequency-dependent Ca^{2+} -desensitization in failing rat hearts. *J Physiol* 2007;582: 695-709.
18. Leineweber K, Seyfarth T, Brodde OE. Chamber-specific alterations of noradrenaline uptake (uptake₁) in right ventricles of monocrotaline-treated rats. *Br J Pharmacol* 2000;131:1438–1444.
 19. Korstjens IJ, Rouws CH, van der Laarse WJ, Van der Zee L, Stienen GJ. Myocardial force development and structural changes associated with monocrotaline induced cardiac hypertrophy and heart failure. *J Muscle Res Cell Motil* 2002;23:93–102.
 20. van Kats JP, Duncker DJ, Haitsma DB, Schuijt MP, Niebuur R, Stubenitsky R, Boomsma F, Schalekamp MA, Verdouw PD, Danser AH. Angiotensin-converting enzyme inhibition and angiotensin II type 1 receptor blockade prevent cardiac remodeling in pigs after myocardial infarction: role of tissue angiotensin II. *Circulation* 2000;102:1556-1563.
 21. van der Velden J, Merkus D, Klarenbeek BR, James AT, Boontje NM, Dekkers DH, Stienen GJ, Lamers JM, Duncker DJ. Alterations in myofilament function contribute to left ventricular dysfunction in pigs early after myocardial infarction. *Circ Res* 2004;95:e85-e95.
 22. Zaremba R, Merkus D, Hamdani N, Lamers JMJ, Paulus WJ, Remedios CD, Duncker DJ, Stienen GJM, van der Velden J. Quantitative analysis of myofilament protein phosphorylation in small cardiac biopsies. *Proteom Clin Applic* 2007;1:1285-1290.
 23. Messer AE, Jacques AM, Marston SB. Troponin phosphorylation and regulatory function in human heart muscle: dephosphorylation of ser23/24 on troponin I could account for the contractile defect in end-stage heart failure. *J Mol Cell Cardiol* 2007;42:247-259.
 24. Hamdani N, Kooij V, van Dijk S, Merkus D, Paulus WJ, Remedios CD, Duncker DJ, Stienen GJ, van der Velden J. Sarcomeric Dysfunction in Heart Failure. *Cardiovasc Res* 2008;77:649-658.
 25. Fraser IDC, Marston SB. In vitro motility analysis of actin-tropomyosin regulation by troponin and Ca^{2+} : the thin filament is switched as a single cooperative unit. *J Biol Chem* 1995;270:7836-7841.
 26. Knott A, Purcell IF, Marston SB. In vitro motility analysis of thin filaments from failing and non-failing human hearts induces slower filament sliding and higher Ca^{2+} -sensitivity. *J Mol Cell Cardiol* 2002;34:469-482.
 27. van der Velden J, Papp Z, Zaremba R, Boontje NM, de Jong JW, Owen VJ, Burton PB, Goldmann P, Jaquet K, Stienen GJ. Increased Ca^{2+} -sensitivity of the contractile apparatus in end-stage human heart failure results from altered phosphorylation of contractile proteins. *Cardiovasc Res* 2003;57: 37-47
 28. Edes IF, Tóth A, Csányi G, Lomnicka M, Chłopicki S, Edes I, Papp Z. Late-stage alterations in myofibrillar contractile function in a transgenic mouse model of dilated cardiomyopathy (Tgαq*44). *J Mol Cell Cardiol* 2008;45:363-372.
 29. Van Heerebeek L, Borbely A, Niessen HW, Bronzwaer JG, van der Velden J, Stienen GJ, Linke WA, Laarman GJ, Paulus WJ. Myocardial structure and function differ in systolic and diastolic heart failure. *Circulation* 2006;113:1966-1973.
 30. Kobayashi T, Solaro RJ. Calcium, thin filaments, and the integrative biology of cardiac contractility. *Annu Rev Physiol* 2005;67:39-67.
 31. Makarenko I, Opitz CA, Leake MC, Neagoe C, Kulke M, Gwathmey JK, del Monte F,

- Hajjar RJ, Linke WA. Passive stiffness changes caused by upregulation of compliant titin isoforms in human dilated cardiomyopathy hearts. *Circ Res* 2004;95:708-716.
32. Nagueh SF, Shah G, Wu Y, Torre-Amione G, King NM, Lahmers S, Witt CC, Becker K, Labeit S, Granzier HL. Altered titin expression, myocardial stiffness, and left ventricular function in patients with dilated cardiomyopathy. *Circulation* 2004;110:155-162.
 33. Neagoe C, Kulke M, del Monte F, Gwathmey JK, de Tombe PP, Hajjar RJ, Linke WA. Titin isoform switch in ischemic human heart disease. *Circulation* 2002;106:1333-1341.
 34. Van Heerebeek L, Hamdani N, Handoko ML, Falcao-Pires I, Musters RJ, Kupreishvili K, Ijsselmuiden AJ, Schalkwijk CG, Bronzwaer JG, Diamant M, Borbely A, van der Velden J, Stienen GJ, Laarman GJ, Niessen HW, Paulus WJ. Diastolic stiffness of the failing diabetic heart: importance of fibrosis, advanced glycation endproducts and myocyte resting tension. *Circulation* 2008;117:52-60.
 35. Krüger M, dos Remedios C, Linke WA. Titin phosphorylation by protein kinases A and G in normal and failing human hearts decreases myocardial passive stiffness. *Circulation* 2007;116:II-301(Abstract).
 36. Hamdani N, Borbely A, Boontje NM, Edes I, Falcao-Pires I, Leite-Moreira AF, Stienen GJM, van der Velden J, Paulus WJ. Protein Kinase G Corrects High Cardiomyocyte Resting Tension in Diastolic Heart Failure. *Circulation* 2007;116:II-708(abstract).
 37. Belin RJ, Sumandea MP, Allen EJ, Schoenfelt K, Wang H, Solaro RJ, de Tombe PP. Augmented Protein Kinase C- α -induced myofilament protein phosphorylation contributes to myofilament dysfunction in experimental congestive heart failure. *Circ Res* 2007;101:195-204.
 38. Solaro RJ, Rosevear P, Kobayashi T. The unique functions of cardiac troponin I in the control of cardiac muscle contraction and relaxation. *Biochem Biophys Res Commun* 2008;369:82-87.
 39. Burkart EM, Sumandea MP, Kobayashi T, Nili M, Martin AF, Homsher E, Solaro RJ. Phosphorylation or glutamic acid substitution at protein kinase C sites on cardiac troponin I differentially depress myofilament tension and shortening velocity. *J Biol Chem* 2003;278:11265-11272.
 40. Sumandea MP, Pyle WG, Kobayashi T, de Tombe PP, Solaro RJ. Identification of a functionally critical protein kinase C phosphorylation residue of cardiac troponin T. *J Biol Chem* 2003;278:35135-35144.
 41. Bowling N, Walsh RA, Song G, Estridge T, Sandusky GE, Fouts RL, Mintze K, Pickard T, Roden R, Bristow MR, Sabbah HN, Mizrahi JL, Gromo G, King GL, Vlahos CJ. Increased protein kinase C activity and expression of Ca²⁺-sensitive isoforms in the failing human heart. *Circulation* 1999;99:384-391.
 42. Takeishi Y, Jalili T, Hoit BD, Kirkpatrick DL, Wagoner LE, Abraham WT, Walsh RA. Alterations in Ca²⁺ cycling proteins and G α q signaling after left ventricular assist device support in failing human hearts. *Cardiovasc Res* 2000;45:883-888.
 43. Braz JC, Gregory K, Pathak A, Zhao W, Sahin B, Klevitsky R, Kimball TF, Lorenz JN, Nairn AC, Liggett SB, Bodi I, Wang S, Schwartz A, Lakatta EG, DePaoli-Roach AA, Robbins J, Hewett TE, Bibb JA, Westfall MV, Kranias EG, Molkenin JD. PKC- α regulates cardiac contractility and propensity toward heart failure. *Nature* 2004;430:248-254.
 44. Huang X, Walker JW. Myofilament anchoring of protein kinase C- ϵ in cardiac

- myocytes. *J Cell Sci* 2004;117:1971-1978.
45. Zabrouskov V, Ge Y, Schwartz J, Walker JW. Unraveling molecular complexity of phosphorylated human cardiac troponin I by top down electron capture dissociation/electron transfer dissociation mass spectrometry. *Mol Cell Proteomics* 2008;7:1838-1849.
 46. Belin RJ, Sumandea MP, Kobayashi T, Walker LA, Rundell VL, Urboniene D, Yuzhakova M, Ruch SH, Geenen DL, Solaro RJ, de Tombe PP. Left ventricular myofilament dysfunction in rat experimental hypertrophy and congestive heart failure. *Am J Physiol Heart Circ Physiol* 2006;291:H2344-53.
 47. Davis JS, Hassanzadeh S, Winitsky S, Lin H, Satorius C, Vemuri R, Aletras AH, Wen H, Epstein ND. The overall pattern of cardiac contraction depends on a spatial gradient of myosin regulatory light chain phosphorylation. *Cell* 2001;107:631-641.
 48. Rajashree R, Blunt BC, Hofmann PA. Modulation of myosin phosphatase targeting subunit and protein phosphatase 1 in the heart. *Am J Physiol* 2005;289:H1736-H1743.
 49. Cazorla O, Szilagyi S, Le Guennec JY, Vassort G, Lacampagne A. Transmural stretch-dependent regulation of contractile properties in rat hearts and its alteration after myocardial infarction. *FASEB J* 2005;19:88-90.
 50. Aït Mou Y, Reboul C, Andre L, Lacampagne A, Cazorla O. Late exercise training improves non-uniformity of transmural myocardial function in rats with ischaemic heart failure. *Cardiovasc Res* 2008;81:555-564.

9

Summary

Conclusion

&

Future perspectives

Summary

In this thesis alterations in cellular function and structure were studied in heart failure with different underlying cause and phenotype to obtain insight into the cellular pathomechanisms underlying progressive deterioration of left ventricle pump function in human heart failure. The results obtained may be used to develop new-targeted therapeutic interventions for the treatment of heart failure in the future. Here, the main findings of the studies are presented and the implications of the findings for clinical practice and future research are discussed.

Chapter 1. In this chapter an introduction to the background and methods of the studies is given. The aim of this thesis is defined.

Chapter 2. In this chapter we focused on the functional role of individual sarcomeric protein isoforms and of post-translational protein modifications such as proteolysis and phosphorylation in diseased myocardium. In failing myocardium, sarcomeric dysfunction includes depressed maximum force development, increased calcium-sensitivity and increased passive stiffness. These changes could be largely explained by altered phosphorylation of sarcomeric proteins including troponin I, titin, myosin binding protein C and myosin light chain 2. Changes in phosphorylation are most likely caused by neurohumoral-induced alterations in the kinase-phosphatase balance inside the cardiomyocytes. A therapy which specifically targets phosphorylation sites within sarcomeric proteins or the kinases and phosphatases involved might be used to improve cardiac function in heart failure.

Chapter 3. Abnormalities in β -adrenergic receptor (β AR) signal transduction are not only involved in impairment of cardiac function, but they also play a role in the structural changes observed in heart failure. An increase in catecholamines resulted in down regulation and desensitization of the β AR. Moreover, it is evident that prolonged adrenergic stimulation causes alterations of the expression and activity of downstream components of the β AR signal transduction cascade.

In Chapter 3 a comparison was made between left ventricular tissue samples from patients with ischemic cardiomyopathy (ISHD) and idiopathic cardiomyopathy (IDCM) in order to investigate whether changes in the β AR signal transduction pathway translate into diverse functional and structural alterations. Donor hearts served as non-failing controls. Diverse changes were found in cellular function and structure in failing human myocardium with different underlying cause. In both groups

a marked reduction was found in the number of β_1 AR and β_2 AR. Different alterations in the expression level of G-coupled receptor kinase 5, G-inhibitory, protein phosphatase 1 and myosin light chain 2 phosphorylation were found between ISHD and IDCM. Furthermore, differences in sarcoplasmic reticulum calcium ATPase (SERCA2a) expression and phospholamban/SERCA2a ratio between ISHD and IDCM were found. Cardiomyocyte force measurements showed differences in calcium sensitivity, which could be explained by a difference in TnI phosphorylation. A lower collagen volume fraction in ISHD was found compared to IDCM using histological analyses.

Our results indicate that alterations in the β AR signaling pathway and in cardiomyocyte structure and function depend on underlying cause. These findings highlight the different alterations in ISHD and IDCM, which may modify heart failure risk, prognosis and response to treatment.

Chapter 4. Fabry disease is an inherited X-linked inborn lysosomal storage disorder characterized by intracellular glycosphingolipid depositions resulting from deficient α -galactosidase A activity. To reveal if alterations in myofilament function and protein composition contribute to left ventricle myocardial dysfunction in Fabry disease patients, both were determined in left ventricle endomyocardial biopsies of patients with the cardiac variant of Fabry disease. In addition cardiomyocyte cross sectional area, area of glycosphingolipid vacuoles, myofibrilolysis and extent of fibrosis were determined. Our data showed high cardiomyocyte passive stiffness and low active tension which may both contribute to left ventricle myocardial dysfunction observed in Fabry disease patients. The high resting tension relates to the observed diastolic LV dysfunction and may be partly explained by decreased phosphorylation of myofibrillar and/or cytoskeletal proteins, while the low active tension relates to reduced tissue Doppler systolic shortening velocity and may be due to proteolysis of troponin I and desmin. As cardiomyocyte stiffness is an important determinant of left ventricle stiffness in heart failure, the augmented passive stiffness in Fabry disease patients may be detrimental for left ventricle diastolic function.

Chapter 5. The aims of β -blocker therapy are to improve survival and quality of life of patients. To investigate if β -blocker therapy induces disparate effects in heart failure with normal ejection fraction (HFNEF) and heart failure with reduced ejection fraction (HFREF), this chapter compared myocardial structure, function and protein composition in HFNEF and HFREF patients without or with β -blocker therapy.

Changes in active tension, calcium sensitivity and troponin I phosphorylation are shared by HFNEF and HFREF and are all beneficial for left ventricle contractility. Changes in collagen volume fraction, cardiomyocyte diameter and passive stiffness are unique to HFNEF and affect diastolic left ventricle function. Lower G-inhibitory is unique to HFREF and may improve left ventricle contractility. β -blocker therapy induces myocardial effects unique to HFNEF or HFREF. This may explain the dissimilar outcome of β -blocker therapy in HFNEF and HFREF phenotype. The clinical benefits obtained with β -blocker therapy are multi-factorial, involving improvement of calcium handling, reversal of cardiac remodeling, improved cardiac efficiency. Our data showed diverse effects of β -blocker therapy on myofilament function. Myofilament contractile reserve to β -adrenergic stimulation (i.e. exogenous PKA) was blunted in HFNEF+ β and enhanced in HFREF+ β . Our data indicate that β -blocker therapy may improve systolic cardiac function in HFNEF patients by an increase in active cardiomyocyte force development and a reduction in cardiomyocyte hypertrophy. However, an increased passive stiffness was observed in cardiomyocytes from HFNEF patients receiving β -blocker therapy, which was no longer corrected to normal values upon PKA treatment. As it is generally believed that the dominant pathophysiological mechanism in HFNEF patients is abnormal diastolic function, our observations do not provide mechanistic evidence to support the use of β -blockers in HFNEF.

Chapter 6. Raised diastolic left ventricle stiffness importantly contributes to heart failure in diabetes mellitus (DM) and results from myocardial deposition of advanced glycation endproducts (AGEs) and interstitial fibrosis. In diabetic patients with heart failure a contribution to this high diastolic left ventricle stiffness of an elevated passive stiffness has so far not been assessed. This study was designed to compare myocardial fibrosis, AGEs deposition and passive stiffness of isolated cardiomyocytes between diabetic and non-diabetic HFNEF patients and between diabetic and non-diabetic HFREF patients. Increased myocardial collagen volume fraction was found only in diabetic patients with HFREF, while elevated cardiomyocyte passive stiffness was present only in diabetic patients suffering from HFNEF. Diabetes increased myocardial AGEs deposition in patients with HFREF and less so in HFNEF patients. The question remains if β -blocker therapy reverses the changes observed in cardiomyocyte function and structure in heart failure patients with diabetes mellitus, especially the high passive stiffness observed in HFNEF patients. It is therefore very important to understand the cellular pathophysiology of

the β -blocker therapy in these patients, to improve the clinical outcome of patients with diabetic cardiomyopathy.

Chapter 7. In this chapter, we investigated whether the antibodies directed against β -adrenergic receptors can be used to determine expression of β -adrenergic receptors (β AR) in human myocardium. Using western blotting we investigated the specificity of commercially available antibodies directed against β_1 AR and β_2 AR in human left ventricular tissue. The antibodies recognized several protein bands at different molecular weights in human myocardial samples and also multiple proteins in Chinese hamster ovary (CHO) cells expressing β_1 AR, β_2 AR and even β_3 AR, indicating that these antibodies are not specific and are not suited to study expression of β -adrenergic receptor in myocardium.

Chapter 8. In this review an overview is given of the perturbed balance between receptor-mediated kinases and phosphatases coordinating phosphorylation of regulatory proteins involved in cardiomyocyte contractility during heart failure. The imbalance between kinases and phosphatases is related to increased neurohumoral stimulation to enhance cardiac pump function in heart failure. The data from different animal and human studies underline the importance of careful biopsy procurement, and the need to investigate localization of kinases and phosphatases within the cardiomyocyte.

Conclusion

The research in this thesis was limited to the most important signal transduction pathway in the heart and the most frequent drug therapy in heart failure, in order to understand the alterations in the pathophysiology of heart failure patients. Despite the different studies performed, it is still unclear how we can improve the quality of life and prolong survival in patients with heart failure. Other options need to be taken in to consideration for a better therapy of patients with heart failure.

Altered maximum force development, calcium sensitivity and increased passive stiffness largely originate from changed sarcomeric proteins in diseased myocardium, caused by neurohumoral-induced alterations in the kinase-phosphatase balance inside the cardiomyocytes. However alterations in β -adrenergic signaling pathway and cardiomyocyte function and structure depend on underlying cause of the cardiomyopathy. Therefore, these differences may explain in part the dissimilar outcome of β -blocker therapy in HFNEF and HFREF.

Overall, the findings presented in this thesis indicate that cellular changes in heart failure depend on underlying cause and phenotype of the disease.

Future perspectives

In the chapter 2, 5 and 6 of this thesis it has been shown that F_{passive} and pCa_{50} remained higher after PKA treatment in β -blocker treated HFNEF patients. This increase may result from changes in the phosphorylation status of different myofilament proteins (e.g. titin, MyBP-C). Apart from protein kinase A (PKA), other kinases are of interest. In particular pretein kinase G (PKG) since myocardial activity of PKG can be increased by nitric oxide (NO) and natriuretic peptides and improve in-vivo diastolic LV stiffness in humans and in experimental rodent models. In pilot experiments (Hamdani et al. Circulation. 2007;116:S_708. Abstract), it has been shown that PKG treatment reduced F_{passive} in HFNEF cells. Moreover the fall in F_{passive} observed after PKG equals the fall in F_{passive} observed after PKA, suggesting that PKG phosphorylates the same myofilament proteins as PKA. *It would be of interest to find out whether PKG can be used as a target in drug therapy.* Apart from phosphorylation, post-translational modifications resulting from oxidative stress might impair sarcomeric function and may explain part of the increased F_{passive} and pCa_{50} . *Further research has to be done to investigate the involvement of such protein alterations in sarcomeric function in heart failure.*

Raised diastolic LV stiffness importantly contributes to heart failure in DM patients and results from myocardial deposition of advanced glycation endproducts

(AGEs), interstitial fibrosis, cardiomyocyte hypertrophy and elevated diastolic F_{passive} of cardiomyocytes (chapter). Pilot data (Hamdani et al. *Circulation*. 2008;116:S_953. Abstract) have shown that in HFNEF patients with diabetic cardiomyopathy, β -blocker therapy lowered CVF but increased F_{passive} of cardiomyocytes. *The role of glycosylation of sarcomeric proteins, in particular in patients with diabetic cardiomyopathy, warrants further research.*

Large-scale trials have shown that different β -blockers (bisoprolol, carvedilol, metoprolol) exert similar effects on clinical outcome. Based on their specific β AR blocking properties these drugs are divided into second generation β -blockers (bisoprolol, metoprolol), which selectively block β_1 ARs and aspecific, third generation, β -blockers (carvedilol), which also block β_2 ARs and α_1 ARs. Despite their similar effects on clinical outcome, the cellular effects might be diverse in both heart failure phenotypes HFNEF and HFREF. *Further research in this area would be important to clarify their effect on the heart.* Moreover it would be of interest to assess whether there are gender differences of β -blockers on the structure and the function of cardiomyocytes.

10

Nederlandse samenvatting

In dit proefschrift zijn de veranderingen in cellulaire functie en structuur in hartfalen met verschillende onderliggende oorzaken en fenotype bestudeerd. Dit om inzicht te krijgen in de cellulaire pathomechanismen die bijdragen aan de progressieve afname in de pompfunctie van het hart in patiënten met hartfalen. De verkregen resultaten kunnen gebruikt worden om nieuwe therapeutische interventies te ontwikkelen voor toekomstige behandeling van hartfalen.

Hoofdstuk 1 bevat een introductie met de achtergrond en de methoden van de studies beschreven in dit proefschrift.

Hoofdstuk 2. In dit hoofdstuk is de functionele rol van de individuele sarcomeer eiwit isovormen en de post-translationele eiwit modificaties, zoals eiwit degradatie en fosforyleringsgraad, beschreven. Door een veranderde eiwitsamenstelling is de functie van de sarcomeren in hartspiercellen van patiënten met hartfalen veranderd. Deze sarcomeer disfunctie betreft een afname in maximale krachtsontwikkeling en een toename van de calcium gevoeligheid en passieve stijfheid. Deze veranderingen kunnen voor een groot deel verklaard worden door de veranderde fosforyleringsgraad van sarcomeer eiwitten zoals troponine I, titine, het myosine bindend eiwit C en myosine lichte keten 2. Veranderingen in fosforylatie kunnen mogelijk verklaard worden door wijzigingen in de kinase-fosfatase balans in de hartspiercellen. Kennis betreffende fosforylatie plaatsen van sarcomeer eiwitten en de kinasen en fosfatasen kan gebruikt worden om nieuwe therapeutische strategieën te ontwikkelen om de pompfunctie van het hart bij hartfalen te verbeteren.

Hoofdstuk 3. afwijkingen in de β -adrenerge signaalroute zijn niet alleen betrokken bij verslechtering van de hartpompfunctie, maar spelen ook een rol bij de structurele veranderingen die geobserveerd zijn bij hartfalen. Een toename in catecholamines resulteert in afname in het aantal β -adrenerge receptoren aan de celmembraan. Tevens zijn de β -adrenerge receptoren minder gevoelig voor catecholamines.

In hoofdstuk 3 is een vergelijking gemaakt tussen hartweefsel van patiënten met een ischemische hartziekte (ISHD) en idiopathische hartspierziekte (IDCM) om te onderzoeken of de veranderingen in β -adrenerge receptor signaalroute een verklaring kunnen bieden voor de verschillen in functie en structuur van het hartspierweefsel. Donor harten zijn gebruikt als gezonde controles. In beide groepen is een duidelijke afname in het aantal β -adrenerge receptoren gevonden. Uiteenlopende veranderingen zijn gevonden in de expressieniveaus van onderdelen

van de β -adrenerge receptor signaalroute tussen ISHD en IDCM harten. Bovendien is er een verschil gevonden in de expressie van het eiwit betrokken bij de calciumhuishouding in de hartspiercel, het sarcoplasmatisch reticulum calcium ATPase (SERCA2a). Krachtmetingen in enkele hartspiercellen toonden aan dat het calcium gevoeligheid hoger was in IDCM dan in ISHD harten, wat verklaard kon worden door het verschil in troponine I fosforyleringsgraad. Histologische analyses toonden minder collageen aan in ISHD ten opzichte van IDCM.

De resultaten laten zien dat componenten van de β -adrenerge receptor signaalroute en de structuur en functie van hartspiercellen verschillen tussen ISHD and IDCM patiënten. Deze verschillen kunnen een basis vormen voor een meer specifieke therapie in de verschillende patiëntgroepen.

Hoofdstuk 4. Fabry ziekte is één van de lysosomale stapelingsziekten. Deze ziekte wordt gekenmerkt door een tekort aan het enzym α -galactosidase A. Om te weten te komen of veranderingen in myofilament functie en eiwitsamenstelling bijdragen aan disfunctie van het hart bij Fabry patiënten, is in dit hoofdstuk onderzoek gedaan naar structuur en functie van hartspierweefsel van patiënten met Fabry. Onze data toonden een hoge passieve stijfheid en een lage actieve kracht in hartspiercellen van Fabry patiënten, welke mogelijk kunnen bijdragen aan de verminderde pompfunctie van het hart. De hoge passieve stijfheid kan oorzaak zijn van de verminderde diastolische functie. Het hart kan zich minder goed ontspannen. Dit kon deels verklaard worden door een verlaagde fosforylatiegraad van contractiele eiwitten. De lage actieve kracht kan leiden tot een verminderde pompfunctie en zou mogelijk veroorzaakt kunnen zijn door degradatie van troponine I en desmine.

Hoofdstuk 5. Het doel van bètablokker therapie is om de mortaliteit en kwaliteit van leven van patiënten te verbeteren. Eerder onderzoek heeft aangetoond dat bètablokkertherapie een gunstig effect heeft op het calcium huishouding in de hartspiercel, de cardiale remodelering tegengaat en een verbetering geeft van de cardiale efficiëntie.

Om te onderzoeken of bètablokker therapie overeenkomstige effecten induceert bij patiënten met hartfalen met normale ejectie fractie (HFNEF) en hartfalen met een verlaagde ejectie fractie (HFREF), zijn in dit hoofdstuk de effecten van de bètablokker therapie bestudeerd op structuur, functie en eiwit samenstelling van hartspierweefsel van HFNEF en HFREF patiënten.

Onze metingen toonden uiteenlopende effecten van bètablokker therapie op

myofilament functie. Onze data gaven aan dat bètablokker therapie de systolische pompfunctie kan verbeteren bij patiënten met een normale ejectie fractie door een toename van de actieve krachtontwikkeling voor de hartspiercellen en een vertraging of omkering van hartspiercelhypertrofie. Echter, een verhoogde passieve stijfheid werd gevonden in hartspiercellen van HFNEF patiënten behandeld met bètablokkers, welke niet meer gecorrigeerd kon worden met proteïne kinase A behandeling. Onze observaties geven geen mechanistisch bewijs om het gebruik van bètablokkers in patiënten met een voornamelijk diastolische disfunctie te ondersteunen.

Hoofdstuk 6. Toegenomen diastolische hartspierstijfheid draagt aanzienlijk bij aan het ontwikkelen van hartfalen in patiënten met diabetes mellitus (DM) en is het gevolg van myocardiale afzetting van zgn. “advanced glycation endproducts” (AGEs) en van interstitiële fibrose. In dit hoofdstuk is onderzocht of passieve stijfheid van geïsoleerde hartspiercellen bijdraagt aan de diastolische disfunctie bij diabetes patiënten met hartfalen. Een vergelijking is gemaakt van myocardiale fibrose, afzetting van AGEs en de passieve stijfheid van hartspiercellen tussen diabetische en niet-diabetische patiënten met hartfalen. Alleen bij diabetes patiënten met een lage ejectie fractie was de myocardiale collageen hoeveelheid verhoogd, terwijl de toegenomen passieve stijfheid van hartspiercellen alleen werd gevonden bij diabetische patiënten met een diastolische disfunctie. De vraag blijft of bètablokkertherapie de veranderingen die geconstateerd zijn in hartspiercel functie en structuur bij hartfalen patiënten met diabetes mellitus, met name de hoge passieve stijfheid, verbetert. Het is daarom van belang om de veranderingen in eiwitsamenstelling, en mate name de post-translationele modificaties van eiwitten verder te onderzoeken in patiënten met diabetische cardiomyopathie voor het optimaliseren van de behandeling.

Hoofdstuk 7. In dit hoofdstuk is onderzocht of de antilichamen gericht tegen β -adrenerge receptoren gebruikt kunnen worden om de expressie van β -adrenerge receptoren in humaan hartspierweefsel te bepalen. Met western blot analyses werd de specificiteit van antilichamen, gericht tegen β_1 en β_2 adrenerge receptoren, in humaan hartspierweefsel onderzocht. De antilichamen herkenden meerdere eiwitten met verschillende moleculaire gewichten in het humane hartspierweefsel. Opvallend was dat deze antilichamen ook verschillende eiwitten herkenden in gekweekte ovarium cellen van de chinese hamster waarin de expressie van β_1 , β_2 en zelfs β_3 adrenerge receptoren verhoogde was. De resultaten duiden aan dat deze

antilichamen niet specifiek zijn en niet geschikt zijn om de expressie van β -adrenerge receptoren in humaan hartspierweefsel te bestuderen.

Hoofdstuk 8. In dit overzichtsartikel wordt de verstoorde balans beschreven tussen receptor-gemedieerde kinasen en fosfatasen die de fosforyleringsgraad van contractiele eiwitten tijdens hartfalen veranderen. De disbalans tussen kinasen en fosfatasen is gerelateerd aan de verhoogde neurohumorale stimulatie om de pomp functie van het hart bij hartfalen te verhogen. De resultaten van diverse proefdier en humane studies verklaren het belang van het op zorgvuldige wijzen verwerven van bioptmateriaal en de noodzaak om de lokalisatie van kinasen en fosfatasen in hartspiercellen te bestuderen.

List of Publications

Full papers

1. Lamberts RR, **Hamdani N**, Soekhoe TW, Boontje NM, Zaremba R, Walker LA, de Tombe PP, van der Velden J, Stienen GJM. Frequency-dependent myofilament Ca^{2+} desensitization in failing rat myocardium. *J Physiol* 2007. 582:695-709.
2. Zaremba R, Merkus D, **Hamdani N**, Lamers JM, Paulus WJ, dos Remedios C, Duncker DJ, Stienen GJM, van der Velden J. Quantitative analysis of myofilament protein phosphorylation in small cardiac biopsies. *Proteomics Clinical Applications* 2007. 1:1285-1290.
3. **Hamdani N**, Kooij V, van Dijk S, Merkus D, Paulus WJ, dos Remedios C, Duncker DJ, Stienen GJM, van der Velden J. Sarcomeric dysfunction in heart failure. *Cardiovasc Res* 2008. 1:649-658.
4. van Heerebeek L, **Hamdani N**, Handoko ML, Falcao-Pires I, Musters RJ, Kupreishvili K, Ijsselmuiden AJ, Schalkwijk CG, Bronzwaer JGF, Diamant M, Borbely A, van der Velden J, Stienen GJM, Laarman GJ, Niessen HWM, Paulus WJ. Diastolic stiffness of the failing diabetic heart: Importance of fibrosis, advanced glycation endproducts and myocyte resting tension. *Circulation* 2008. 117:43-51.
5. **Hamdani N***, Chimenti C*, Boontje NM, DeCobelli F, Esposito A, Jean GF, Bronzwaer JGF, Stienen GJM, Russo MA, Paulus WJ, Frustaci A, van der Velden J. Myofilament degradation and dysfunction in human cardiomyocytes with Fabry disease *Am J Pathol* 2008. 172:1482-1490. ***Both authors contributed equally.**
6. van Heerebeek L, **Hamdani N**, Handoko ML, Falcao-Pires I, Musters RJ, Borbely A, van der Velden J, Stienen GJM, Paulus WJ. Response to letter regarding article: Diastolic stiffness of the failing diabetic heart: Importance of fibrosis, advanced glycation end products, and myocyte resting tension". *Circulation* 2008. 117:e484.
7. **Hamdani N**, van der Velden J. Specificity of antibodies directed against human beta-adrenergic receptors. *Naunyn Schmiedebergs Arch Pharmacol* 2009, 379:403-407
8. **Hamdani N**, de Waard M, Messer AE, Boontje NM, Kooij V, van Dijk S, Versteilen A, Lamberts R, Merkus D, dos Remedios C, Duncker DJ, Borbely A, Papp Z, Paulus W, Stienen GJ, Marston SB, van der Velden J. Myofilament dysfunction in cardiac disease from mice to men. *J Muscle Res Cell Motil* 2009, 29:189-201.
9. van Dijk SJ, **Hamdani N**, Stienen GJM, van der Velden J. Myocardial

- adaptations in the failing heart: cause or consequence. *J Muscle Res Cell Motil* 2009.
10. Borbély A, Falcao-Pires I, Heerebeek L, **Hamdani N**, Édes I, Leite-Moreira AF, Bronzwaer JGF, van der Velden J, Stienen GJM, Paulus WJ. Hypophosphorylation of the stiff N2B titin isoform raises cardiomyocyte resting tension in failing human myocardium. *Circ Res* 2009.
 11. Lamberts RR*, Onderwater G*, **Hamdani N**, Vreden J, Steenhuisen J, Eringa E, Loer SA, Stienen GJM, Bouwman RA,. Reactive oxygen species-induced activation of 5'AMP-activated protein kinase mediates sevoflurane-induced cardioprotection. *Circulation* 2009. ***Both authors contributed equally.**
 12. Swinnen M, Vanhoutte D*, Van Almen G, **Hamdani N**, Vandenberghe A, Schellings MWM, Herijgers P, D'Hooge J, van der Velden J, Sage HE, Bornstein P, Verheyen FK, Paulus WJ, van de Werf F, Schroen B, Carmeliet P, Pinto YM, Heymans S. Absence of thrombospondin-2 causes age-related dilated cardiomyopathy. *Submitted*. ***Both authors contributed equally.**
 13. **Hamdani N**, Paulus WJ, van Heerebeek L, Borbély A, Boontje NM, Zuidwijk MJ, Simonides WS, Niessen HWM, Stienen GJM, van der Velden J. Distinct myocardial effects of beta-blocker therapy in heart failure with normal or reduced left ventricular ejection fraction. *Revision European heart journal*.
 14. **Hamdani N**, Borbely A, Veenstra SPGR, Zaremba R, dos Remedios C, Niessen HWM, Paulus WJ, Stienen GJM, van der Velden J. Diverse alterations in sarcomeric protein composition and function in ischemic and idiopathic dilated cardiomyopathy. *Submitted*.
 15. Bouwman AR, Jumoke MA. Vreden, **Hamdani N**, Wassenaar LEJ, Loer SA, Stienen GJM, Regis R. Lamberts. Bupivacaine and sevoflurane-induced cardioprotection in isolated rat hearts. *Submitted*.

Abstracts

1. Lamberts RR, Soekhoe TW, **Hamdani N**, Boontje NM, Zaremba R, van der Velden J, Stienen GJM. Frequency-dependent alterations in calcium sensitivity in healthy and failing rat myocardium. *Biophys J* 2005, 88:538A. Part 2, Suppl. S.
2. Lamberts RR, **Hamdani N**, Soekhoe TW, Walker LA, de Tombe PP, van der Velden J, Stienen GJM. Origin of frequency-dependent alterations in calcium sensitivity in failing rat myocardium. *Biophys J* 2006, 90: Suppl. S.
3. **Hamdani N**, van der Velden J, Boontje NM, Stienen GJM, Frustaci A, Paulus WJ, Chimenti C. Myofilament dysfunction in Fabry disease. The European Young Physiologist Symposium and The German Society of Physiology and The Federation of European Physiological Societies 2006 in Munich. **Poster presentation.**
4. **Hamdani N**, van Heerebeek L, Borbély A, Boontje NM, Niessen HWM, Stienen GJM, Paulus WJ, van der Velden J. Beta-blocker therapy alters myofilament function in patients with congestive heart failure. *Circulation* 2006, 114:376. Suppl.S. **Poster presentation.**
5. Falcao-Pires I, **Hamdani N**, van der Velden J, Stienen GJM, Niessen HWM, Gavina C, Leite-Moreira AF, Paulus WJ. Stiffness of hypertrophied cardiomyocytes differs in aortic stenosis and arterial hypertension. *Circulation* 2006, 114:666. Suppl.S.
6. Chimenti C, **Hamdani N**, Boontje NM, Stienen GJM, Paulus WJ, Frustaci A, van der Velden J. Myofilament dysfunction in human cardiomyocytes with Fabry disease. *Circulation* 2006, 114:667. Suppl. S.
7. van Heerebeek L, Handoko ML, Hamdani N, Niessen HWM, van der Velden J, Stienen GJM, Paulus WJ. Fibrosis, AGEs or stiff cardiomyocytes: Which one to blame for the high diastolic stiffness of the diabetic heart? *Circulation* 2006, 114:802. Suppl. S.
8. **Hamdani N**, van Heerebeek L, Borbély A, Boontje NM, Niessen HWM, Stienen GJM, Paulus WJ, van der Velden J. Opposite Effects Of Chronic Beta-blocker Therapy On Myofilament Function In Heart Failure With Reduced Or Normal Left Ventricular Ejection Fraction. *Circulation* 2007, 116: 302. Suppl. S. **Oral presentation.**
9. **Hamdani N**, Borbély A, Falcao-Pires I, Boontje NM, Niessen HWM, Stienen GJM, van der Velden J, and Paulus WJ. Protein Kinase G Corrects High Cardiomyocyte Resting Tension in Diastolic Heart Failure. *Circulation* 2007,

- 116:708. Suppl. S. **Oral presentation.**
10. Borbély A, **Hamdani N**, Falcao-Pires I, Édes I, Leite-Moreira AF, Stienen GJM, van der Velden J, Paulus WJ. Titin Isoform phosphorylation in failing human myocardium. *Circulation* 2007, 116: 301. Suppl. S.
 11. Borbély A, **Hamdani N**, Falcao-Pires I, Édes I, Leite-Moreira AF, Stienen GJM, van der Velden J, Paulus WJ. Myocardial titin isoform phosphorylation in diastolic heart failure. *Circulation* 2007, 116:420-421. Suppl. S.
 12. Heerebeek L, Attila Borbély, **Hamdani N**, Falcao-Pires I, Édes I, Leite-Moreira AF, Stienen GJM, van der Velden J, Paulus WJ. Myocardial titin isoform expression in concentric and eccentric left ventricular remodeling. *Circulation* 2007, 116:622.
 13. Lamberts RR, Onderwater G, **Hamdani N**, Loer SA, Bouwman RA. Sevoflurane preconditioning increases AMPK activation during ischaemia and reperfusion in isolated rat hearts. *ESA 2008 Copenhagen*.
 14. Lamberts RR, **Hamdani N**, Walker LA, Tombe PP, van der Velden J, Stienen GJM. Calcium-dependent protein kinase C alpha and the frequency dependent increase in phosphorylation of troponin I in failing hearts. *Experimental Biology FASEB Journal* 2008, 22:751. Suppl. S.
 15. Onderwater G, **Hamdani N**, Vreden MAJ, Steenhuisen J, Eringa EC, Stienen GJM, Loer SA, Bouwman RA, Lamberts RR. Reactive oxygen species-induced activation of 5'AMP-activated protein kinase mediates cardioprotection against ischemia and reperfusion injury. *Circulation* 2008, 118:706. Suppl. S.
 16. van Heerebeek L, **Hamdani N**, Handoko ML, van der Velden J, Stienen GJM, Niessen HWM, Laarman GJ, Somsen A, Paulus WJ. Myocardial protein kinase G activity differs in heart failure with normal and reduced ejection fraction. *Circulation* 2008, 118:865. Suppl. S.
 17. van Heerebeek L, **Hamdani N**, Handoko ML, van der Velden J, Stienen GJM, Niessen HWM, Laarman GJ, Somsen A, Paulus WJ. Low myocardial protein kinase G activity raises cardiomyocyte resting tension in diastolic heart failure. *Circulation* 2008, 118: 349-349 Suppl. S.
 18. **Hamdani N**, van der Velden J, van Heerebeek L, Borbely A, Boontje NM, Zuidwijk M, Simonides WS, Niessen HWM, Stienen GJM, Paulus WJ. Distinct myocardial effects of beta-blocker therapy in heart failure with normal and reduced left ventricular ejection fraction. *Circulation* 2008, 118:952. Suppl. S. **Oral presentation.**

- 19. Hamdani N**, van der Velden J, van Heerebeek L, Borbely A, Boontje NM, Stienen GJM, Paulus WJ. Myocardial effects of beta-blocker therapy in the failing diabetic heart. *Circulation* 2008, 118:953. Suppl. S. ***Oral presentation.***



Dankwoord

Het lijkt nog als de dag van gisteren dat ik begonnen ben met mijn promotieonderzoek, maar inmiddels zijn er 4 jaar voorbij. Ik heb mijn werk altijd met veel plezier en genot gedaan. Het waren mooie jaren, waarin ik veel heb geleerd. Natuurlijk doe je een proefschrift niet alleen. Je hebt altijd mensen nodig, mensen die je kunnen helpen en steunen. Hierbij wil ik de vele mensen bedanken voor hun hulp en steun.

Mijn co-promotor dr. Jolanda van der Velden, altijd met een brede glimlach. Bij jou wil ik even stil staan: je bent mijn co-promotor en mijn directe begeleidster. Ten eerste wil ik je bedanken voor de mogelijkheid die je mij hebt gegeven om onderzoek bij je te mogen doen, voor de vrijheid die je mij gaf en voor je vertrouwen. Ik heb veel van je geleerd, alles wat betreft onderzoek, nadenken over de experimenten, plannen, uitvoeren en schrijven. Samen hebben we het altijd leuk gehad en ook in de toekomst met het project van ESC en wie weet bij misschien nog meer projecten in de toekomst. Wat ik vooral enorm aan je waardeer, is je enthousiasme voor het vak en onderzoek, je positieve instelling, je goede ideeën, je creativiteit, je volledige toewijding aan de wetenschap en de goede balans die je hebt tussen werk en privé met 4 mannetjes thuis. Verder verraste je mij keer op keer door de enorme hoeveelheid energie die jij hebt en het warme persoonlijke contact dat je onderhoudt met mij en met andere mensen. Jouw deur stond letterlijk altijd open voor vragen. Je nam altijd de tijd om mijn manuscripten en proefschrift kritisch te lezen ondanks de drukte. Bedankt voor alles en voor wat je me geleerd hebt binnen dit vakgebied, maar ook voor de overige dingen die geen betrekking hebben op het werk, onder anderen je gastvrijheid. Natuurlijk wil ik jouw mannetjes niet vergeten. Bas bedankt voor alle gezelligheid en voor het feit dat ik altijd welkom bij jullie was. Tomas, Mike en Boris bedankt voor de kusjes, de knuffeltjes en de tekeningen.

Mijn promotoren Prof. dr. Walter J. Paulus en Prof. dr. Ger J.M. Stienen, jullie enthousiasme, ideeën, enorm gedrevenheid, inzet en relativiseringsvermogen waren zeer belangrijk voor het succes van dit onderzoek. Betere promotoren en co-promotor zoals jullie kan een AIO zich niet wensen.

Prof. dr. Walter J. Paulus, je hebt ervoor gezorgd dat ik naast mijn promotieonderzoek ook verschillende samenwerkingsprojecten deed zowel in het binnen als het buitenland. Je enthousiasme voor het vak en je grote ideeën heb ik veel van geleerd en hebben mij enorm geïnspireerd. Bedankt voor het meedenken en jouw kritische inbreng, bedankt voor alles wat ik van je heb geleerd en vooral het

schrijven.

Prof. dr. Ger J.M. Stienen, hartelijk dank voor je kritische blik op zowel een manuscript, als een aanvraag. Jouw gehele overzicht van probleemstellingen heeft niet alleen tot aanzienlijk betere artikelen geleid, maar heeft mij ook een breder inzicht gegeven. Jouw deur stond en staat altijd voor mij en voor alle andere AIO's open, voor zowel korte als lange vragen, je zegt nooit nee ondanks het feit dat je het erg druk hebt. Ik heb veel van jou geleerd, van kritisch naar dingen kijken tot schrijven. Bedankt voor alles en ook voor de snelle commentaren en correcties. Ik ben erg blij dat ik de komende tijd nog als post-doc in de groep blijf werken en nog meer van jullie kan leren.

Mijn paranimfen Nicky en Pauline. Lieve Nicky, vanaf het eerste moment had ik het idee dat we elkaar altijd wel 'begrepen', al was het maar om de bepaalde cynische humor die jij en ik hebben. Met jou kan ik altijd veel lachen, dus niet gek dat je mijn paranimf bent. Ik heb van jou alle technieken geleerd, je stond altijd klaar voor mij. Bovendien, je bent mijn grootste sushi-, bioscoop-, lekker-eten- maatje en af en toe samen met *de trein!* reizen naar Londen, rarararara hoe komt dat? Een kaartje kopen voor de musical Chicago voor 25 pond en vervolgens slapen tijdens de show, dat doe je goed! Binnenkort ga je een grote reis maken met Thomas. Ik wens je veel plezier en succes, geniet en maak er wat van. Bedankt voor al je hulp en gezelligheid.

Lieve Pauline, je bent mijn beste vriendin we kennen elkaar al jaren. Het is dus voor mij logisch dat je mijn paranimf bent. Het is voor mij een eer dat je 4 juni naast mij zal staan als ik mijn proefschrift moet verdedigen, we hebben het altijd leuk samen bedank voor je hulp, voor alle goede zorgen en luisterend oor. Ik ben erg blij met je vriendschap. Bedankt voor alles.

Kamer B-156, een onvergetelijke kamer. De afgelopen jaren was dit mijn thuisbasis en het heeft vele verschillende bewoners gehad: Viola, Loek, Attila, Ines, Nadija, Sander, Koen en Daniel. Jullie allen ontzettend bedankt voor de gezelligheid. Beste Viola, of anders gezegd "snoepmonster" die niet zomaar snoepmonster wordt genoemd. Je bent mijn koffie- en theemaatje. Het is altijd leuk om jou als kamergenoot te hebben. Ik ben blij dat ik nog even mag blijven tot eind november en je gezelschap kan houden. Bedankt voor je steun, gezelligheid, snoepjes en natuurlijk je luisterend oor. Jij en Nicky zorgden voor de nodige afleiding en gemeente belangstelling die ik nodig had tijdens de vele uren werk. Veel succes met

je verdere carrière en met je eigen promotie de komende anderhalf jaar! Loek, ik heb altijd een goede en fijne samenwerking met jou gehad. Ook was het super gezellig om met jou koffie te drinken. Veel succes met je opleiding als cardioloog en met je eigen promotie.

Ik heb met verschillende collega's in zowel binnen- als buitenland mogen samenwerken:

Dr. C. Chemilti from Italy, I. Falcao-Pires from Portugal, dr. A. Borbely and D. Czurigad from Hungary, prof.dr. MC. Michel from Amsterdam, M. Swinnen and D. Vanhoutte from Maastricht.

Dr. C. Chimenti, thank you for the collaboration. Attila, during your stay in Amsterdam we had lots of fun! Cleaning and taking care of the room was the major part that I missed of you when you left. Changing your habits to Dutch habits was my biggest challenge like eating dropjes as part of the Dutch course that I gave you. But also working together with you appears to turn into a great success (CircRes), thank you for everything. Daniel, thank you as well. Ines, we worked together and we had a great time with the myocytes, I am happy that you will come to my defense since you are also busy with finalizing your own thesis. I hope everything will go as fast as with your CircRes paper. Good luck! And see you the 4th of June. Prof.dr. MC. Michel van het AMC hartelijk dank voor de samenwerking en ben erg blij dat u deel uitmaakt van de promotiecommissie. Mellissa en Davy, het was erg gezellig met jullie in de AHA van 2008, dank voor de samenwerking. Thank you for the opportunity to collaborate with all of you which already resulted in a couple of articles and I hope to continue this collaboration.

Regis, ik ben begonnen bij de afdeling als student. Als student heb ik aan jouw project gezeten, sindsdien werken we samen. Onze samenwerking heeft mooie publicaties opgeleverd en nu zit je ook in mijn promotiecommissie, daar ben erg blij mee. Ik hoop dat we nog meer gaan samenwerken in de komende tijd. Succes met je aanvraag. Coen, je hebt Viola ingehaald, je weet wel wat ik bedoel. Bedankt voor de goede tips voor de Rubicon en voor je gezelligheid. Ruud, bedankt voor de technische ondersteuning. Je bent erg gezellig, maar nog gezelliger als je een biertje op hebt. Sabine bedankt voor de fijne tijd en succes met je promotieonderzoek.

Charissa, Frances, Kanita, Louis en Rob, inmiddels zijn jullie ook sushi-, The Basket- en pannenkoekmaatjes. Ik ben blij dat jullie mijn promotie zullen bijwonen. Rob, wel

goed opletten op de ceremonie. Veel succes met jullie promotieonderzoek. Kanita, je bent weg gegaan, verhuisd naar Utrecht en straks ook nog naar Maastricht, maar toch lijkt het alsof je nog steeds bij ons rondloopt. Het is altijd lachen met je. Heel veel succes en plezier met je promotieonderzoek, je verdere carrière en met verhuizen.

Foppo en Duncan, bedankt. Jullie hebben veel bijgedragen op het gebied van software en elektronica. Dirk de Jong, bedankt voor de posters en het afmaken van de omslag. Aimee en Hans, bedankt voor alle jullie klusjes en de administratieve ondersteuning. Daarnaast wil ik ook de medewerkers van de instrumentmakerij bedanken met name Peter voor de transducers. Chris Zwart, ooit gaan we samen lopen☺, beloofd en wie weet misschien lopen we samen de Dam tot Dam.

Ook heb ik tijdens mijn promotieonderzoek verschillende stagiaires mogen begeleiden. Brain, Imad, Kai, Ashwyn, Sophie, Sebastian, Wellimijn en Wim, jullie hebben veel werk uit mijn handen genomen, maar het was vooral een genot om met jullie samen te werken. Ik hoop dat jullie net zo veel van mij hebben geleerd als ik van jullie.

Alle andere collega's van de afdeling wil ik hartelijk danken voor de stimulerende omgeving en de heerlijke tijd.

Alle AIO's: Everaldo, Yeung-Ying, Sabine, Wineke, Koen, Robert, Jacqueline, Nora, Melanie, Lonneke, Ester, Evi, Christine, Cora en Kakkhee, ik wens jullie veel succes met het afronden van jullie eigen promotie. Alle post-docs: Amanda, Lynda, Coen en Ed, succes met jullie projecten. Roland, veel succes in Utrecht. Het gaat je goed, je hebt het daar naar je zin en dat is erg belangrijk. Alle analisten: Caro-Lynn, Ingrid, Dorine, Sylvia, Michiel en Jan bedankt voor de leuke tijd en de gezelligheid.

Sjoukje Bonekamp, ik ben je zeer dankbaar voor al je hulp en steun, hoewel ik nog steeds denk dat ik niet eigenwijs ben☺.

De leden van de lees- en promotiecommissie, prof.dr. DJ. Duncker, prof.dr. HW. Niessen, dr. JG. Bronzwaer, dr. RG. Schoemaker, prof.dr. MC. Michel, dr. RR. Lamberts, dr. AJ. Ijsselmuiden en prof.dr. GJ. Tangelder, hartelijk dank voor de goedkeuring en voor de bereidheid om zitting te nemen in de

beoordelingscommissie.

Mijn vrienden Pauline, Nadia, Santi, Mieke, Amber, Kamar, Farnoush, Soumia, Nasreen, Davi en Mary, ik wil jullie bedanken voor al jullie steun en begrip.

Nadia, Pauline, Santi en Far, jullie zijn mijn beste en gouden vriendinnen, hoewel we vaak hebben afgesproken en ik op het laatste moment afzegde, wist 100% zeker dat jullie het begrepen. Jullie antwoord was altijd "ik weet dat jij het druk hebt". Bedankt voor jullie begrip.

Nu iets speciaals voor mijn prachtige familie: mijn zussen, broers, neefje en nichtjes, bedankt voor al jullie steun, liefde en jullie begrip.

Lieve mama en papa, ik wil jullie bedanken voor alle steun en zorg die ik altijd van jullie gekregen heb. Mama, bedankt voor je lekkere koffie en papa bedankt voor je lekkere soep. Jammer dat er geen gelegenheid is om jullie in het openbaar te bedanken, dus wil ik van deze gelegenheid gebruik maken. Ik weet zeker dat jullie zullen genieten van de hele ceremonie en *vooral niet klappen tijdens de ceremonie papa!*

Natuurlijk kan ik nu een hele lijst mensen opnoemen die de afgelopen jaren belangrijk zijn geweest, zowel binnen als buiten mijn promotieproject. Hier noemde ik slechts enkele speciaal bij naam, hoewel misschien diegene die niet expliciet werden genoemd nog belangrijker waren, op welke wijze dan ook.

Nazha Hamdani,

Amsterdam, 8 april 2009

Curriculum vitae

Nazha Hamdani geboren te Amsterdam. In 1994 behaalde zij haar VWO diploma aan Calandlyceum te Amsterdam. In hetzelfde jaar begon zij met studie geneeskunde en economie aan de vrije universiteit van Brussel (Université Libre de Bruxelles) en in 1998 behaalde zij haar economie doctoraalexamen. In 1998 begon zij aan de vrije universiteit van Amsterdam met studie de Farmaceutische wetenschappen met specialisatie Farmacologie als eerste afstudeeropdracht en Toxicologie als tweede afstudeeropdracht.

In 2005 behaalde zij haar doctoraalexamen. Tijdens haar afstudeeropdrachten kwam zij voor het eerste in aanraking met het wetenschappelijk onderzoek. In februari 2005 begon zij met haar promotieonderzoek bij de vakgroep Fysiologie aan de Vrije Universiteit Medisch Centrum (VUMC) te Amsterdam. De resultaten van haar promotieonderzoek staan in dit proefschrift met de publicaties beschreven.

Vanaf 1 maart 2009 is zij werkzaam als post-doc bij de vakgroep Fysiologie van het VUMC. Vanaf mei 2009 tot en met mei 2010 wordt de samenwerking met de Vakgroep Fysiologie van de Universiteit van Bochum voortgezet en uitgebreid met de ESC beurs die zij toegekend gekregen heeft. Vanaf december 2009 is haar bedoeling naar Baltimore, USA te vertrekken. Zij zal in Johns Hopkins University School of Medicine Peadiatric cardiology research voor twee jaar een postdoctoral fellowship beginnen.